TECHNICAL REPORT HL-82-15

THE ATCHAFALAYA RIVER DELTA

Report 5
THE ATCHAFALAYA RIVER DELTA QUASI-TWO-DIMENSIONAL MODEL OF DELTA GROWTH AND IMPACTS ON RIVER STAGES

by

W. A. Thomas, R. E. Heath, J. P. Stewart, D. G. Clark

Hydraulics Laboratory

DEPARTMENT OF THE ARMY
Waterways Experiment Station, Corps of Engineers
PO Box 631, Vicksburg, Mississippi 39181-0631

December 1988
Report 5 of a Series

US Army Corps of Engineers

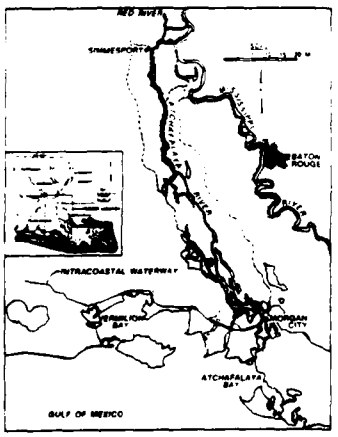

HYDRAULICS LABORATORY

Destroy this report when no longer needed. Do not return it to the originator.

The findings in this report are not to be construed as an official Department of the Army position unless so designated by other authorized documents.

The contents of this report are not to be used for advertising, publication, or promotional purposes. Citation of trade names does not constitute an official endorsement or approval of the use of such commercial products.

Unclassified
SECURITY CLASSIFICATION OF THIS PAGE

REPORT DOCUMENTATION PAGE

Form Approved
OMB No. 0704-0188

1a. REPORT SECURITY CLASSIFICATION Unclassified	1b. RESTRICTIVE MARKINGS
2a. SECURITY CLASSIFICATION AUTHORITY	3. DISTRIBUTION/AVAILABILITY OF REPORT Approved for public release; distribution unlimited.
2b. DECLASSIFICATION/DOWNGRADING SCHEDULE	
4. PERFORMING ORGANIZATION REPORT NUMBER(S) Technical Report HL-82-15	5. MONITORING ORGANIZATION REPORT NUMBER(S)
6a. NAME OF PERFORMING ORGANIZATION USAEWES Hydraulics Laboiatory 6b. OFFICE SYMBOL (If applicable) CEWES-HP-M	7a. NAME OF MONITORING ORGANIZATION
6c. ADDRESS (City, State, and ZIP Code) PO Box 631 Vicksburg, MS 39181-0631	7b. ADDRESS (City, State, and ZIP Code)
8a. NAME OF FUNDING/SPONSORING ORGANIZATION USAED, New Orleans 8b. OFFICE SYMBOL (If applicable)	9. PROCUREMENT INSTRUMENT IDENTIFICATION NUMBER
8c. ADDRESS (City, State, and ZIP Code) PO Box 60267 New Orleans, LA 70160-0267	10. SOURCE OF FUNDING NUMBERS PROGRAM ELEMENT NO. / PROJECT NO. / TASK NO. / WORK UNIT ACCESSION NO.
11. TITLE (Include Security Classification) The Atchafalaya River Delta; The Atchafalaya River Delta Quasi-Two-Dimensional Model of Delta Growth and Impacts on River Stages	
12. PERSONAL AUTHOR(S) Thomas, W. A.; Heath, R. E.; Stewart, J. P.; Clark, D. G.	
13a. TYPE OF REPORT Report 5 of a series 13b. TIME COVERED FROM _____ TO _____	14. DATE OF REPORT (Year, Month, Day) December 1988 15. PAGE COUNT 172
16. SUPPLEMENTARY NOTATION Available from National Technical Information Service, 5285 Port Royal Road, Springfield, VA 22161.	

17. COSATI CODES		
FIELD	GROUP	SUB-GROUP

18. SUBJECT TERMS (Continue on reverse if necessary and identify by block number)
Alluvial plains, Louisiana, (LC) Sedimentation, Deposition. (AW)
Atchafalaya River (La.)--Delta (LC)
Deltas--Louisiana (LC) (see reverse)

19. ABSTRACT (Continue on reverse if necessary and identify by block number)

A quasi-two-dimensional sediment movement computer program was verified to historical bed deposition and scour and used to forecast delta growth for the next 50 years. The results are compared with growth rates predicted by several other methods in Report 6 of this series, Interim Summary Report of Growth Prediction.

Coastal Army Planning, Resource Management, Subaerial land Bays, Flood elevation,

20. DISTRIBUTION/AVAILABILITY OF ABSTRACT ☒ UNCLASSIFIED/UNLIMITED ☐ SAME AS RPT. ☐ DTIC USERS	21. ABSTRACT SECURITY CLASSIFICATION Unclassified
22a. NAME OF RESPONSIBLE INDIVIDUAL	22b. TELEPHONE (Include Area Code) / 22c. OFFICE SYMBOL

DD Form 1473, JUN 86 Previous editions are obsolete. SECURITY CLASSIFICATION OF THIS PAGE

Unclassified

18. SUBJECT TERMS (Continued).

Sedimentation and Deposition--Research (LC)

PREFACE

This report documents the processes by which the Quasi-Two-Dimensional Sediment Transport model was applied in the Atchafalaya River Delta Study to simulate delta growth and how the impact of that growth on flood peak elevations was calculated by the computer program, "Simulated Open Channel Hydraulics, Multiple Junctions."

The study was authorized by the US Army Engineer District, New Orleans, and was conducted by personnel of the US Army Engineer Waterways Experiment Station (WES), under the direction of Messrs. H. B. Simmons and F. A. Herrmann, Jr., former and present Chiefs, Hydraulics Laboratory (HL); R. A. Sager, Assistant Chief, HL; M. B. Boyd, Chief, Waterways Division (WD); W. H. McAnally, Jr., Chief, Estuaries Division (ED), Project Manager; and J. V. Letter, Jr., Chief, Estuarine Simulation Branch, ED, Task Coordinator. The plan of study of which this task is one part was developed by Messrs. McAnally and Samuel B. Heltzel, Estuarine Engineering Branch, ED. This study was performed and this report written by Messrs. W. A. Thomas, WD; R. E. Heath, Math Modeling Group, WD; J. P. Stewart, Office of Technical Programs and Plans; and CPT D. G. Clark, Coastal Ecology Group, Environmental Resources Division, Environmental Laboratory. Tables 3 and 4 were compiled by Mr. James D. Ethridge, Jr., Estuarine Simulation Branch. This report was edited by Mrs. M. C. Gay, Information Technology Laboratory, WES.

COL Dwayne G. Lee, EN, is the Commander and Director of WES. Dr. Robert W. Whalin is the Technical Director.

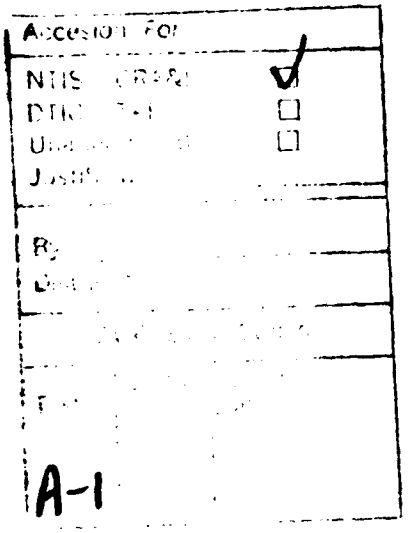

CONTENTS

CONVERSION FACTORS, NON-SI TO SI (METRIC) UNITS OF MEASUREMENT

Non-SI units of measurement used in this report can be converted to SI (metric) units as follows:

Multiply	By	To Obtain
acres	4,046.873	square metres
cubic feet	0.02831685	cubic metres
cubic yards	0.7645549	cubic metres
feet	0.3048	metres
miles (US statute)	1.609347	kilometres
pounds (force) per square foot	47.88026	pascals
pounds (mass) per cubic foot	16.01846	kilograms per cubic metre
square miles	2.589998	square kilometres
tons (2,000 pounds, mass)	907.1847	kilograms
tons (force) per square foot	95.76052	kilopascals

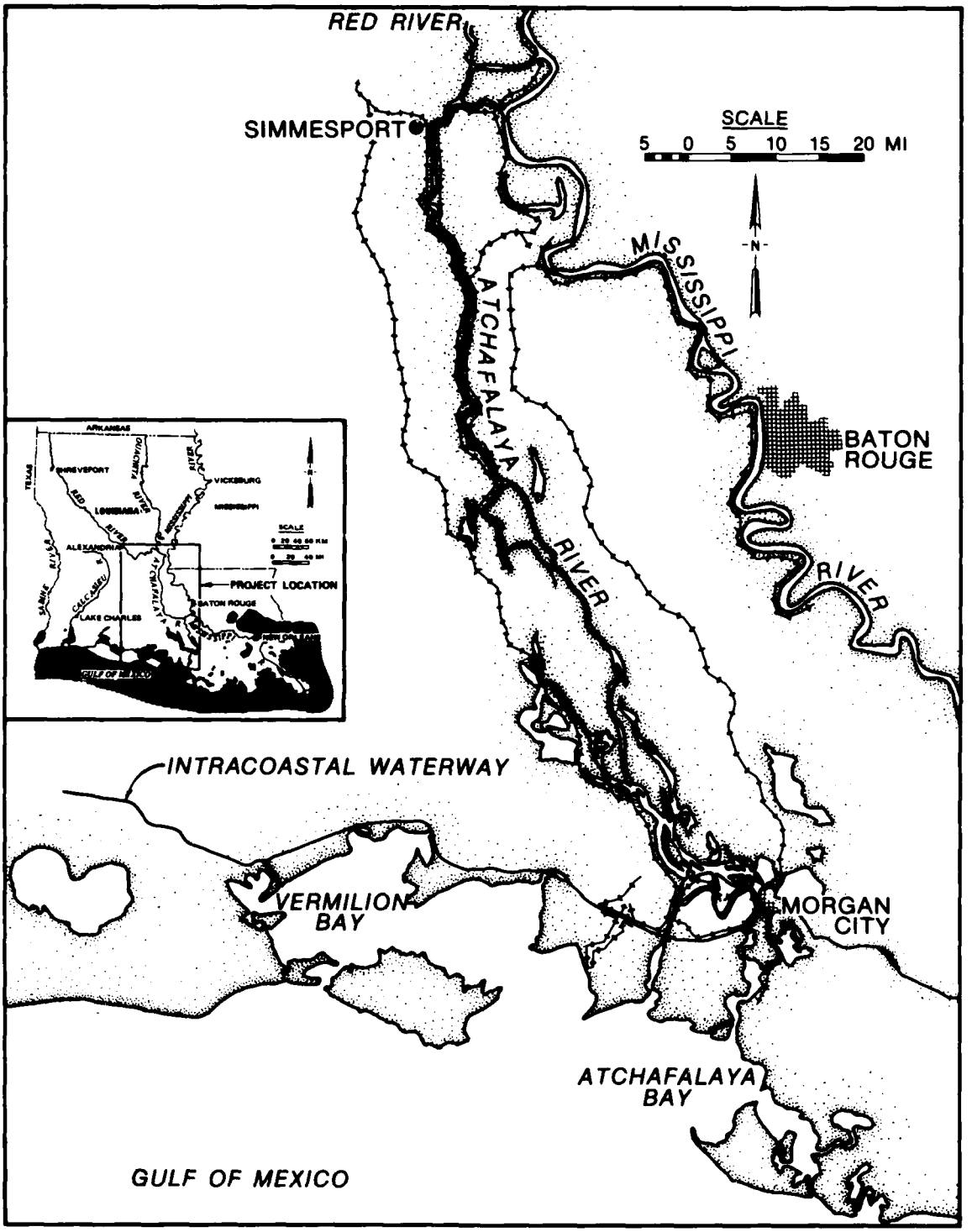

Figure 1. Project location

THE ATCHAFALAYA RIVER DELTA QUASI-TWO-DIMENSIONAL MODEL OF DELTA GROWTH AND IMPACTS ON RIVER STAGES

PART I: INTRODUCTION

Background

1. The Atchafalaya Basin, a natural floodway, became part of the Mississippi River and Tributaries (MR&T) flood-control project as a result of the 1928 Flood Control Act of the United States Congress. Figure 1 shows the location of the basin, and Figure 2 shows the major role it plays in the MR&T plan. Not only does the Atchafalaya Floodway carry half the discharge of the MR&T system during a design flood, but it also carries 30 percent of the daily flow. The annual sediment yield into the floodway is about 100 million tons.* Since the emergence of the delta in Atchafalaya Bay, during the 1973 flood, it has become one of the most dynamic in the world with initial growth rates estimated at 5.5 to 6.5 square miles per year (Shlemon 1975 and Shlemon and Gagliano 1972).

2. Delta growth is, therefore, an ongoing subject of extensive study by aerial and land reconnaissance. Through those studies, past development has been cataloged and projections of future deltas have been made. The impact on flood elevations in the Atchafalaya River is expected to be substantial at the latitude of the present coastline, and that impact is expected to extend upstream, even beyond Morgan City, Louisiana, although it will decrease with distance from the present coastline. The extent to which Wax Lake Outlet will be affected, maintenance of navigation, the environmental impact, and changes in salinity as the delta grows are other questions vital to the US Army Corps of Engineers flood-control and navigation planning. The study reported here used 2 of the 12 numerical models and the physical model the US Army Engineer Waterways Experiment Station (WES) is developing for predicting the growth of

---

* A table of factors for converting non-SI units of measurement to SI (metric) units is found on page 3.

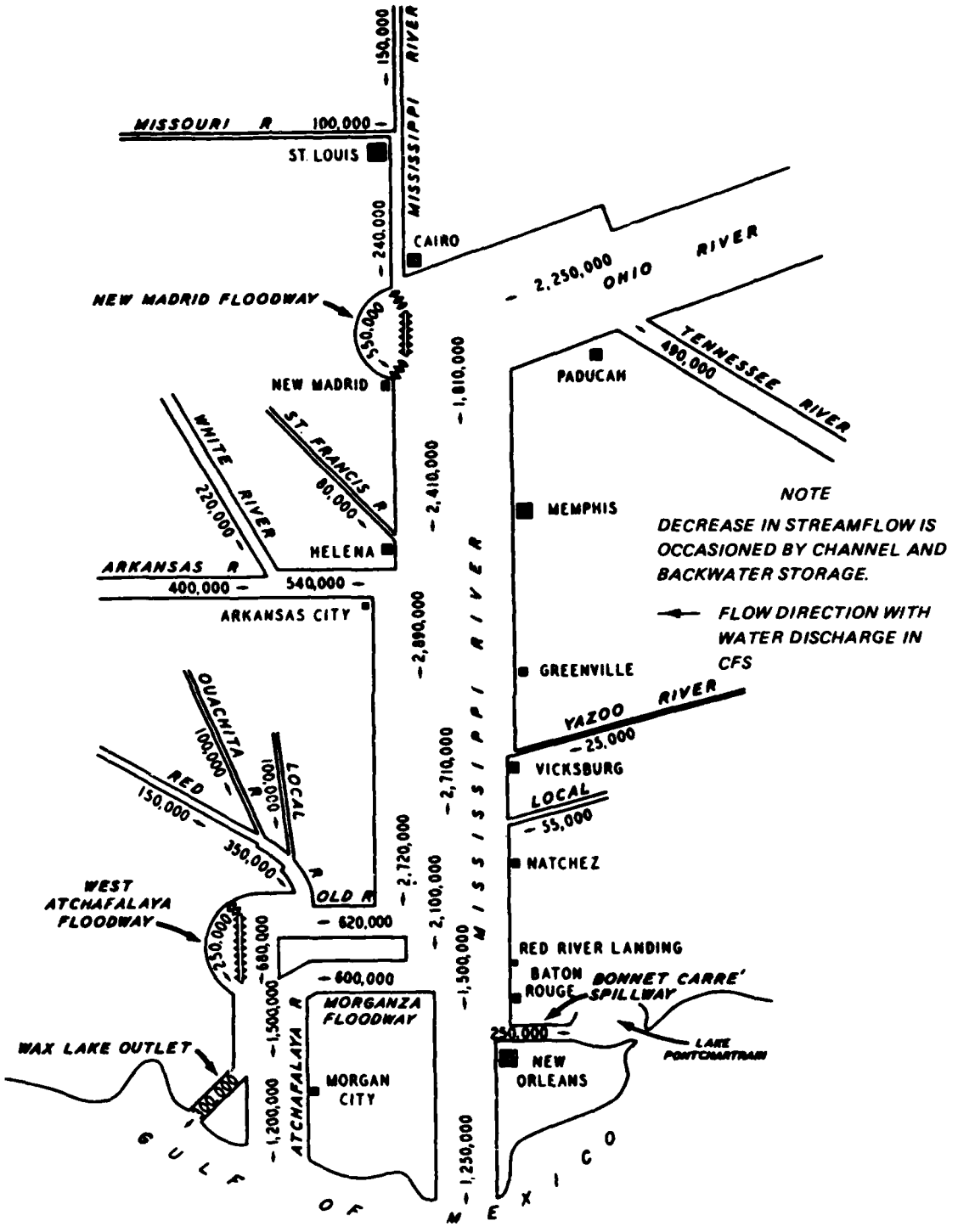

Figure 2. Project design flood

this delta as well as the MR&T system's response to it.

Study Authority

3. This study was conducted at the request of the US Army Engineer District (USAED), New Orleans. It is a portion of their overall study to develop a comprehensive plan for the management and preservation of the water and related land resources of the Atchafalaya Basin. Their overall study area boundary is shown in Figure 3. The portion of that comprehensive plan

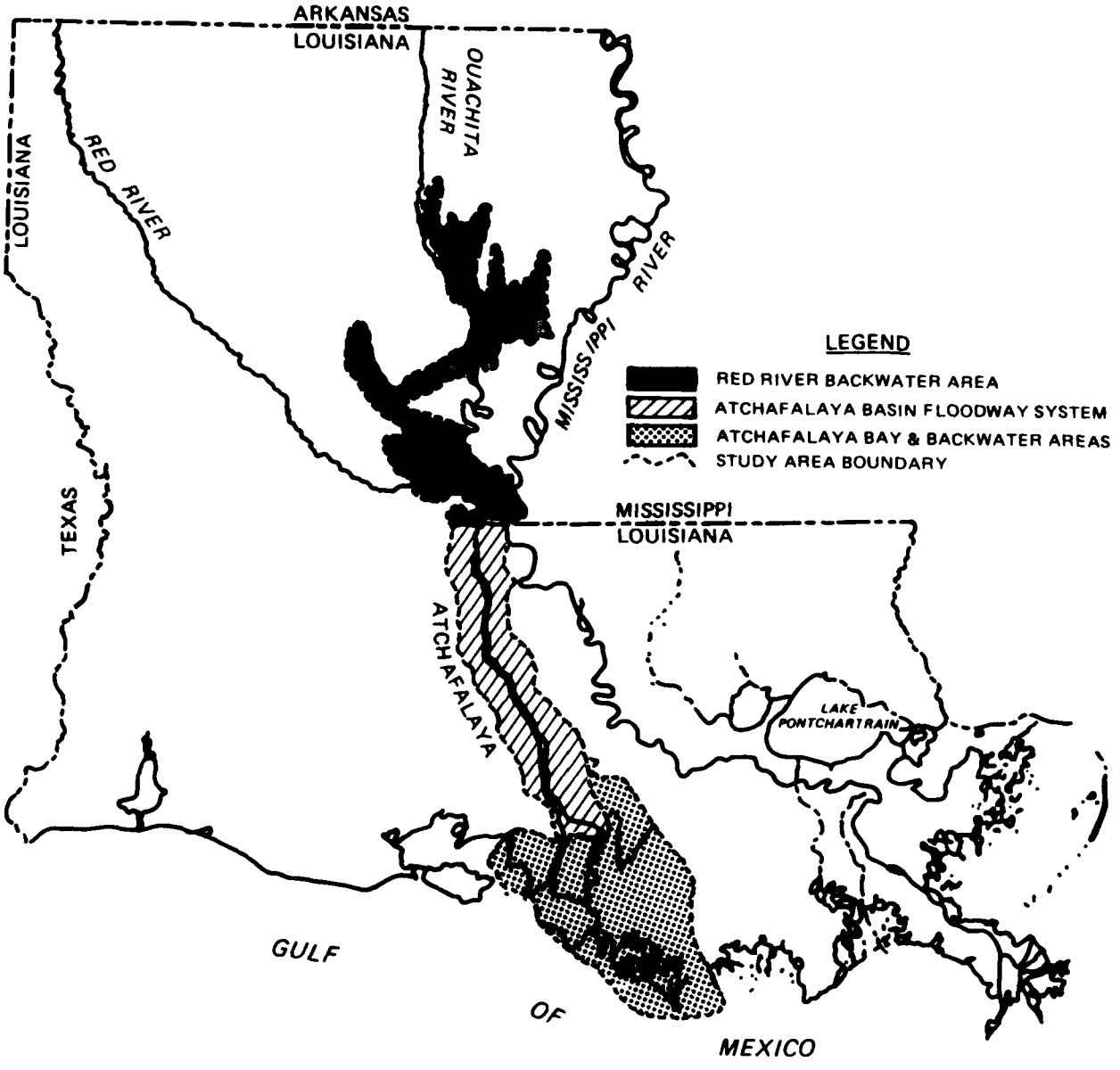

Figure 3. Study area boundary (from USAED, New Orleans)

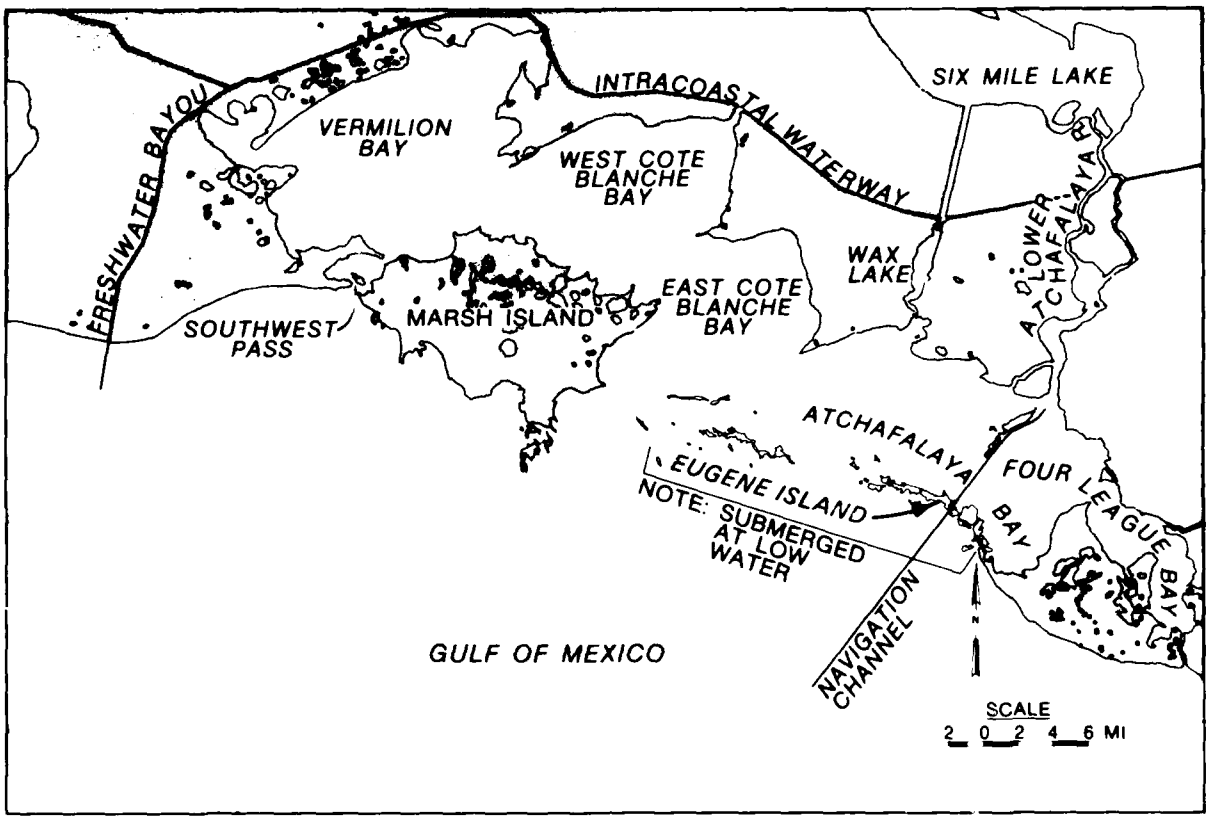

Figure 4. Atchafalaya Bay area

investigated herein is confined to the Atchafalaya Bay (Figure 4). Subsequent uses of the term "study area" in this report refer to the Atchafalaya Bay.

Purpose and Scope

4. This report documents one task in a multidisciplinary study of the development of the Atchafalaya Delta. The purpose of this task was to predict the area of new subaerial land, the volume of sediment deposition in the bay, and the resulting change in flood elevations for a period of 50 years into the future.

5. The plan of study, for which this task is one part, was developed at the request of the New Orleans District by McAnally and Heltzel (in preparation).

6. Because of the complex interactions of the many processes going on in this study area, four basically different approaches were planned for predicting delta growth:

a. A regression analysis of historical prototype data from which future growth patterns can be extrapolated.

b. A generic analysis from the geological perspective which includes historical growth patterns at this site plus comparisons with other deltas.

c. An analytical approach based on theoretical hydraulics and sediment transport mechanics.

d. Processes-based numerical models which treat delta growth as a boundary value problem:

(1) "Quasi-Two-Dimensional Sediment Computation" (HAD-1).

(2) "Sediment Transport in Unsteady, Two-Dimensional Flow, Horizontal Plane" (STUDH and its companion hydrodynamic model, RMA-2V).

(3) A special treatment of the saline density currents, deep-water waves, and hurricane surges.

This report documents the Quasi-Two-Dimensional Sediment Computation approach and compares results to those determined by the regression analysis (Letter 1982) and the generic analysis (Wells, Chinburg, and Coleman 1984).

7. Finally, the scope of this phase of the delta study is limited to forecasting rate of delta growth and the resulting impact on flood stages, maintenance dredging, and flow distribution for a do-nothing alternative. That is, if man's activities in the study area were to cease except for maintenance dredging for navigation, how much would the delta grow over the next 50 years? Later studies will address salinity and other alternatives for managing the land and water resources in the bay. The techniques being developed in the present study are designed to handle other alternatives, also. Because these techniques are intended for use by others, this report describes their development and presents the bases for decisions made during their application in more detail than normally is presented.

Related Studies

8. The related studies are grouped into two categories: those by others which give insight into the growth and behavior of the Atchafalaya Basin Floodway and companion studies to this one.

9. The New Orleans District (USAED, New Orleans) prepared a feasibility report. It is a comprehensive document presenting the historical development in the Atchafalaya Basin starting with records from de Soto's exploration

of the area in 1542. It addresses natural and man-made changes in terms of physical and environmental characteristics, cultural and natural resources, and past as well as proposed water and land uses. It cites 17 documents of the US Senate or House of Representatives bearing on the role of the Atchafalaya Basin in the MR&T Project. Thirty-five studies that others have made in the basin are listed in Appendix A and abstracted in Appendixes I and J of that document. Engineering, environmental, geologic, and economic investigations are presented for historical record as well as future forecasts. Alternatives for managing this important natural resources are assessed. Although that study focused on the floodway portion of the Atchafalaya Basin, it mentioned the bay as well as the delta which was expected to develop there. It included the predicted effect from that delta growth on water and sediment movement in the floodway and cited the more extensive and intensive studies of delta growth in the bay. The current study, in all its many parts, is that investigation cited.

10. Two reports by Keown, Dardeau, and Causey (1980) and Keown, Dardeau, and Kennedy (1977) give pertinent data and comments on sedimentation in the Mississippi River Basin. Of particular interest are the general comments on the reduction of sediment concentration in the lower Mississippi during the past 3 decades.

11. Information from Roberts, Adams, and Cunningham (1980) was used as a guide in establishing sediment yield, trap efficiency in the basin, and the distribution of sediment between the Lower Atchafalaya River and Wax Lake Outlet.

12. The following studies and reports are companion to this one in the present investigation:

a. "A Plan for Predicting the Evolution of Atchafalaya Bay, Louisiana" (McAnally and Heltzel in preparation) which recommended a three-phase approach for evaluating the evolution of the Atchafalaya Delta, including development of the plan of study, implementation of the plan of study, and monitoring the behavior of the prototype.

b. Field Data Program (Coleman et al. 1988) which documents the data collected especially for this problem and the methods used in its collection by WES.

c. "The Atchafalaya River Delta: Extrapolation of Delta Growth" (Letter 1982) predicts the delta will extend even beyond Eugene Island within the next 50 years, which agrees with predictions

by Garrett, Hawxhurst, and Miller.* In that work, the delta is defined as not only subaerial land but also the area where water depth is less than 3 ft.

d. Wells, Chinburg, and Coleman (1984) predicted that the delta will grow to fill the entire bay, a surface area of about 200 square miles, except for channels which will persist between the Atchafalaya and adjacent bays, within the next 50 years. Not all the land will be subaerial but depths in the bay will be generally less than 3 ft, the criteria adopted by Garrett, Hawxhurst, and Miller* and employed also by Letter. The work by Wells, Chinburg, and Coleman indicates a decline in delta size after this 50-year growth period based on their analyses of Mississippi River subdeltas. The work of others is so extensive that only selected references are included in this report.

13. In addition to these completed studies, Wang (1985) conducted an analytical analysis of delta development in which two-dimensional turbulent theory was used to forecast the hydrodynamic aspects of delta development; mass transport with a bed source term was used to convey sediment and interact with the bed.

Conceptual Model of the Growth of Atchafalaya Delta

14. With delta growth defined as the emergence of land from beneath the water surface at the mouth of a river, the conceptual model of delta growth rate adopted for this study is based on four processes: (a) sediment deposition by grain size, (b) subsidence of the area, (c) reentrainment of the deposited sediment, and (d) growth of vegetation on the newly formed subaerial lands. The most significant process is sediment deposition. Whether sediment deposits or not depends on flow velocity, flow depth, the concentration of sediment in the water column, particle setting velocity, water temperature, and water chemistry. Once sediment is deposited, reentrainment will occur if energy forces in the flow exceed the inertia/electrochemical bonds of the deposited particles. The same list of parameters is significant in the reentrainment process as itemized for deposition; however, the critical threshold values increase.

15. The second most significant process is apparent subsidence (or

---

* Committee on Tidal Hydraulics (CTH), Corps of Engineers, US Army. 1969. Committee on Tidal Hydraulics, Minutes of the 66th Meeting, July 15-16, 1969, New Orleans, LA.

apparent sea level rise) (Shlemon 1973 and Swanson and Thurlow 1973). In Shlemon (1973), the average, apparent sea level rise from 1940 to 1970 was estimated to be 1.3 cm/year (0.0425 ft/year). The term "apparent sea level rise" combines regional subsidence with sea level rise to produce the significant change of interest in this delta growth study.

16. Energy levels vary, from point to point in a flow field as well as from time to time at any given point, over a sufficiently large range to shift conditions back and forth among the processes of deposition-reentrainment-transportation. Consequently, the third most important process in growth of the Atchafalaya Delta is reentrainment of deposited sediment. Included in this variation of energy are freshwater discharge, tidal energy, regional setup or setdown of the Gulf due to winds, the dissipation of wave energy inside the bay, and density currents.

17. The fourth significant process is growth of vegetation on the delta. Willow growth will reduce hydraulic efficiency significantly in only one season, and newly formed subaerial delta space will then merely store water rather than contribute to conveyance.

18. There are two aspects of delta growth not considered to be processes but which strongly influence the analytical approach selected for this analysis: (a) sediment discharge at the coastline, and (b) the long time required for a delta to develop. The supply of sediment at the coastline determines growth rate. Because the time of development spans decades rather than single storm events or annual periods, sediment supply is not completely independent of delta growth. That is, delta growth creates backwater up the river which, in turn, increases sediment deposition upstream from the coastline. On the other hand, it is possible to locate the boundary of the study area sufficiently far inland to be out of that backwater influence during the forecast period, which is the approach taken in this study.

19. The significance of slow growth (i.e., developing over decades) is that it burdens any computation technique in a process-based, numerical-integration model. The scheme adopted for this study is based on the Exner equations of bed surface change rather than the convection-diffusion equation. That allows relatively long computation time-steps because bed elevation changes proceed at 10^{-3} to 10^{-5} times the rate of the flow velocity. The time rate of change of concentration, velocity, and depth during a single flood event is much less significant in delta building than is the spatial variation

of energy and sediment concentration as long as depths and velocities are approximately correct.

20. Finally, these processes are deterministic within the study area. The randomness associated with delta growth rates and patterns is due to boundary conditions which, for lack of anything better, engineers consider to be random events. Boundary conditions in the Atchafalaya Delta are freshwater inflows, sediment inflows, properties of the sediment load, Gulf elevations, the wind field, wave energy, and tide.

Background Information for This Task

Selection of model limits

21. This study addresses delta growth in the Atchafalaya River miles 137 to 145. The approach uses two numerical models: one which routes flood hydrographs by a numerical solution of the St. Venant equations, thereby predicting flow distribution and flood peak attenuation, and the other which calculates the movement of the water-sediment mixture along with the resulting deposition and scour of the bed. Both of these are process-based simulation models and therefore require geometry of the model area, the initial water discharge in the model, a continuous record of the inflowing water discharge to the model, and a continuous record of stage at the downstream boundary of the model. In addition, the sediment gradation in the model bed and the concentration of sediment by particle size in the inflowing water discharge must be supplied. Model limits should coincide with gage locations.

22. The long-term gaging stations closest to the study area are Simmesport, Louisiana, at Atchafalaya River mile 4.9, which is about 131 river miles upstream from the bay, and Eugene Island, projected Atchafalaya River mile 145.0±, which is the downstream or oceanward limit of the bay. These are shown in Figure 5.

23. The Simmesport gage is separated from the bay by the Atchafalaya Basin, which extends from Simmesport to the latitude of Morgan City/Calumet--a distance of 110 river miles. At that point, flows leave the basin through two outlets. The Lower Atchafalaya River is the primary outlet. It passes the Morgan City gage, river mile 117.7, and the Gulf Intracoastal Waterway, river mile 121, and then flows for 16 river miles through a marsh zone to the coastline where it enters the bay. The other outlet, Wax Lake, passes the Calumet

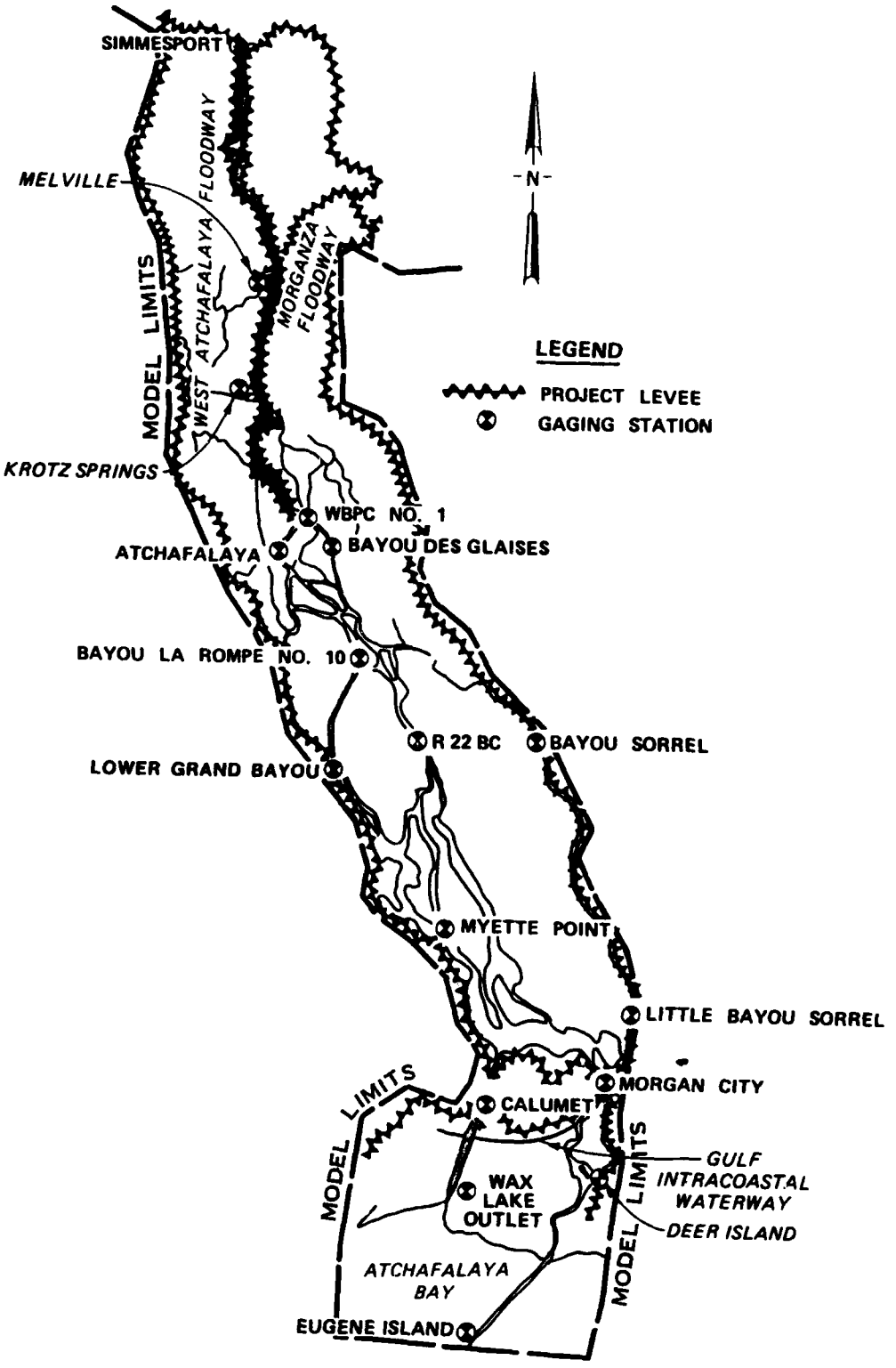

Figure 5. Gaging stations

gage and the Gulf Intracoastal Waterway, and flows for 9 miles through the marsh zone to the bay. The flow distance from the basin to the bay is 23 miles via the Wax Lake Outlet, whereas it is 35 miles by way of the Lower Atchafalaya River.

24. Table 1, obtained from New Orleans District, illustrates the variability in both water and sediment yields at Simmesport. The sediment yields and the trap efficiencies are shown in Table 2 for two periods of time: 1967-1971 and 1973-1975. This variability makes it necessary to extend the model boundaries as far inland as possible to pick up these boundary values. The numerical models must then include the dominant processes in the basin and marsh to provide the proper amount of water and sediment discharge passing the coastline into the bay. The riverflow model met these requirements even when extended to the latitude of Simmesport because its network feature allowed the basin to be partitioned into several subbasins; therefore, Simmesport was selected as the upstream boundary for the computation grid. The sediment movement model is a strip model, not a network model. That is, the width can be partitioned into strips in the direction of flow, but the entire width of the floodway is modeled in a single cross section. Moreover, it is a one-dimensional model, requiring the water surface to be horizontal across the entire cross section. That requirement makes modeling the expanding flow near the Whiskey Bay Pilot Channel (WBPC) No. 1 gage (Figure 5) very difficult. Since water in the prototype is conveyed toward both levees via access and freshwater diversion channels in the vicinity of the Bayou La Rompe No. 10 gage, the upstream boundary of the HAD-1 grid was located near R 22 BC gage, a few miles downstream from the east and west channels. Simmesport sediment and water data were then translated to that point, without change, for the HAD-1 model (Figure 6).

25. Except during 1973, all water entered the basin via the main Atchafalaya River channel at Simmesport. However, there are actually three potential inflow points: the Main Atchafalaya Floodway, the Morganza Floodway, and a fuseplug levee leading to the West Atchafalaya Floodway. Morganza was operated for a few months during the 1973 flood, but the West Atchafalaya Floodway has never been used. Therefore, Morganza is included in the Simulated Open Channel Hydraulics in Multiple Junction Systems (SOCHMJ) model, but flows from the West Atchafalaya Floodway, required only for the project design flood, were treated as local inflows near the Bayou La Rompe No. 10 gage. The total

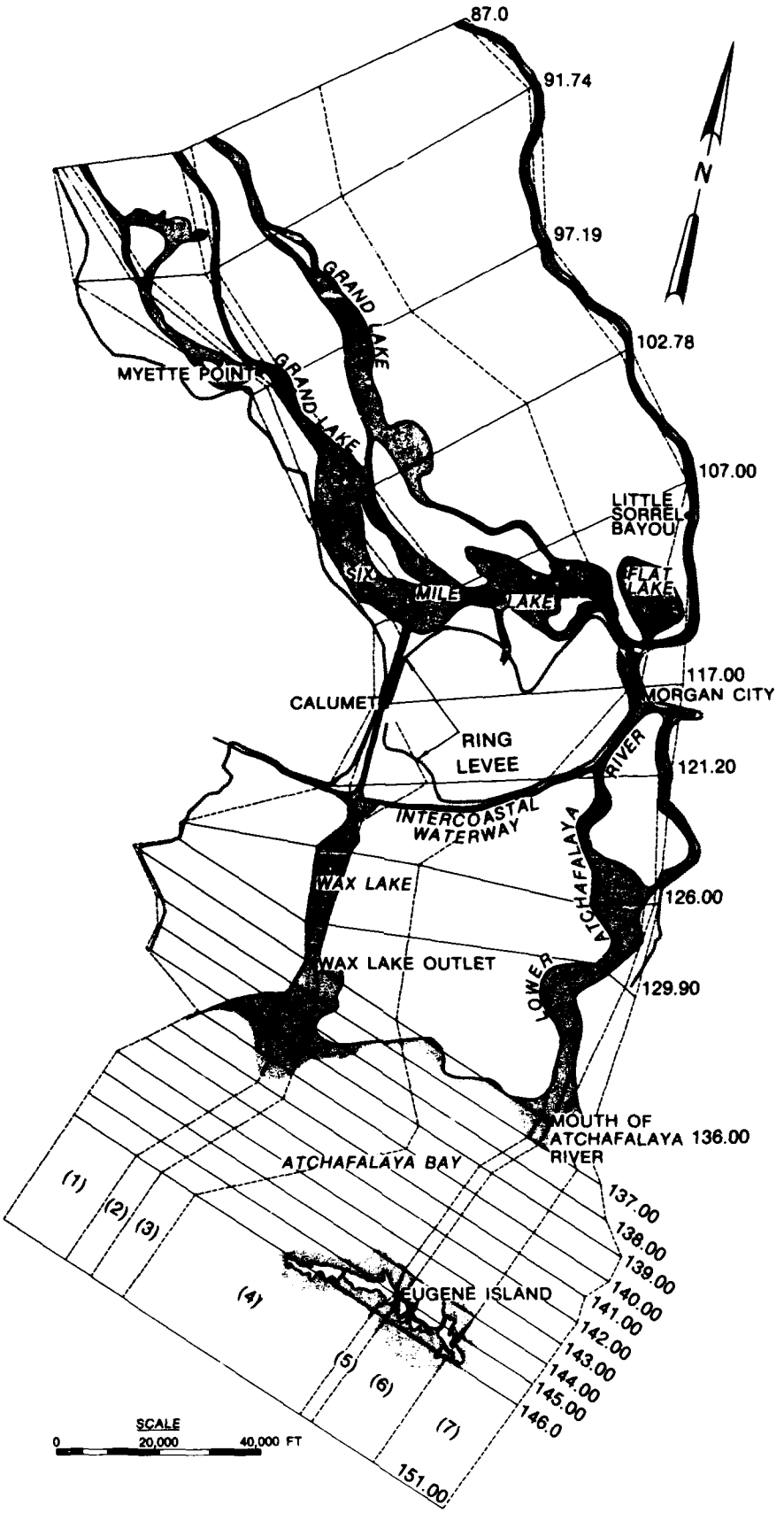

Figure 6. HAD-1 grid

flow was also used in the HAD-1 model, but sediment concentration was limited to that passing the Simmesport gage plus silts and clays from Morganza. In the absence of other field data, Simmesport concentrations were used for all inflowing sediment discharges.

26. Once in the bay, flow passes generally toward the west--subject to wind and tidal currents. The resulting depositional pattern is shown in Figure 7. Because substantial bed changes are evident even beyond Eugene Island, the ocean boundary of the model grid was shifted 5 miles beyond Eugene Island. Data from the Eugene Island gage were shifted to the boundary without water level change.

27. For constructing boundary conditions, the lateral limits of the model grid were developed along surveyed data limits. That is, flow in the prototype is free to expand to the west once it passes Point Chevreuil, but that area was not surveyed and consequently was omitted from this model grid.

28. The model limits shown in Figure 5 coincide with the Atchafalaya portion of the Mississippi Basin Model (MBM) at Clinton, Mississippi, except in the bay portion where the MBM was enlarged for this study.

Sedimentation within the model limits

29. The bay is not the only active area within the model limits. Both recent history (the last 50 years) and recent geologic history demonstrate significant changes in the basin. According to recent geologic history, Calumet, Morgan City, and the marsh zone, as described in model development, are on an alluvial ridge from an earlier Mississippi River delta. This alluvium, the Teche Ridge, is a well compacted clay, more compacted than modern deltaic material, so subsidence is significantly less than it is at other locations around the bay.

30. According to recent history, the 50 years just prior to 1972 showed the type of sediment reaching the bay to be primarily silt and clay. The sand deposited in the basin along with a significant portion of the silt/clay load passing Simmesport. These values, illustrated in Figure 7, were taken from Roberts, Adams, and Cunningham (1980). Deposition has not been uniformly distributed over the basin. Rather, it has been concentrated in the area of Grand and Six Mile lakes to the extent that those lakes are essentially filled. The ridge on either side of the main channel is partially natural and partially the result of dredging activity to provide authorized flood protection to the area. Figure 8, a cross-basin sediment range, illustrates the

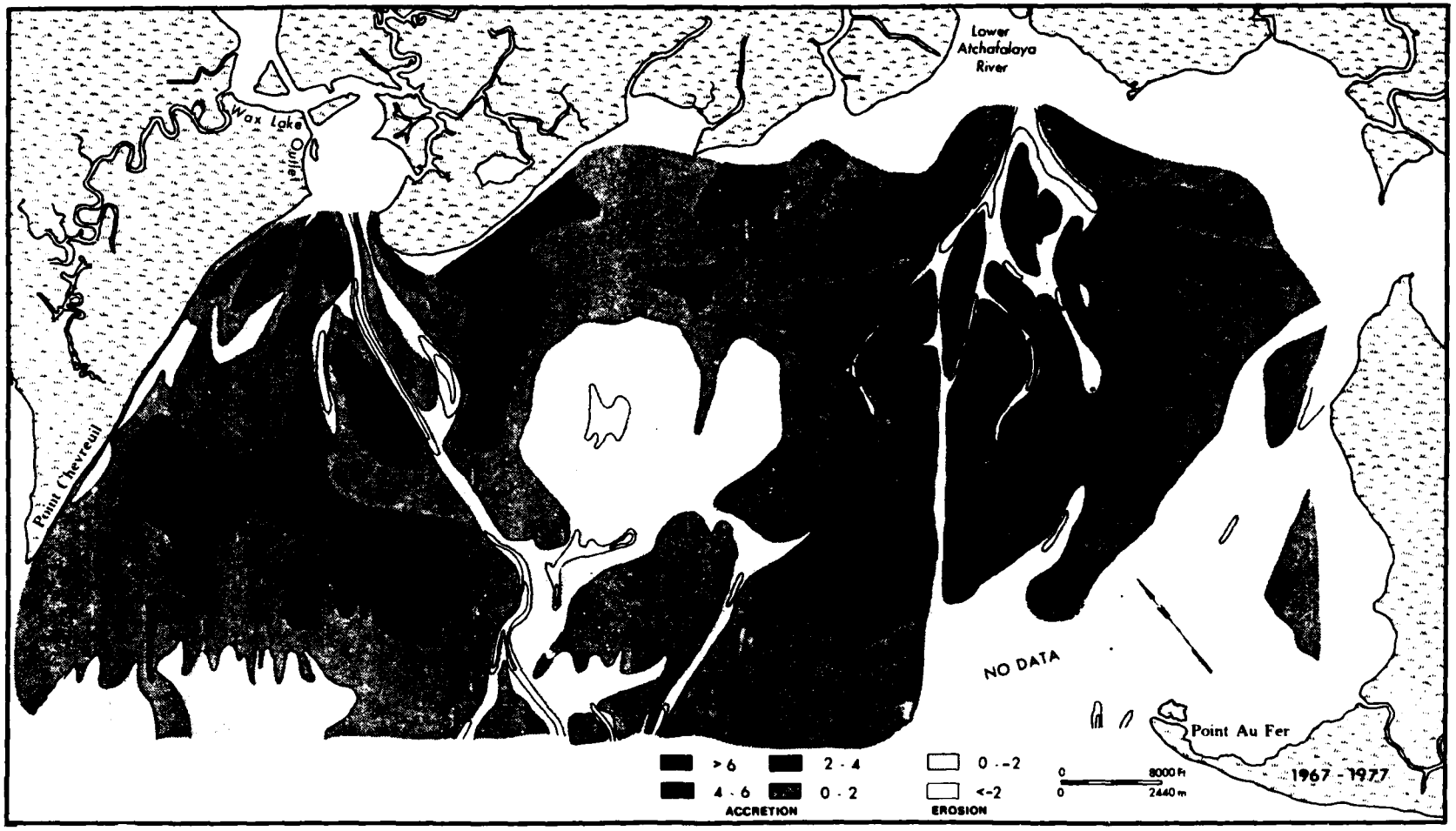

Figure 7. Isopach map of Atchafalaya Bay, 1967-1977 (depths in feet)
(from Adams and Baumann 1980, courtesy of Dr. Robert H. Baumann)

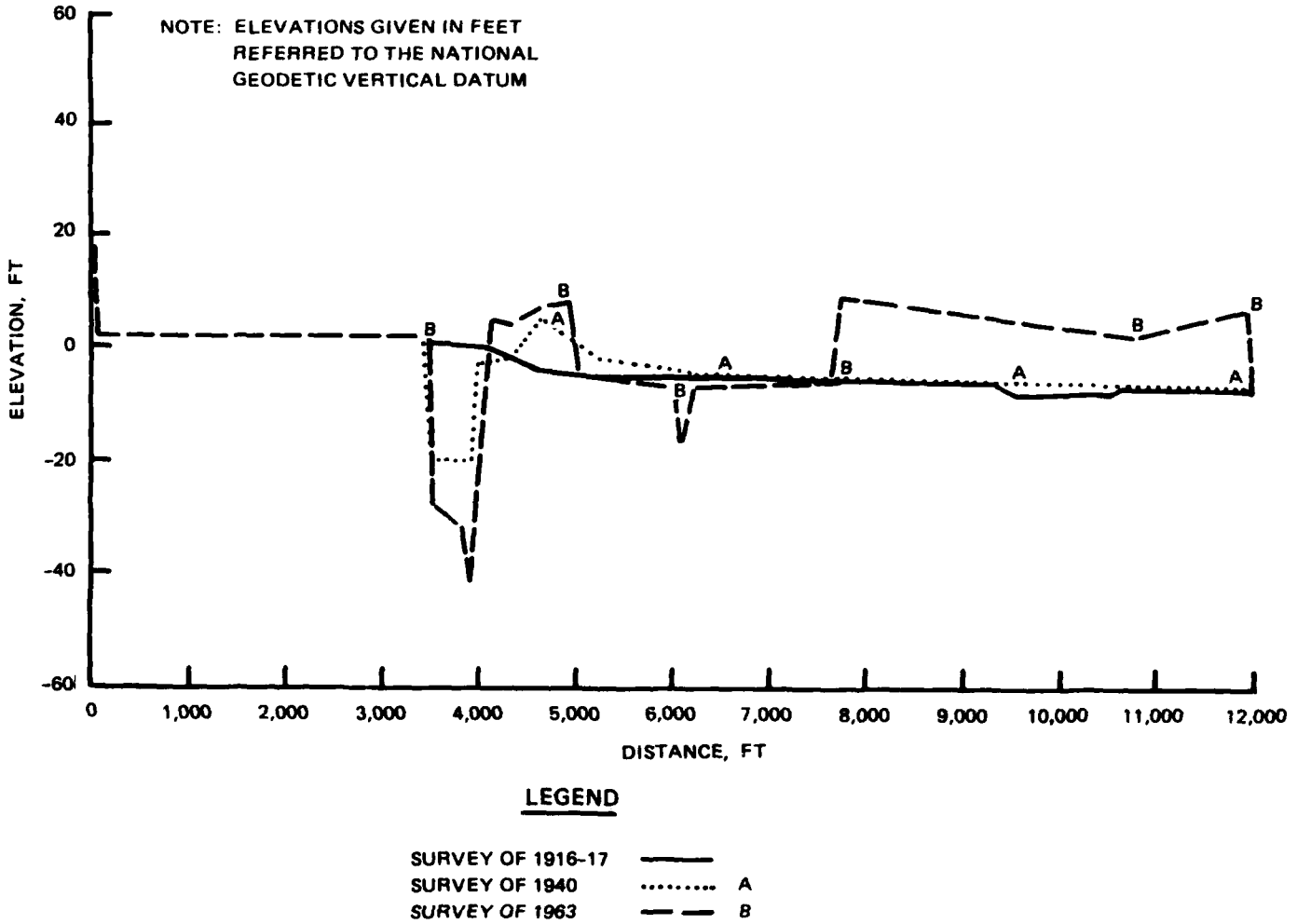

Figure 8. Floodway deposition based on sedimentation range

magnitude of basin changes during that period. That information was an aid in the adjustment of HAD-1.

31. The significance of these observations to delta growth forecasts is as follows:

a. Sediment yield at latitudes of the marsh and of the coastline has changed substantially in both magnitude and particle size during the past 50 years and is expected to continue to do so during the next 50;

b. The shape of cross sections inside the floodway must be used with caution when confirming the shape of deposits in the bay because dredged material was disposed on top of the natural levees prior to 1968;

c. The shape of cross sections in the marsh, even if available, should not be used to predict a shape of future bay cross sections because the marsh zone is left over from a much earlier delta.

Data sources within the model limits

32. Bay geometry, marsh geometry, basin geometry, hydrologic data, sediment data, land use data, and water use data provide the required information for both the sediment movement model (HAD-1) and the flood routing model (SOCHMJ).

33. Bay geometry. Atchafalaya Bay is that portion of the HAD-1 grid (Figure 6) between river miles 136.0 and 145.0. The surface area is 128,000 acres (200 square miles). Four recent surveys are available as documented by Letter (1982). They are, by year surveyed, the 1961, 1967, 1972, and 1977 surveys made by the New Orleans District. Areas covered generally follow the open water boundary identified in Figure 5 as "Model Limits" except that the 1961 survey covered only the eastern half of the bay. The 1977 survey is considered the best data set because a correction was applied by Louisiana State University to account for changes in tidal elevations during each passage of the hydrographic survey boat.

34. Marsh geometry. The marsh zone in the HAD-1 grid is between sections 121.2 and 136.0. The surface area of the marsh zone is estimated to be 9,000 acres (14 square miles). Hydrographic surveys are available for the Lower Atchafalaya River and Wax Lake Outlets for 1962-1964 and again for 1974-1976 (USAED, New Orleans, 1967 and 1977a, respectively). The lateral extent of coverage is shown in Figure 9. Areas outside of the hydrographic survey maps have no surveyed information. Environmental land use maps published in USAED, New Orleans, show this zone to be largely freshwater marsh.

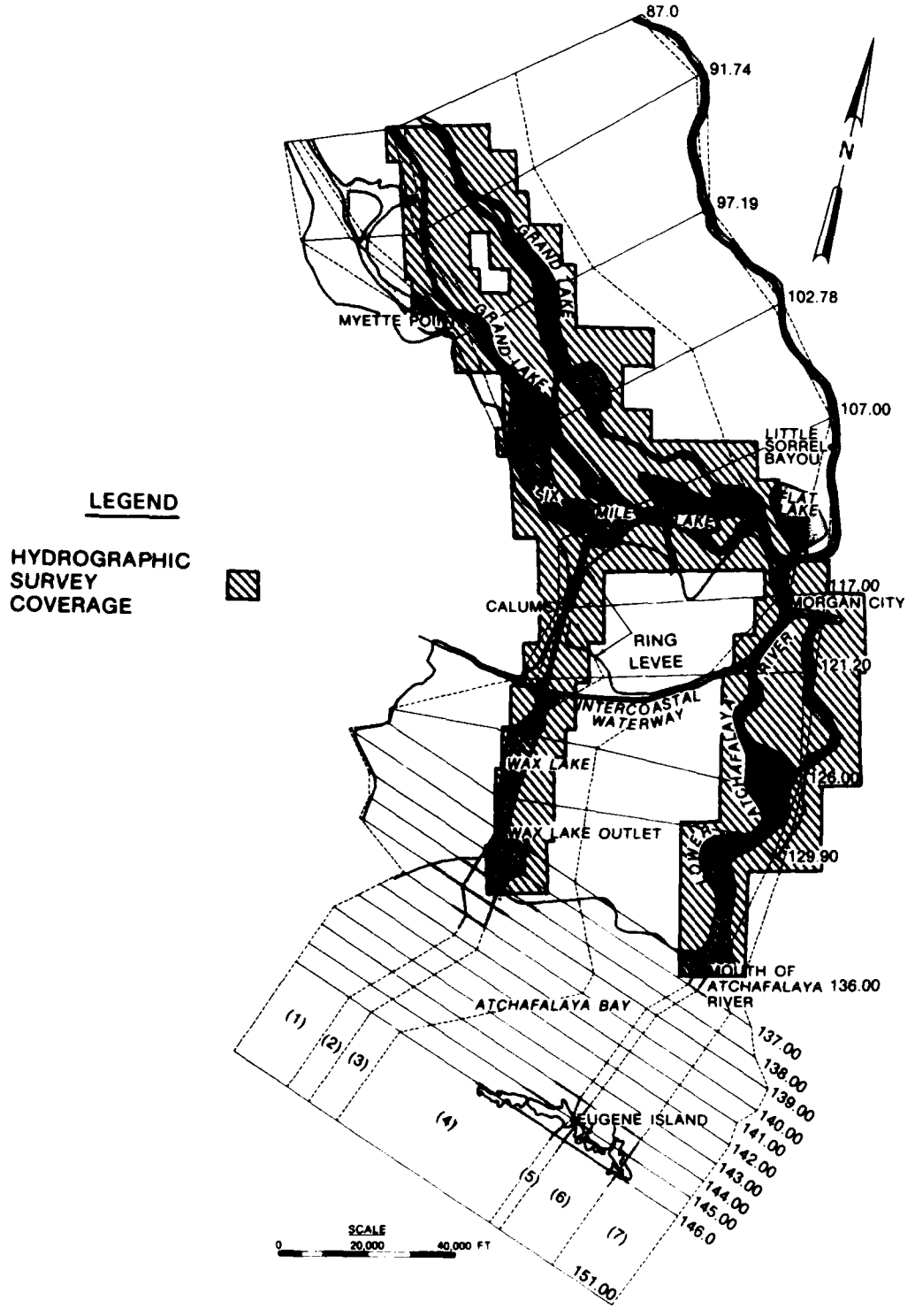

Figure 9. Hydrographic survey coverage

Numerical models of geometry, furnished by New Orleans District from other studies, were used along with this information to establish that marsh surface elevation for the present study.

35. Atchafalaya Basin Floodway geometry. The Atchafalaya Basin Floodway lies upstream from river mile 107.0 in the HAD-1 grid (Figure 6). Figure 9 shows coverage of the lower portion of the floodway by the hydrographic survey of 1962-1964 (USAED, New Orleans, 1967a). This area was resurveyed in 1974-1976 (USAED, New Orleans, 1977a). Unlike the marsh, however, cross-basin sediment ranges have been surveyed on 5-mile intervals in the floodway since 1916. These provide an excellent time-history of changes between Krotz Springs and the basin outlets.

36. Hydrographic survey coverage of the main channel of the Atchafalaya River extends to the Old River Structure (USAED, New Orleans, 1967 and 1977a). However, the upper half of Atchafalaya Floodway is partitioned into three separate floodways: (a) the Atchafalaya River, (b) the Morganza Floodway, and (c) the West Atchafalaya Floodway. The West Atchafalaya Floodway was not modeled, and Morganza Floodway geometry is available only on US Geological Survey (USGS) quadrangle maps.

37. Hydrologic data. Figure 5 shows the 11 prototype gages used in the study. These were selected from about 40 gages in the basin, because they contained the most data for the 1967-1977 verification period. A summary of data by year, prepared from USAED, New Orleans (1977b), is shown in Tables 3 and 4.

38. MBM data. The MBM has been used extensively in studies of flood wave movement through the Atchafalaya Basin as well as in the Mississippi River. In addition, steady-state discharges have been run through the model and the resulting elevations and flow distributions recorded.* Whereas prototype data often have gaps, the MBM data are synoptic, and consequently are valuable for both the SOCHMJ and HAD-1 water-surface profile adjustment.

39. Sediment data. Suspended sediment samples are available at Simmesport from 1951 to the present. Morgan City and Calumet gages have periodic suspended sediment data since the 1973 flood. In addition to these data, bed surface samples, collected by the New Orleans District during 1975-1976, are

---

* Personal Communication, 29 May 1979, WESHR, from H. B. Simmons, WES, to District Engineer, USAED, New Orleans, New Orleans, La., subject: "Transmittal of Test Results for Hypothetical Flood 58AEN (Modified) in the Atchafalaya Basin Portion of the Mississippi Basin Model."

available at about 10-mile intervals along the Atchafalaya River, and bottom sediment samples were collected at about 300 locations in the bay for this study. A separate data report presents all data collected for this study (Coleman et al. 1988).

40. Land and water use data. The need for such data comes from the need to identify homogeneous regions for assigning hydraulic roughness values. In this study, attention focused on land and water inside the model boundary, and USAED, New Orleans, is the primary reference.

Computer Codes Selected

41. No single computer code embodies all the processes required to predict flood stages, navigation maintenance dredging, and flow distribution into the bay. Consequently, two primary codes were selected: (a) HAD-1 for sedimentation related to delta growth and dredging, and (b) SOCHMJ for flow distribution and flood stages.

42. These programs are described in more detail in Thomas* and Johnson and Senter (1973), respectively. In summary, the HAD-1 code is a modification to HEC-6 to permit multiple strips across the bay and basin for sediment movement calculations. It is essentially one-dimensional in energy loss calculations but two-dimensional in sediment movement and bed deposition or erosion.

43. The SOCHMJ code is a numerical solution for the St. Venant equations of unsteady flow. It has the capability for calculating flow around islands automatically by balancing discharges and energy losses.

44. Several utility programs were developed to support these primary codes.

45. The application of those computer codes is summarized in the following paragraph and described in detail in the following parts of this report.

Study Procedure

46. Starting with 1961 geometry, delta growth was simulated and a 1977

---

* W. A. Thomas. 1982. "Quasi Two-Dimensional Sediment Computations (HAD-1)" (unpublished), US Army Engineer Waterways Experiment Station, Vicksburg, Miss.

geometry calculated with HAD-1. That HAD-1 model was adjusted until calculated deposition and erosion in the bay matched values observed in the prototype. A 50-year forecast was then made, 1980 through 2030, and the predicted deposition added to 1980 geometry. Meanwhile the SOCHMJ code was adjusted to 1975 geometry by reconstituting MBM steady-flow water-surface profiles and the 1973 and 1975 historical floods in the prototype. The 50-year delta growth geometry was taken from HAD-1 and converted for SOCHMJ. Future flood stages and flow distributions were calculated with SOCHMJ.

PART II: THE SEDIMENT STUDY WITH HAD-1

Introduction

47. HAD-1 is a simulation model which treats sedimentation as a boundary value problem. "Simulation" in this case means reconstituting physical processes with equations which are continuous in time. "Boundary value problem" in this case means that water discharge, water temperature, and sediment concentrations are prescribed at the upstream boundary of the numerical model grid, and Gulf elevations are prescribed at the downstream boundary of the model grid. The equations are formed to calculate the rate of movement of those boundary values throughout the interior space of the model grid, the resulting interaction between sediment in the water and sediment in the bed, and the resulting water-surface and bed surface profiles.

48. This sedimentation study was conducted in two phases: model adjustment followed by delta growth prediction. Both phases used the same computation grid, but the adjustment phase required boundary values which were observed during the adjustment period whereas the growth prediction phase required boundary values anticipated during the forecast period, 1980 through 2030. This section describes the development of the data and the interpretation of results for both phases of the sedimentation study. The SOCHMJ model application for future water-surface elevations and flow distributions is described in Part III, "Stages and Flow Distribution Study with SOCHMJ."

Model Adjustment Procedure and Coefficients

49. Because HAD-1 is a simulation model, verification of the movable-bed computation requires at least two hydrographic surveys of the prototype separated by enough time to allow a wide range of boundary values to occur in the prototype. The starting survey is referred to as the initial condition of the model, and the model development begins by encoding the cross sections of the initial condition survey. Beginning at the time of that survey, a continuous, time-dependent record of each boundary variable is coded up to the time of the second survey. The simulation proceeds as the computer program solves the flow-sediment equations for the boundary value at each time-step between the dates of the two hydrographic surveys. The simulation ends when

the program reaches the final boundary value set.

50. Model performance is evaluated by comparing the calculated results to measured prototype data. For example, the calculated bed elevations at the end of the simulation should match the data from the second survey. Calculated stage, discharge, and sediment loads at interior points of the model should match prototype values at those locations on the same date and time. The steps in the adjustment process are summarized as follows in the order of work and are discussed in the following paragraphs.

a. Select the time period for adjustment and code the starting geometry.

b. Develop hydraulic boundary conditions (water inflow and Gulf stages) for the adjustment period.

c. Develop sediment boundary conditions for verification period.

d. Adjust for apparent subsidence.

e. Reconstitute observed water-surface elevations at gages within the study area.

f. Reconstitute measured stage-discharge values at the Morgan City and Calumet gages.

g. Reconstitute flow distribution across the floodway.

h. Develop gradation curve for bed sediment.

i. Develop unit weights for bed deposits.

j. Select the transport function.

k. Reconstitute sediment trap efficiency in the basin.

l. Reconstitute measured sediment discharge rates at Morgan City and Calumet.

m. Reconstitute average depth of sediment deposition in the bay.

n. Reconstitute depth of sediment deposition or erosion in each cell in the bay.

Model Coefficients

51. There are 14 coefficients to adjust during the adjustment process, as summarized in Table 5. The first coefficient, the set of Manning's n values, applies to hydraulic calculations. The next eight apply to the deposition and erosion of clays and silts. The last five apply to the bed deposit. HAD-1 treats the erosion and deposition of silts and clays as proposed by Ariathurai and Arulanandan (1978). Procedures for unit weight of a mixture and for consolidation of silts and clays are from Vanoni (1975). These 14 coefficients can neither be independent from each other nor can the

values be arbitrary. An n value may be changed in each strip and at each cross section whereas only one value for each sediment erosion and deposition coefficient can be prescribed for the entire model. Values are prescribed at the beginning and are not changed during the entire simulation, including the prediction period, unless physical circumstances dictate a change. The only coefficient to change during this forecast period was the n value, and that change was required to simulate the growth of vegetation on newly formed islands.

Selection of time period

52. The 1967 and 1977 hydrographic surveys were selected for the adjustment period for the following reasons. No model coefficients were involved with the selection of the time period.

a. Hydrographic surveys were made in the bay in 1961, 1967, 1972, and 1977, but surveys in the basin and outlets were available only for 1962-1964 and 1974-1976. The magnitude of the 1973 flood dominated energy in the system, thereby making it desirable to include that event in the adjustment period.

b. The initiation of sand movement past Morgan City, as well as sand deposition in the bay, occurred during the 1973 flood.

c. The prototype measurement program for water and sediment data was intensified during and following the 1973 flood.

d. The Corps of Engineers ceased major dredging activities in the basin in 1968.

53. The first approach considered for the adjustment time period used a split record test during which model performance was to be adjusted between 1961 and 1967 and was to be confirmed by comparison to the remaining surveys. Two problems were encountered: (a) the 1961 hydrograph survey covered only the east half of the bay, and (b) man's activities in the basin made it impossible to interpret model performance because conditions upstream from Morgan City were difficult to establish. Therefore, the split record approach was abandoned in favor of a "warm-up" period from 1961 to 1967 followed by model adjustment between 1967 and 1977. The 6 years from 1961 to 1967 were adopted as a warm-up period to allow the model to smooth out bed irregularities that occurred when 1961 and 1967 surveys were combined to obtain coverage for the initial bed geometry.

Coding the starting geometry

54. The selection of boundaries for the numerical model grid was presented in the section, "Background Information for This Task," but the

details for developing the HAD-1 grid are as follows.

55. Geometry is described by cross sections and reach lengths. The cross sections, identified by river mile, are located at 1-mile intervals across the bay and at approximately 5-mile intervals through the marsh and basin (Figure 6). Each cross section is partitioned into seven parts, called subsections, and the subsection boundaries are connected to form strips. Cross sections are plotted in Plates 1-21 facing upstream with strip boundaries across the top.

56. Cross-section alignment is a critical issue. The HAD-1 code will calculate a velocity in each strip, but the water-surface elevation is forced to remain horizontal across the entire cross section. Consequently, cross sections are skewed to correct for the fact that observed lateral water-surface elevations in the prototype are not horizontal laterally. That is, prototype and MBM water surfaces are generally higher on the west side than the east side of the basin within the limits of the HAD-1 grid. Therefore, the eastern ends of HAD-1 cross sections were shifted upstream in that part of the model. (Note: The SOCHMJ model demonstrated that the water-surface slope through Six Mile Lake controlled the water-surface elevations along the west levee of the floodway whereas the geometry of the eastern access and fresh-water diversion channels throttled the flow to the east side resulting in lower stages along the east levee.) Downstream from the basin, the orientation of cross sections was estimated in an attempt to create an alignment which would be normal to the anticipated flow direction.

57. The 1961 hydrographic survey was selected for initial geometry in the bay, but it covered only a portion of the eastern half. The 1961 bed elevations for the rest of the bay grid were determined from the 1967 survey. That is, the 1961 survey was subtracted from the 1967 survey where they overlapped, and the results showed that a foot should be subtracted from the bed elevations. The resulting bay bathymetry was adopted for initial conditions.

58. The 1962-1964 hydrographic survey was used to extend the HAD-1 model from the bay to its upstream boundary, river mile 87 in Figure 6. Some areas inside the floodway were not covered by that survey as shown in Figure 9. The initial geometry in those areas was developed from the cross-basin sediment ranges. In the 14-square-mile marsh zone downstream from the Intracoastal Waterway, no field surveys were available outside the area of the

hydrographic survey limits shown in Figure 9. That zone was treated as freshwater marsh at el +2.0* based on information presented in the land and water use appendix of USAED, New Orleans, and spot elevations along the edges of the hydrographic survey maps.

Steps in Fixed Bed Adjustment

Hydraulic boundary conditions during calibration period (water inflow and Gulf stages)

59. In employing the joint probability approach to boundary conditions, the following two points were considered: (a) the problem of relating the magnitude of deposition or scour in the bay to the probability of hydrologic events and (b) the problem of demonstrating that the elevation of the Gulf of Mexico at the Eugene Island gage is independent of the water discharges at Simmesport. Regarding deposition and scour in the bay, hydraulic and sediment conditions near a point of interest will affect bed change at that point immediately, whereas it may take years for a change in the sediment discharge at Simmesport, the inflow boundary location, to reach the bay. In this delta growth forecast, however, the period of interest is measured in decades and the primary influence on delta growth is expected to be the amount and grain size of sediment passing Simmesport. The primary mechanisms influencing the transport of this sediment from Simmesport to the Atchafalaya Bay are water discharges at Simmesport and Gulf elevations at Eugene Island. These mechanisms are hydrologic events which can be addressed statistically. Since sediment discharge measurements are not as abundant as water discharge or stage measurements, a correlation approach was used to fill in the missing values. In this case the correlation was made between sediment discharge and water discharge. Simmesport flow records provide the statistical basis for the long-term water discharges, and Eugene Island gage records provide the statistical basis for the Gulf elevations. Jointly these records depict the hydrologic events necessary for the long-term forecast of delta growth.

60. The second point involves the possible dependency of stage at Eugene Island on flow at Simmesport. That question was addressed by calculating the rate of energy dissipation in the vicinity of Eugene Island for a range

---

* All elevations (el) and stages cited herein are in feet referred to the National Geodetic Vertical Datum (NGVD) except where noted.

of water discharges. Even at 1 million cubic feet per second, approximately the peak of the 1973 flood, the calculated increase in stage at Eugene Island was less than half a foot whereas the observed stage range is ±3.5 ft. That impact approaches zero rapidly as water discharge decreases. Consequently, the Eugene Island stage was considered to be independent of the Simmesport water discharge.

61. The joint probability for the HAD-1 model was constructed from individual probability functions of Simmesport flows and Eugene Island stages. In this case, however, it is not only the peak annual flood discharge or peak annual stage that is of interest but also the daily events. In terms of water discharges, the mean daily flows during the warm-up period were grouped into class intervals, and a probability density function was constructed showing the probability that any mean daily flow would be equaled or exceeded. Figure 10 shows that density function, called a flow duration curve, and Table 6 shows the probability for each class interval. As a check, the annual water yield from the flow duration curve is 71,912,000 cfs-days (2.1 million cubic metres per year) compared to 84,512,000 cfs-days (2.4 million cubic metres per year) from records. That is satisfactory agreement for HAD-1 water yield since the model actually performs steady-state calculations.

62. Eugene Island stages were analyzed in a similar manner by ranking the 8:00 a.m. readings into the stage duration curve shown in Figure 11. When the ranking was made, datum changes were discovered as shown in Table 7. The bias caused by aliasing tidal constituents in the 8:00 a.m. readings was also evaluated. Since mean tidal amplitude is only 0.8 ft and the record is 17 years long, the record was used without change. Table 8 shows the joint probability of occurrence for each discharge class $P(Q)$ with each of the 1-ft class intervals of the Eugene Island stage $P(H)$. Extreme stages occurred higher and lower than the +2 to -2 ft range, but the duration was only 3 percent of the time. Consequently, these extremes were omitted from Figure 11 and the time for +2 to -2 ft rounded off to 100 percent. The joint probability coefficients, shown in columns 4 through 7 of Table 8, were calculated with the following equation (Benjamin and Cornell 1970)

$$P_{Q,H}(q,h) = P(Q_1 \leq q \leq Q_2)\ (H_1 \leq h \leq H_2) \qquad (1)$$

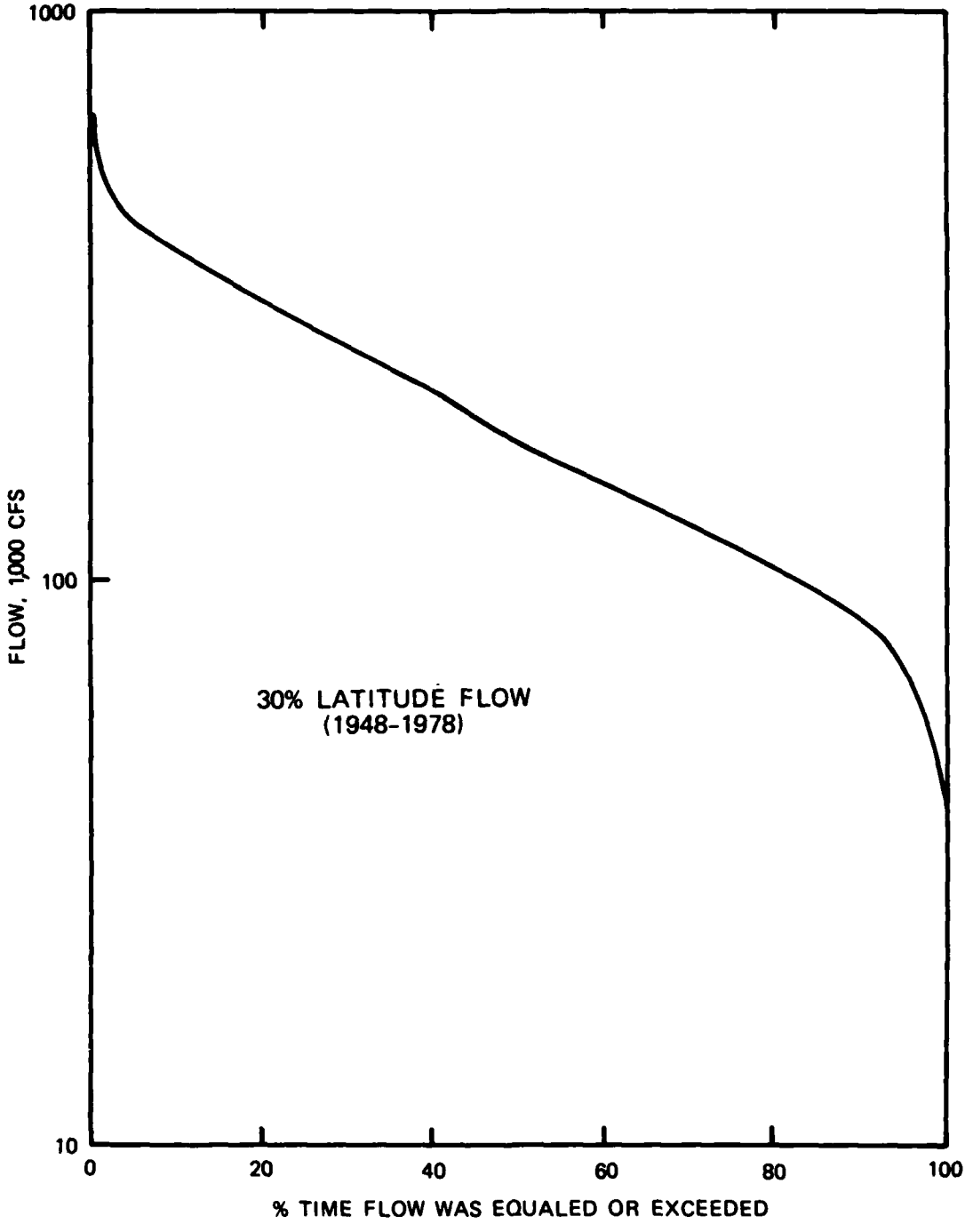

Figure 10. Flow duration curve, Atchafalaya River at Simmesport gage

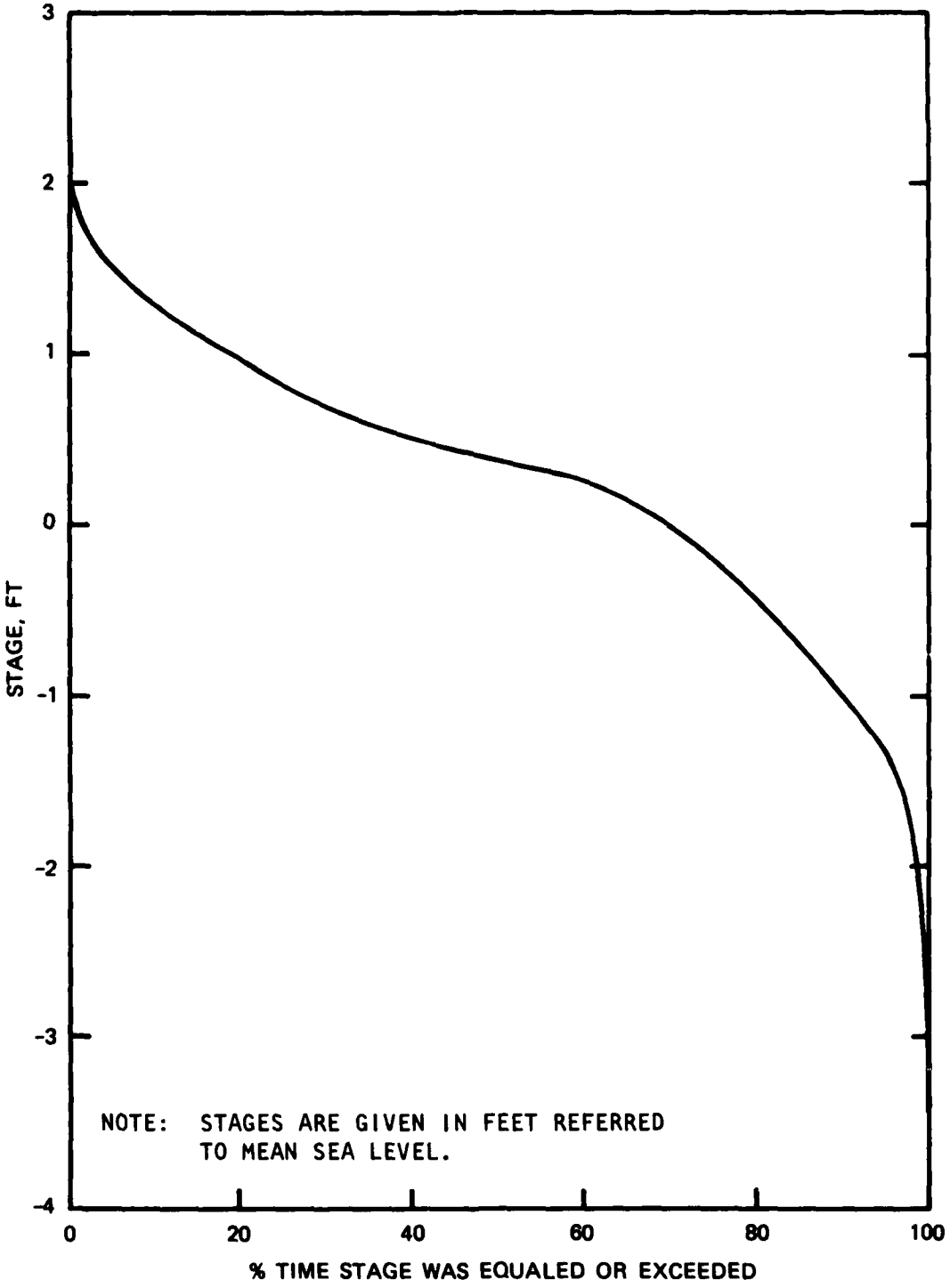

Figure 11. Stage duration curve, Atchafalaya River at Eugene Island gage, for the period 1962-1978

where

$P_{Q,H}(q,h)$ = joint probability

$P(Q_1 \leq q \leq Q_2)$ = probability that q lies between Q_1 and Q_2

$P(H_1 \leq h \leq H_2)$ = probability that h lies between H_1 and H_2

Q = water discharge class intervals

H = Eugene Island stage class intervals

Σ = summation over all possible Q and H

63. The expected value of rate of bed change, expressed as feet per day of deposition or erosion, is the product of the rate of bed change times its probability where probability is the joint probability from Table 8. The equation is:

$$\Delta Y_{si}^{j} = \sum_{i=1}^{ALL} \Delta Y_{si}^{j} \, Pi \qquad (2)$$

where

ΔY_{si}^{j} = calculated rate of bed change in cell j during the i^{th} combination of events in Table 8.

Pi = joint probability of occurrence

64. The expected rate is converted to expected value of bed change by multiplying it by the duration of the adjustment period, 3,650 days. To facilitate using HAD-1, the time period weighted by probability of occurrence of the combination of events was calculated (Table 9). The Eugene Island mean interval stages are shown above columns 4-7. A year of histograms was developed for the Eugene Island el -1.5 by combining the 14 discharge events of column 3 with their respective days of column 4. The Eugene Island stage was changed to -0.5 ft, column 5, and the discharge histogram from columns 3 and 4 was repeated twice to represent column 5 in the table. The Eugene Island stage was changed to +0.5 and five sets of the annual flow duration histogram were created to represent column 6. Two more sets of the annual histogram were developed for a Eugene Island stage of +1.5 ft to represent column 7. These 10 sets of the annual flow histogram were placed in sequence from low to high Eugene Island stage class to form the adjustment hydrology data set.

65. A disadvantage of the probability approach is the loss of serial correlation. That is, it is not possible to compare model to prototype behavior during the hydrograph. Comparisons can be made only for the ending condition, which is 1977 in this case. Furthermore, the major event of record

occurred during this period. Care was taken to include it separately in the simulation hydrograph. By including it separately, the discharge from Morganza Floodway, which was not included in the histogram analysis, was added to the measured Simmesport flow.

66. Energy forces which are neglected in these boundary conditions (e.g., winds, wind waves, tides, and tropical storms) are also neglected in the HAD-1 analysis. These, as well as salinity- and temperature-induced density currents, are being treated in the multidimensional approaches and will be reported later. Although the mean tidal range is 0.8 ft, fluctuations in Gulf elevation from -3.5 to +3.8 ft have been recorded at the Eugene Island gage. These fluctuations are captured in the Eugene Island stage duration curve and thereby in the downstream boundary condition of HAD-1.

Development of sediment boundary conditions for adjustment

67. Tuttle and Combe (1981) reported that while water yield of the Mississippi River has remained stable, sediment yield has decreased by 50 percent over the past 3 decades. Measurements at the Simmesport gage indicate a corresponding reduction in the Atchafalaya suspended sediment yield. Figure 12 illustrates the trend by using annual sediment yield divided by annual water yield. An average sediment discharge was developed for the adjustment period as shown in Figure 13.

68. Because of significantly different characteristics in behavior between very small particles and large particles, the sediment discharge is partitioned into six sizes using the American Geophysical Union classification size classes: clay for particle diameters less than 0.004 mm, silt for particle diameters between 0.004 and 0.0625 mm, and four classes of sand for particle sizes between 0.0625 and 1 mm. Sediment coarser than 1 mm is found in such small quantity that it is considered negligible in this task. Figure 14 shows the fraction of each type of sediment in the total load. A further breakdown of silt and sand is presented in Table 10.

69. The annual sediment yield, calculated using the flow histogram and the average sediment discharge curve, is 98,708,000 tons per year compared to 97,000,000 tons per year measured during the adjustment period.

70. These Simmesport sediment discharge data were translated to the HAD-1 grid, 82 river miles downstream. Between that point, Atchafalaya River mile 87, and the outlets from the basin, the trend is primarily deposition.

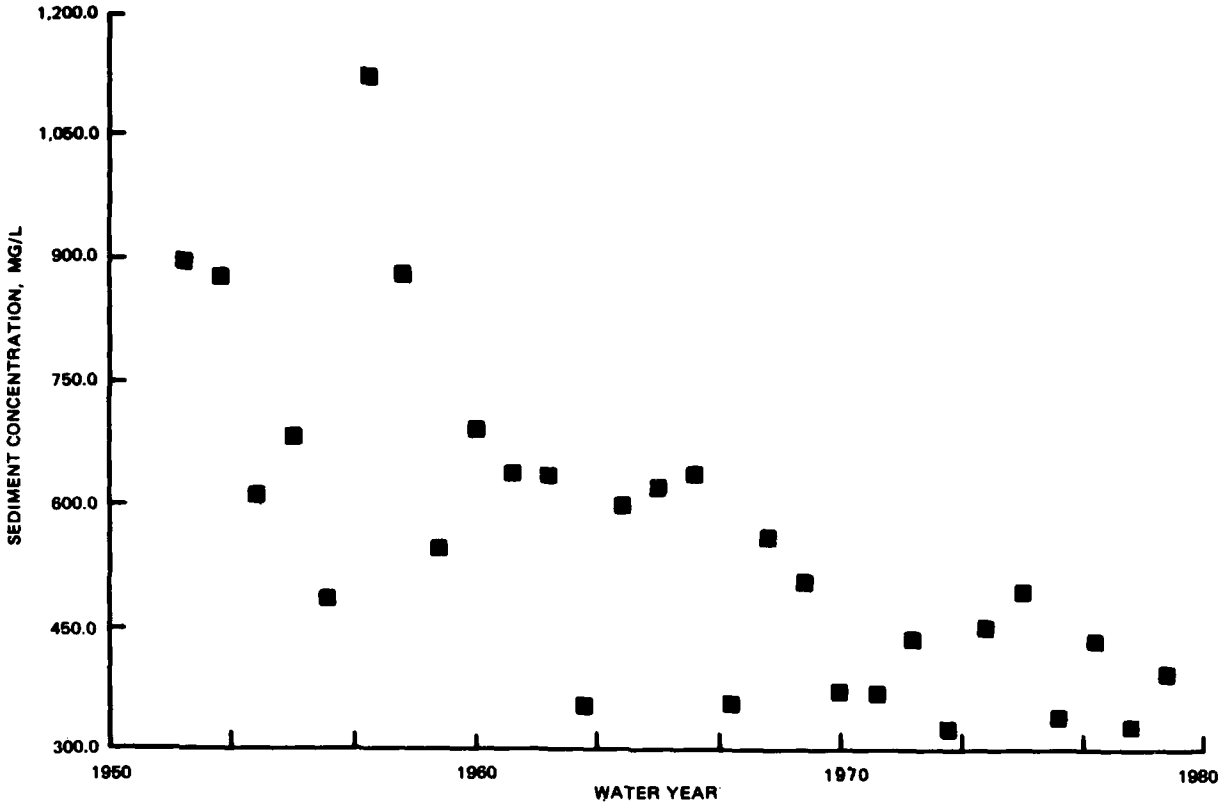

Figure 12. Average annual sediment concentration at Simmesport

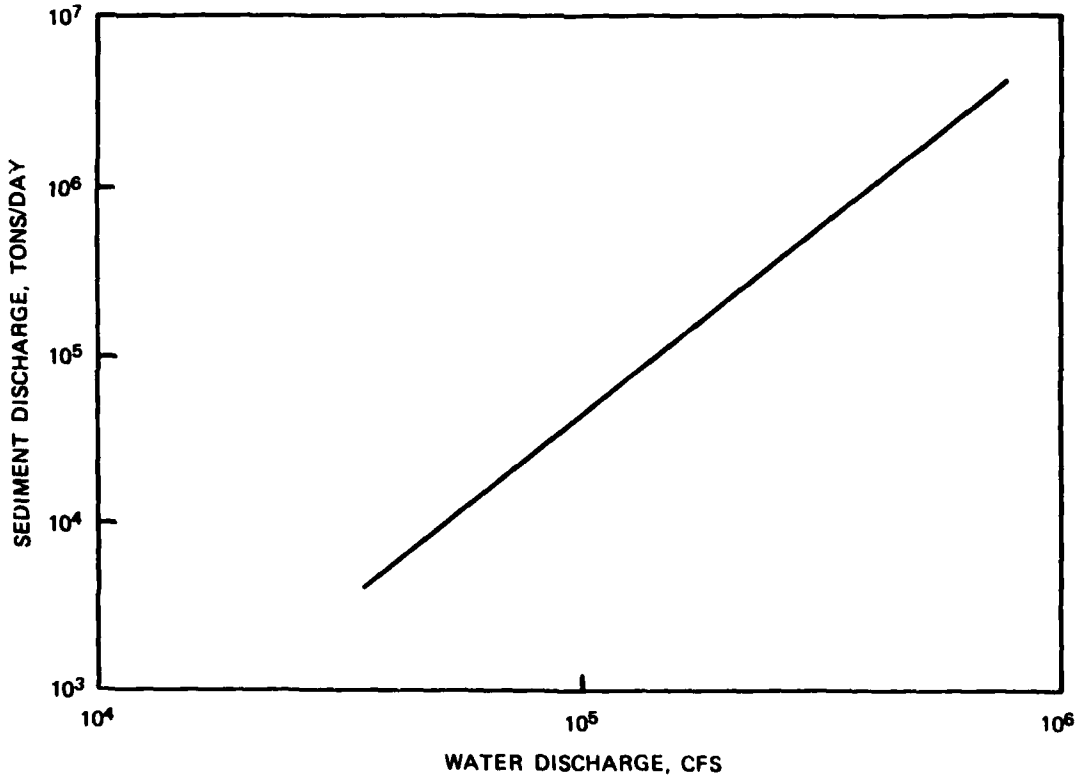

Figure 13. Sediment rating curve for the period 1966-1977, Atchafalaya River at Simmesport gage

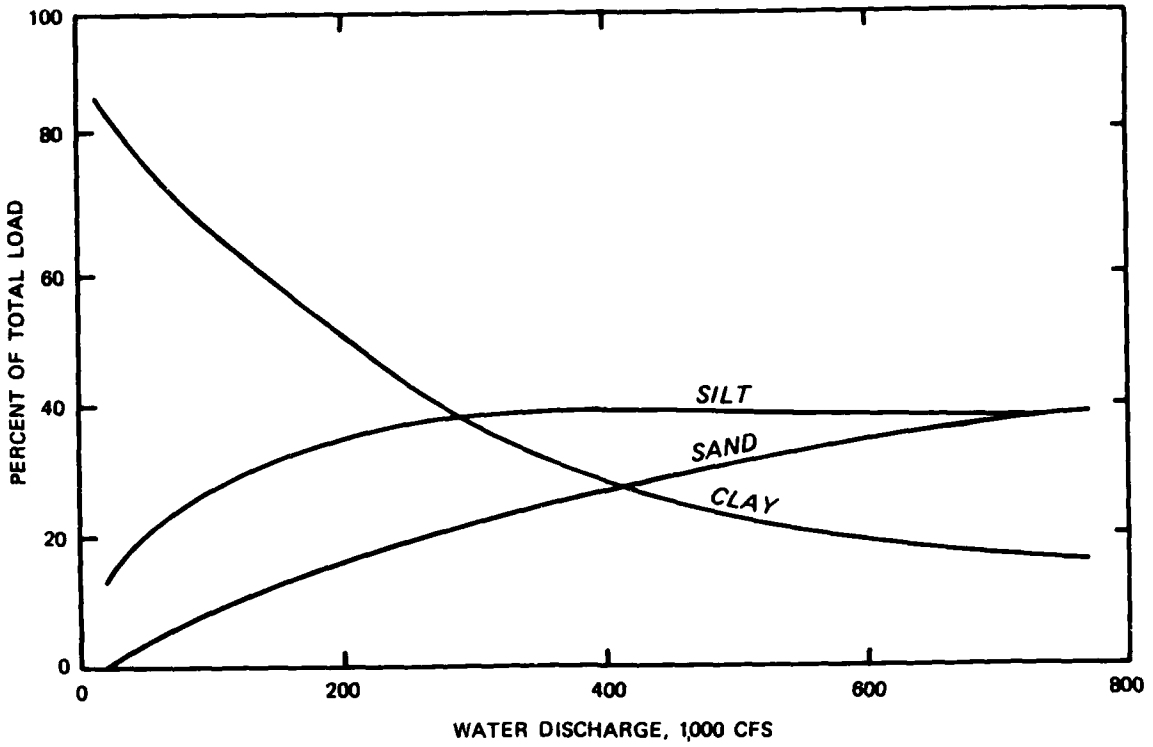

Figure 14. Distribution of total load, Atchafalaya River at Simmesport gage

Consequently, any inaccuracy in the rate of sand discharge which might have resulted from the translation is filtered out by deposition before the HAD-1 flows reach the coastline.

Adjustment for apparent subsidence

71. Although not an adjustment parameter, subsidence has been included in this calculation. The primary factors in apparent subsidence are (a) actual sea level rise, (b) basement sinking, and (c) consolidation of sediments. Subsidence is the latter two of these factors; and when sea level rise is included, the term becomes "apparent subsidence." Estimates of rates vary from 0.30 to 4 cm per year in the general area. The rate adopted for this study was 1.3 cm per year (0.5 ft per decade) after the work of Swanson and Thurlow (1973). Details of the investigation into apparent subsidence rates for this delta growth study are presented in McAnally et al. (1984). The entire HAD-1 grid was allowed to settle at the rate of the apparent subsidence.

Fixed Bed Adjustments

72. The numerical model was adjusted in two steps: (a) fixed bed, in

which n values were adjusted to reconstitute MBM water-surface profiles and flow distribution; and (b) mobile bed, in which the critical shear stress threshold was adjusted to reconstitute observed values for trap efficiency in the basin, the sediment-water discharge relationships at Morgan City and Calumet, average change in bed elevation in the bay, and the change in bed elevation in each cell of the bay grid.

Reconstitution of observed water-surface elevations

73. Both the MBM and prototype water-surface elevations were used in water-surface profile adjustment. Three discharges were selected: 350,000, 800,000, and 1,500,000 cfs. Prototype data are available for floodway flows up to 965,000 cfs; only MBM data are available for 1.5 million cubic feet per second.

74. The prototype discharges used are shown in the following tabulation along with their time of occurrence. Because these events are unsteady, whereas HAD-1 uses a steady-state calculation, the water-surface elevations were averaged over 5 days to get each prototype data point. Variation was always less than a foot and usually only a few tenths. The observed and calculated stages are shown in Table 11.

Date	Total Discharge Across Floodway, cfs
21-25 April 1977	350,000
14-15 May 1972	375,000
6-15 April 1978	425,000
16-18 April 1975	710,000
13-20 May 1973	965,000

75. The adjustment parameter is Manning's n value. By adjusting that parameter, both the water-surface elevations and the cross-section flow distribution are made to agree with observed values. Adjustments are not arbitrary, however; hydraulically similar regions were assigned similar roughness as illustrated in the following tabulation. These regions are shown in Figure 15.

Hydraulically Similar Region	n value
Primary channels and open water	0.025
Marsh and emerging land with willows	0.20
Cypress and bottomland hardwood with underbrush	0.20

76. The comparisons between calculated and observed stages were quite

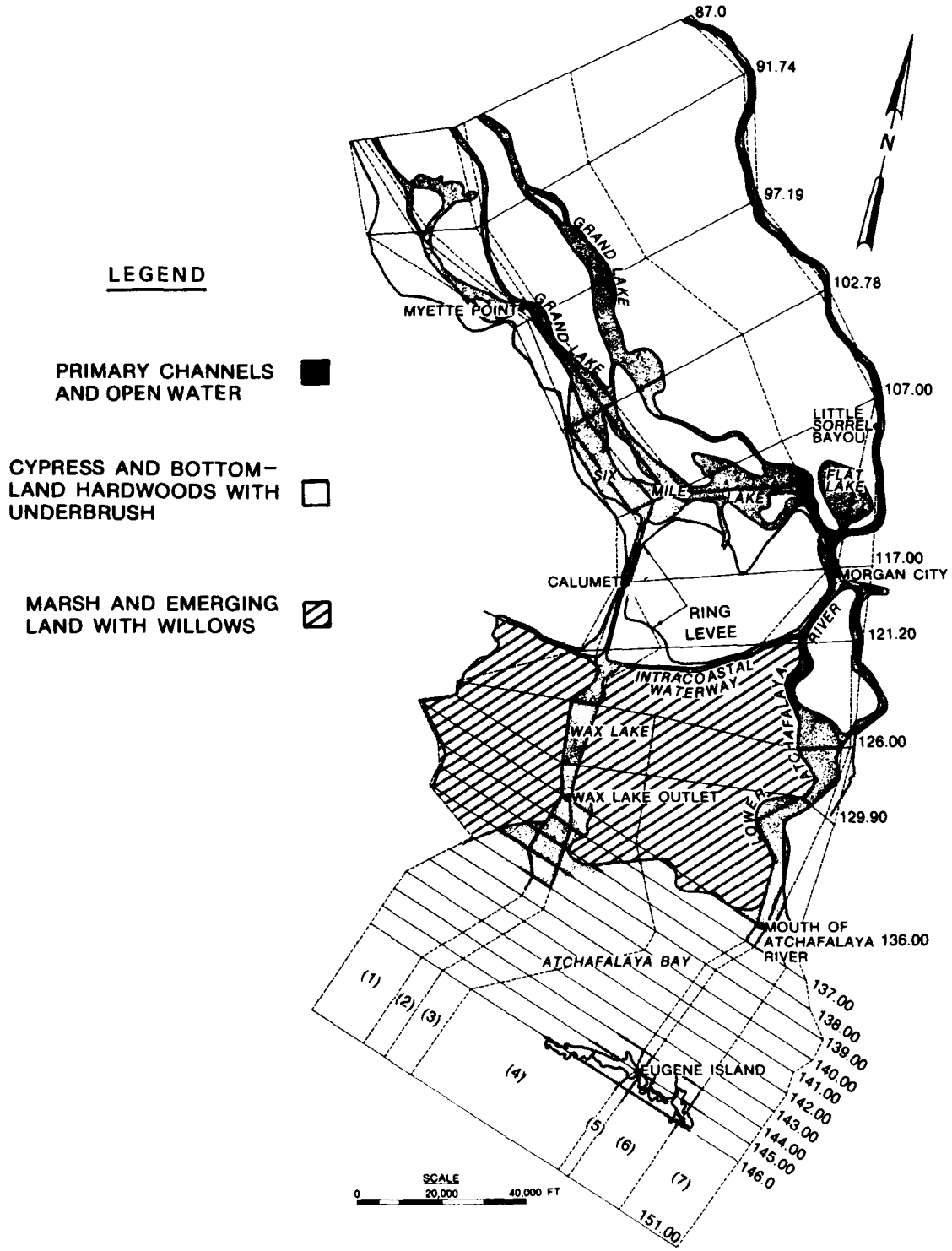

Figure 15. Hydraulically similar regions

good up to 965,000 cfs--the range of observed data. The only data set available for comparison with the 1,500,000-cfs flow lines was from the MBM, shown in column 12 of Table 11. In the vicinity of Morgan City, the HAD-1 profile was 3 ft lower than that MBM elevation, which is attributed to different sets of cross sections being used to design the two models. In addition, the MBM has a fixed bed whereas HAD-1 can scour. To further test the HAD-1 adjustment, observed stages at Morgan City were plotted versus total latitude flow (Figure 16). Although that data set stops well short of 1.5 million cubic feet per second, a straight-line extrapolation on log-log paper indicated that 15 ft is a reasonable estimate of the stage. The n values in paragraph 75 were accepted.

Reconstitution of the Morgan City and Calumet stage discharge data

77. Figure 16 is also very useful in assessing the difference in

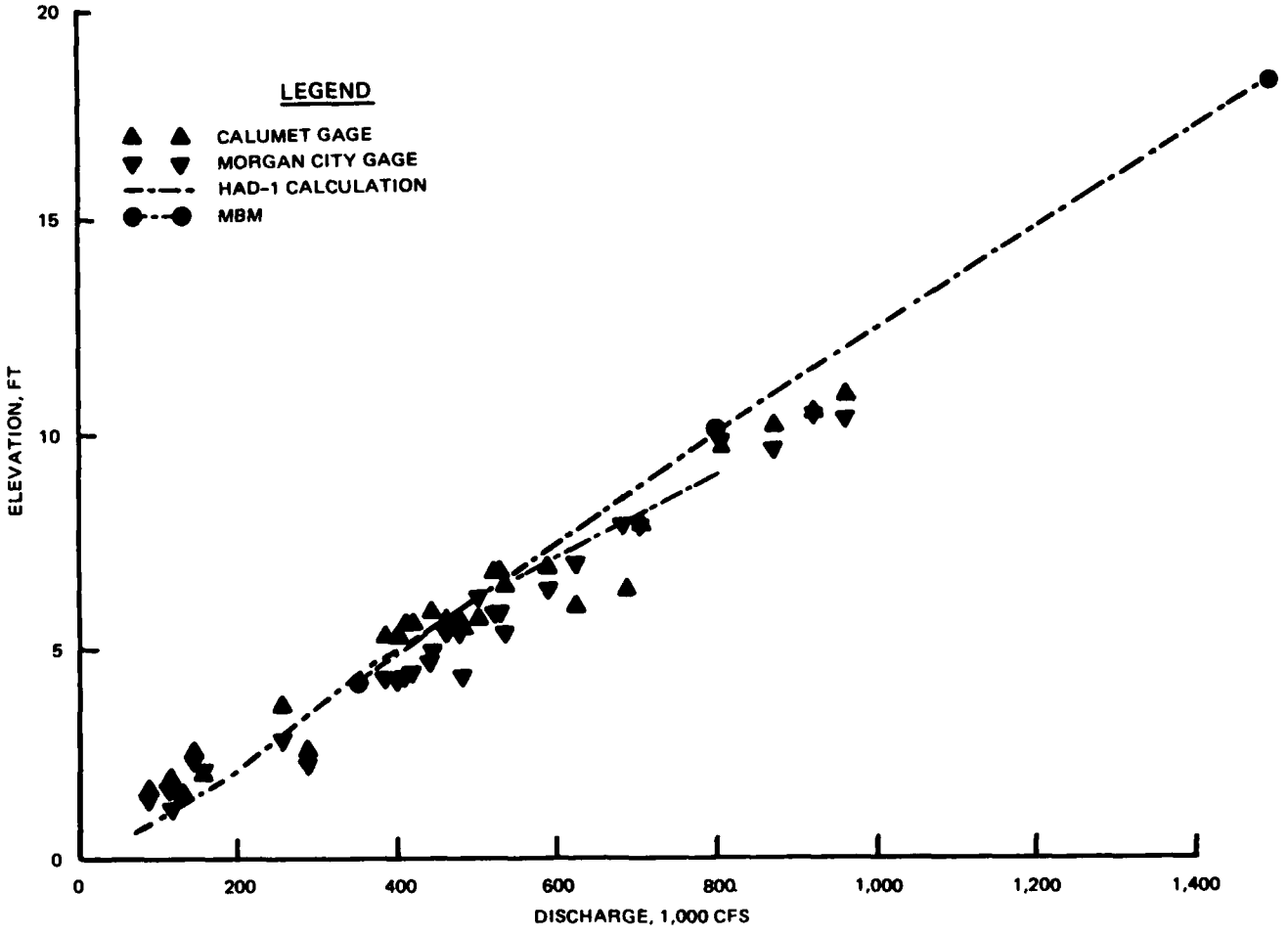

Figure 16. HAD-1 stage verification, Morgan City-Calumet gages

water-surface elevation between Morgan City and Calumet. In most cases, stages at Calumet were higher than at Morgan City, but usually the difference was small. That supports a basic assumption in the HAD-1 model (the water surface is horizontal across each cross section) and allows the HAD-1 model to establish a reasonable flow distribution between the outlets.

78. Another criterion used in fixed-bed adjustment is flow distribution. Figure 17 shows measured prototype data for Morgan City-Calumet, the only locations on the Lower Atchafalaya Basin where such measurements are available. During low-flow periods, Wax Lake Outlet passed 40 percent of the flow and the Lower Atchafalaya River passed 60 percent. As water discharge increased to 300,000 cfs, the prototype flow distribution became 35 percent/65 percent for Wax Lake Outlet and Lower Atchafalaya River, respectively. By 965,000 cfs, which is the maximum flow of record, Wax Lake Outlet carried 27 percent and the main river channel carried 73 percent. The HAD-1 calculation is also shown in Figure 17. For discharges greater than 350,000 cfs, the calculated values fell well within the observed scatter of data. Since most delta growth is associated with the larger floods, these results are considered acceptable.

Reconstitution of flow distribution across the floodway

79. Average annual values of water distribution had been calculated by others for the Atchafalaya Floodway (Figure 18). These were used to guide in the HAD-1 flow distribution test. An example of the HAD-1 flow distribution is shown in Table 12 for 350,000 cfs.

Movable-Bed Adjustments

80. Fixed-bed adjustment proceeded without the sedimentation data set, so prior to the adjustment of sediment parameters, the following sediment data set was assembled.

Development of the bed gradation data

81. Sediment boundary conditions were discussed earlier. The bed sediment data were assembled from measurements made by the New Orleans District during the period 1975-1976. Figure 19 shows bed gradation, expressed as percent finer by weight, plotted versus river mile. The solid line separates sand, above the line, from silt size particles below the line. Although a

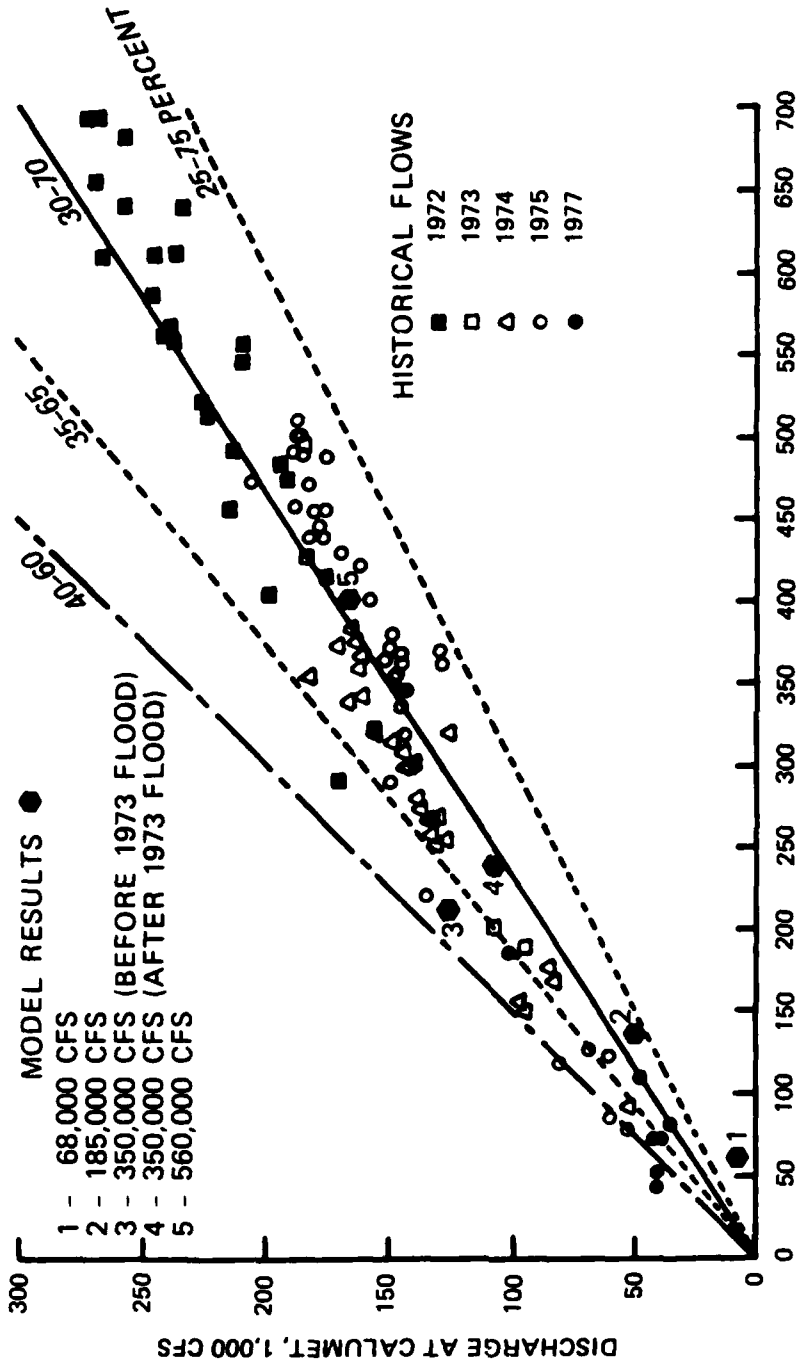

Figure 17. Distribution of flow for the period 1972-1977, Atchafalaya River at Calumet and Morgan City

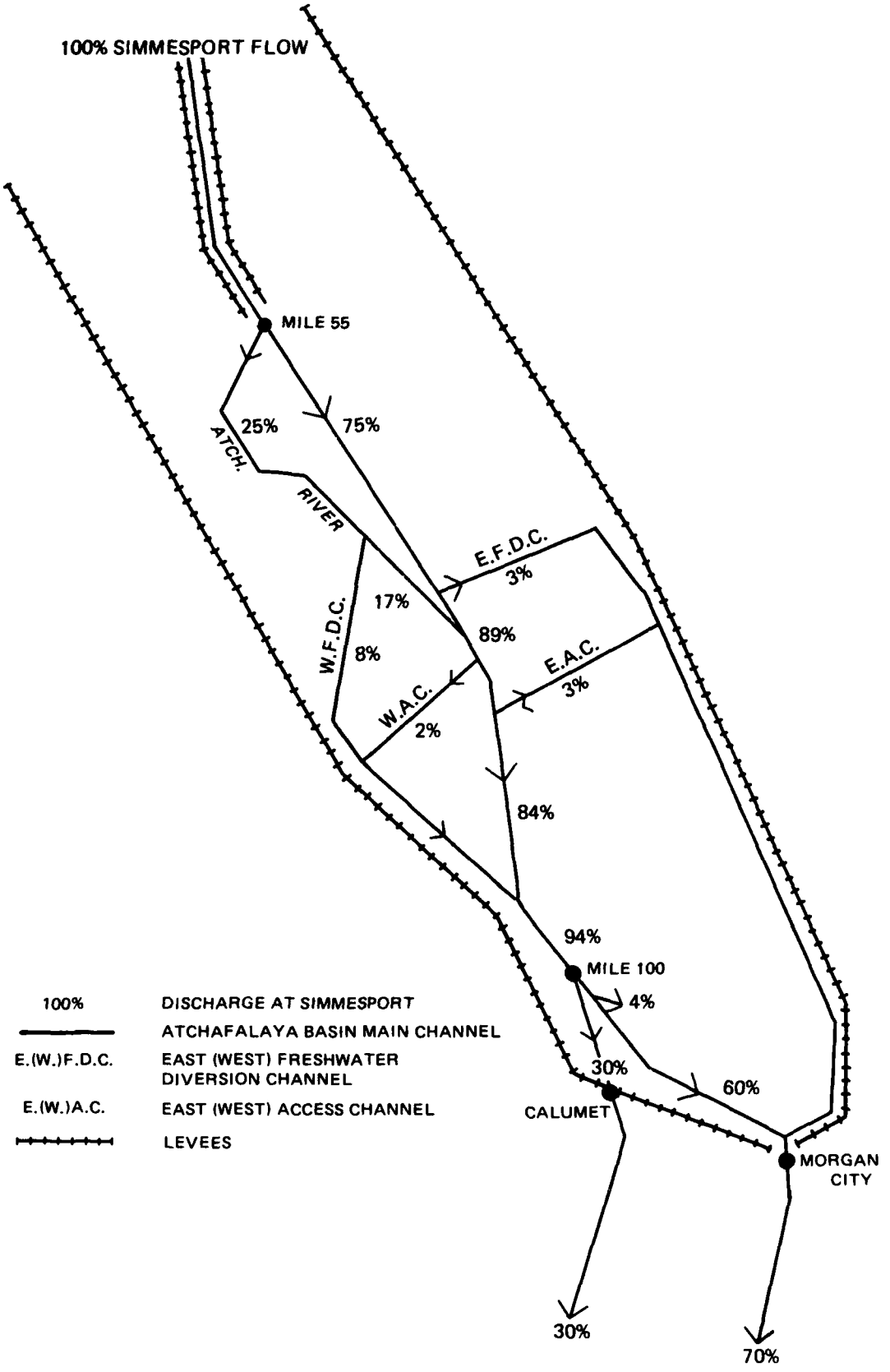

Figure 18. Diversion from the Atchafalaya Basin main channel during average annual flood (courtesy of van Beek et al. 1979)

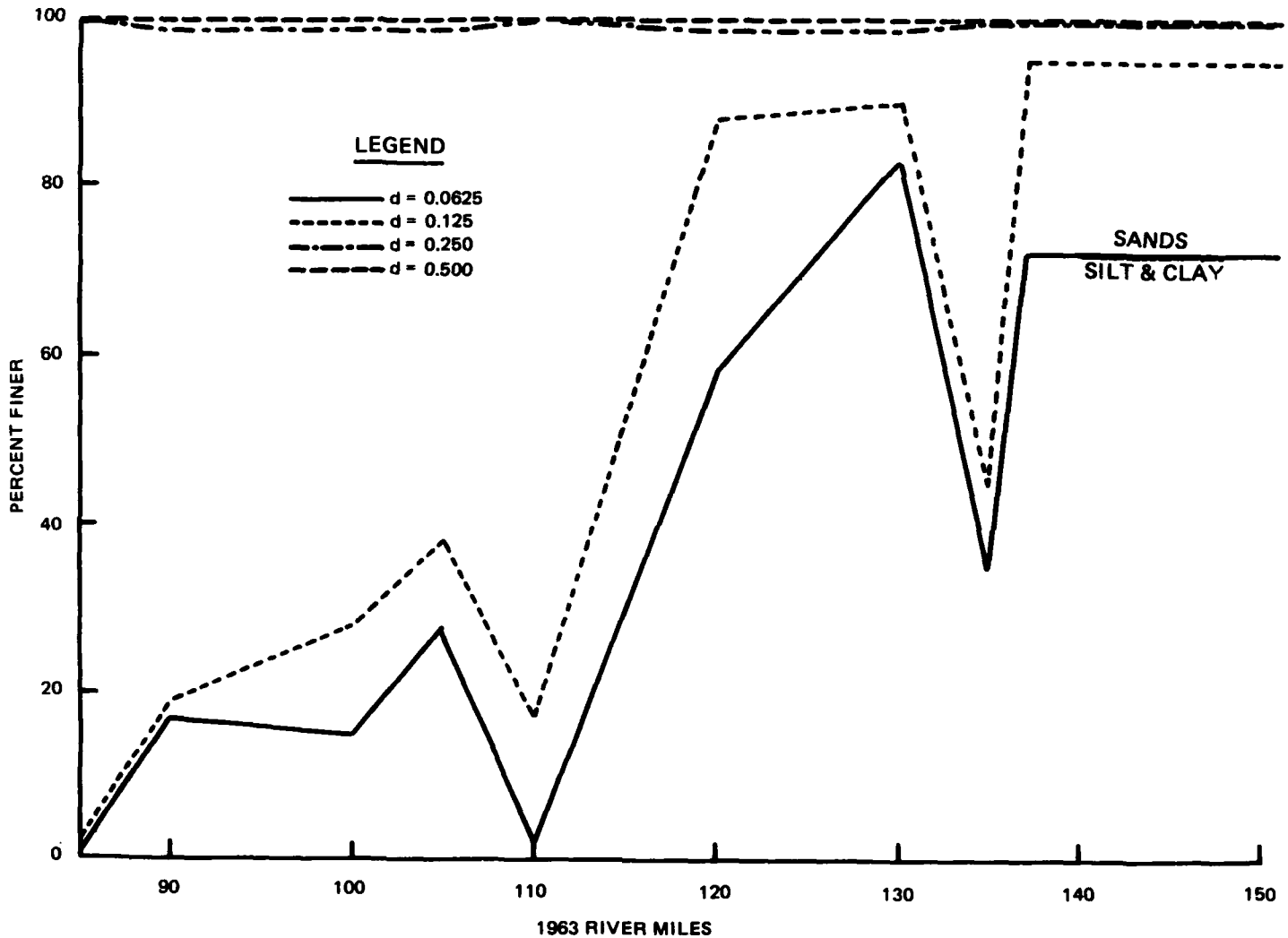

Figure 19. Gradation of bed surface, Atchafalaya River, 1975-1976 samples

considerable quantity of silt was deposited in the downstream end of the basin, the samples used to form this figure were taken from the channel, which has a predominately sand bed.

82. Bed sediment gradation of the bay, based on the 330 samples from the top 1 to 2 ft of the bed deposit, is as follows: 10 percent clay, 62 percent silt, and 28 percent sand. Figure 20 shows sample locations in the bay, and Figure 21 is the composite bed gradation curve for all bay samples (Coleman et al. 1988).

Development of unit weights for bed deposits

83. The final required bed sediment property is composite unit weight of the bed deposit. Measured values shown in Figure 22 are referenced by letter to locations plotted on Figure 23. The lightweight sample is representative of an initial clay deposit because it came from a deep hole on the Wax Lake Outlet side of the bay taken at sta S, during the low flow season. Averaging the other samples gave a unit weight of 65 lb/cu ft on the bed surface, increasing to 68 lb/cu ft at 1 ft of depth.

84. The HAD-1 program requires separate unit weights for clay, silt, and sand. It then calculates the composite unit weight of the deposit using the equation:

$$\frac{1}{\gamma_B} = \frac{\frac{\% \text{ Clay}}{\gamma_{Clay}} + \frac{\% \text{ Silt}}{\gamma_{Silt}} + \frac{\% \text{ Sand}}{\gamma_{Sand}}}{100} \tag{3}$$

where

γ_B = composite unit weight of the mixture, lb/cu ft

γ = unit weight of each sediment class in the bed deposit

Using the average gradation curve and initial unit weights of 25, 60, and 93 lb/cu ft for clay, silt, and sand, respectively, HAD-1 would calculate an initial unit weight of the mixture of 58 lb/cu ft as follows:

$$\frac{1}{\gamma_B} = \frac{\frac{10}{25} + \frac{62}{60} + \frac{28}{93}}{100} \tag{4}$$

where γ_B = 57.7 lb/cu ft.

Figure 20. Sample locations (from Coleman et al. 1988)

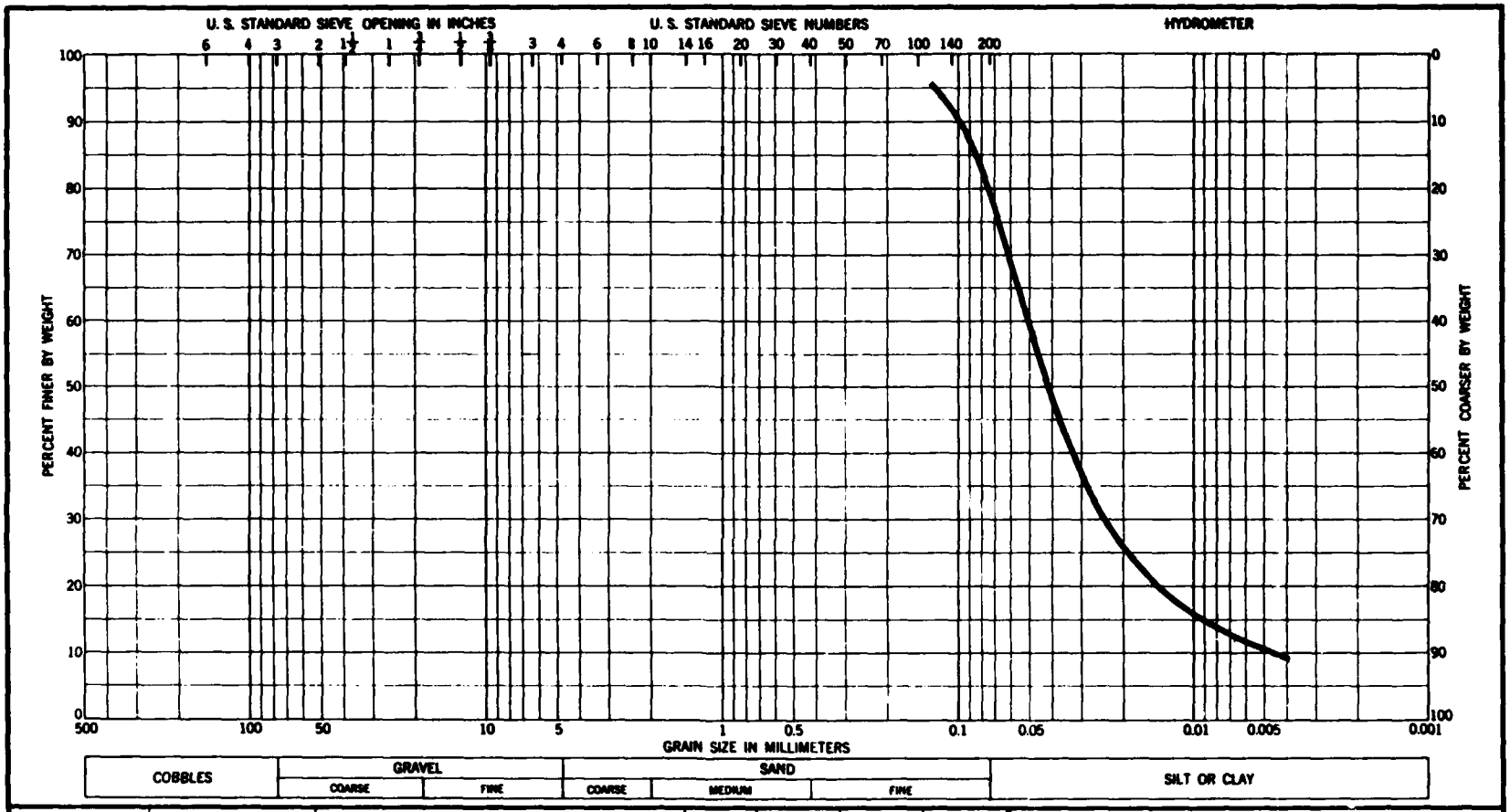

Sample No.	Elev or Depth	Classification	Nat w %	LL	PL	PI

GRADATION CURVES

Project

Area

Boring No.

Date 2/3/82

ENG FORM 1 MAY 63 2087

Figure 21. Composite bed gradation curve for all bay samples

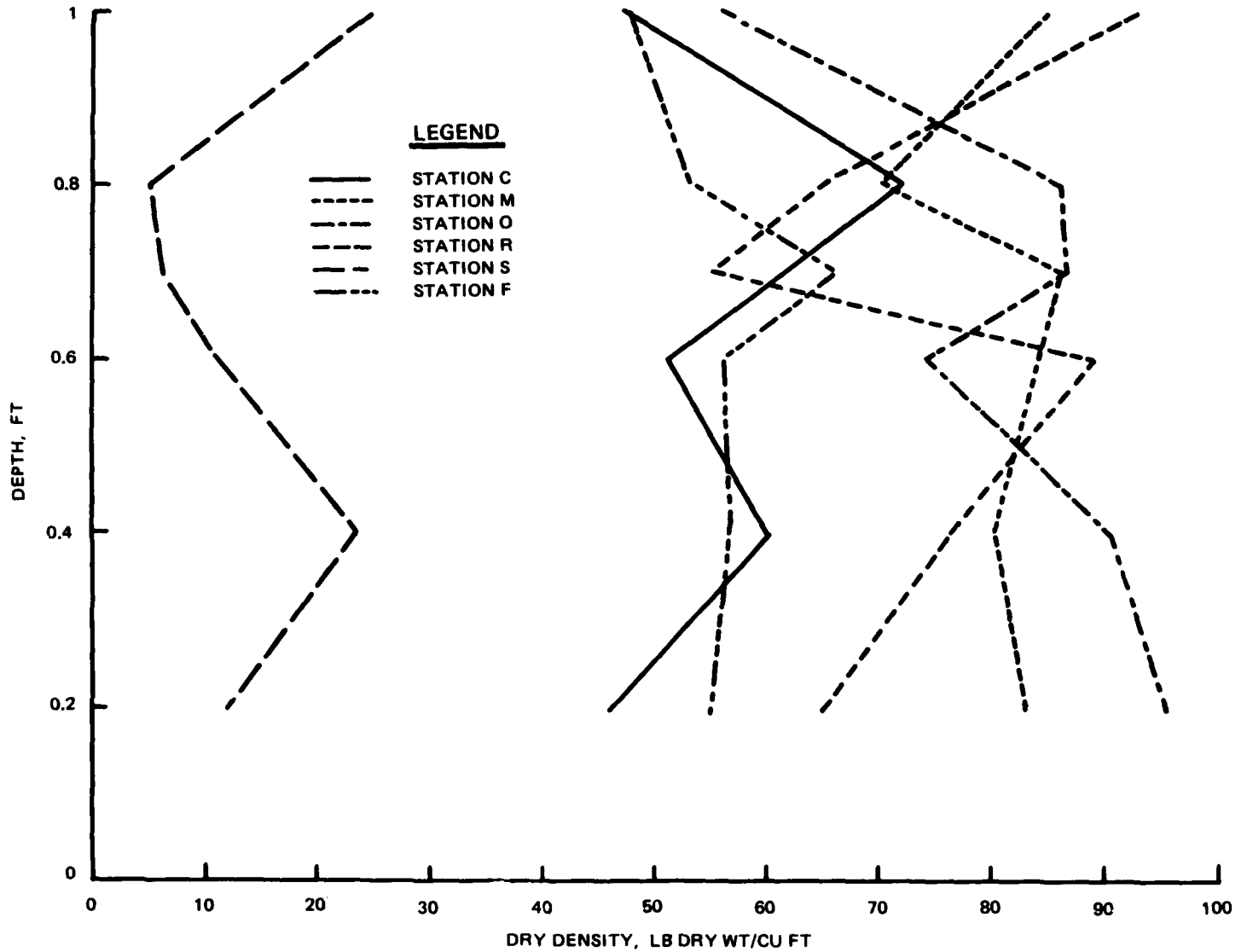

NOTE: SEE FIGURE 23 FOR LOCATIONS OF STATIONS.

Figure 22. Composite unit weight of bed deposit

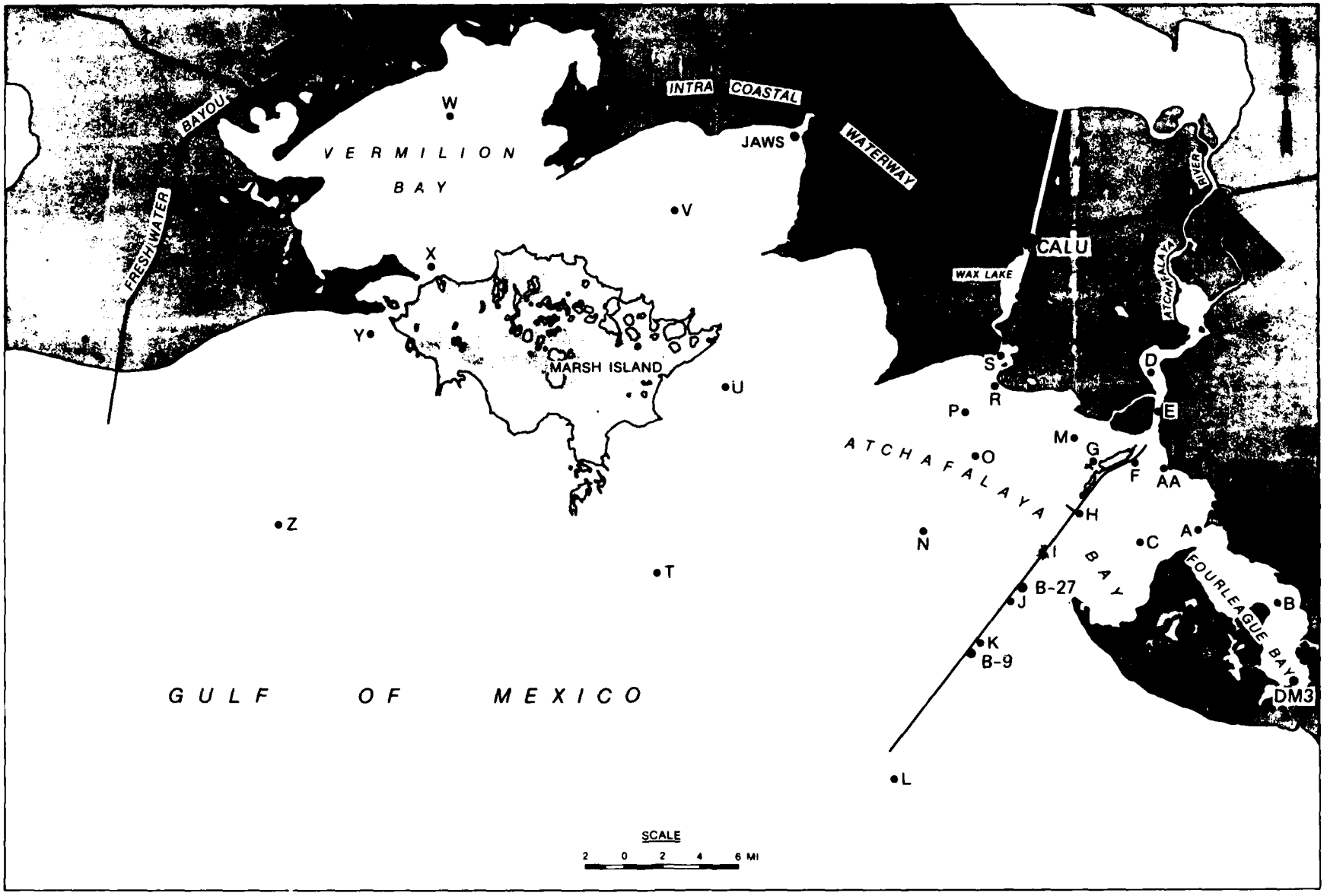

Figure 23. Sampling locations

85. The HAD-1 program allows silt and clay to consolidate with time according to the following equation (Vanoni 1975):

$$\gamma_T = \gamma_i + B \log_{10} T \tag{5}$$

where

γ_T = consolidated unit weight at the end of year T

T = time in years

γ_i = the unit weight at T = 1 year

B = the consolidation coefficient

86. For a period of 10 years (i.e., length of adjustment period), the calculated consolidated weights of clay and silt are

$$\text{Clay: } \gamma_{10} = 25 + 16 \log_{10} (10) = 41 \text{ lb/cu ft} \tag{6}$$

$$\text{Silt: } \gamma_{10} = 60 + 5.7 \log_{10} (10) = 66 \text{ lb/cu ft} \tag{7}$$

Sand remains at the unit weight of the initial deposit, 93 lb/cu ft. The consolidated unit weight of the mixture by applying Equation 3 is 67.2 lb/cu ft, which compares favorably with the measured value of 68 lb/cu ft at 1 ft below the bed surface. Consequently, the initial unit weights and consolidation coefficients shown in Equations 6 and 7 were adopted for the entire HAD-1 grid.

Selection of transport function

87. The rate of sand transport was calculated with the Toffaleti method. Clay and silt movement was calculated using cohesive transport concepts with deposition processes patterned after the work of Krone (1962), and erosion concepts developed by WES based on work published by Partheniades (Shen 1971) and Ariathurai (Ariathurai, MacArthur, and Krone 1977).

Particle Settling Velocities

88. Particle settling velocities were calculated by HAD-1 using the procedure documented in Vanoni (1975). Silt and clay settling velocities were checked against values measured in laboratory tests of Atchafalaya Bay sediments and compared satisfactorily.

Reconstitute sediment
trap efficiency in the basin

89. Values for the critical shear stress thresholds and erosion rate coefficients for clay and silt were established by trial and error using trap efficiency of the floodway as estimated by Roberts, Adams, and Cunningham (1980) and the following field data as guides: measured sediment load at Morgan City, measured sediment load at Calumet, total deposit in the bay, and deposit in each cell in the bay. Table 13 shows the resulting coefficients for deposition and erosion symbols, as defined in Table 5. The deposition threshold τ_{cd} for clay is 0.0004 lb/sq ft, and for all silt sizes is 0.001 lb/sq ft. The threshold for erosion of both silt and clay τ_{ce} is 0.0024 lb/sq ft. The processes are assumed to be constrained by the clay erosion. By that same reasoning the erosion rate coefficients are the same for silt as for clay. Clay erosion shifts from individual particles to flocs at a bed shear stress τ_m of 0.015 lb/sq ft. The erosion rate, ERM, is thus 0.001 ton/sq ft/day. As the actual bed shear stress, τ, increases above τ_m, the erosion rate increases by the amount $B_m(\tau - \tau_m)$ where B_m is 0.3 and the product is in tons per square foot per day. Similarly, if the bed shear stress drops below τ_m, the erosion rate is decreased by the amount $B_p(\tau - \tau_m)$ where B_p is 0.06 and the product is in tons per square foot per day. Steps in arriving at these values are described in the following paragraphs. When the bed shear stress falls between τ_d and τ_e, silt and clay are transported without erosion or deposition.

90. The calculated sediment retention in the basin was compared to results published by Roberts, Adams, and Cunningham (1980). The comparison is tabulated in Table 14. The first entry in that table shows agreement at Simmesport, the upstream boundary condition for HAD-1. During that portion of the HAD-1 adjustment period which overlapped with Roberts, Adams, and Cunningham, the total sediment inflow of each investigator was 105 million tons per year. The distribution between sand and silt/clay fractions is slightly different between the two studies. The second entry in Table 14 shows the sediment outflow from the basin. The outflow points are the Morgan City and Calumet discharge ranges, and the outflow calculated by HAD-1 matches very closely that calculated by Roberts, Adams, and Cunningham in both total yield, 78 million tons per year versus 80 million tons per year, and also yield by size class. That comparison is the most significant in the table because it

confirms the volume of sediment being delivered to the bay by the HAD-1 model. The overall trap efficiency calculated by HAD-1 agrees well with that calculated by Roberts, Adams, and Cunningham. The disagreement in trap efficiency of sand is to be expected since Roberts, Adams, and Cunningham used a different inflowing sediment load at Simmesport than was used in HAD-1. The average annual outflow is the more important parameter and was given first priority in this adjustment test.

Reconstitute measured sediment discharge rates at Morgan City and Calumet gages

91. Whereas the previous test demonstrated that the combined Morgan City-Calumet average annual sediment yield as calculated by HAD-1 matched the work of others, this test demonstrates that the short-interval discharge calculated by HAD-1 also matches that measured in the prototype, and that in addition, the distribution between the Lower Atchafalaya River and the Wax Lake Outlet matches the prototype. The results are displayed in Figures 24 and 25 for the Morgan City gage and the Calumet gage, respectively.

Reconstitute average depth of sediment deposition in the bay

92. The 1967 and 1977 hydrographic surveys of the bay were digitized using a 1,000-ft-square mesh, and the digital maps were subtracted to obtain the change in bed elevation during the adjustment period. The HAD-1 grid was superimposed over the digitized surveys, and the change in bed elevation calculated in each cell by averaging the values for all mesh points in the cell. Only the bay portion of the grid was included as shown by the grid cell numbers in Figure 26. Results are shown in Table 15. Positive values are deposition and negative values reflect a lowering of the bed surface as by subsidence, dredging, or scour.

93. The average change in bed elevation of all cells between cross sections 136.00 and 145.00 is +1.05 ft (Table 15). Some cells in that computation are in the marsh zone rather than the bay. When confined to the bay, the average depth of change is +1.19 ft. By comparison, the calculated change in HAD-1 is +1.31 ft. The surface area in that calculation is 176.14 square miles. Although prototype data are not available to verify the HAD-1 sediment yield at the coastline, the good agreement between calculated and measured depth of bay deposits, the tests presented in the calculation of trap efficiency in the basin, and the calculated sediment discharge rates at the Morgan

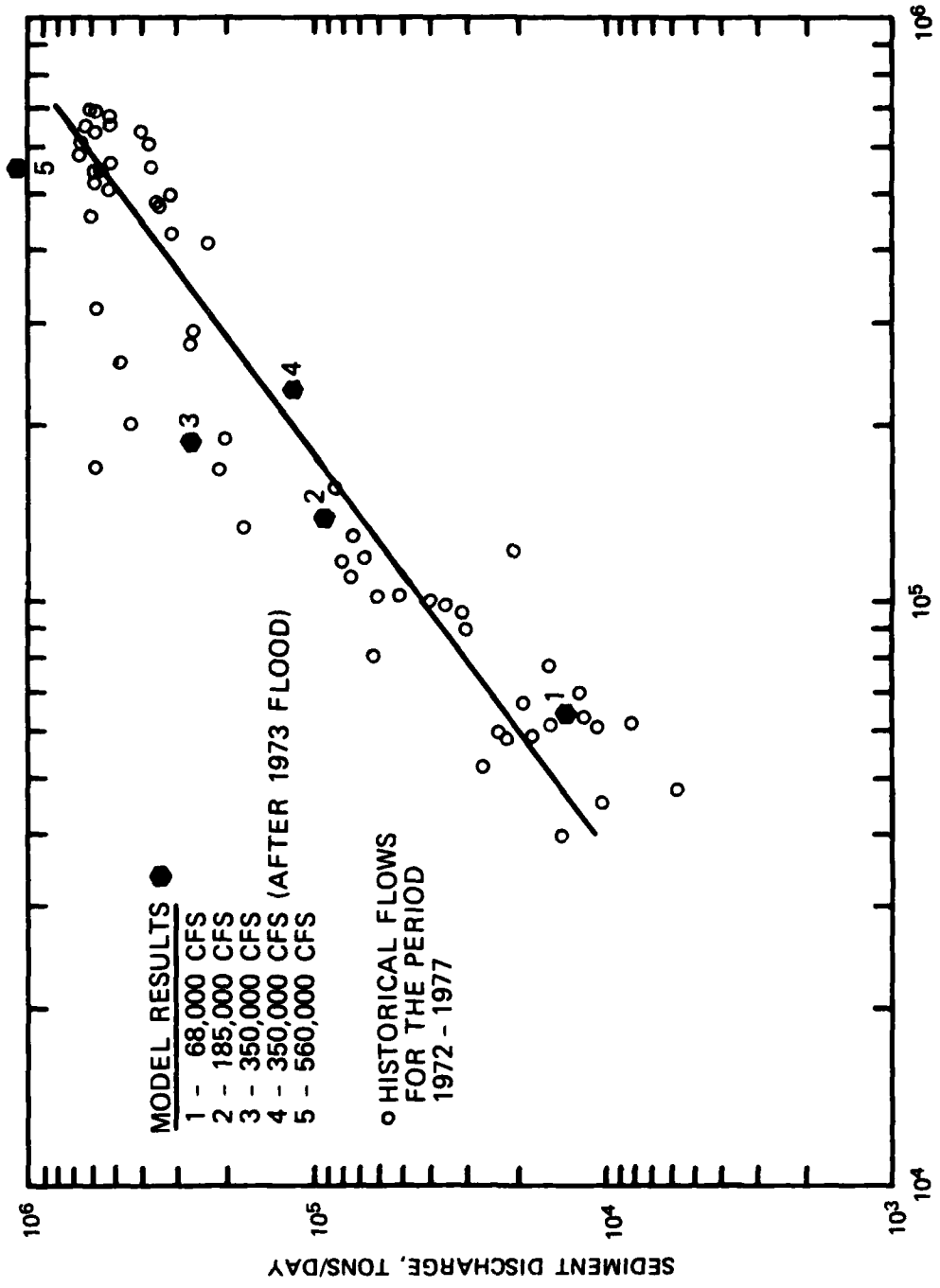

Figure 24. Sediment rating curve, Atchafalaya River at Morgan City

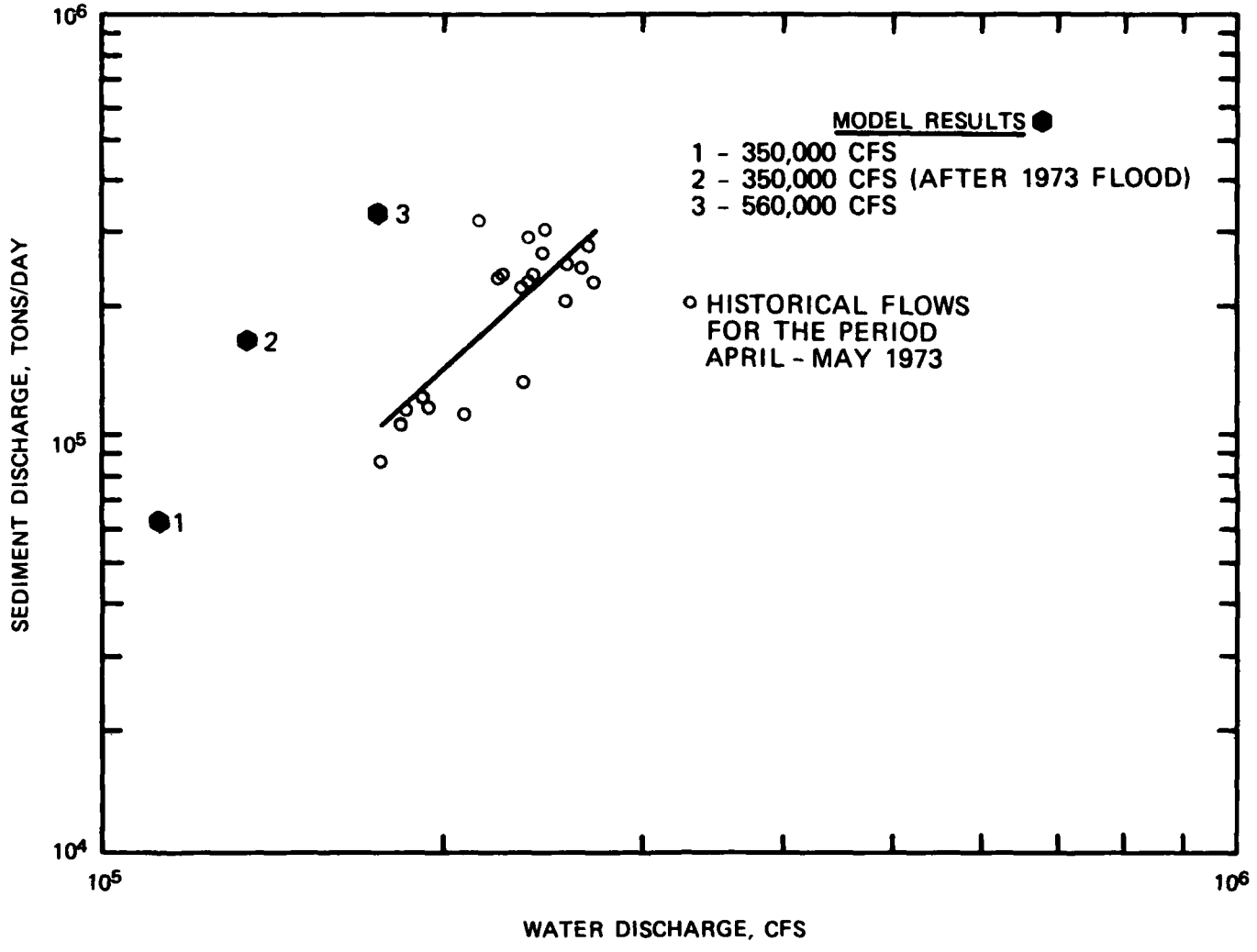

Figure 25. Sediment rating curve, Atchafalaya River at Calumet

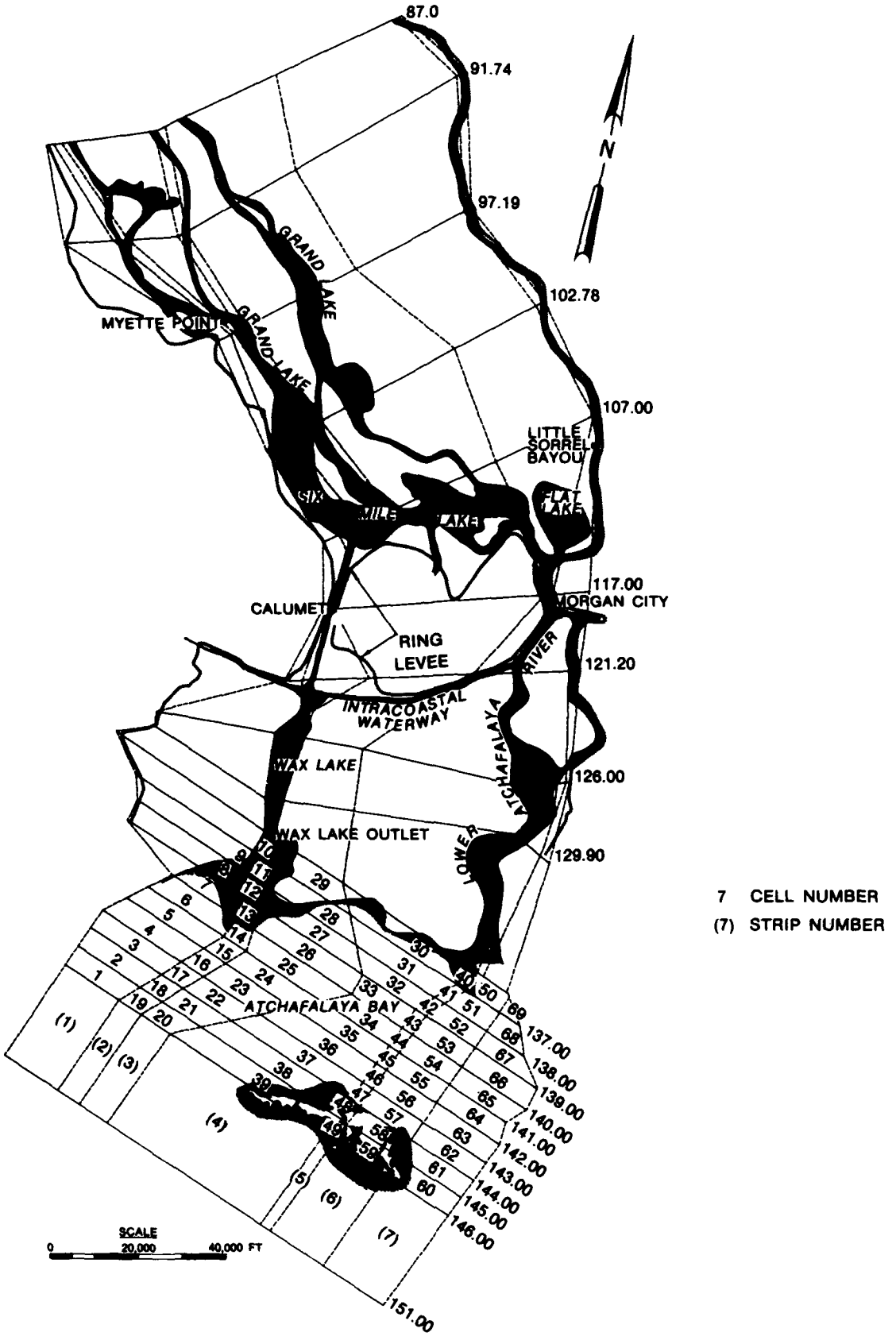

Figure 26. Index of cell numbers for calculating changes in bed elevations

City and Calumet gages support the reasonableness of the results. Other evidence of reasonableness is the consistency between the calculated trap efficiency in the basin and in the bay, 31 percent compared to 26 percent. Of the calculated 70 million tons per year of sediment passing the coastline during the adjustment period, only 1 percent was sand. All of that deposited in the bay. The average annual amount of silt and clay passing through the bay into the Gulf of Mexico was calculated to be 50 million tons per year.

Reconstitute depth of sediment deposition or erosion in each cell of the bay

94. The changes in bed elevation calculated by HAD-1 compared to the prototype values are shown in Plates 22-28. Those results demonstrate the trends observed in the prototype surveys although some point values deviate from the prototype significantly. For example, the prototype surveys show two deposition zones in strip 1 (Plate 22). One is located near the cross section for river mile 139 and the other at 142. HAD-1 results also showed two deposition zones, but the first is located near river mile 140 rather than 139. Calculated deposition in strip 2 (Plate 23) is about 1.5 miles gulfward of the prototype location. The conclusion from this cell-by-cell comparison is that the model will give trends on a cell-by-cell basis, but the location of islands and channels may be different in the prototype. However, the average bed elevation change by strip correlates with prototype data as shown in the following tabulation. The mean μ and standard deviation ρ of bed

	Prototype		HAD-1	
Strip	μ	ρ	μ	ρ
1	1.2	0.8	0.9	0.8
2	1.4	0.6	1.2	1.9
3	0.2	0.6	0.2	1.0
4	1.4	0.4	1.1	1.1
6	0.6	0.8	1.2	1.5
7	0.4	0.9	0.8	1.2

elevation change in the bay were calculated for all cells in each strip, and compared to the prototype values in the tabulation. At the strip level of adjustment, the model performance is adequate. Consequently, questions addressed to this model should be at or coarser than the strip level of resolution.

95. A significant difference still exists between HAD-1 and the prototype in the gulfward ends of strips 6 and 7 (Plates 27 and 28, respectively).

These strips lie east of the navigation channel. That difference is due either to an energy source not included in HAD-1, such as a cross current, or some activity which has not been included in the modeling process, such as shell dredging. The quantity of sediment involved lends itself to the latter explanation. Consequently, the model was accepted as shown and a sensitivity test was devised to measure the impact of location of deposits on the calculated water-surface profile at Morgan City and Calumet for the predicted future delta.

96. Deposition in the area of strips 6 and 7 will be investigated in more detail with the two-dimensional models in the final phase of this study.

97. In conclusion, this adjustment supports the overall rate of deposition as well as the general distribution of deposits in the bay; however, model results should be interpreted as a general pattern and not as the specific location for land growth.

Delta Growth Prediction

Procedure followed in prediction

98. The procedure followed in prediction was to change the boundary conditions in the adjusted model to represent the future rather than the verification period. Otherwise, no changes were made to the adjusted model until deposition produced islands in the bay. At that point, Manning's n values were changed from 0.025 to 0.20 to reflect willow growth on the new subaerial land.

Time period selected for predictions

99. A short-term prediction was made 10 years into the future with year zero being 1980. A total of 50 years was also simulated in the model, ending in 2030.

Development of boundary conditions

100. The future water discharge at the latitude of Old River was to be 30 percent of the total latitude flow. Eugene Island stage was not changed from the adjustment. The annual sediment concentration at Simmesport decreased during the 1950's and 1960's (Figure 12). It seems to have stabilized during the decade 1970 to 1980, and data from that period were used to develop a sediment discharge curve for the forecast. The resulting concentration at Simmesport, based on annual water and sediment yields, is 450 mg/ℓ which

approximates the upper limit of field data for the period 1970 to 1980. The annual yield is 91 million tons per year.

Rate and distribution of apparent subsidence

101. The value adopted for the adjustment period, 1.3 cm per year, was used throughout the model for the forecast period also. That amounts to 0.47 ft per decade for a total of 2.35 ft during the 50-year forecast period.

Predicted delta volume and growth of subaerial land

102. Figure 27 shows the predicted delta growth in terms of new subaerial land as well as the volume of deposition in the bay. Calculated yields by sediment type are shown in Table 16. The total yield at Simmesport during years 0-10 was calculated from the boundary condition load curve to be 910 million tons, or an average of 91 million tons per year. Calculations show that 79 percent of that reaches Morgan City; 68 percent reaches the coastline; and 49 percent passes the Eugene Island range (section 145) into the Gulf of Mexico. Furthermore, the calculated clay discharge passing the Morgan City-Calumet gages is 93 percent of the clay passing the Simmesport gage. The other 7 percent deposits in the basin. Between the latitude of the Morgan City-Calumet gages and the coastline, deposition is quite active amounting to 7 percent, 12 percent, and 13 percent of the Simmesport yield for clay, silt, and sand, respectively.

103. The total trap efficiency between Simmesport and Eugene Island, shown in the last column of Table 16, was 51 percent during years 0-10. The calculated trap efficiency of the bay during that time was 28 percent (i.e., trap efficiency, E, of the bay is the coastline yield minus Eugene Island yield divided by the coastline yield with values expressed in tons).

104. The 50-year total sediment yield at the coastline (Table 16) is 3,339 million tons, and at the Eugene Island range it is 2,767 million tons. Therefore, the average trap efficiency of the bay during the 50-year forecast period is 17 percent, and the resulting deposition is 572 million tons. That converts to an average depth of 4-1/2 ft over the entire bay. Because of the mixtures of sediment types involved, the details of converting the bay deposit from weight to volume are shown in Tables 17, 18, and 19.

105. Table 17 summarizes the calculated weight of deposits by decade and sediment type. The values were determined from Table 16 by subtracting

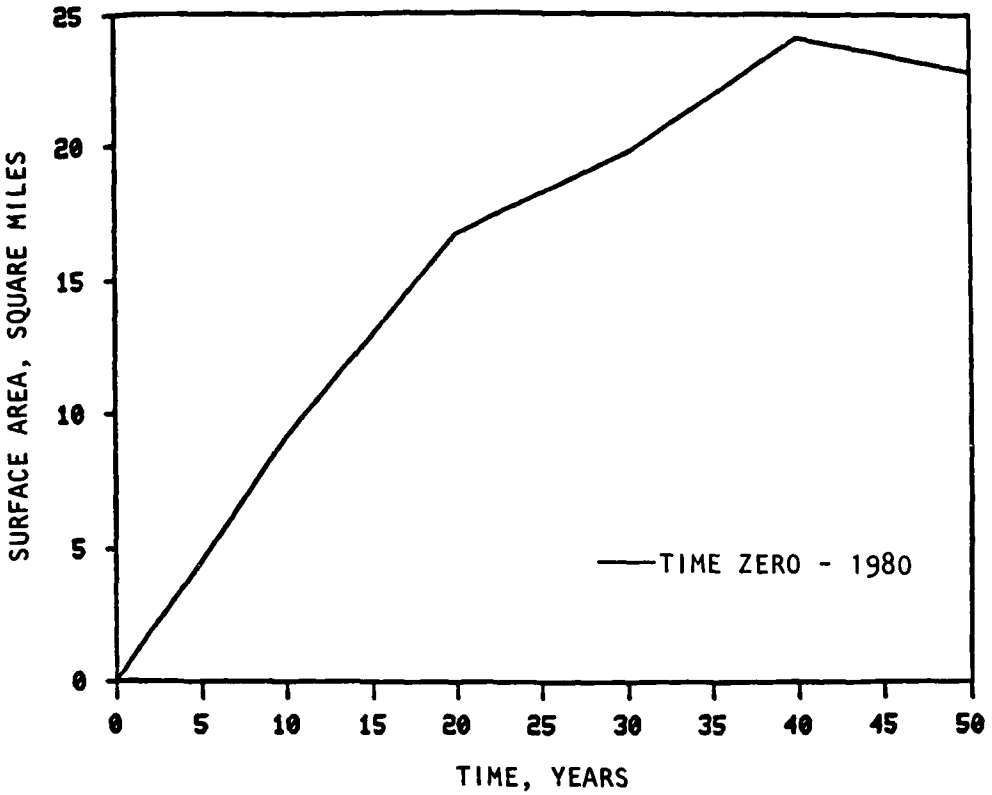

a. Predicted subaerial land growth

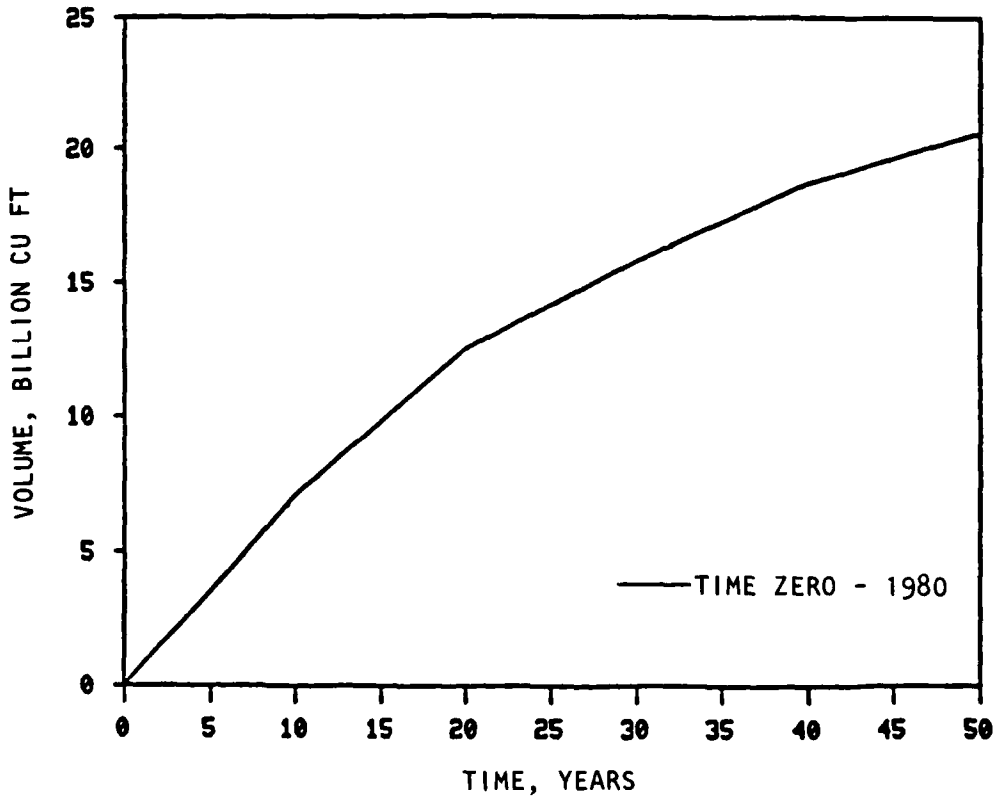

b. Predicted volume of deposition

Figure 27. Predicted delta growth in terms of new subaerial land and volume of deposition in the bay

the sediment yield at Eugene Island from that at the coastline. Accumulated deposits by sediment type are shown for the forecast period as is the accumulated total of sand/silt/clay. The percentage of each type present in the deposit is also shown for each decade and for the accumulated deposits. These percentages were used in Equation 3 to determine the composite unit weight of deposits, and the results are shown in Table 18. Silt and clay sediments consolidate with time, and Equation 5, along with coefficients shown in Equations 6 and 7, was used to predict future unit weights. The resulting depths of deposit, shown in Table 19, were calculated with values from Tables 17 and 18.

106. Whereas the accumulated depth of the sediment deposit continually increases with time as shown in the last column of Table 19, Figure 27 shows that subaerial land growth peaks at year 40 and declines during the next decade. That increase in depth of deposits was expected, but the decrease in subaerial land over the entire delta was a surprise. Several reasons have been considered: (a) poor model performance in that the model is not properly simulating the prototype; (b) the Atchafalaya and Mississippi River deltas must be studied together since either is only a subdelta of the whole; (c) subdeltas are subject to local fluctuation in sediment availability and hydraulic controls; and (d) subsidence is allowing land to sink below the water surface at too high a rate in the model. These are discussed in the following paragraphs.

107. Regarding model performance, the decrease in subaerial land does not seem to be related to the detailed cell-by-cell deposition process. Since adjustment included a check against total volume deposited, model performance should adequately forecast the total land surface.

108. Wells, Chinburg, and Coleman (1984) studied the combined growth of the Atchafalaya and Mississippi River deltas in a generic analysis of this river system. Concentrating on subdeltas, they discovered the growth and decay of subaerial lands was a common characteristic in the delta growth process. Even when subdeltas were combined, the decrease in subaerial land was a common occurrence. Not all subdeltas peaked at the same time, and the access to sufficiently accurate data limited the study to the most recent 50-100 years. Consequently, the next inflection point in the growth curve, the point where the decline in area ceases and growth resumes, is beyond this forecast period.

109. Regarding local fluctuations in sediment availability and hydraulic controls, the HAD-1 model indicated that both of these affected the growth and decline of subaerial land. The average amount of sediment entering the bay during the forecast period, from Table 16, is 660 million tons per decade with a standard deviation of 22 million tons whereas the average amount discharged from the bay is 515 million tons per decade with a standard deviation of 70 million tons. Two points are pertinent. First, beginning the decade 10-20 years into the forecast in Table 16, 553 million tons of sediment is being transported out of the bay which exceeds the average for the forecast period. Second, the standard deviation of outflow, 70 million tons, is three times that of the inflow, 22 million tons, showing the relatively large fluctuations in local sediment yield from one decade to the next. Such fluctuations are also logical in nature and would indeed contribute to shifts between growth and decline of the prototype delta.

110. Vegetation growth on subaerial land is a significant hydraulic control in the prototype. It was reproduced in the HAD-1 model by increasing n values from 0.025 for subaqueous to 0.20 for subaerial land. That shift reduces the conveyance of water over subaerial land; and even though deposition should have become more likely, the quantity of deposited sediment was reduced.

111. Regarding the subsidence between years 30 and 40, the net gain in bed elevation was 0.15 ft over the bay. That comes from 0.62 ft of deposition (Table 19) and 0.47 ft of subsidence during that decade. During the following decade, the net gain in bed surface elevation relative to subsidence is predicted to be zero. Consolidation of the deposit is continuing. That trend is expected to continue until sand begins to dominate the deposition process. Thereafter subaerial land growth is expected to increase. According to HAD-1 predictions, that reversal will not occur during the 50-year forecast period.

Predicted delta configuration

112. The calculated delta configurations are shown in Plates 29-34 for year 0 through year 50, respectively. The TØ (base condition) delta corresponds to 1980 conditions as calculated by HAD-1 during adjustment. The resolution of the model grid is considerably coarser than the size of deltaic lobes presently visible in the prototype; however, the volume of sediment entering the bay has been adjusted to the prototype yield. Therefore the growth of

subaerial land in the model is slower than it has been in the prototype.

113. The year 10 (T10) delta shows considerable filling to the east of the navigation channel (Plate 30). Adjustment showed this portion of the model to fill at twice the rate of the prototype. Therefore, either the energy forces which dominate this portion of the prototype are not considered in the HAD-1 model or some activity is occurring in the field that is not included in the model. For example, there could be a cross current between Atchafalaya Bay and Four League Bay (Figure 4). That simulation is beyond the capability of HAD-1, but the next phase of this study will investigate cross currents using fully two-dimensional numerical models. Another possible factor is shell dredging in the prototype during the 1967-1977 time period. The difference in the quantity of bed sediment between model calculations and prototype bed change is 14 million cubic yards. Although no actual data are available, it is feasible to remove such a quantity during a decade. If that is the case, the two-dimensional models will also show deposition in this portion of the bay. A conclusion must await results from the more detailed two-dimensional modeling.

114. In assessing model behavior west of the navigation channel, it is interesting that the model showed a dominant channel developing toward the southwest from the present navigation channel. In this study the explanation is related to the geometry used in the model. That is, when the survey used as initial condition for these computations was made in 1961, a barrier reef separated Atchafalaya Bay from the Gulf of Mexico along the alignment from Eugene Island to Marsh Island as indicated in Figure 4. That condition is emulated at cross section 146.00 by setting the bed elevation at -2.0 across strips 4, 6, and 7. Consequently, flow passed either through the deep, 500-ft-wide outlet of strip 5, or over the shallow reef, or across Atchafalaya Bay toward the southwest. (Note: subsequent to this study, a fathometer survey of the bay conducted along the historical alignment of the barrier reef showed that the reef is gone. The depths from that survey were used in two-dimensional model grid, and the results from the two-dimensional model study will be better indicators of the likelihood of having a dominant channel which is misaligned with the navigation channel.)

115. The model showed new land extending the present coastline into the bay and extensive shoaling on the west side of Wax Lake Outlet.

116. During the next decade, ending with T20, the T10 trend continued

as subaerial land appeared east of the navigation channel, and shoals to the west became larger. By T30 the dominant flow channel had developed to the west, linking Wax Lake Outlet with the Lower Atchafalaya River and moving toward Marsh Island. The T40 and T50 deltas continued to grow in that same pattern. Superimposed on top of this general pattern will be the crow's foot delta associated with a sand system. Whereas the silts provide the largest volume of sediment and shape the subaqueous delta, sand deposition is expected to shape the subaerial land. That is, the sand particles are heavier than silt and therefore deposit in the center of the channel, forming islands which divide the flow. Silt particles are swept to either side of the main current forming side boundaries for the flow and are easily resuspended by waves.

117. Because the cell-by-cell adjustment was weak, an alternate delta shape was produced by adding the average depth of HAD-1 deposits in the bay to the 1977 hydrographic survey. That result is shown in Plate 35. The total volume of sediment is the same as that in Plate 34; only the pattern of delta growth is changed. The resulting surface area is 12,000 acres by year 50 as compared with 18,000 acres from the HAD-1 results. The volume of deposits at and above el -3 is 12 billion cubic feet as compared with 6 billion in the HAD-1 pattern, illustrating the reduction in sediment passing over subaerial land when hydraulic roughness was increased to reproduce vegetation growth. The one major difference between the delta pattern developed from the 1977 survey and average deposit as compared with the HAD-1 calculated pattern is the absence of the cross-bay channel. That suggests the reef did not exist in 1977 because that survey showed no accelerated deposition upstream (landward) from the historical location of the reef.

118. In summary, the two approaches for expressing the 50-year forecast differ by only 4.5 square miles of surface area in a total of 24 square miles. The pattern will probably be more like Plate 35 than Plate 34 because the reef no longer appears to control flow at any Gulf elevations. The delta will, by year 50, occupy 80 percent of the bay if defined as in Letter (1982) and Wells, Chinburg, and Coleman (1984). Those studies defined delta areas as that area where bed elevation is equal to or greater than el -3.

PART III: STAGES AND FLOW DISTRIBUTION STUDY WITH SOCHMJ

Introduction

119. SOCHMJ is an unsteady flow program which can simulate the movement of flows in a network of streams including closed loops (i.e., sometimes referred to as island flow). This fixed-bed calculation determines water-surface elevation, water velocity, water discharge, and flood wave travel time. Flow reversals are accommodated. The network of streams in this study, called the Multiple Channel Model (MCM), is illustrated in Figure 28.

120. Each "branch" of the network is numbered as well as each point where branches intersect, called junctions. The network starts at Simmesport, the upstream end of branch 1; it includes flows from Morganza, branch 2; and allows flows to exit the floodway through the Lower Atchafalaya River, branch 13; and the Wax Lake Outlet, branch 11. The interior of the basin is modeled by multiple interconnected channels called closed loops such that hydraulic calculations determine the amount and distribution of flow as the program routes the flood hydrograph through the system.

Study Area

121. The MCM network begins at the same points offshore as the HAD-1 grid but it extends further inland. The upstream boundaries are located at Simmesport, Atchafalaya River mile 4.7, and the Morganza control structure.

122. The resulting numerical model, MCM, consists of the computer program, SOCHMJ, plus the digital description of the network, channel overbank geometry, initial water discharge, initial water-surface elevations, and boundary conditions for inflows and tailwater controls. As in the case of the HAD-1 study, attention was focused on the Atchafalaya Bay. The upstream portion of the model was used only to establish the proper flow distribution into the bay. To forecast the effect of delta growth on flood stages, the results from HAD-1 were added to the 1977 geometric data for the MCM; and the 1973, 1975, and 58AEN project flood hydrographs were routed through the model. Stages at Morgan City/Calumet and Eugene Island were calculated.

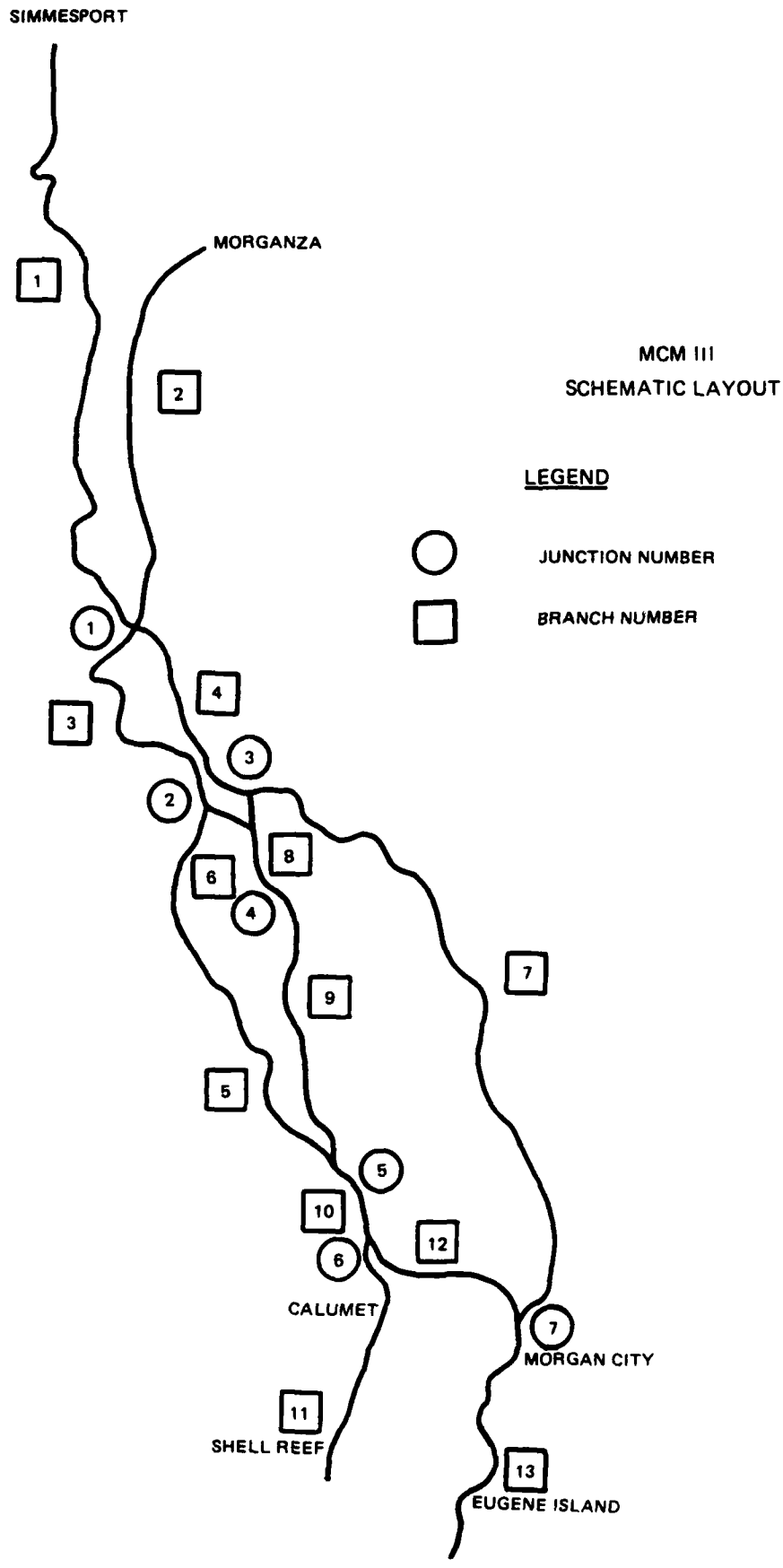

Figure 28. MCM network

Model Evolution

123. Three versions of the MCM were developed during the course of the study. The first, MCM I, was used to test the application of SOCHMJ to networks containing multiple closed loops at the scale of Atchafalaya and to test preliminary designs of the network system. MCM II, a partial implementation of the selected network, was used to expedite the first stage of adjustment by using the Calumet and Morgan City gages as the downstream boundary. MCM III, the full network implementation shown in Figure 28, was used to complete verification and to forecast the effects of deltaic growth on flood stages.

Network Design

124. The first step in the development of the MCM was to design a network which could reconstitute the magnitude, shape, and phase of a flood hydrograph passing through the Lower Atchafalaya River and the Wax Lake Outlet given the recorded discharge hydrograph at Simmesport, the recorded discharge hydrograph at Morganza, and the recorded water-surface elevations at Eugene Island. In addition, the selected network was required to distribute flows into each region of the basin in a manner that would reproduce the water-surface elevation and storage volume in that region.

125. As shown in Figure 18, 75 percent or more of the total flow at any section is accounted for by three primary channels down the basin: Atchafalaya River, Morganza Floodway to East Side, and West Side Floodway. However, a significant difference has been observed between water-surface elevation on the west side and the water-surface elevation on the east side of the basin for the same point in time.

126. To account for the lateral distribution of storage, more than three pathways were used in the MCM (Figure 28). In planform, each branch can be drawn as a quadrilateral region. Flow may enter and leave a region only through the ends; the sides are treated as barriers to flow. In the absence of obvious barriers, such as levees, the layout of branch boundaries is based largely on engineering judgment.

127. Topographic maps, cross-section plots, flow distribution estimates, and stage records from the prototype and MBM were used to identify obvious barriers to flow, the number of pathways needed in the model, and the

approximate location of branch boundaries. Additional sources of data used to refine the network were flooded area maps from the MBM, the computer program GEDA (Geometric Data from Cross-Section Coordinates) which calculated cross-section properties such as incremental conveyance and area across the section, and velocity vector plots from early runs of the two-dimensional, hydrodynamic model of Atchafalaya Bay.

128. Several attempts were made to develop quantitative procedures for determining branch and storage boundary locations. Some insights were gained into the behavior of the system during the development of these procedures, but the single most useful method of determining suitable branch and storage zone boundaries was observation of flow patterns in the MBM.

129. The MCM III has 13 branches, 7 junctions, and 4 exterior boundary nodes. Branch 1, as shown in Plate 36, is the leveed reach of the Atchafalaya River from the discharge range at Simmesport, Louisiana, to its junction with the WBPC at river mile 55. Branch 2 (Plate 37) is the Morganza Floodway from the Morganza Control Structure to the cross section marking the lower end of branch 1. Branch 3 (Plate 38) represents the old, main channel of the Atchafalaya River from its junction with the WBPC to its junction with the West Freshwater Diversion Channel near the Bayou La Rompe No. 10 gaging station. Branch 4 (Plate 39) represents the WBPC from its junction with the Atchafalaya River to its junction with the East Freshwater Diversion Channel (Little Tensas Bayou). Branch 5 (Plate 40) represents the West Freshwater Diversion Channel from its junction with the old main channel of the Atchafalaya River to the West Floodway Channel and along the western levee to a junction with the existing main channel of the Atchafalaya River near Myette Point. Branch 6 (Plate 41) represents the old main channel of Atchafalaya River from its junction with the West Freshwater Diversion Channel to its confluence with the WBPC. Branch 7 (Plate 42) represents the East Freshwater Diversion Channel from its junction with the WBPC to its junction with the East Floodway Channel and along the eastern levee to the main channel of the Atchafalaya River above Morgan City. Branch 8 (Plate 43) represents the WBPC (Lake Mongoulois) from its junction with the East Freshwater Diversion Channel to its confluence with the old main channel of the Atchafalaya River. Branch 9 (Plate 44) represents the Atchafalaya River from its confluence with the WBPC to its confluence with the Western Floodway. Branch 10 (Plate 45) begins at the lower end of branches 5 and 9, and ends near the upper end of Cypress

Island where a portion of the flow is diverted toward the Wax Lake Outlet. Branch 11 (Plate 46) begins at the lower end of branch 10 and represents a portion of Grand Lake, the Wax Lake Outlet, the western third of Atchafalaya Bay, and a portion of the Gulf of Mexico. Branch 12 (Plate 47) representing Six Mile Lake, begins at the lower end of branch 10 and ends at the confluence of Strouts Pass and the Eastern Floodway. Starting at this confluence, branch 13 (Plate 48) represents the Lower Atchafalaya River, the eastern two-thirds of Atchafalaya Bay, and a portion of the Gulf of Mexico.

Network Performance

130. Because some of the prototype's two-dimensional behavior could not be reproduced by the SOCHMJ model, the network design incorporated two major compromises. First, in circumstances where the model could not accurately reproduce both low and high flows, the network was designed to reproduce high flows. Second, in conflicts between the upper and lower parts of the basin, the network was designed to reproduce events in the lower parts of the basin with greater accuracy. For example, the East and West Access Channels were not included in the network because they would have interrupted the longitudinal pathways down the east and west sides of the basin that exist under high flow conditions. In order to preserve the flow distribution in the lower parts of the basin, the flow that would have been diverted away from the main channel by the East and West Access Channels was added to the flow in the East and West Freshwater Diversion Channels.

Geometric Data

131. Cross-section locations are shown in Figure 29. Cross sections of the Upper Atchafalaya River, the Lower Atchafalaya Basin Floodway, and the marsh were derived from the 1974-1976 Atchafalaya River Hydrographic Survey (USAED, New Orleans, 1977a), topographic maps, and cross sections developed by New Orleans District for HEC-2 and HEC-6 studies of the basin (USAED, New Orleans, Appendix C). Morganza Floodway cross sections were digitized from USGS 7.5-min topographic maps. Cross sections of the Atchafalaya Bay were developed from the 1977 hydrographic survey furnished by New Orleans District.

132. Each cross section was partitioned into three to seven subsections. Channel subsections were assigned an initial Manning's n value of

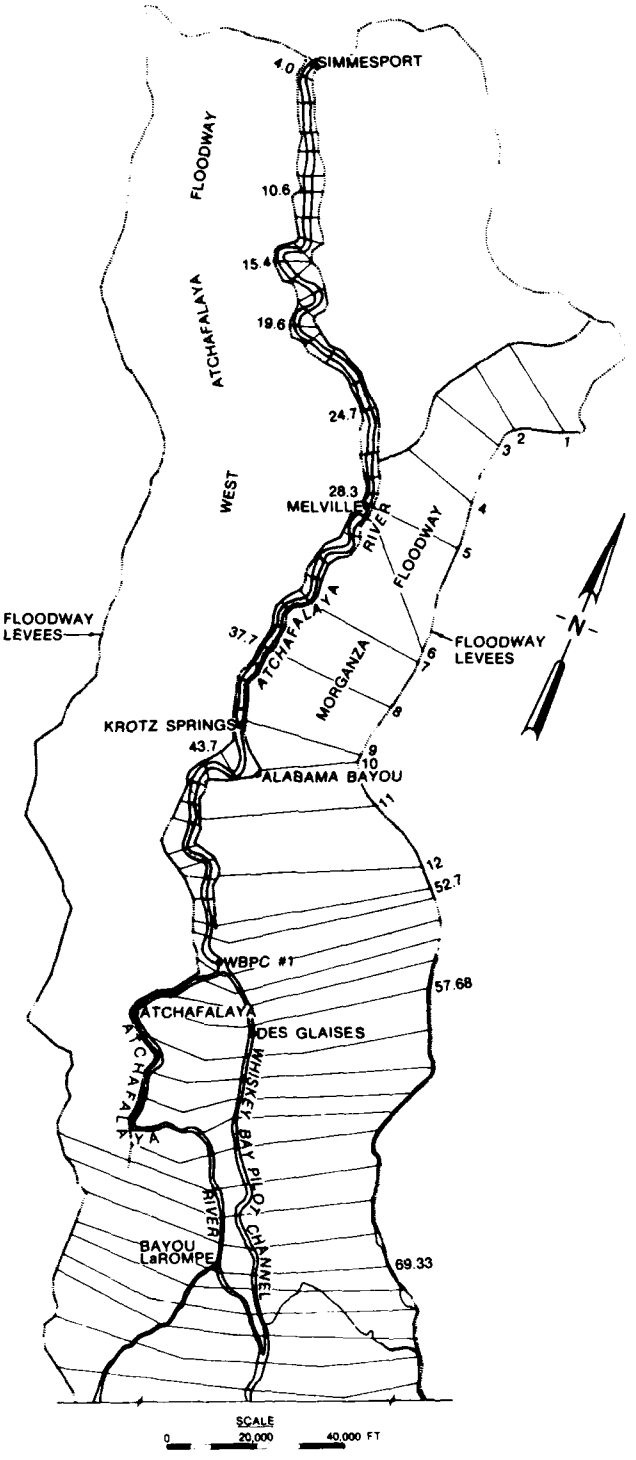

Figure 29. Cross-section locations, MCM (Continued)

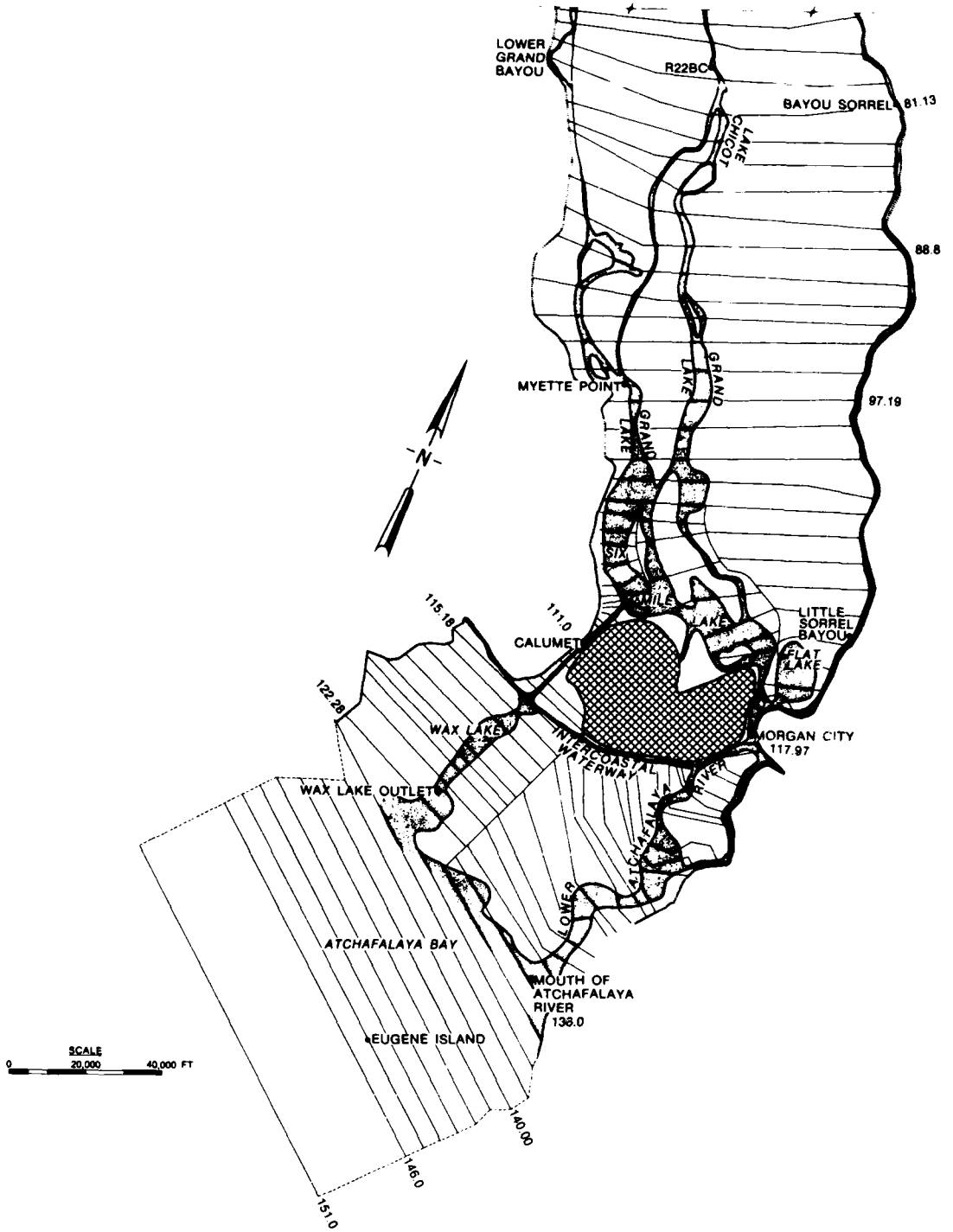

Figure 29. (Concluded)

0.030; a value of 0.140 was used for overbank subsections; and a value of 0.025 was used in Atchafalaya Bay. The cross-section geometry was processed with the computer program GEDA, and the resulting geometric data tables were saved for input into SOCHMJ. A summary of branch characteristics, including spatial step size ΔX , is given in Table 20.

Boundary Conditions

133. SOCHMJ is a flood-routing model which solves boundary value problems. That is, for prescribed hydrographs of water discharge or stage at the external boundaries of the MCM network, SOCHMJ calculates the water-surface elevation, water discharge, and flow velocity at all internal computational nodes and junctions. There are two types of boundaries: (a) the computational node at the model limit and (b) lateral inflow (i.e., a tributary or rainfall input) at the internal computational nodes.

134. There are four external boundary locations in the MCM network: (a) the Simmesport gage, (b) the Morganza Control Structure, (c) the Gulf end of the Wax Lake Outlet branch, and (d) the Gulf end of the Lower Atchafalaya River branch. In addition, a lateral inflow point was included near the Bayou La Rompe No. 10 gage for the project design flood discharge from the West Atchafalaya Floodway.

135. During model adjustment, a series of steady state water discharges were run from the Simmesport boundary to Morgan City and Calumet. These started at 50,000 cfs and ranged up to 450,000 cfs. Later, 350,000-cfs and 800,000-cfs steady flow discharges were run all the way to the Gulf. MBM data were used to adjust n values and the flow distribution among the several branches.*

136. Later in the verification tests, the 1973 and 58AEN flood hydrographs from the MBM were run in SOCHMJ. The 58AEN hydrograph is a version of the design flood producing 1.5 million cubic feet per second at Eugene Island. The 1975 flood hydrograph and corresponding Eugene Island gage record provided the one prototype data set analyzed.

---

* Personal Communication, 29 May 1979, WESHR, from H. B. Simmons, WES, to District Engineer, USAED, New Orleans, New Orleans, La., subject: "Transmittal of Test Results for Hypothetical Flood 58AEN (Modified) in the Atchafalaya Basin Portion of the Mississippi Basin Model."

137. Recorded peaks at the latitude of Morgan City/Calumet are shown in the following tabulation along with the stage for the project design flood, the 58AEN hydrograph, as predicted by the MBM.

	Morgan City		Calumet		
	Flow 1,000 cfs	Stage, ft*	Flow 1,000 cfs	Stage, ft*	Total Flow 1,000 cfs
1975 Flood	511	7.95 (18 Apr)	205	8.82 (19 Apr)	716
1973 Flood	692	10.53 (23 May)	272	11.02 (26 May)	964
58AEN Hydrograph**		18.3			

* Stages are given in feet referred to mean sea level.
** MBM data.

Adjustment

138. Water-surface elevations from the steady-flow adjustment tests are shown in Tables 21 and 22 for 350,000 cfs and 800,000 cfs, respectively. Since the MBM was adjusted to 1973 flood conditions, the MBM results were considered adequate for this test. The adjustment parameter in SOCHMJ is a composite Manning's n value, and the final values are shown in Table 23.

139. The East Floodway branch, branch 7, was more difficult to adjust than the West Floodway branch because a geometry control is present near the upstream end. The control corresponds to Little Tensas Cut/Upper Grand River/East Freshwater Diversion Channel in the prototype, and indicates that the natural overbank is a very inefficient passage for conveying water away from the main channel.

140. The old Atchafalaya River Channel near the Atchafalaya gage, branch 3, showed the most difference between MCM and MBM water-surface elevations, -1.1 ft at 800,000 cfs. This is acceptable because the location is well away from the study area.

141. The flow distribution calculated with SOCHMJ is superimposed in Figure 30, the results from van Beek et al. (1979). This comparison shows very good agreement between MCM and prototype flow distribution.

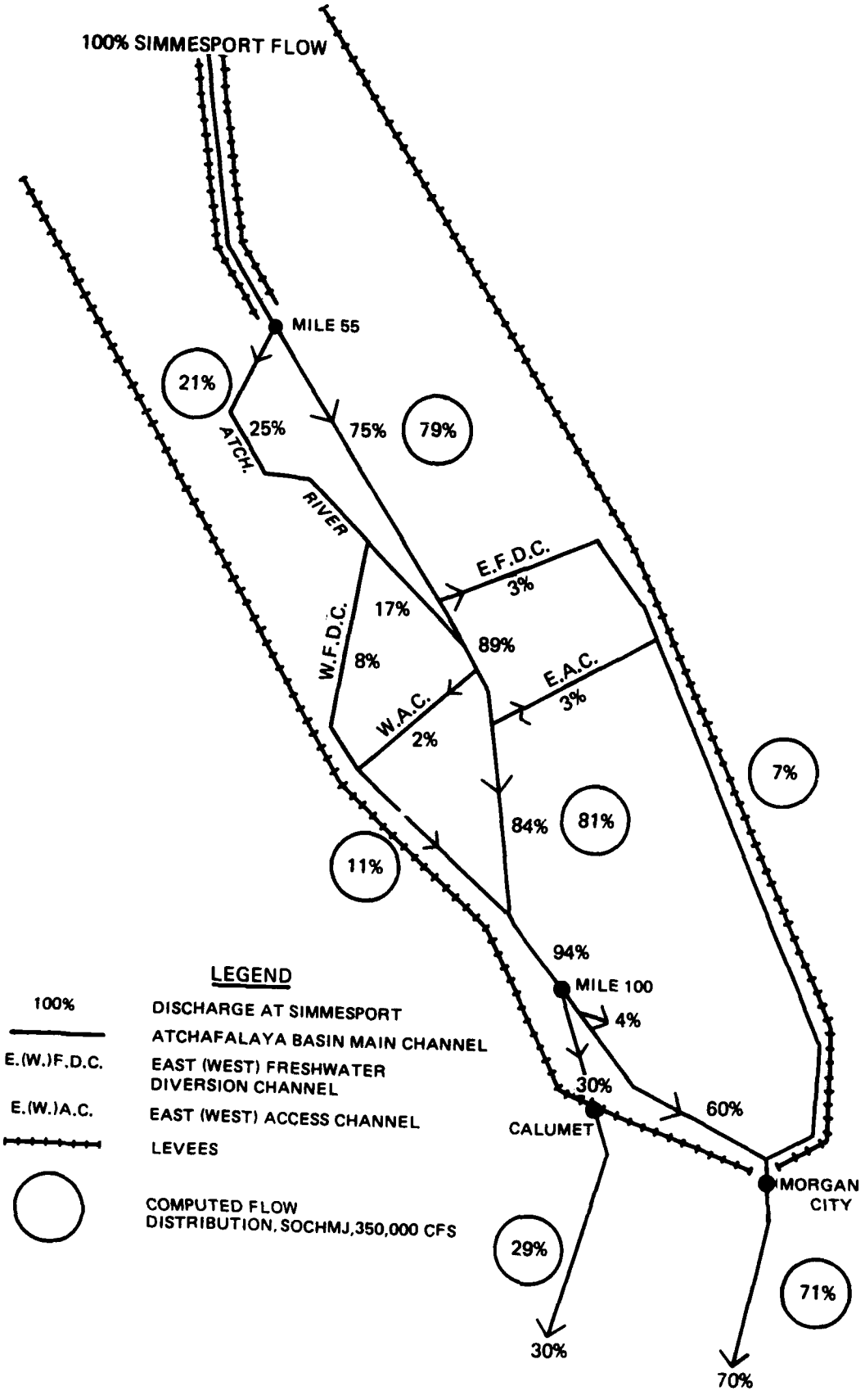

Figure 30. Comparison of flow distribution calculated with SOCHMJ and by van Beek et al. (1979)

Verification

142. The 1973 and 1975 flood hydrographs were also used in the verification process. Peak water-surface profiles, peak water discharges, and hydrograph shape are the parameters observed in this test. Only the 1975 results are described here because they reflect prototype data. The 1975 Simmesport inflow and Eugene Island tailwater are shown in Plates 49 and 50, respectively. Plates 51 and 52 are calculated stages at Morgan City and Calumet, respectively. Plates 53 and 54 are the corresponding discharge hydrographs at Morgan City and Calumet; and although discharge is a much more sensitive parameter than stage, the MCM reconstituted both the peak and shape of the hydrograph very nicely.

Forecast

143. The delta deposit calculated with HAD-1 was transferred from the HAD-1 numerical model to the MCM by changing cross-section elevation. Figure 31 is a HAD-1 cross section showing the TØ and calculated T50 bed elevations for section 138.0. The amount of bed change is constant across a strip. These constants, called bed change in Tables 24 and 25, were added to the TØ (1977) SOCHMJ bed elevations to develop the T50 conditions. Since the T50 delta is expected to be vegetated, all new subaerial land was assigned n values equal to the present marsh values.

144. Future water-surface profiles were calculated for only one time--the end of the 50-year forecast period. These results are labeled as T50 conditions whereas the beginning of the forecast period is labeled TØ. In calendar time, the beginning of the forecast period coincides with the end of the adjustment period, which is 1977. However, the T50 delta and water-surface profiles are referred to as 2030 conditions, and the 50-year forecast is actually 53 years of simulation.

145. Three possible T50 futures were considered: (a) the delta deposit calculated with HAD-1 shown in Table 24; (b) a delta created by simply extending the present marsh geometry to Eugene Island without regard to the volume of sediment required to accomplish that extension; and (c) a delta having the volume of sediment predicted by HAD-1 calculations but deposited, starting at

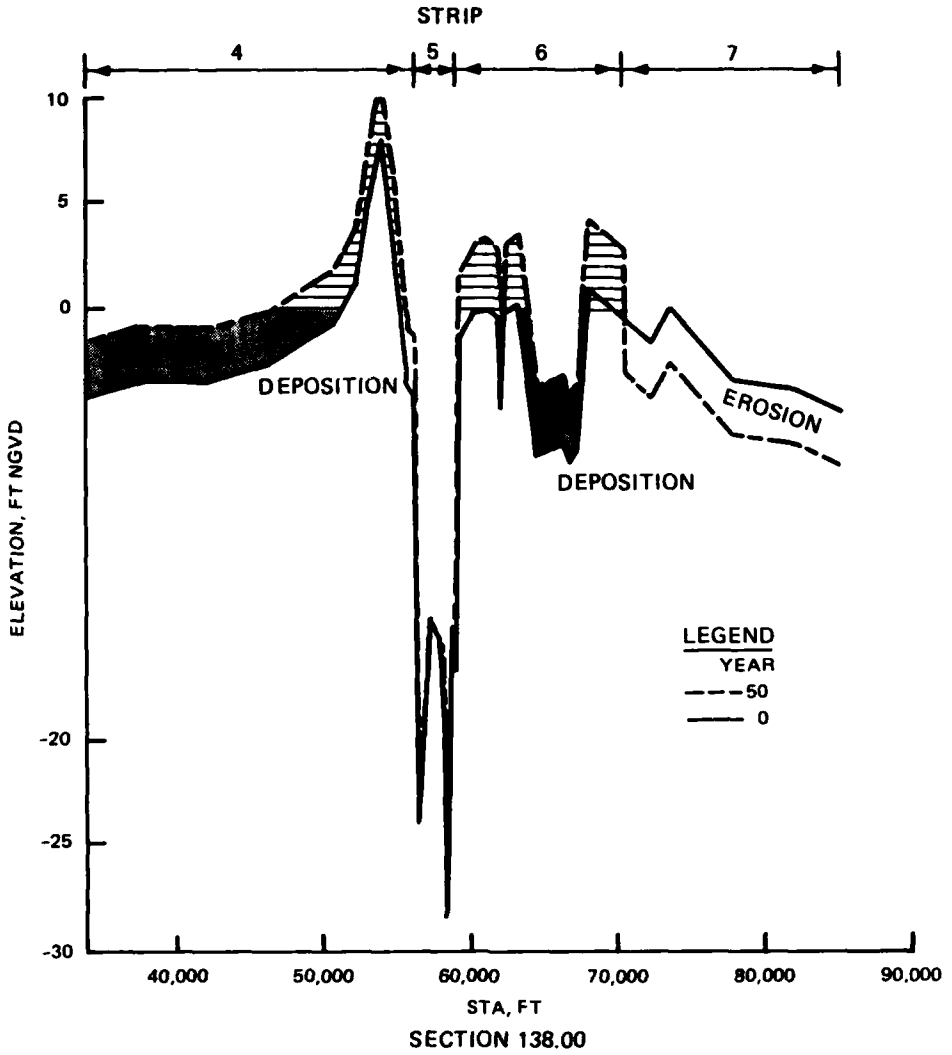

Figure 31. HAD-1 cross section showing TØ and T50 bed elevations (section 138)

the present coastline, oceanward as far as that volume permitted shown in Table 25.

146. The 1975, 1973, and 58AEN flood hydrographs were rerun in the MCM and results plotted over TØ conditions. Plate 55 illustrates the results of the 1975 hydrograph run. Both Wax Lake and the Lower Atchafalaya River are plotted as Atchafalaya River miles. The largest increase in water-surface elevation occurred at the location of the present coastline, mile 137. The TØ elevation is 3.4 ft and the T50 elevation is predicted to be 5.2 ft for the Lower Atchafalaya River outlet. The T50 water-surface profile approaches the TØ profile as distance from the coastline increases. By Morgan City, mile 117.6, the predicted water surface is only 0.6 ft higher than present

conditions. Table 26 shows the calculated stages at T0 and T50.

147. The rather modest change on the Wax Lake Outlet side of the bay demonstrated a similar pattern. Of particular interest are the water-surface profiles because the Wax Lake side is lower than the Lower Atchafalaya River side, indicating a gradient toward the west. That would produce the southwestern movement of water through the bay as indicated in HAD-1. A major factor in that prediction is the extent to which the shell reefs exist in the prototype. They extended over the eastern two-thirds of this model grid.

148. The rather small increase in calculated water-surface elevations at Morgan City/Calumet during the forecast period, 1980-2030, is the result of two processes: (a) subsidence in the HAD-1 model and (b) channel deepening as the delta building establishes a marsh along each side.

149. As the delta grows, water will be confined to the channel, resulting in erosion and the corresponding increase in conveyance. The stream slope across the present marsh is about 0.5 ft per mile. That converts to a head loss between Morgan City and Eugene Island of 13-14 ft. In the 1973 flood the head was measured at 10 ft. That additional 3-4 ft is a reasonable long-term estimate of water-surface rise, but computations indicate that a longer time than 50 years will be required to create the entire 3-4 ft.

150. The other factor is subsidence. The HAD-1 numerical model permitted a uniform subsidence rate over the entire grid. That was transferred to the MCM via the bed change. For example, Table 19 shows the quantity of deposits in the bay to amount to a depth of 4.57 ft. Subsidence, at the HAD-1 rate of 1.3 cm per year, amounts to 2.35 ft in 50 years. The nominal bed change is the difference between those two or a value of 2.2 ft. A realistic consideration of subsidence is also to let structures along the river subside. In that case, 2.4 ft should be added to all stage changes to determine what grade structures should be built to assure that protection 50 years in the future will be equivalent to that of today.

151. Profiles for the 1973 flood and the 58AEN hydrograph are shown in Plates 56 and 57, respectively. Eventually, this study was limited to the bay and the Lower Atchafalaya River. Therefore the basin portion of these models was not modified for T50 geometry. In addition, the bed of the Lower Atchafalaya River is sand, and as overbank deposition forced more water into the channel, degradation occurred. Wax Lake Outlet passes through a clay plug and no erosion was allowed. These two factors combine and shift outflows from Wax

Lake Outlet into the Lower Atchafalaya River in the future. The calculated values for the project design flood were 29 percent through Wax Lake Outlet and 71 percent in the Lower Atchafalaya River, presently shifting to 21/79 percent, respectively, for T50 conditions. The significance of this prediction is that two refinements should be made for the next phase of this study: (a) deposition should be considered inside the basin and (b) an estimate of the erodibility of the Wax Lake Outlet clay plug should be made.

Sensitivity of Water Profiles to Size and Shape of Delta

152. A sensitivity analysis of two conditions was tested. First, the existing coastline was extended to Eugene Island at the elevation of the present marsh, 2 ft. The channel in the present marsh, which is estimated to be half a mile wide and 40 ft deep, was extended along with the marsh geometry. The volume of deposition required to create such a deposit is estimated at 39 billion cubic feet (1.4 billion cubic yards). The expected value of the 50-year yield of sand, silt, and clay inflow at Simmesport is 140 billion cubic feet, and 40 billion of that is predicted to deposit before reaching the bay. Consequently, that condition could develop in 50 years; and since it represents an extreme case, it was tested. The results are shown in Plates 58, 59, and 60 for the 1975, 1973, and 58AEN flood peaks, respectively. Except for the 58AEN profile, they agree rather well with water-surface profiles for the delta predicted with HAD-1 upstream from river mile 130.

153. The second test was to accept the HAD-1 volume of deposits as being the best estimate, to start at the present coastline and marsh elevation, and to extend the delta into the bay until the volume of deposits was exhausted. That procedure set the T50 coastline at about river mile 142 of the HAD-1 grid. For the same channel size adopted in the preceding paragraph, no new information would be gained from this delta size; therefore, the impact of channel dimensions was introduced. The average channel width through the present marsh zone (i.e., between the intracoastal canal and the coastline) is estimated to be half a mile. Where the existing channel is that width, it is 40 ft deep. The present bay is only 4 ft deep, and it has a 400-ft-wide navigation channel maintained at 14 ft deep. The sensitivity question posed is "What water-surface profile would result if the present bed of the bay cannot erode as the marsh zone grows toward Eugene Island?" This result is shown in

Plates 58-60 as the remolded HAD-1 volume. It shows that the ultimate water-surface profile will depend more strongly on the ultimate size of the channel cross section which develops through the bay than it will on the size, shape, or roughness of the delta deposit.

PART IV: DISCUSSION OF RESULTS AND CONCLUSIONS

154. Although the model limits in this study extend from the Gulf, 6 miles beyond Eugene Island, to well inside the floodway, the study area is limited to Atchafalaya Bay (i.e., in terms of the grid, cross sections that correspond to Atchafalaya River mile 137 to Atchafalaya River mile 145). These locations correspond to the present coastline and Eugene Island shell reefs, respectively. The surface area of the bay is 200 square miles, and the average water depth in the 1977 survey was 5 ft.

155. Although the tidal range is less than a foot, setup and setdown of the Gulf water surface ranged from +3.8 to -3.5 ft at the Eugene Island gage. Seasonal trends in Gulf water-surface elevation at Eugene Island ranged from a low of 0.7 ft for the average of all Januarys to a high of 1.6 for the average of all Augusts.

Sedimentation

156. Adjustment of HAD-1 was satisfactory for total quantity trapped in the basin and deposited in the bay, for the distribution of water and sediment between the Lower Atchafalaya River and the Wax Lake Outlet, and for the distribution of sediment deposits by strips west of the Lower Atchafalaya River. More deposition occurred east of the navigation channel in the model than detected by the prototype surveys. Two possibilities for that are proposed: Either (a) a strong cross current between Four League Bay and the vicinity of Eugene Island prevents water from flowing toward Point Au Fer or (b) shell dredging removed bed sediments from the prototype. The quantity of dredging would have had to be only 13 million cubic yards between 1967 and 1977 to cause the difference between prototype and HAD-1 behavior.

157. The increase in subaerial land peaked at about 24 square miles in year 40 and decreased during the next decade to about 22-1/2 square miles. Three factors in the decline in subaerial land are as follows: (a) the sediment yield at the coastline increases from year 0 to year 20, then remains about constant from year 20 to year 40, (b) during the decade of years 30 to 40, predicted sediment transport through the bay becomes much more efficient resulting in a smaller quantity of deposits than in the earlier decade, and (c) apparent subsidence continues at the constant rate of 1.3 cm per year

causing previously formed subaerial deposits to sink beneath the water surface.

158. Wells, Chinburg, and Coleman (1984) showed a similar trend in the generic analysis approach. They show the peak growth occurring in year 50 and the reduction in subaerial land continuing for 2 decades thereafter. The generic analysis indicated the peak growth of new land would be 48-72 square miles or from 2 to 3 times that predicted by HAD-1. A major difference between the two study approaches is in the way the inflowing sediment discharge was treated. The generic analysis assumed historical growth rates and patterns in predicting the future. The HAD-1 used historical growth rates and sediment inflows to adjust the model, but it used predicted future water and sediment inflows to predict future delta growth. Presumably, if historical and future inflows were the same, the HAD-1 model should produce the same results as the generic analysis, but in this system the estimated future annual sediment yield is 80 percent of historical. That showed up in the HAD-1 delta forecast, but not in the generic approach.

159. Letter (1982) estimated the total deposition within his study grid will be 60 billion cubic feet of sediment, but that approach did not estimate the amount of newly formed, subaerial land surface. In comparison the HAD-1 model predicted a total deposition, within the model limits, of 57 billion cubic feet, a good agreement with Letter's results. The generic approach focused on land surface growth rather than total volume of the deposit.

160. Subaerial land in the HAD-1 study was defined to be those cells whose surface elevation was equal to or greater than el 0. Many cells in the grid fell slightly below zero, and to include a comparison with the original estimate of Garrett, Hawxhurst, and Miller,* the aerial extent of the -3 contour was also calculated. This resulted in 109 square miles inside the reef, that is 62 percent of the entire bay, plus 16 square miles outside the reef.

161. Total sediment yield at the coastline is estimated to be 3.3 billion tons which converts to 100 billion cubic feet. Trap efficiency of the bay is estimated to be about 25 percent of that yield with essentially all inflowing sand, 24 percent of the silt, and 5 percent of the clay depositing. Because 78 percent of the Simmesport sand discharge deposited before reaching the coastline, the major bay filling resulted from silts. Consequently, resuspension turned out to be important in the modeling process.

---

* CTH, op cit.

162. The preliminary investigation into subsidence revealed that it is a dominant process in the delta growth problem. Defined as apparent subsidence to include both sea level rise and all settlement type factors, the rate in Atchafalaya Bay is 1-4 cm per year. A value of 1.3 cm per year (2.4 ft per 50 years) was adopted for this study.

163. The sediment yield at Simmesport has decreased over the past 3 decades because sediment concentrations have decreased (Figure 12). This is probably the single most important boundary parameter to establish in forecasting delta growth because the water yield does not demonstrate such a trend. The concentrations used in this forecast reflect the decade of the 1970's with annual values ranging from 300 to 500 mg/ℓ.

Stages and Flow

164. When delta growth was translated into changes in water level, subsidence of the bay and marsh were considered along with increased vegetation. The net effect at Morgan City and Calumet was an increase in peak stage of about 1 ft for the design flood. The increased storage in the basin, resulting from the tendency to increase the stage at Morgan City/Calumet, did not significantly change the discharge.

Comparison to Other Approaches in This Study

165. The results from this phase of the overall study support the results from Wells, Chinburg, and Coleman (1984) and from Letter (1982). The study highlighted problem areas needing extra attention during the two-dimensional phase. Current patterns due to interaction between Atchafalaya and Four League bays or between Atchafalaya and Cote Blanche bays need defining since silt resuspension may be a dominant activity there. Subsidence rates are sufficiently high in the bay to require additional refinement. Of particular interest are different rates of subsidence between Morgan City, Calumet, and the bay. Deposition in the marsh zone should be considered in more detail since that affects the sediment yield at the coastline. The basin should be linked to the bay model for that same reason plus the fact that deposition in the basin will probably affect flow distribution between Morgan City and Wax Lake Outlets. The forecast should be extended beyond 50 years

since the model indicates the delta is on the verge of a more rapid growth at about that time.

166. Although modeling inside the basin was for the sole purpose of establishing boundary conditions for this delta, having the flood-routing model extend to Simmesport and Morganza makes it a potentially useful tool for routing floods through the basin.

REFERENCES

Adams, R. D., and Baumann, R. H. 1980. "Land Building in Coastal Louisiana: Emergence of the Atchafalaya Bay Delta," Center for Wetlands Resources, Louisiana State University, Baton Rouge, La.

Ariathurai, Ranjari, and Arulanandan, Kandiah. 1978 (Feb). "Erosion Rates of Cohesive Soils," Technical Note, Journal, Hydraulics Division, American Society of Civil Engineers, Vol 104, No. HY2, pp 279-283.

Ariathurai, R., MacArthur, R. C., and Krone, R. B. 1977. "Mathematical Model of Estuarial Sediment Transport," Technical Report D-77-12, US Army Engineer Waterways Experiment Station, Vicksburg, Miss.

Benjamin, Jack R., and Cornell, C. Allin. 1970. Probability, Statistics and Decision for Civil Engineers, McGraw-Hill, New York.

Coleman, C. J., Teeter, A. M., Donnell, B. P., Fisackerly, G. M., Crouse, D. A., Parman, J. W. 1988 (Jun). "The Atchafalaya River Delta; Field Data," Technical Report HL-82-15, Report 2, US Army Engineer Waterways Experiment Station, Vicksburg, Miss.

Johnson, B. H., and Senter, P. K. 1973 (Jun). "Flood Routing Procedure for the Lower Ohio River," Miscellaneous Paper H-73-3, US Army Engineer Waterways Experiment Station, Vicksburg, Miss.

Keown, M. P., Dardeau, E. A., Jr., and Causey, E. M. 1980. "Characterization of the Suspended-Sediment Regime and Bed-Material Gradation of the Mississippi River Basin," Potamology Investigations Report 22-1, US Army Engineer Waterways Experiment Station, Vicksburg, Miss.

Keown, M. P., Dardeau, E. A., Jr., and Kennedy, J. G. 1977 (Mar). "Inventory of Sediment Sample Collection Stations in the Mississippi River Basin," Technical Report M-77-1, US Army Engineer Waterways Experiment Station, Vicksburg, Miss.

Krone, R. B. 1962 (Jun). "Flume Studies of the Transport of Sediment in Estuarial Shoaling Processes," University of California, Berkeley, Calif.

Letter, J. V., Jr. 1982 (Jul). "The Atchafalaya River Delta; Extrapolation of Delta Growth," Technical Report HL-82-15, Report 3, US Army Engineer Waterways Experiment Station, Vicksburg, Miss.

McAnally, W. H., Jr., and Heltzel, S. B. "A Plan for Predicting the Evolution of Atchafalaya Bay, Louisiana" (in preparation), Technical Report HL-82-15, Report 1, US Army Engineer Waterways Experiment Station, Vicksburg, Miss.

McAnally, W. H., Jr., Thomas, W. A., Letter, J. V., Jr., Stewart, J. P. 1984 (Jul). "The Atchafalaya River Delta; Interim Summary Report of Growth Predictions," Technical Report HL-82-15, Report 6, US Army Engineer Waterways Experiment Station, Vicksburg, Miss.

Roberts, H. H., Adams, R. D., and Cunningham, R. H. W. 1980 (Feb). "Evolution of Sand-Dominant Subaerial Phase, Atchafalaya Delta, Louisiana," American Association of Petroleum Geologists Bulletin, Vol 64, No. 2, pp 264-279.

Shen, Hsieh Wen, ed. 1971. River Mechanics (In 2 vols), Colorado State University, Fort Collins, Colo.

Shlemon, R. J. 1973. "Atchafalaya Bay, Louisiana: Regional Subsidence and Contemporary Delta Formation," Transactions, Gulf Coast Association of Geological Societies, Vol 23, pp 22-26.

_____. 1975. "Subaqueous Delta Formation-Atchafalaya Bay, Louisiana," Deltas: Models for Exploration, M. L. Broussard, ed., Houston Geological Society, Houston, Tex., pp 209-221.

Schlemon, R. J., and Gagliano, S. M. 1972. "Birth of a Delta, Atchafalaya Bay, Louisiana," 24th International Geological Congress, Sec. 6, Montreal, Canada, pp 437-441.

Swanson, R. L., and Thurlow, C. I. 1973. "Recent Subsidence Rates Along the Texas and Louisiana Coasts as Determined from Tide Measurements," Journal of Geophysical Research, Vol 78, pp 2665-2671.

Tuttle, J. R., and Combe, A. J., III. 1981 (Oct). "Flow Regime and Sediment Load Affected by Alterations of the Mississippi River," Proceedings, National Symposium on Freshwater Inflow to Estuaries, US Department of the Interior, US Fish and Wildlife Service, Vol 1, pp 334-348.

US Army Engineer District, New Orleans. "A Feasibility Report/Environmental Impact Statement on the Atchafalaya Basin Floodway System, Louisiana" (draft), Vols 1-5, New Orleans, La.

_____. 1967 (Jun). "Atchafalaya River Hydrographic Survey, 1962-1964; Old River to Atchafalaya Bay Including Main Channel and Distributaries," New Orleans, La.; prepared for Mississippi River Commission, Vicksburg, Miss.

_____. 1977a (Jul). "Atchafalaya River Hydrographic Survey, 1974-1976; Old River to Atchafalaya Bay Including Main Channel and Distributaries," New Orleans, La.; prepared for Mississippi River Commission, Vicksburg, Miss.

_____. 1977b. "Stages and Discharges of the Mississippi River and Tributaries and Other Watersheds in the New Orleans District," New Orleans, La.

US Geological Survey. 1977. "Hydrology and Water Quality of the Atchafalaya River Basin," Water Resources Technical Report No. 14, US Department of the Interior, Washington, DC; in cooperation with Louisiana Department of Transportation and Development, Office of Public Works, Baton Rouge, La.

van Beek, J. L., Harmon, A. L., Wax, C. L., Wicker, K. M. 1979 (Nov). "Operation of the Old River Control Project, Atchafalaya Basin; An Evaluation from a Multiuse Management Standpoint," EPA 600/4-79-073, US Environmental Protection Agency, Environmental Monitoring and Support Laboratory, Las Vegas, Nev.

Vanoni, V., ed. 1975. "Sedimentation Engineering," Manual No. 54, American Society of Civil Engineers, New York.

Wang, F. C. 1985 (Sep). "The Atchafalaya River Delta; Analytical Analysis of the Development of the Atchafalaya River Delta," Technical Report HL-82-15, Report 7, US Army Engineer Waterways Experiment Station, Vicksburg, Miss.; prepared under Contract No. DACW39-81-C-0004 by Louisiana State University, Baton Rouge, La.

Wells, John T., Chinburg, Susan J., and Coleman, James M. 1984 (Jan). "The Atchafalaya River Delta; Generic Analysis of Delta Development," Technical Report HL-82-15, Report 4, US Army Engineer Waterways Experiment Station, Vicksburg, Miss.; prepared under Contract No. DACW39-80-C-0082 by Coastal Studies Institute, Louisiana State University, Baton Rouge, La., for US Army Engineer District, New Orleans, New Orleans, La.

Table 1

Annual Water and Sediment Yields at Simmesport*

Water Year (Oct-Sep)	Total Measured Sediment Load 1,000 tons	Sand/Silt Ratio** Sand 1,000 tons	Sand %	Silt 1,000 tons	Silt %	Water Year Discharge 1,000 DSF†	Average Sediment Concentration, ppm
1951-1952	196,000	49,000	25	147,000	75	80,800	900
1952-1953	135,000	28,000	21	107,000	79	57,000	880
1953-1954	54,100	13,000	24	41,000	76	32,000	627
1954-1955	93,400	24,100	26	69,300	74	50,400	686
1955-1956	67,200	15,500	23	51,700	77	49,100	507
1956-1957	225,000	55,000	25	170,000	75	74,100	1,126
1957-1958	214,000	48,000	22	166,000	78	89,400	887
1958-1959	83,200	20,900	25	62,300	75	55,700	553
1959-1960	132,000	24,000	18	108,000	82	69,300	704
1960-1961	133,000	40,000	30	93,000	70	76,800	643
1962-1963	44,900	8,600	19	36,300	81	47,100	353
1963-1964	52,600	10,400	20	42,200	80	33,100	588
1964-1965	109,000	28,000	25	81,000	75	66,400	607
1965-1966	88,500	17,500	20	71,000	80	51,000	642
1966-1967	55,700	6,800	12	48,900	88	57,300	360
1967-1968	121,000	16,000	14	105,000	86	80,100	561
1968-1969	115,000	27,000	24	88,000	76	83,300	512
1969-1970	75,100	19,800	26	55,300	74	74,300	374
1970-1971	72,400	19,600	27	52,800	73	71,700	374
1971-1972	89,600	18,700	21	70,900	79	75,400	440
1972-1973	124,000	45,000	36	79,000	64	140,000	329
1973-1974	143,000	32,000	23	111,000	77	117,000	453
1974-1975	158,000	35,000	22	123,000	78	117,000	499
1975-1976	56,100	8,500	15	47,600	85	65,900	315
1976-1977	57,100	6,000	11	51,100	89	47,800	443
1977-1978	71,200	12,500	18	58,700	82	79,700	331
1978-1979	112,300	25,500	23	86,800	77	104,800	346
Average	108,000	25,000	23	83,000	77	72,000	500

* Personal Communication, 1980, to W. A. Thomas, US Army Engineer Waterways Experiment Station, Vicksburg, Miss.

** The sand fraction is the material retained on the No. 230 sieve (0.062 mm). The silt fraction includes all of the fine material passing the No. 230 sieve.

† DSF = day-second-feet (cubic feet per second for 1 day).

Table 2

Average Annual Suspended Load Budget, Atchafalaya River

(Roberts, Adams, and Cunningham 1980, reprinted by permission of American Association of Petroleum Geologists)

Fraction	Input for Simmesport (near Diversion Point)		Distribution of Input						
			Basin Retention		Wax Lake Outlet		Lower Atchafalaya River		Total
	1,000 tons	%	1,000 tons	%	1,000 tons	%	1,000 tons	%	%
			1967-1971						
Sand	19,342	22	14,491	75	1,153	6	3,968	19	100
Sand/Clay	67,905	78	10,179	15	15,590	23	42,136	62	100
Total	87,247	100	24,670	29	16,743	19	45,834	52	100
			1973-1975						
Sand	37,506	25	3,668	10	5,748	15	28,090	75	100
Silt/Clay	100,704	75	21,256	19	21,789	20	67,650	61	100
Total	148,210	100	24,924	17	27,546	19	95,740	65	100

Note: Computations from measured data and sediment rating curves, USACOE.

Table 3

Stage Data Available

Station Name Available	Station No.	1 9 3 9 0	1 9 4 1 2	1 9 5 3 4	1 9 6 5 6	1 9 7 7 8	1 9 8 9 0
Atchafalaya River at Barbre Landing, LA	03015	**********	**********	**********	**********	**********	**********
Atchafalaya River at Simmesport, LA	03045	**********	**********	**********	**********	**********	**********
Atchafalaya River at Melville, LA	03060	**********	**********	**********	**********	**********	**********
Atchafalaya River at Krotz Springs, LA	03075	**********	**********	**********	**********	**********	**********
Atchafalaya River at Atchafalaya, LA	03090	--**********	**********	**********	**********	**********	**********
Atchafalaya River at Butte La Rose, LA	03120	**********	**********	**********	**********	**********	**********
Bayou La Rompe at Lake Long, LA	03210	---0000000000000	----------	----------	-000-------	------**00	******
Whiskey Bay Pilot Channel Below Head, LA	03240	----------	----------	----------	-0**********	*0--***	******
Blind Tensas Cut Below Upper Grand River (LA)	03315	----------	----------	----------	-0**********	---0****	******
Bayou Chene Below Bayou Chene Cut (LA)	03420	----------	----------	----------	----------	----------	***
Chicot Pass at West Fork Chicot Pass (LA)	03465	----------	----------	----------	**********	**00****	******
Chicot Pass Near Myette Point (LA)	03540	----------	----------	----------	---------0	**********	******
Grand Lake at Charenton Floodgate (LA)	03550	----------	----------	----------	----------	----------	*****
Keelboat Pass Below Lake Chicot (LA)	03615	**********	**********	**********	**********	-----*****	******
Six Mile Lake Near Verdunville, LA	03645	----0**********	**********	**********	**********	**********	**********
Wax Lake Outlet at Calumet, LA	03720	----------0	**********	**********	**********	**********	**********
Lower Atchafalaya River at Berwick Lock (LA) (West)	03650	----------	----------	----------	**********	**********	******
Lower Atchafalaya River at Morgan City, LA	03780	**********	**********	**********	**********	**********	**********
Lower Atchafalaya River Below Sweet Bay Lake (LA)	03820	----------	----------	----------	**********	**********	******
Wax Lake Outlet Vicinity at Belle Isle, LA	03830	----------	----------	----------	----------	----------	--0**0**
Round Bayou at Deer Island (LA)	03850	----------	----------	----------	----------	----------	0****
Bayou Latenache Above Pointe Coupee Drainage Structure (LA)	40900	----------	----------	----------	---------0	**********	******
Bayou Latenache Below Pointe Coupee Drainage Structure	43500	----------	----------	----------	**********	**********	******
Bayou Courtableau Outlet Channel at Sta 225+00 (LA) (East Auto.)	49075	----------	----------	----------	---------0	**********	**********
WABPL (FWS) at Cleon, LA	49120	-----00-*--00000	----------	----------	-0**********	**********	******
WABPL Borrow Pit (FWS) at Opelousas Bay (LA)	49135	------0--0------00--00	----------	----------	----------	-0-0********	******
WABPL Borrow Pit (FWS) at Bayou Mersier (LA)	49150	----------	----------	-00000----	---0---0----	***----*****	******
WABPL (FWS) at Lower Grand Bayou (LA)	49195	----0000000000-0	**********	**********	**********	**********	**********
Arm of Grand Lake Near Crook Chene Cove (LA)	49197	----------	----------	----------	----------	----------	---00*
WABPL (FWS) at Little Lake Long (LA)	49230	----------	----------	----------	----------	----------	********
Buffalo Cove at Round Island (LA)	49235	----------	----------	----------	----------	----------	***
Bayou Fordoche Near Krotz Springs, LA	49255	----------	----------	----------	**********	**********	******
Alabama Bayou (FWS) at Sherburne, LA	49400	----------	----------	----------	----------	----------	********
Upper Grand River at Little Tensas Bayou (LA)	49440	----------	----------	----------	----------	----------	********
EABPL Borrow Pit (FWS) at Dixie Bayou (LA)	49510	----------	----------	---0---0----	--00--000000000000000		
EABPL Borrow Pit (FWS) at Ramah, LA (Above Railroad Fill)	49525	----------	----------	----------	--00--000000000000000		
EABPL Borrow Pit (FWS) at Ramah, LA (Below Railroad Fill)	49540	------00	--------0	---0----	-00--00000000000	-********	
Upper Grand River (FWS) at Dike (LA)	49670	----0000000000000	---0----	0********	000**********	**********	**********
EABPL Borrow Pit (FWS) at Bayou Sorrel Lock (LA)	49630	----------	----------	----------	-0**********	**********	**********
Big Bayou Pigeon (FWS) Near Pigeon, LA	49635	----------	-------000	----------	-00----------	----------	********
Old River (FWS) at Junction with GIWW	49645	-----0**000000000	---0----	----------	----------	----------	********
Intracoastal Waterway Near Pierre Pass, LA	49690	----------	----------	---0----	----------	--00**********	**********
Little Bayou Sorrel at Junction with GIWW (Morgan City-Port Allen Route)	49725	----------	----------	----------	----------	----------	---0********
Lower Grand River at Bayou Sorrel Lock, LA	52560	----------	----------	----------	*00-**********	**********	**********
Charenton Drainage Canal Near Floodgate (LA)	64400	----------	----------	**00**********	**********	**********	**********
Charenton Drainage Canal at Baldwin, LA	64450	----------	----------	0**********	**********	**********	**********
Bayou Teche at West Calumet Floodgate (LA)	64650	----------	----------	----------	-0**********	**********	**********
Bayou Teche at East Calumet Floodgate (LA)	64700	----------	----------	----------	-0**********	**********	**********
Vermilion River Near Bancker, LA	67875	----------	----------	----------	----------	**********	**********

(Continued)

Note: This information was extracted from "Stages and Discharges of the Mississippi River and Tributaries and Other Watersheds in the New Orleans District" for 1977.

Any data available prior to 1929 were ignored.

Data available throughout a year on a daily basis signified by "*."

Data available partially or intermittently during a year signified by "0."

Unless specified otherwise, the notes refer to feet msl. Example: 3.81(-74) means gage zero was 3.81 ft msl thru 1974. 0.00(75-) means gage zero was 0.00 ft msl from the beginning of 1975 to the present.

The pamphlet is very hard to decipher in respect to changes in gage zero over the years and is ambiguous as to the meaning of the "to" in respect to the years that data were collected. (Example: does 1933 to 1941 mean 1933 thru 1940 or 1933 thru 1941). "To" is assumed to mean "to," not "thru."

The gage zero information was so difficult to decipher that it is strongly recommended that this information be reverified.

Table 3 (Concluded)

Station Name Available	Station No.	1 9 3 9 0	1 9 4 1 2 3 4 5 6 7 8 9 0	1 9 5 1 2 3 4 5 6 7 8 9 0	1 9 6 1 2 3 4 5 6 7 8 9 0	1 9 7 1 2 3 4 5 6 7 8 9 0	1 9 8 1 2 3 4 5 6 7 8 9 0
Bayou Boeuf (IWW) at Bayou Boeuf Lock (LA) (East)-----	76360				0**********		
Bayou Boeuf (IWW) at Bayou Boeuf Lock (LA) (West)-----	76400				0**********		
Intracoastal Waterway at Wax Lake----------	76440				0**********		
Wax Lake East Borrow Pit (LS) Near Calumet, LA (North)	76460					0-0--000	
Wax Lake East Drainage Area at Control Structure (LA)-	76480				0**********		
Wax Lake West Drainage Area at Control Structure (LA)-	76520				0**********		
Intracoastal Waterway at Wax Lake---------- West Control Structure	76560				0**********		
Freshwater Canal Above Reef Ridge (LA)----------	76590					0**********	
Freshwater Canal at Freshwater Bayou Lock (LA) (South)	76593					0**********	
Schooner Bayou (Inland Waterway) at Control---------- Structure (LA) (East Auto.)	76600	**********	**********	**********	**********	**********	**********
Schooner Bayou (Inland Waterway at Control---------- Structure (LA) (East Staff)	76640	**********	**********	**********	**********	**********	**********
Schooner Bayou (Inland Waterway) at Control---------- Structure (LA) (West)	76680	**********	**********	**********	**********	**********	**********
Intracoastal Waterway at Vermilion Lock---------- (LA) (East Auto.)	76720		0**********	**********	**********	**********	**********
Intracoastal Waterway at Vermilion Lock---------- (LA) (East Staff)	76760		0**********	**********	**********	**********	**********
Intracoastal Waterway at Vermilion Lock (LA) (West)---	76800		0**********	**********	**********	**********	**********
Intracoastal Waterway at Calcasieu Lock (LA) (East)---	76880			**********	**********	**********	**********
Atchafalaya Bay Near Eugene Island (LA)----------	88550						***
Atchafalaya Bay at Eugene Island (LA)----------	88600		0**********	**********	**********	00******	
East Cote Blanche Bay at Lukes Landing, LA----------	88800			**********	**********	**********	
Mississippi River Near Knox Landing, LA----------	01080			0******	0**********	**********	
Mississippi River at Tarbert Landing, MS----------	01100	0000000000000000000000000000000000000000000000000000					
Mississippi River at Red River Landing, LA----------	01120		0**********	**********	**********	**********	**********
Mississippi River at Bayou Sara, LA----------	01140	**********	**********	**********	**********	**********	**********
Mississippi River at Baton Rouge, LA----------	01160	**********	**********	**********	**********	**********	**********
Old River Inflow Channel Near Knox Landing, LA--------	02050				0**********	**********	
Old River Outflow Channel Near Knox Landing, LA-------	02100				0**********	**********	
Old River at Torras, LA (Lock Forebay)----------	02725	**********	**********	**********	**********	**********	**********
Old River at Torras, LA (Lock Tailbay)----------	02750			**********	**********	**********	**********

Table 4

Discharge Data Available

Station Name Available	Station No.	1 9 3 9 0	1 9 4 1 2	1 9 5 3 4	1 9 6 5 6	1 9 7 7 8	1 9 8 9 0
Atchafalaya River at Barbre Landing, LA	03015	----------	----------	----------	----------	----------	
Atchafalaya River at Simmesport, LA	03045	**********	**********	**********	**********	**********	
Atchafalaya River at Melville, LA	03060	----------	----------	----------	----------	----------	
Atchafalaya River at Krotz Springs, LA	03075	-----0*****	**********	**********	**********	*0----------	
Atchafalaya River at Atchafalaya, LA	03090	----------	-00000----	-00000----	----00000-	0000000000	
Atchafalaya River at Butte La Rose, LA	03120	----------	----------	----------	----------	----------	
Bayou La Rompe at Lake Long, LA	03210	---0000000	0000000---	----------	---000----	------**00	****
Whiskey Bay Pilot Channel Below Head, LA	03240	----------	----------	----------	----0*****	***0--***	
Blind Tensas Cut Below Upper Grand River (LA)	03315	**********--000000----	----000000	-------000000	------0000	0000000000	
Bayou Chene Below Bayou Chene Cut (LA)	03420	----------	----------	----------	----------	----------	
Chicot Pass at West Fork Chicot Pass (LA)	03465	----------	----------	----------	----*******	******00**	**
Chicot Pass Near Myette Point (LA)	03540	------0000	0000000000	0000-----0	00000---0-	---00000000	00
Grand Lake at Charenton Floodgate (LA)	03550	----------	----------	----------	----------	----------	*****
Keelboat Pass Below Lake Chicot (LA)	03615	----------	----000000	-----00000	0----------	----------	
Six Mile Lake Near Verdunville, LA	03645	----------	----------	----------	----0000000	0000000000	0000000000
Wax Lake Outlet at Calumet, LA	03720	----------	----*****	---*******	--0000000000	0000000000	0000000000
Lower Atchafalaya River at Berwick Lock (LA) (West)	03650	----------	----------	----------	----------	----------	
Lower Atchafalaya River at Morgan City, LA	03780	0000000000	0000000000	0000000000	0000000000	0000000000	0000000000
Lower Atchafalaya River Below Sweet Bay Lake (LA)	03820	----------	----------	----------	----------	----------	
Wax Lake Outlet Vicinity at Belle Isle, LA	03830	----------	----------	----------	----------	----------	
Round Bayou at Deer Island (LA)	03850	----------	----------	----------	----------	----------	0****
Bayou Latenache Above Pointe Coupee Drainage Structure (LA)	40900	----------	----------	----0*****	**********	**********	
Bayou Latenache Below Pointe Coupee Drainage Structure	43500	----------	----------	----------	**********	**********	
Bayou Courtableau Outlet Channel at Sta 225+00 (LA) (East Auto.)	49075	----------	----------	----------	----0*****	**********	
WABPL (FWS) at Cleon, LA	49120	-----00-*-	-00000----	----------	--0*******	**********	
WABPL Borrow Pit (FWS) at Opelousas Bay (LA)	49135	------0--0	------00--	00----------	----------	-0-0*******	*
WABPL Borrow Pit (FWS) at Bayou Mersier (LA)	49150	----------	----00000-	------0---0	----***---	-*******	
WABPL (FWS) at Lower Grand Bayou (LA)	49195	----000000	0000-0*****	**********	**********	**********	
Arm of Grand Lake Near Crook Chene Cove (LA)	49197	----------	----------	----------	----------	----------	00*
WABPL (FWS) at Little Lake Long (LA)	49230	----------	----------	----------	----------	**********	
Buffalo Cove at Round Island (LA)	49235	----------	----------	----------	----------	----------	***
Bayou Fordoche Near Krotz Springs, LA	49255	----------	----------	----******	**********	**********	
Alabama Bayou (FWS) at Sherburne, LA	49400	----------	----------	----------	----------	----------	*******
Upper Grand River at Little Tensas Bayou (LA)	49440	----------	----------	----------	----------	----------	********
EABPL Borrow Pit (FWS) at Dixie Bayou (LA)	49510	----------	----------	----0---0-	----00--00	0000000000	0000000000
EABPL Borrow Pit (FWS) at Ramah, LA (Above Railroad Fill)	49525	----------	----------	----------	----00--00	0000000000	0000000000
EABPL Borrow Pit (FWS) at Ramah, LA (Below Railroad Fill)	49540	------00--	------0---	0---0-----	00--000000	0000-*****	**
Upper Grand River (FWS) at Dike (LA)	49670	----000000	0000000---	0---0----	0********0	00**********	**
EABPL Borrow Pit (FWS) at Bayou Sorrel Lock (LA)	49630	----------	----------	----------	----0*****	**********	**********
Big Bayou Pigeon (FWS) Near Pigeon, LA	49635	-------000	----------	--00------	----------	----------	********
Old River (FWS) at Junction with GIWW	49645	-----0**0	0000000000	---0------	----------	----------	********
Intracoastal Waterway Near Pierre Pass, LA	49690	----------	----------	----0---0-	----------	--00******	**********
Little Bayou Sorrel at Junction with GIWW (Morgan City-Port Allen Route)	49725	----------	----------	----------	----------	----------	0********
Lower Grand River at Bayou Sorrel Lock, LA	52560	----------	----------	----------	----*00-**	**********	**********
Charenton Drainage Canal Near Floodgate (LA)	64400	----------	----------	----**00**	**********	**********	**********
Charenton Drainage Canal at Baldwin, LA	64450	----------	----------0	**********	**********	**********	**********
Bayou Teche at West Calumet Floodgate (LA)	64650	----------	----------	----------	----0*****	**********	**********
Bayou Teche at East Calumet Floodgate (LA)	64700	----------	----------	----------	----0*****	**********	**********
Vermilion River Near Bancker, LA	67875	----------	----------	----------	----------	----------	**********

(Continued)

Note: This information was extracted from "Stages and Discharges of the Mississippi River and Tributaries and Other Watersheds in the New Orleans District" for 1977.

Any data available prior to 1929 were ignored.

Data available throughout a year on a daily basis signified by "*."

Data available partially or intermittently during a year signified by "0."

Unless specified otherwise, the notes refer to feet msl. Example: 3.81(-74) means gage zero was 3.81 ft msl thru 1974. 0.00(75-) means gage zero was 0.00 ft msl from the beginning of 1975 to the present.

The pamphlet is very hard to decipher in respect to changes in gage zero over the years and is ambiguous as to the meaning of the "to" in respect to the years that data were collected. (Example: does 1933 to 1941 mean 1933 thru 1940 or 1933 thru 1941). "To" is assumed to mean "to," not "thru."

The gage zero information was so difficult to decipher that it is strongly recommended that this information be reverified.

Table 4 (Concluded)

Station Name Available	Station No.	1 9 3 9 0	1 9 4 1	2	3	4	5	6	7	8	9	0	1	2	3	4	5	6	7	8	9	0	1	2	3	4	5	6	7	8	9	0
Bayou Boeuf (IWW) at Bayou Boeuf Lock (LA) (East)	76360	-	-	-	-	-	-	-	-	-	-	-	-	-	-	-	-	-	-	-	-	-	-	-	-	-	-	-	-	-	-	-
Bayou Boeuf (IWW) at Bayou Boeuf Lock (LA) (West)	76400	-	-	-	-	-	-	-	-	-	-	-	-	-	-	-	-	-	-	-	-	-	-	-	-	-	-	-	-	-	-	-
Intracoastal Waterway at Wax Lake	76440	-	-	-	-	-	-	-	-	-	-	-	-	-	-	-	-	-	-	-	-	-	-	-	-	-	-	-	-	-	-	-
Wax Lake East Borrow Pit (LS) Near Calumet, LA (North)	76460	-	-	-	-	-	-	-	-	-	-	-	-	-	-	-	-	-	-	-	-	-	-	-	-	-	-	-	-	-	-	-
Wax Lake East Drainage Area at Control Structure (LA)	76480	-	-	-	-	-	-	-	-	-	-	-	-	-	-	-	-	-	-	-	-	-	-	-	-	-	-	-	-	-	-	-
Wax Lake West Drainage Area at Control Structure (LA)	76520	-	-	-	-	-	-	-	-	-	-	-	-	-	-	-	-	-	-	-	-	-	-	-	-	-	-	-	-	-	-	-
Intracoastal Waterway at Wax Lake West Control Structure	76560	-	-	-	-	-	-	-	-	-	-	-	-	-	-	-	-	-	-	-	-	-	-	-	-	-	-	-	-	-	-	-
Freshwater Canal Above Reef Ridge (LA)	76592	-	-	-	-	-	-	-	-	-	-	-	-	-	-	-	-	-	-	-	-	-	-	-	-	-	-	-	-	-	-	-
Freshwater Canal at Freshwater Bayou Lock (LA) (South)	76593	-	-	-	-	-	-	-	-	-	-	-	-	-	-	-	-	-	-	-	-	-	-	-	-	-	-	-	-	-	-	-
Schooner Bayou (Inland Waterway) at Control Structure (LA) (East Auto.)	76600	*	*	*	*	*	*	*	*	*	*	*	*	*	*	*	*	*	*	*	*	*	*	*	*	*	*	*	*	*	*	*
Schooner Bayou (Inland Waterway at Control Structure (LA) (East Staff)	76640	*	*	*	*	*	*	*	*	*	*	*	*	*	*	*	*	*	*	*	*	*	*	*	*	*	*	*	*	*	*	*
Schooner Bayou (Inland Waterway) at Control Structure (LA) (West)	76680	*	*	*	*	*	*	*	*	*	*	*	*	*	*	*	*	*	*	*	*	*	*	*	*	*	*	*	*	*	*	*
Intracoastal Waterway at Vermilion Lock (LA) (East Auto.)	76720	-	-	0	*	*	*	*	*	*	*	*	*	*	*	*	*	*	*	*	*	*	*	*	*	*	*	*	*	*	*	*
Intracoastal Waterway at Vermilion Lock (LA) (East Staff)	76760	-	-	-	-	0	*	*	*	*	*	*	*	*	*	*	*	*	*	*	*	*	*	*	*	*	*	*	*	*	*	*
Intracoastal Waterway at Vermilion Lock (LA) (West)	76800	-	-	-	-	0	*	*	*	*	*	*	*	*	*	*	*	*	*	*	*	*	*	*	*	*	*	*	*	*	*	*
Intracoastal Waterway at Calcasieu Lock (LA) (East)	76880	-	-	-	-	-	-	-	-	-	-	-	-	-	*	*	*	*	*	*	*	*	*	*	*	*	*	*	*	*	*	*
Atchafalaya Bay Near Eugene Island (LA)	88550	-	-	-	-	-	-	-	-	-	-	-	-	-	-	-	-	-	-	-	-	-	-	-	-	-	-	-	-	*	*	*
Atchafalaya Bay at Eugene Island (LA)	88600	-	-	-	-	-	-	-	-	-	-	-	-	-	-	-	-	-	-	-	-	-	-	-	-	-	-	-	-	-	-	-
East Cote Blanche Bay at Lukes Landing, LA	88800	-	-	-	-	-	-	-	-	-	-	-	-	-	-	-	-	-	-	-	*	*	*	*	*	*	*	*	*	*	*	*
Mississippi River Near Knox Landing, LA	01080	-	-	-	-	-	-	-	-	-	-	-	-	-	-	-	-	-	-	-	-	-	-	-	-	-	-	-	-	-	-	-
Mississippi River at Tarbert Landing, MS	01100	-	-	-	0	0	0	*	*	*	*	*	*	*	*	*	*	*	*	*	*	*	*	*	*	*	*	*	*	*	*	*
Mississippi River at Red River Landing, LA	01120	-	-	-	-	-	-	-	-	-	0	*	*	*	*	*	*	*	*	*	*	*	*	*	*	*	*	*	*	*	*	*
Mississippi River at Bayou Sara, LA	01140	-	-	-	-	-	-	-	-	-	-	-	-	-	-	-	-	-	-	-	-	-	-	-	-	-	-	-	-	-	-	-
Mississippi River at Baton Rouge, LA	01160	*	-	*	*	*	*	*	*	*	*	*	*	*	*	*	-	-	-	-	-	-	-	-	-	-	-	-	-	-	-	-
Old River Inflow Channel Near Knox Landing, LA	02050	-	-	-	-	-	-	-	-	-	-	-	-	-	-	-	-	-	-	-	-	-	-	-	-	-	-	-	-	-	-	-
Old River Outflow Channel Near Knox Landing, LA	02100	-	-	-	-	-	-	-	-	-	-	-	-	-	-	-	-	-	-	-	-	-	*	*	*	*	*	*	*	*	*	*
Old River at Torras, LA (Lock Forebay)	02725	-	-	-	-	-	-	-	-	-	-	-	-	-	-	-	-	-	-	-	-	-	-	-	-	-	-	-	-	-	-	-
Old River at Torras, LA (Lock Tailbay)	02750	-	-	-	-	-	-	-	-	-	-	-	-	-	-	-	-	-	-	-	-	-	-	-	*	*	-	-	-	-	-	-

Table 5

Model Coefficients for HAD-1

Coefficient	Description
n value	Manning's n value. It is used for friction and vegetation loss, and is calibrated in fixed bed node using water-surface elevations and flow distribution for performance criteria
τ_{cd}	Critical bed shear stress for deposition of clay
τ_{ce}	Critical bed shear stress for erosion of clay. τ_{ce} must be equal to or greater than τ_{cd}
τ_{sd}	Critical bed shear stress for deposition of silt
τ_{se}	Critical bed shear stress for erosion of silt. In the present version of HAD-1, τ_{se} must equal τ_{ce}
τ_m	Bed shear stress at which mass erosion begins
ERM	Erosion rate, tons/day/ft^2, corresponding to τ_m
B_p	Slope of erosion rate curve for particle erosion
B_m	Slope of erosion rate curve for mass erosion
γ_{ci}	The unit weight, lb/ft^3, of a freshly deposited clay bed
B_{clay}	The consolidation coefficient for the compaction of clay deposits
B_{silt}	The consolidation coefficient for the compaction of silt deposits
γ_s	The unit weight of sand deposits. No compaction of the sand bed is expected
γ_{si}	The unit weight, lb/ft^3, of a freshly deposited silt bed

Table 6

Events in Flow Duration Curve

Event No.	Duration: Percent Exceeded	Duration: P	Duration: DD 365 × P	Water Yield: Q	Water Yield: $\bar{Q}$	Water Yield: $\bar{Q}$ × DD 1,000 cfs-days	Sediment Yield: QS 1,000 tons/day	Sediment Yield: QS × DD 1,000 tons
	100			35				
1		0.10	36		68	2,448	17	612
	90			85				
2		0.10	36		95	3,420	36	1,296
	80			102				
3		0.10	36		115	4,140	56	2,016
	70			125				
4		0.10	36		133	4,788	78	2,808
	60			145				
5		0.10	36		156	5,616	110	3,960
	50			170				
6		0.10	36		185	6,660	161	5,796
	40			200				
7		0.10	36		230	8,280	265	9,540
	30			255				
8		0.10	36		280	10,080	410	14,760
	20			310				
9		0.10	36		330	11,880	530	19,080
	10			370				
10		0.05	18		390	7,020	900	16,200
	5			410				
11		0.01	4		420	1,680	1,020	4,080
	4			430				
12		0.01	4		440	1,760	1,190	4,760
	3			450				
13		0.01	4		475	1,900	1,350	5,400
	2			500				
14		0.01	4		560	2,240	2,100	8,400
	1			560				
					Total	71,912		98,709
					Measured*	84,527		97,000

Note: P = probability
DD = Duration, days
Q = discharge, 1,000 cfs
$\bar{Q}$ = average discharge, 1,000 cfs
S = sediment load, tons
* Average of years 1967-1977, Table 1.

Table 7

Eugene Island Gage Datum Changes, Atchafalaya River

USGS Gage No. 8860010

Period	Gage Zero*	Shift ft
26 May 1939-31 Dec 1943	-2.99	+0.3
1 Jan 1944-31 Dec 1958	-2.99	-0.7
1 Jan 1959- 3 May 1972	-2.99	0
12 Apr 1973-31 Dec 1974	-1.59	0
1 Jan 1975-1978	0	0

* Given in feet referred to mean sea level (msl).

Table 8

Joint Probability Table

Class Interval No.	Simmesport Water Discharge 1,000 cfs	P(Q)	Eugene Island Stage Class Intervals* ft msl -2 to -1 (0.10)	-1 to 0 (0.20)	0 to +1 (0.50)	+1 to +2 (0.20)
1	35- 85	0.10	0.01	0.02	0.05	0.02
2	85- 100	0.10	0.01	0.02	0.05	0.02
3	100- 125	0.10	0.01	0.02	0.05	0.02
4	125- 145	0.10	0.01	0.02	0.05	0.02
5	145- 170	0.10	0.01	0.02	0.05	0.02
6	170- 200	0.10	0.01	0.02	0.05	0.02
7	200- 255	0.10	0.01	0.02	0.05	0.02
8	255- 310	0.10	0.01	0.02	0.05	0.02
9	310- 370	0.10	0.01	0.02	0.05	0.02
10	370- 410	0.05	0.005	0.01	0.025	0.01
11	410- 430	0.01	0.001	0.002	0.005	0.002
12	430- 450	0.01	0.001	0.002	0.005	0.002
13	450- 500	0.01	0.001	0.002	0.005	0.002
14	500- 560	0.01	0.001	0.002	0.005	0.002
--**	560-1,500	<<0.01	0.001	0.002	0.005	0.002
Marginal Distribution Function			0.10	0.20	0.50	0.20
Joint Cumulative Distribution			0.10	0.30	0.80	1.00

* The probability of occurrence P(H) for each stage class interval is given in parentheses under that class.

** These values are required to make the results total 100 percent.

Table 9

Flow Duration in Days for the Joint Probability Mass Function

Class Interval No.	Simmesport Class 1,000 cfs	Discharge Event Q 1,000 cfs	Eugene Island Stage for H Value* -2 to -1 (-1.5)	-1 to 0 (-0.5)	0 to 1 (+0.5)	+1 to +2 (+1.5)
1	35- 85	68	36	72	180	72
2	85-100	95	36	72	180	72
3	100-125	115	36	72	180	72
4	125-145	133	36	72	180	72
5	145-170	156	36	72	180	72
6	170-200	185	36	72	180	72
7	200-255	230	36	72	180	72
8	255-310	280	36	72	180	72
9	310-370	330	36	72	180	72
10	370-410	390	18	36	90	36
11	410-430	420	3.6	7.2	18	7.2
12	430-450	440	3.6	7.2	18	7.2
13	450-500	475	3.6	7.2	18	7.2
14	500-560	560	3.6	7.2	18	7.2
	Marginal		356.4	712.8	1,782	712.8
	In terms of years		1	2	5	2
	Accumulative		1	3	8	10

* The mean value of stage H for each class interval is given in parentheses under that class.

Table 10

Sediment Discharge by Grain Size Class

Class	Particle Size mm	Discharge, tons/day, for Water Discharge, cfs 700	35,000	70,000	400,000	775,000
Clay	<0.004	700	3,300	13,000	265,000	720,000
$Silt_1$	0.008 -0.016	30	200	1,400	120,000	600,000
$Silt_2$	0.016 -0.032	30	200	1,400	120,000	600,000
$Silt_3$	0.032 -0.062	30	200	1,400	120,000	600,000
Very fine sand	0.062 -0.125	1	40	350	165,000	1,200,000
Fine sand	0.0125-0.250	1	40	280	80,000	500,000
	Total	792	3,980	17,830	870,000	4,220,000

Table 11

Observed and Calculated Stages, HAD-1 Calibrations

Gage Name	Gage No.	Approximate river mile (1963)	Stage, ft, msl for Discharge, 1,000 cfs								
			350* 1977**	375* 1972**	425* 1978**	350†	710* 1975**	800†	965* 1973†	1,500†	1,500 MBM
Atchafalaya River at Eugene Island	88600	146	0.4	--	0	0	1.7	0	2.3	5.0	5.0
Round Bay at Deer Island	3850	136	1.4	--	2.0	2.2	3.2	4.9	--	7.8	--
Lower Atchafalaya River Below Sweet Bay Lake	3820	129.5	2.2	3.6	2.5	2.8	4.6	6.4	5.7	10.1	10.0
Lower Atchafalaya River at Morgan City	3780	117.7	3.8	4.6	4.2	3.9	7.8	8.3	10.5	15.0	18.3
Chicot Pass near Myette Point	3540	95.4	9.0	10.2	10.3	9.0	14.9	15.0	17.3	23.3	26.0
Chicot Pass at West Fork Chicot Pass	3465	83.2	12.0	13.3	14.0	--	18.3	--	20.1	--	--

* Observed in prototype.
** Year of flow event.
† Calculated by HAD-1.

Table 12

Distribution of Flow in HAD-1, Percent,

Q = 350,000 cfs, 1977

Cross Section by river mile	Strip 1	2	3	4	5	6	7
			Bay				
151.00	13.4	5.8	7.8	44.8	2.4	10.8	14.9
146.00	27.0	11.3	15.1	27.2	5.1	13.8	0.5
145.00	19.8	6.7	14.8	37.0	6.3	9.0	7.2
144.00	23.5	13.4	19.8	25.4	2.4	6.0	9.4
143.00	22.7	6.4	18.0	26.1	3.7	12.4	10.6
142.00	26.6	6.5	19.9	22.2	3.7	9.8	11.2
141.00	18.3	7.4	33.5	16.6	4.0	9.2	11.0
140.00	14.3	9.0	40.9	11.8	3.9	9.5	10.7
139.00	2.2	14.7	39.6	24.6	2.1	2.2	14.5
138.00	0.0	12.9	7.5	72.1	5.1	1.5	0.9
137.00	0.3	34.5	3.0	4.7	33.9	1.2	22.3
			Marsh				
136.00	0.7	18.7	0.8	0.3	64.5	9.2	5.8
129.90	0.5	16.0	0.3	0.5	82.6	0.1	0.0
126.00	1.3	10.6	0.2	0.7	84.6	2.6	0.0
121.20	0.0	29.0	0.0	0.0	63.0	--	8.0
117.00	0.0	29.0	0.0	34.9	30.8	3.0	2.3
			Basin				
107.00	0.3	38.7	0.0	49.8	2.6	2.0	6.6
102.78	0.1	18.4	0.0	76.3	2.2	1.0	1.9
97.19	0.8	20.5	0.0	68.5	1.6	4.2	4.4
91.74	0.8	9.8	0.3	83.7	1.2	2.9	1.4
87.0	0.0	13.1	2.0	72.5	2.9	4.3	5.2

Table 13

Calibration Coefficients for Deposition and Erosion of Silt and Clay

Particle Sediment Type	Size mm	Bed Shear Threshold Settling Velocity fps	τ_{cd} lb/sq ft	Erosion Rate Coefficients τ_{ce} lb/sq ft	τ_m lb/sq ft	ERM	B_p	B_m
Clay	<0.004	0.000016	0.0004	0.0024	0.015	0.001	0.06	0.30
$Silt_1$	0.004-0.008	0.000067	0.001	*	*	*	*	*
$Silt_2$	0.008-0.016	0.00026	0.001	*	*	*	*	*
$Silt_3$	0.016-0.032	0.0010	0.001	*	*	*	*	*
Very fine sand	0.062-0.125	0.016	--	--	--	--	--	--
Fine sand	0.125-0.250	0.052	--	--	--	--	--	--

Note: Symbols are defined in Table 5.
* Same as used for clay.

Table 14

Basin Retention

Fraction	Roberts, Adams, and Cunningham (1980) Millions of Tons	%	HAD-1 Millions of Tons	%
Inflow, Simmesport Gage				
Average annual yield				
Sand	25	24	31	30
Silt/clay	80	76	74	70
Total	105	100	105	100
Outflow, Morgan City Plus Calumet Gages				
Average annual yield				
Sand	13	16	12	15
Silt/clay	67	84	66	85
Total	80	100	78	100
Average Annual Retention and Trap Efficiency				
Sand	12	50*	19	61*
Silt/clay	13	16*	8	8*
Total	25	24*	27	26*

Note: Data from US Geological Survey (1977).
* Trap efficiency, E = (Inflow-Outflow)/Inflow . Total trap efficiency is not the summation of the parts.

Table 15

Prototype Bed Change

Cell No.	1977 Survey* Area square miles	1977 Survey* Number of Measurements	1977 Survey* Avg Depth ft	1967 Survey* Area square miles	1967 Survey* Number of Measurements	1967 Survey* Avg Depth ft	Bed Change ft
1	5.56	155	8.22	6.28	175	8.33	0.11
2	5.92	165	7.04	5.92	165	8.00	0.96
3	6.31	176	6.63	6.31	176	7.82	1.19
4	5.56	155	4.64	5.49	153	7.08	2.44
5	4.73	132	3.48	4.66	130	5.46	1.98
6	3.55	99	3.28	3.62	101	3.60	0.32
7	2.19	61	2.67	2.19	61	3.18	0.51
8	0.97	27	1.11	1.22	34	3.48	2.37
9	0.11	3	1.41	0.07	2	3.25	1.85
10	0.14	4	9.66				
11	1.15	32	6.43	0.14	4	8.97	2.54
12	1.18	33	5.41	1.18	33	7.50	2.09
13	1.15	32	4.71	1.15	32	5.59	0.88
14	1.18	33	3.67	1.18	33	4.07	0.40
15	1.08	30	3.83	1.08	30	6.12	2.29
16	1.15	32	4.65	1.15	32	7.40	2.75
17	1.18	33	6.83	1.18	33	7.62	0.79
18	1.11	31	6.95	1.11	31	8.01	1.06
19	1.36	38	7.92	1.51	42	8.72	0.80
20	4.27	119	7.94	5.02	140	8.25	0.31
21	3.41	95	7.06	3.41	95	7.56	0.50
22	3.26	91	7.17	3.26	91	6.98	-0.19
23	3.59	100	6.39	3.59	100	6.38	-0.01
24	3.73	104	6.15	3.73	104	5.54	-0.61
25	5.02	140	5.36	5.02	140	5.21	-0.15
26	5.38	150	4.12	5.38	150	5.56	1.44
27	4.52	126	3.93	4.05	113	5.20	1.27
28	2.33	65	3.38	1.51	42	4.85	1.47
29	0.32	9	1.93				
30	4.23	118	1.84	0.18	5	4.73	2.8
31	5.06	141	2.21	2.98	83	4.02	1.8
32	3.44	96	2.57	3.44	96	4.22	1.65
33	3.08	86	2.46	3.08	86	4.71	2.25
34	2.80	78	2.59	2.80	78	3.81	1.25
35	2.73	76	3.60	2.73	76	4.18	0.58

(Continued)

* USAED, New Orleans, 1967 and 1977a.

Table 15 (Concluded)

Cell No.	1977 Survey Area square miles	1977 Survey Number of Measurements	1977 Survey Avg Depth ft	1967 Survey Area square miles	1967 Survey Number of Measurements	1967 Survey Avg Depth ft	Bed Change ft
36	2.73	76	4.24	2.73	76	5.37	1.13
37	2.83	79	5.06	2.83	79	6.43	1.37
38	2.87	80	4.75	2.73	76	6.80	2.05
39	3.30	92	6.47	3.23	90	7.06	0.59
40	0.61	17	7.81	0.22	6	12.35	4.54
41	0.39	11	2.10	0.39	11	8.91	6.81
42	0.32	9	5.11	0.32	9	7.85	2.74
43	0.50	14	2.19	0.50	14	5.50	3.31
44	0.50	14	1.79	0.50	14	3.46	1.57
45	0.50	14	4.97	0.50	14	4.21	-0.76
46	0.57	16	4.84	0.57	16	5.58	0.7
47	0.50	14	2.76	0.50	14	6.54	3.78
48	0.36	10	6.22	0.25	7	7.44	1.22
49	0.29	8	5.47	0.22	6	6.28	0.81
50	1.15	32	8.88	0.54	15	11.99	3.11
51	1.83	51	6.44	1.69	47	8.09	1.65
52	2.40	67	5.63	2.40	67	6.10	0.47
53	2.69	75	4.47	2.69	75	5.62	1.15
54	2.55	71	3.41	2.55	71	4.79	1.38
55	2.44	68	3.52	2.44	68	5.27	1.75
56	2.73	76	5.31	2.73	76	6.03	0.72
57	2.73	76	6.99	2.73	76	6.70	-0.29
58	2.62	73	7.13	1.97	55	6.76	-0.37
59	3.55	99	7.78	1.79	50	7.04	-0.74
60	3.37	94	5.21	1.11	31	4.71	-0.50
61	3.08	86	5.60	3.16	88	4.99	-0.61
62	3.41	95	6.00	3.44	96	5.38	-0.62
63	3.34	93	5.86	3.12	87	5.41	-0.45
64	3.12	87	5.26	2.62	73	5.47	0.21
65	3.23	90	3.96	2.40	67	4.92	0.96
66	3.59	100	3.27	3.16	88	4.71	1.44
67	3.10	89	2.46	2.87	80	3.88	1.42
68	2.33	65	1.70	1.69	47	3.37	1.67
	172.28**	4,806**	4.95†	156.21**	4,355**	6.00†	+1.05†

** Total value.
† Average value.

Table 16

Summary of Calculated Sediment Yield in Millions of Tons per Decade

Fraction	Forecast Period years	Simmesport	Morgan City/ Calumet mile 117.7	Coast-line mile 136	Eugene Island mile 145	Percent of Simmesport			E
						Morgan City/ Calumet	Coastline	Eugene Island	Simmesport to Eugene Island
Clay	0-10	340	316	293	269	93	86	79	
Silt		360	334	292	177	93	81	49	
Sand		210	65	37	1	31	18	--	
	Total	910	715	622	447	79	68	49	51
Clay	10-20	340	320	314	302	94	92	89	
Silt		360	337	320	249	94	89	69	
Sand		210	78	39	2	37	18	1	
	Total	910	735	673	553	81	74	61	39
Clay	20-30	340	321	312	301	94	92	89	
Silt		360	340	318	260	94	88	72	
Sand		210	82	43	2	39	20	1	
	Total	910	743	676	563	82	74	62	38
Clay	30-40	340	324	315	306	95	93	90	
Silt		360	341	321	277	95	89	77	
Sand		210	73	36	2	35	17	1	
	Total	910	738	672	585	81	74	64	36
Clay	40-50	340	326	319	313	96	94	92	
Silt		360	351	334	302	97	93	84	
Sand		210	86	46	4	41	22	2	
	Total	910	763	699	619	84	77	68	32
50-Year Total		4,550	3,694	3,339	2,767				

Table 17

Sediment Deposition in Bay in Millions of Tons

Forecast Period years	By Decade				Accumulative			
	Clay	Silt	Sand	Total	Clay	Silt	Sand	Total
			Millions of Tons					
10	24	115	35	174	24	115	35	174
20	12	71	37	120	36	186	72	294
30	11	58	41	110	47	244	113	404
40	9	44	34	87	56	288	147	491
50	6	32	42	80	62	320	189	572
			Percent by Sediment Type					
Calibration	12	57	31		12	57	31	
10	14	66	20		13	61	26	
20	10	59	31		12	61	27	
30	10	53	37		12	59	29	
40	10	51	39		12	58	30	
50	7	40	53		11	56	32	

Table 18

Composite Unit Weights of Bay Deposits

	Clay		Silt		Sand		Composite
Year	γ_T lb/cu ft	%	γ_T lb/cu ft	%	γ_T lb/cu ft	%	γ_B lb/cu ft*
10	41	12	54	57	93	31	59
20	45	13	55	61	93	26	60
30	48	12	56	61	93	27	61
40	50	12	57	59	93	29	63
50	51	12	58	58	93	30	64

* Composite unit weight at the end of year specified.

Table 19

Average Depth of Deposits

Forecast Period years	Incremental, ft				Accumulated, ft			
	Clay	Silt	Sand	Total	Clay	Silt	Sand	Total
0-10	0.27	1.00	0.31	1.58	0.27	1.00	0.31	1.58
10-20	0.20	0.83	0.16	1.19	0.47	1.83	0.47	2.77
20-30	0.07	0.48	0.16	0.71	0.54	2.31	0.63	3.48
30-40	0.07	0.37	0.18	0.62	0.61	2.68	0.81	4.10
40-50	0.06	0.27	0.14	0.47	0.67	2.95	0.95	4.57

Table 20

SOCHMJ Branch Characteristics

Branch	No. of Nodes	Spatial Step Size, ft	Total Channel Length, miles
1	13	21,078.8	47.9
2	9	18,687.5	28.3
3	5	19,775.0	15.0
4	5	18,912.5	14.3
5	9	16,775.0	25.4
6	5	5,375.0	4.3
7	13	19,600.0	44.5
8	5	4,087.5	3.1
9	7	19,300.0	21.9
10	5	7,650.0	5.8
11	17	12,300.0	37.3
12	5	19,025.0	14.4
13	43	4,575.0	36.4
Total	141		Total 299.0

Table 21

SOCHMJ Water-Surface Calibration at 350,000 cfs

Branch	Gage	Stage, ft NGVD MBM Observed	Stage, ft NGVD MCM Computed	Difference ft*
1	Simmesport	33.3	33.38	+0.1
	Melville	26.2	26.66	+0.5
	Krotz Springs	23.7	23.61	-0.1
	WBPC No. 1	20.8	20.88	+0.1
3	Atchafalaya	20.0	20.50	+0.5
	La Rompe No. 10	17.0	17.40	+0.4
4	Des Glaises	20.4	19.93	-0.5
5	Lower Grand Bayou	12.7	13.24	+0.5
7	Bayou Sorrel	7.5	8.06	+0.6
	Little Bayou Sorrel	5.4	5.58	+0.2
9	R 22 BC	15.4	15.56	+0.2
10	Myette Point	10.0	10.04	-0.1
11	Calumet	4.1	4.22	-0.2
	Wax Lake Outlet	0.6	0.56	T
13	Morgan City	4.2	4.08	-0.1
	Deer Island	1.3	1.31	T
	Eugene Island	0.0	0.02	T

* T = less than 0.1 ft.

Table 22

SOCHMJ Water-Surface Calibration at 800,000 cfs

Branch	Gage	Stage, ft NGVD MBM Observed	Stage, ft NGVD MCM Computed	Difference ft*
1	Simmesport	57.1	56.71	-0.4
	Melville	46.3	47.04	+0.7
	Krotz Springs	40.1	39.51	-0.6
	WBPC No. 1	30.8	30.61	-0.2
3	Atchafalaya	29.7	28.64	-1.1
	La Rompe No. 10	22.7	21.84	-0.9
4	Des Glaise	29.1	28.80	-0.3
5	Lower Grand Bayou	20.5	20.74	+0.2
7	Bayou Sorrel	17.2	17.56	+0.4
	Little Bayou Sorrel	13.7	14.04	+0.3
9	R 22 BC	20.0	20.32	+0.3
10	Myette Point	16.6	16.82	+0.2
11	Calumet	10.3	10.40	+0.1
	Wax Lake Outlet	1.9	1.97	+0.1
13	Morgan City	10.0	9.96	T
	Deer Island	2.3	2.20	-0.1
	Eugene Island	0.0	-0.02	T

* T = less than 0.1 ft.

Table 23

Manning's n Values, SOCHMJ 1975 Adjustment

Branch	Channel		Overbanks	
	From	To	From	To
1	0.021	0.030	0.098	0.140
2	0.030	0.030	0.140	0.140
3	0.030	0.030	0.140	0.140
4	0.042	0.042	0.196	0.196
5	0.030	0.030	0.140	0.140
6	0.030	0.030	0.140	0.140
7	0.024	0.036	0.112	0.168
8	0.042	0.042	0.196	0.196
9	0.033	0.036	0.154	0.168
10	0.030	0.030	0.140	0.140
11	0.023	0.045	0.023	0.252
12	0.021	0.030	0.098	0.140
13	0.018	0.030	0.018	0.140

Table 24

HAD-1 Delta Growth, T = 50 years; SOCHMJ Model

Bed Change in ft*

Wax Lake Outlet Branch				Lower Atchafalaya River Branch				
X-Section	Strip			X-Section	Strip			
miles**	1	2	3	miles**	4	5	6	7
146†	2.1	-4.9	2.3	146	1.8		2.8	-1.8
145	1.5	3.4	2.2	145	2.0		2.6	0.6
144	-0.2	1.8	4.9	144	2.0		1.3	3.4
143	-1.7	3.5	2.1	143	-1.8		6.9	1.6
142	-1.1	0.8	-1.4	142	3.4		4.2	2.5
141	0.6	3.1	0.6	141	-0.9		3.0	3.3
140	1.6	3.3	3.4	140	-4.1		2.8	3.7
139	0.08	701	2.6	139	-2.5		-0.9	4.0
				138	2.6		3.2	-2.5
				137	-1.2		10.4	4.1
				136	1.0		9.0	1.3
122.28	-1.9	-2.6	1.5	135.8	1.5	7.5		0.7
120.84	-0.1	1.7	1.6	135.1	1.7	6.1		0.3
119.95		0.6	0.2	134.28	1.8	4.6		-0.2
119.38	-0.7	3.1	-0.3	133.12	2.0	2.6		-0.8
118.81	-1.2	6.3	-0.4	131.65	2.1	1.8		-1.5
117.90	-0.5	10.5	-0.6	130.50	2.2	0.6		-1.5
116.95	-0.2	14.5	-0.8	129.55	1.4	0.7		-1.5
116.00	-0.2	7.6	-0.2	129.00	1.0	1.2		-1.5
115.18	-0.2	2.6	-0.2	127.13	0.1	2.9		-1.5
114.48	-0.2	-2.3	-0.2	126.50	1.1	2.2		-1.6
113.73	-0.3	-2.3	-0.3	125.63	5.3	1.1		-1.6
112.40	-0.4	-2.3	-0.4	124.35	9.6	-0.1		-1.6
111.83	-0.5	-2.3	-0.5	123.40	10.5	-0.5		-1.7
111.00	-0.5	-2.3	-0.5	122.20	11.6	-1.0		-1.7
				121.73	12.7	-1.7		-1.7
				120.77	12.1	-2.2		-1.4
				120.22	9.4	-2.2		-1.1
				119.28	-0.5	-2.3		-0.5
				118.49	-1.3	-2.3		-0.4
				118.00	-2.4		-0.2	
				117.97				
				117.16	-3.2	-2.3		
				116.40				
				115.90				

* + is deposition; - is erosion.

** This position in table corresponds to relative location in bay.

† 146 to 136 corresponds to Atchafalaya River miles extended along Navigation Channel.

Table 25

Delta, Remolded HAD-1 Volume, T = 50 years; SOCHMJ Model

Bed Change in ft*

Wax Lake Outlet Branch				Lower Atchafalaya River Branch				
X-Section	Strip			X-Section	Strip			
miles**	1	2	3	miles**	4	5	6	7
145	0.0	0.0	0.0		0.0	0.0	0.0	0.0
144	0.0	0.0	0.0		0.0	0.0	0.0	0.0
143	0.0	0.0	0.0		0.0	0.0	0.0	0.0
142	0.0	0.0	0.0		0.0	0.0	0.0	0.0
141	0.0	0.0	0.0		0.0	0.0	0.0	0.0
140	0.0	0.0	1.0		3.0	0.0	3.0	3.3
139	3.5	3.3	4.5		3.5	0.0	3.5	3.7
138	2.5	7.1	4.5		3.5	0.0	3.5	4.0
137					4.0	0.0	4.0	4.0
136				136	4.0	0.0	10.4	4.0
				135.0	4.5	0.0	9.0	4.5
122.28	-1.9	-2.6	1.5	135.80	1.5	7.5		0.7
120.48	-0.1	1.7	1.6	135.10	1.7	6.1		0.3
119.95		0.6	0.2	134.28	1.8	4.6		-0.2
119.38	-0.7	3.1	-0.3	133.12	2.0	2.6		-0.8
118.81	-1.2	6.3	-0.4	131.65	2.1	1.8		-1.5
117.90	-0.5	10.5	-0.6	130.50	2.2	0.6		-1.5
116.95	-0.2	14.5	-0.8	129.55	1.4	0.7		-1.5
116.00	-0.2	7.6	-0.2	129.00	1.0	1.2		-1.5
115.18	-0.2	2.6	-0.2	127.13	0.1	2.9		-1.6
114.48	-0.2	-2.3	-0.2	126.50	1.1	2.2		-1.6
113.73	-0.3	-2.3	-0.3	125.63	5.3	1.1		-1.6
112.40	-0.4	-2.3	-0.4	124.35	9.6	-0.1		-1.6
111.83	-0.5	-2.3	-0.5	123.40	10.5	-0.5		-1.7
111.0	-0.5	-2.3	-0.5	122.20	11.6	-1.0		-1.7
				121.73	12.7	-1.7		-1.7
				120.77	12.1	-2.2		-1.4
				120.22	9.4	-2.2		-1.1
				119.28	-0.5	-2.3		-0.5
				118.49	-1.3	-2.3		-0.4
				118.00	-2.4		-0.2	
				117.97				
				117.16	-3.2	-2.3		

Note: There are no entries in cross-sections 145-141 because there were no changes in these cross sections.

* + is deposition; - is erosion.

** This position in table corresponds to relative location in bay.

† 146 to 136 corresponds to Atchafalaya River miles extended along Navigation Channel.

Table 26

Calculated Stage Changes, T = 50 years

Gage	Wax Lake Outlet: Water-Surface Stage NGVD T0	Wax Lake Outlet: Stage Change T50	Wax Lake Outlet: Discharge 1,000 cfs	Gage	Lower Atchafalaya River: Water-Surface Stage NGVD T0	Lower Atchafalaya River: Stage Change T50	Lower Atchafalaya River: Discharge 1,000 cfs
			1975 Flood				
Calumet	9.3	+0.3	188	Morgan City	8.2	+0.6	512
Coastline	1.7	+1.2	188	Coastline	3.4	+1.8	512
Shell Reef	0.6	+1.2	186	Eugene Island	8.0	+0.1	511
			1973 Flood				
Calumet	11.2	0	236	Morgan City	10.0	0.5	636
Coastline	3.8	+0.2	236	Coastline	4.5	+1.8	636
Shell Reef	2.0	0.2	236	Eugene Island	2.1	+0.1	636
			58AEN				
Calumet	16.7	0	447	Morgan City	14.7	+0.5	1,096
Coastline	7.5	+0.2	447	Coastline	7.8	1.8	1,096
Shell Reef	5.2	+0.3	447	Eugene Island	5.3	0.1	1,096

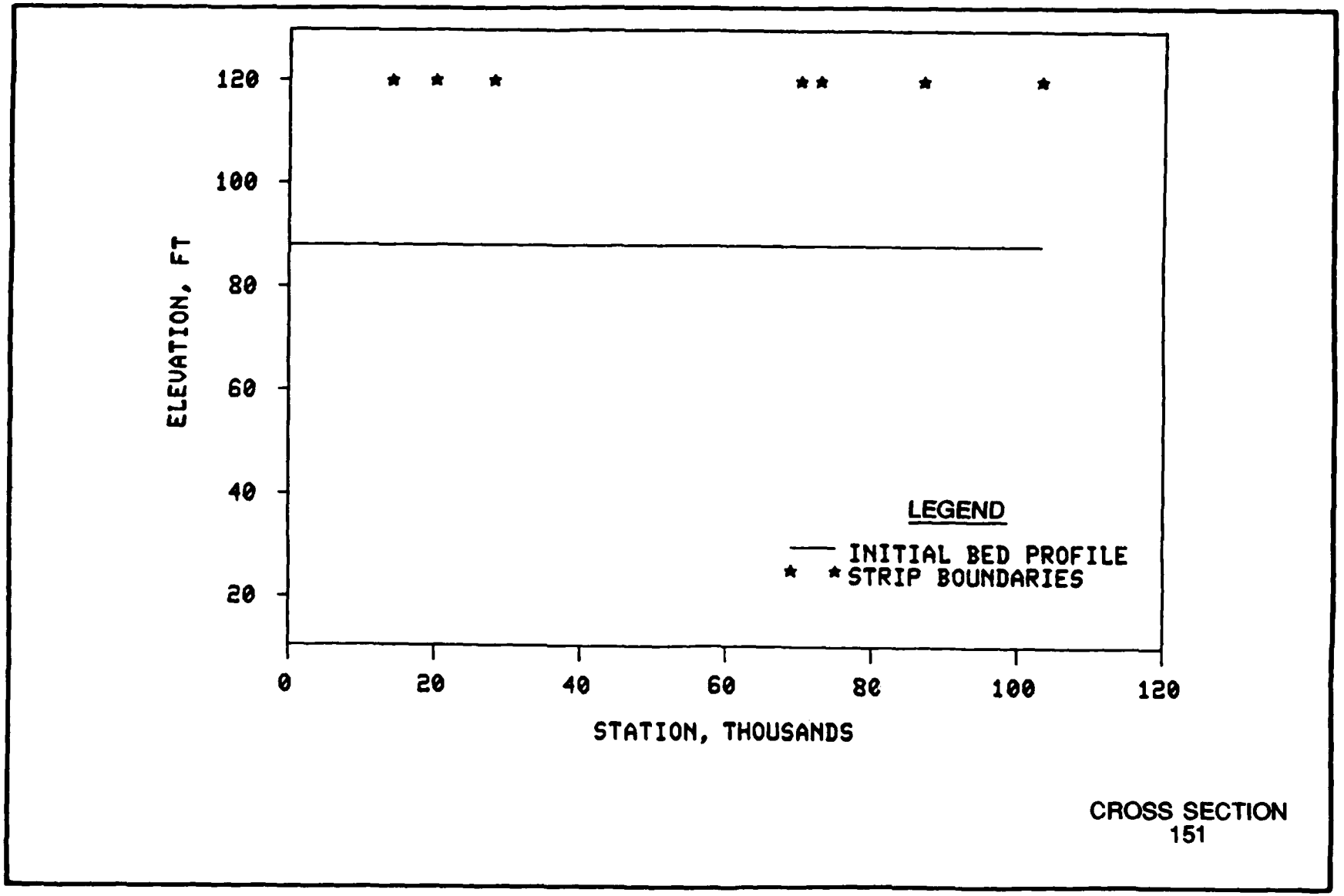

CROSS SECTION
151

PLATE 1

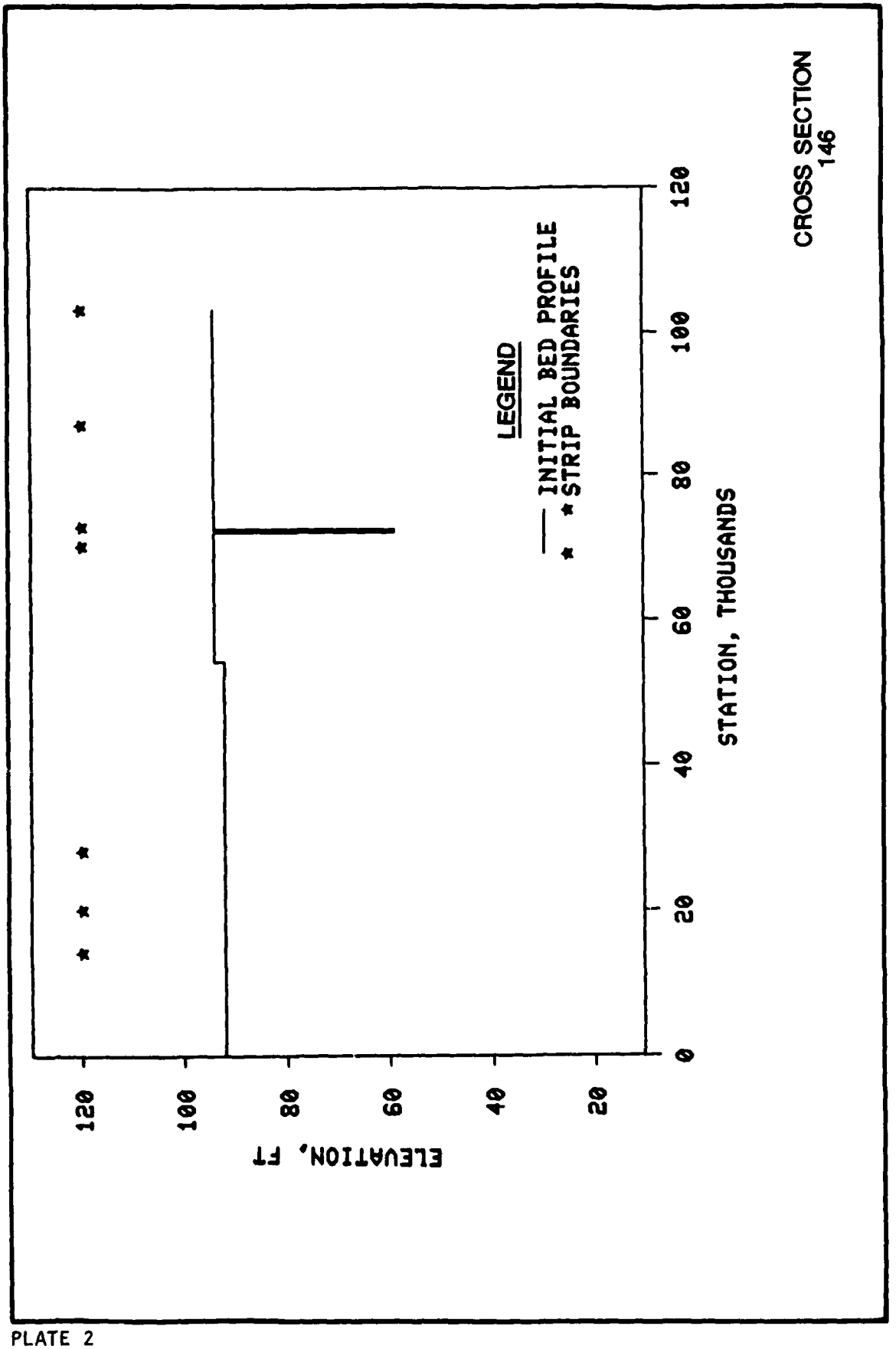
CROSS SECTION
146
LEGEND
INITIAL BED PROFILE
STRIP BOUNDARIES
STATION, THOUSANDS
0
20
40
60
80
100
120
ELEVATION, FT
120
100
80
60
40
20

PLATE 2

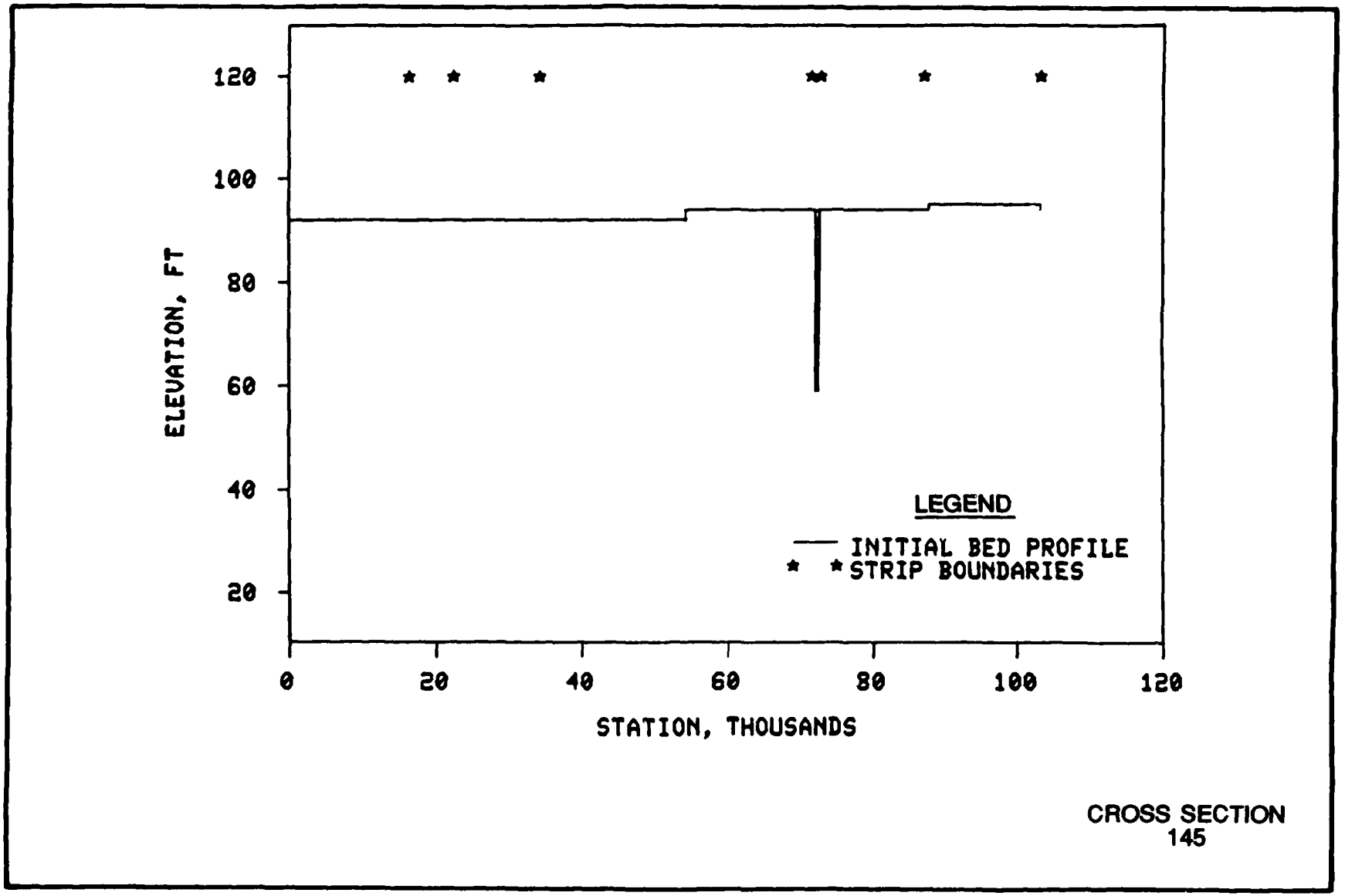

CROSS SECTION
145

PLATE 3

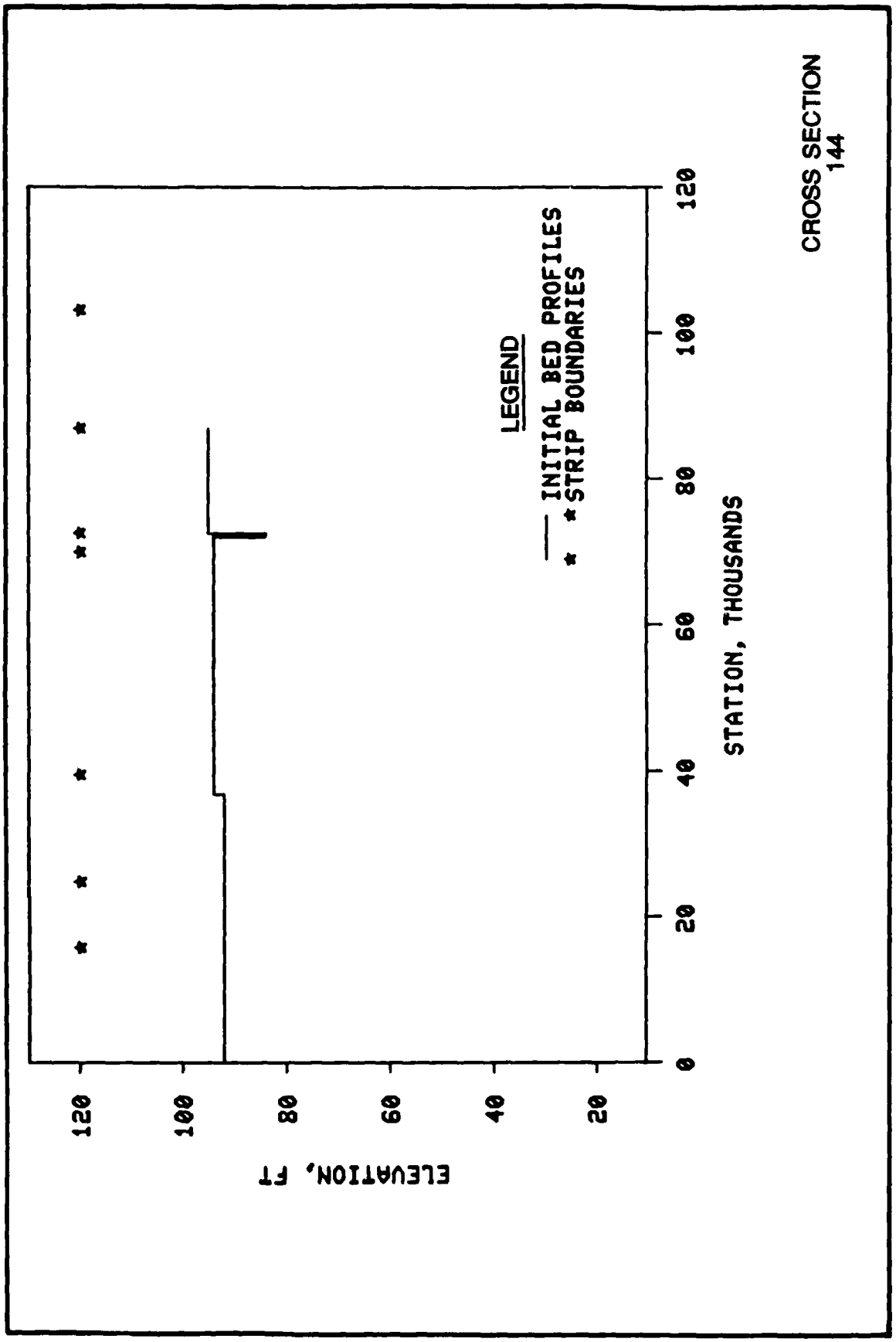
CROSS SECTION
144
LEGEND
INITIAL BED PROFILES
STRIP BOUNDARIES
STATION, THOUSANDS
0
20
40
60
80
100
120
ELEVATION, FT
20
40
60
80
100
120

PLATE 4

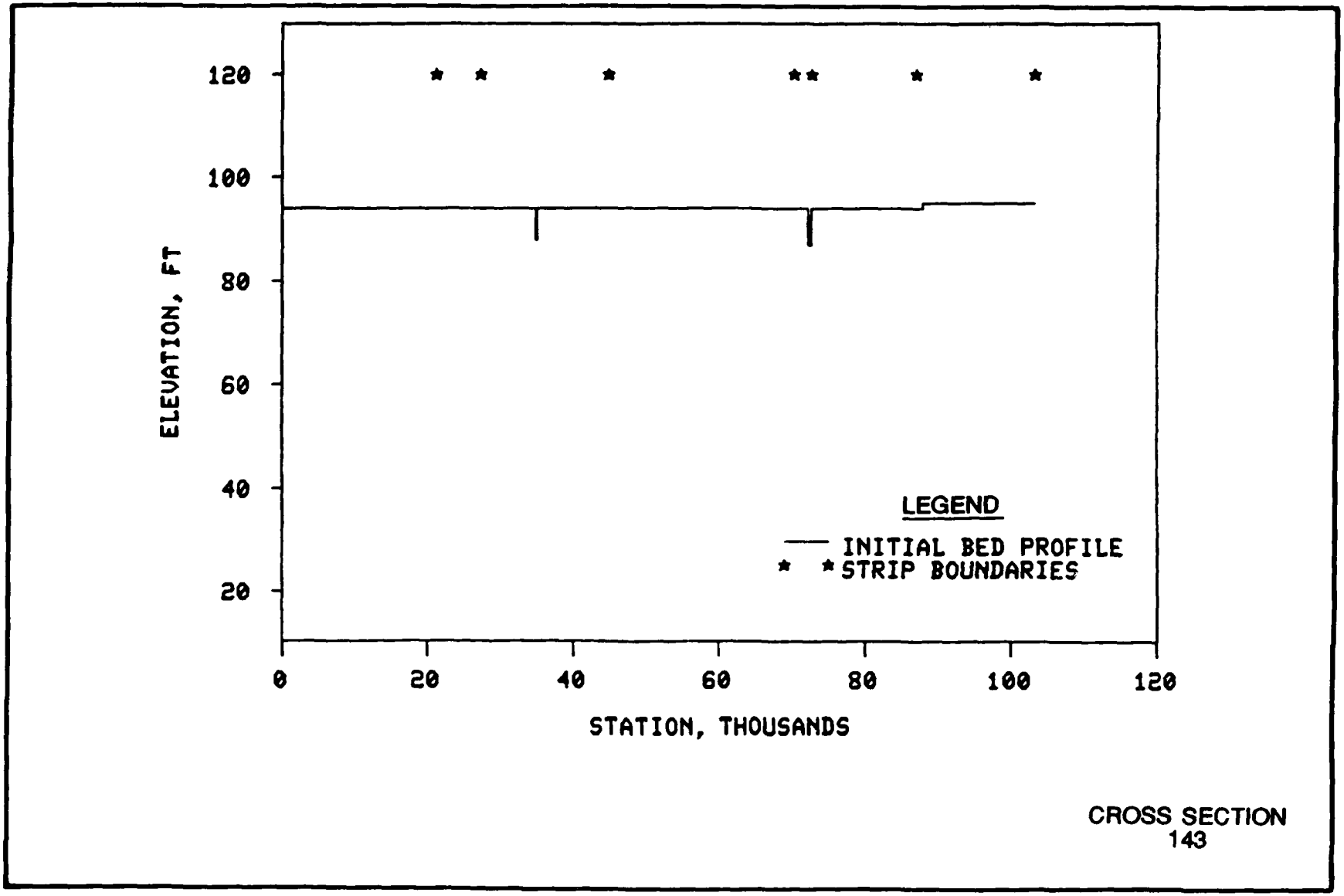
120
100
80
60
40
20
ELEVATION, FT
0
20
40
60
80
100
120
STATION, THOUSANDS
LEGEND
INITIAL BED PROFILE
STRIP BOUNDARIES
CROSS SECTION
143

PLATE 5

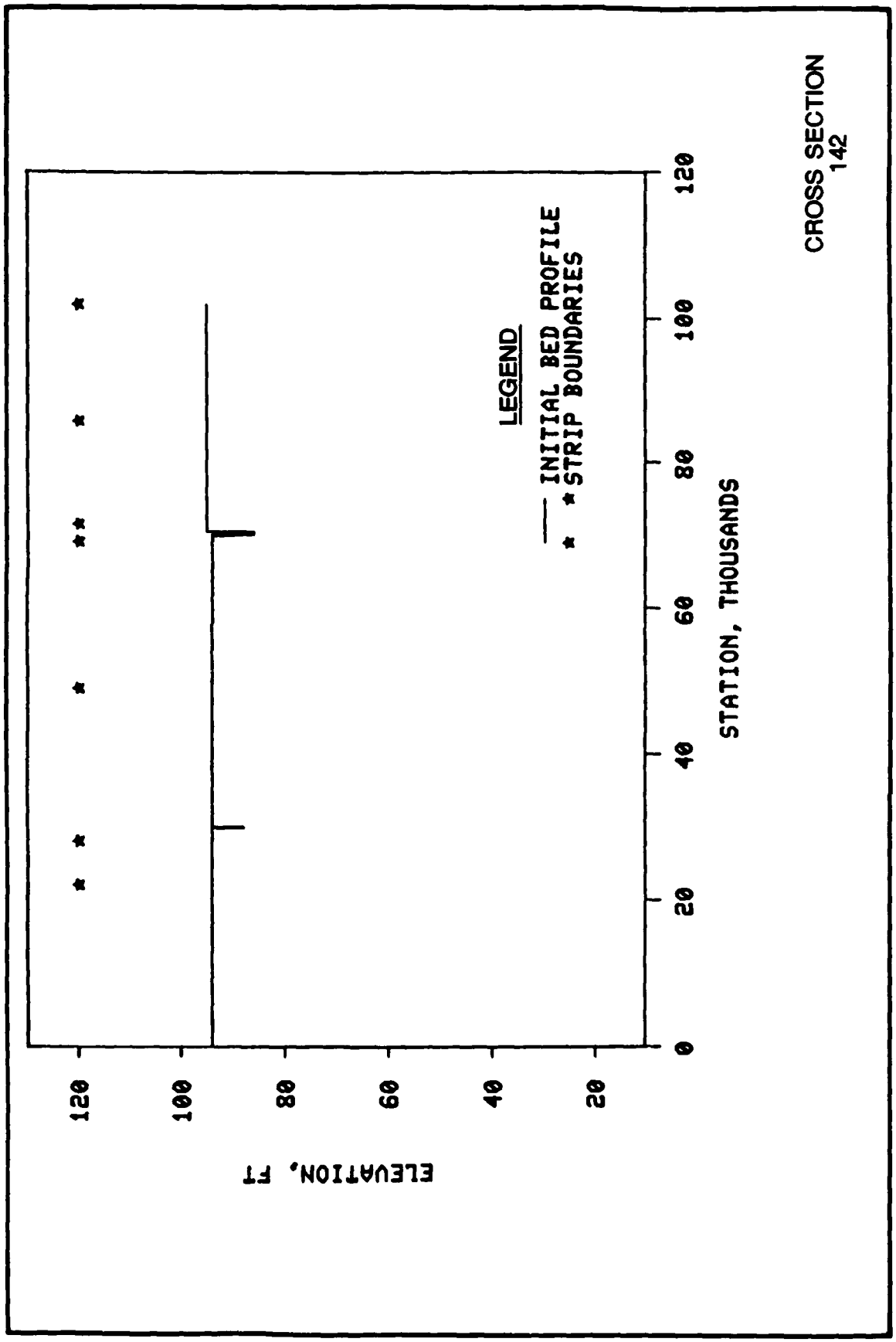
CROSS SECTION
142
LEGEND
INITIAL BED PROFILE
STRIP BOUNDARIES
STATION, THOUSANDS
0
20
40
60
80
100
120
ELEVATION, FT
120
100
80
60
40
20

PLATE 6

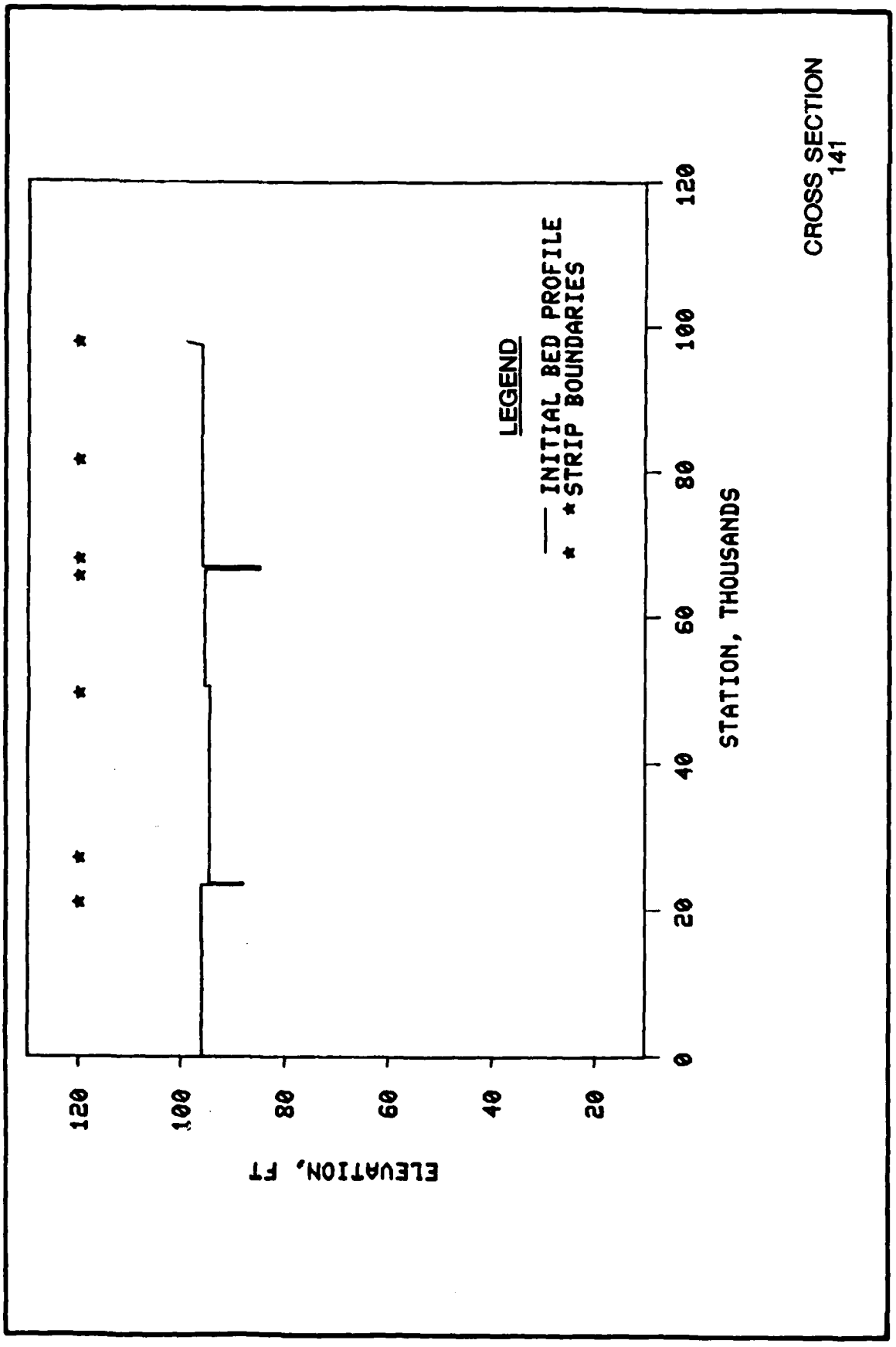
CROSS SECTION
141
LEGEND
INITIAL BED PROFILE
STRIP BOUNDARIES
STATION, THOUSANDS
0
20
40
60
80
100
120
ELEVATION, FT
120
100
80
60
40
20

PLATE 7

PLATE 8

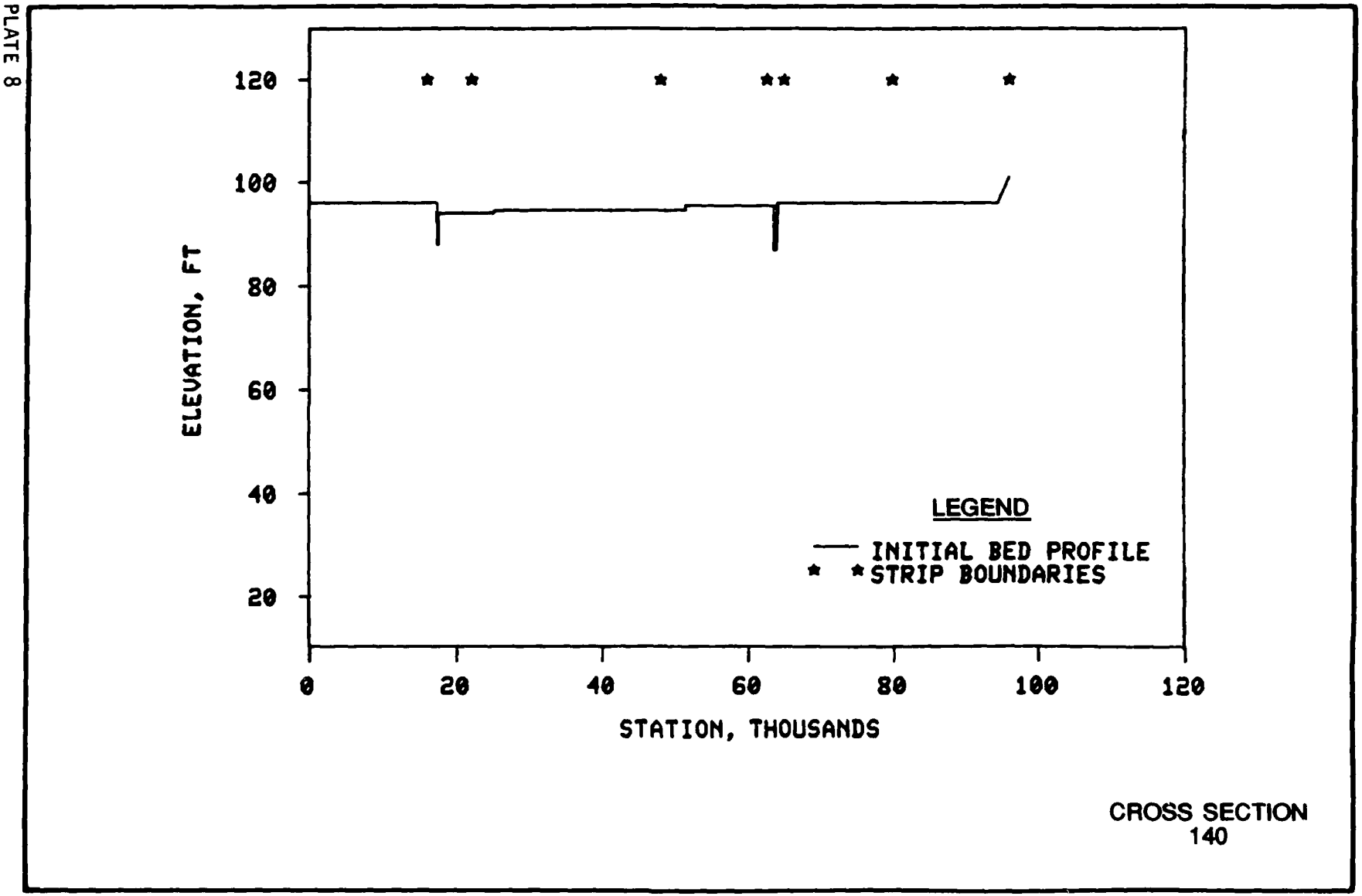
120
100
80
60
40
20
ELEVATION, FT
0
20
40
60
80
100
120
STATION, THOUSANDS
LEGEND
INITIAL BED PROFILE
STRIP BOUNDARIES
CROSS SECTION
140

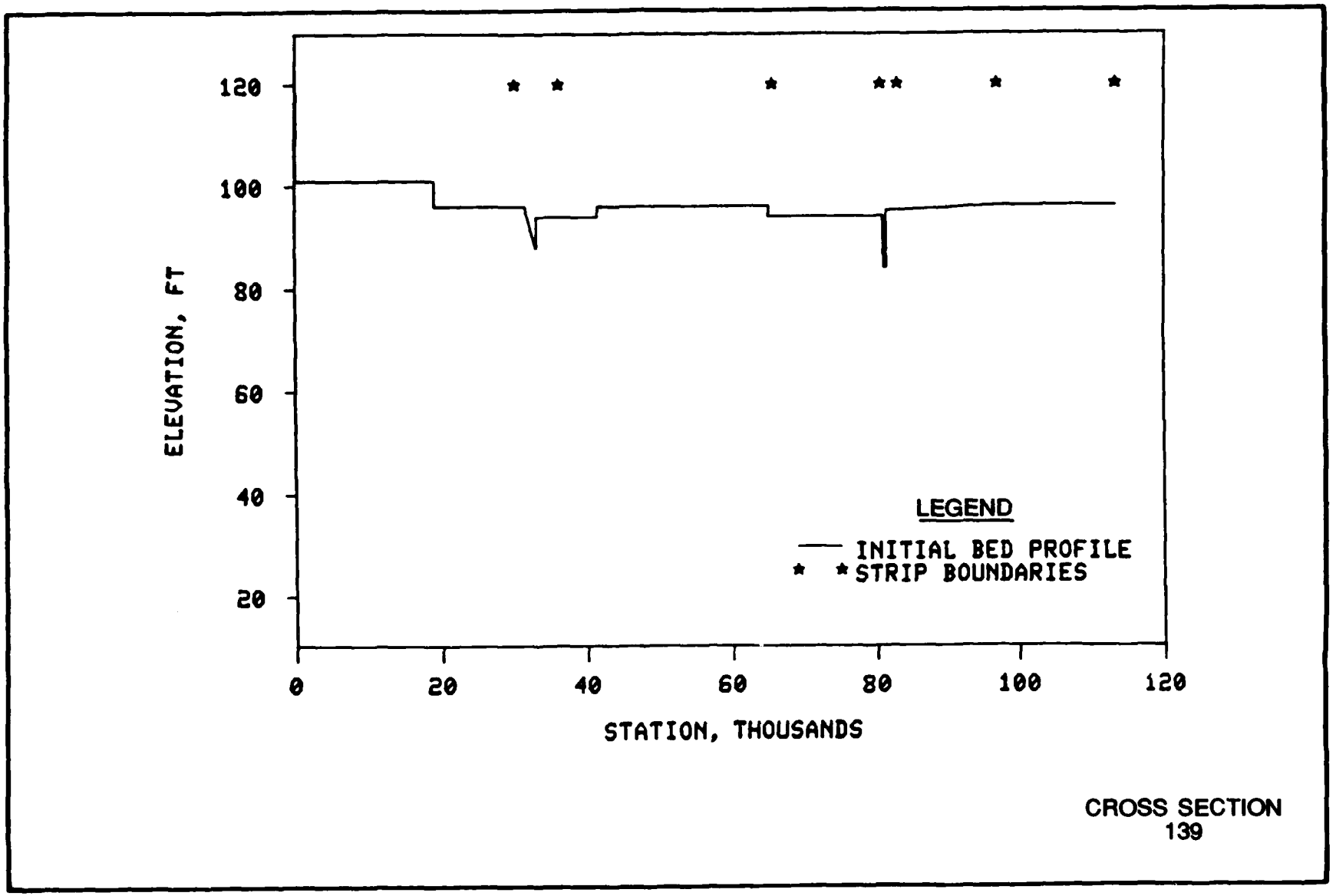
120
100
80
60
40
20
ELEVATION, FT
0
20
40
60
80
100
120
STATION, THOUSANDS
LEGEND
INITIAL BED PROFILE
STRIP BOUNDARIES
CROSS SECTION
139

PLATE 9

PLATE 10

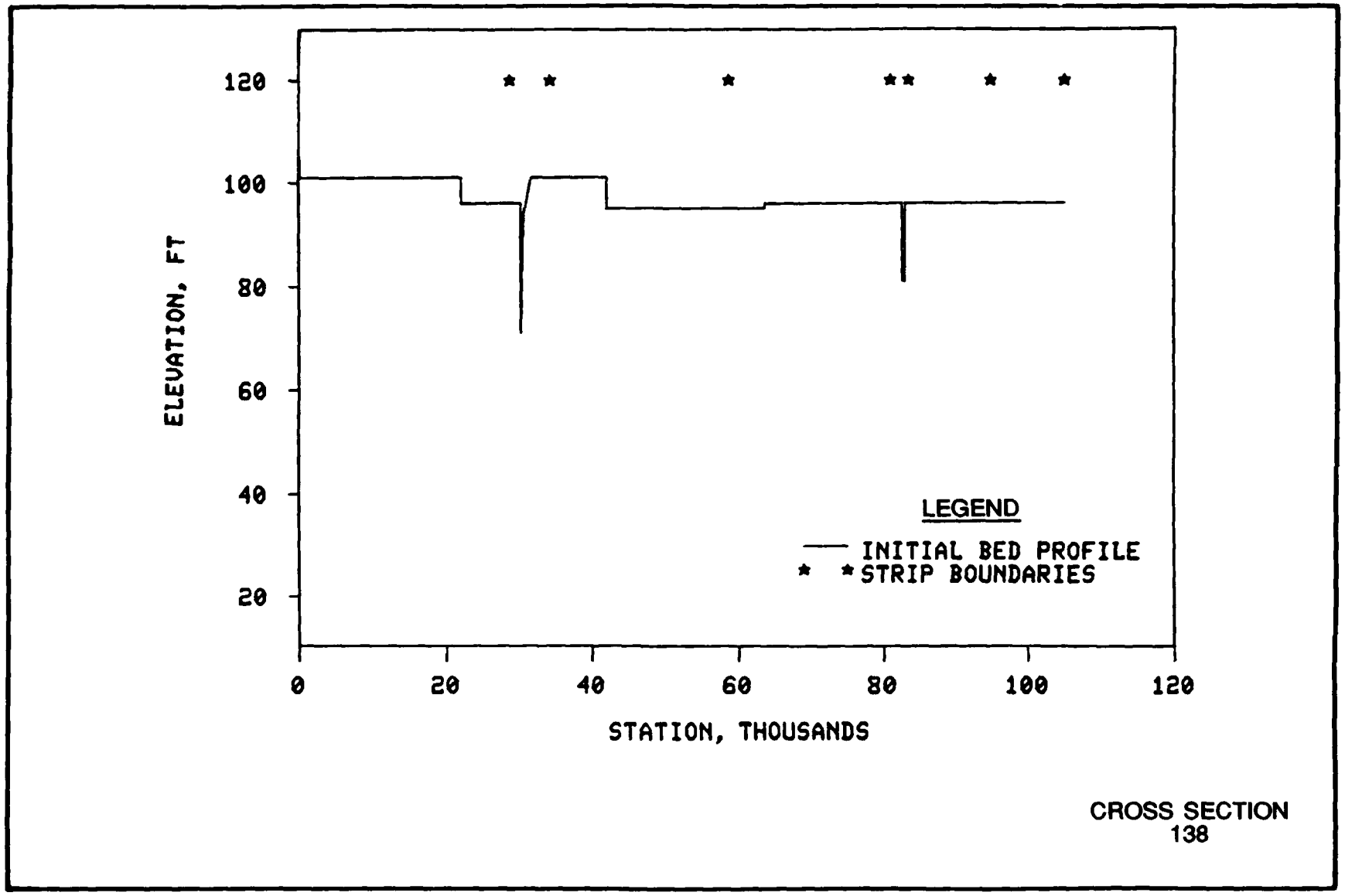
120
100
80
60
40
20
ELEVATION, FT
0
20
40
60
80
100
120
STATION, THOUSANDS
LEGEND
INITIAL BED PROFILE
STRIP BOUNDARIES
CROSS SECTION
138

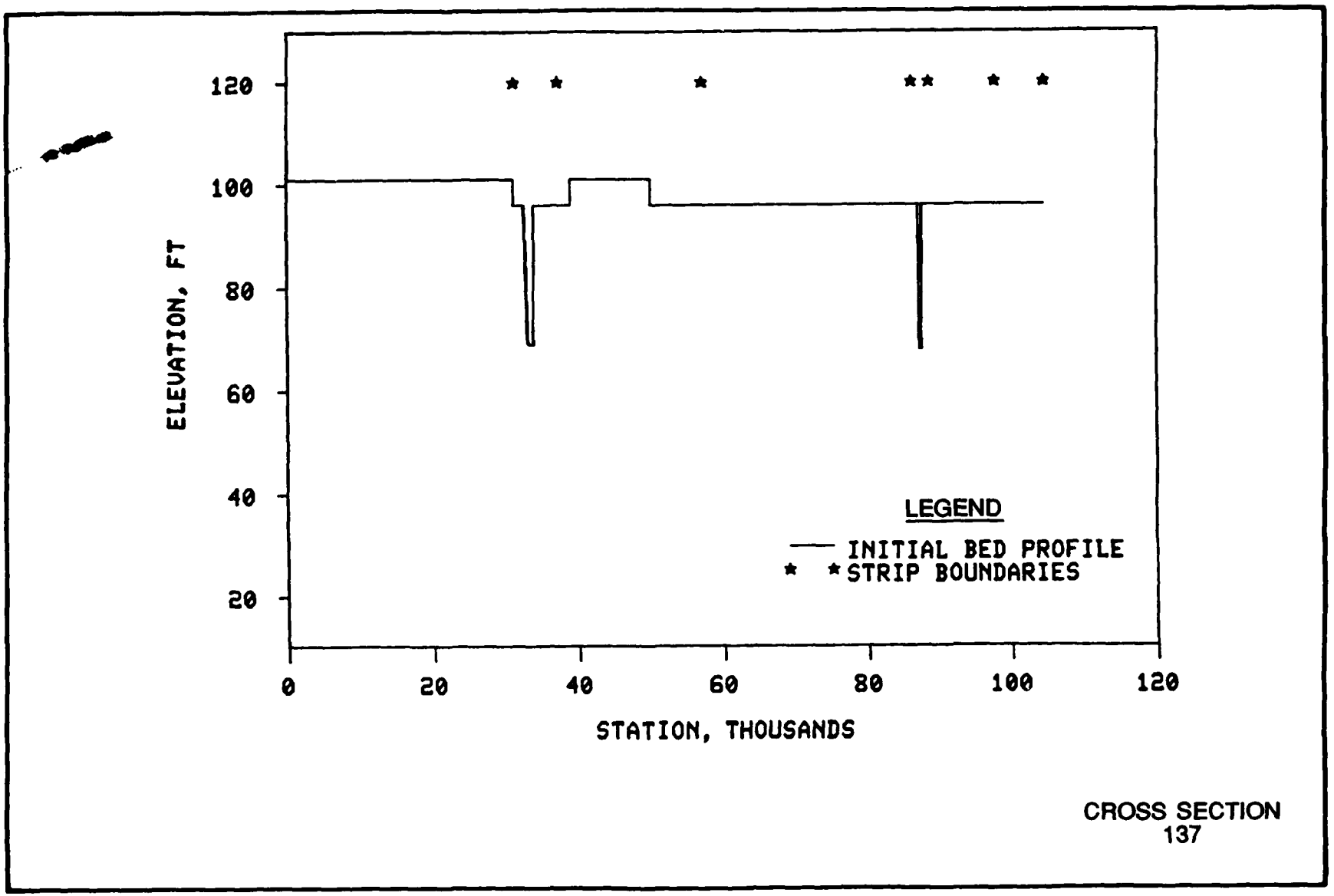

CROSS SECTION
137

PLATE 11

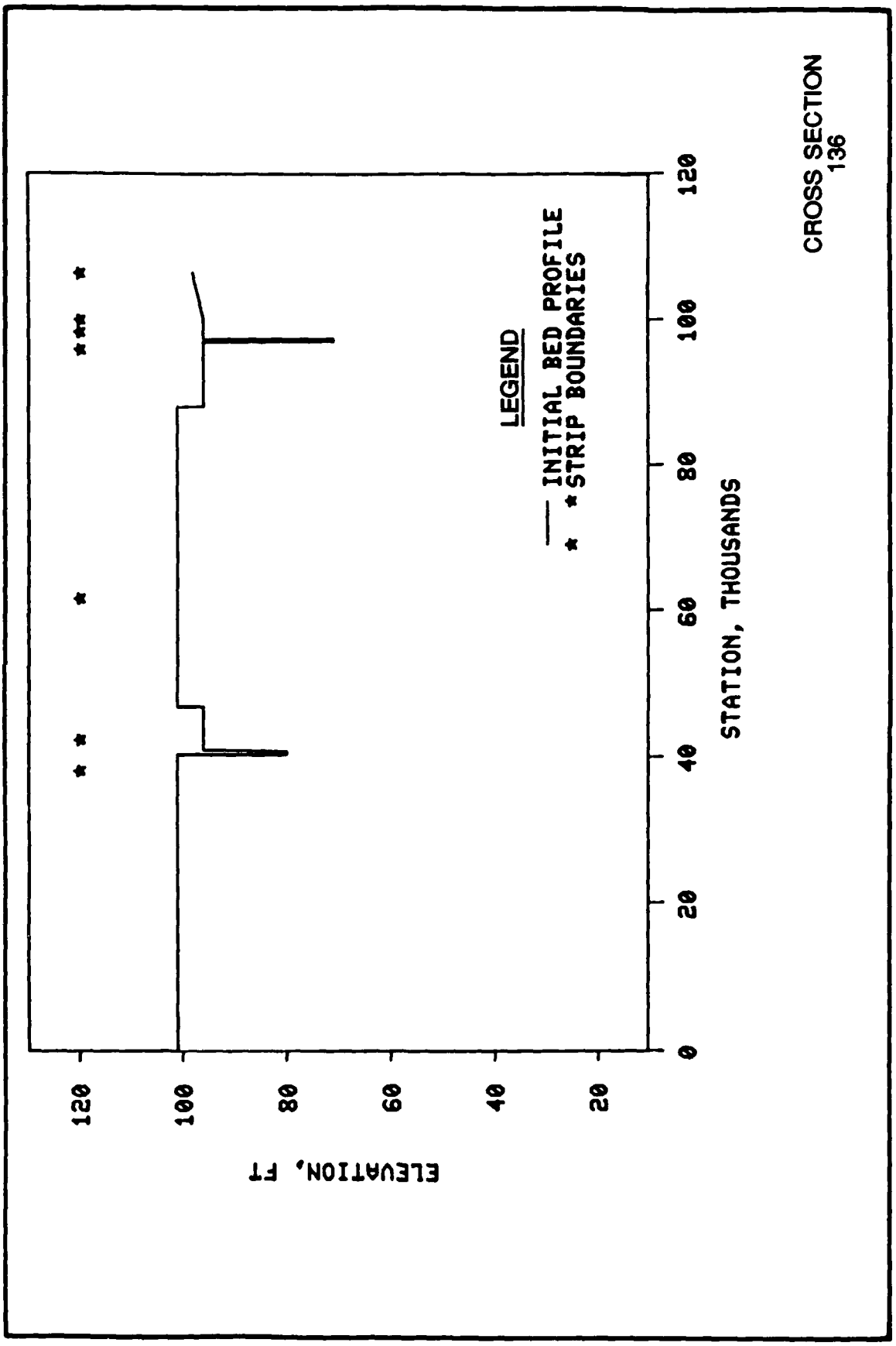
CROSS SECTION
136
LEGEND
INITIAL BED PROFILE
*STRIP BOUNDARIES
STATION, THOUSANDS
0
20
40
60
80
100
120
ELEVATION, FT
120
100
80
60
40
20

PLATE 12

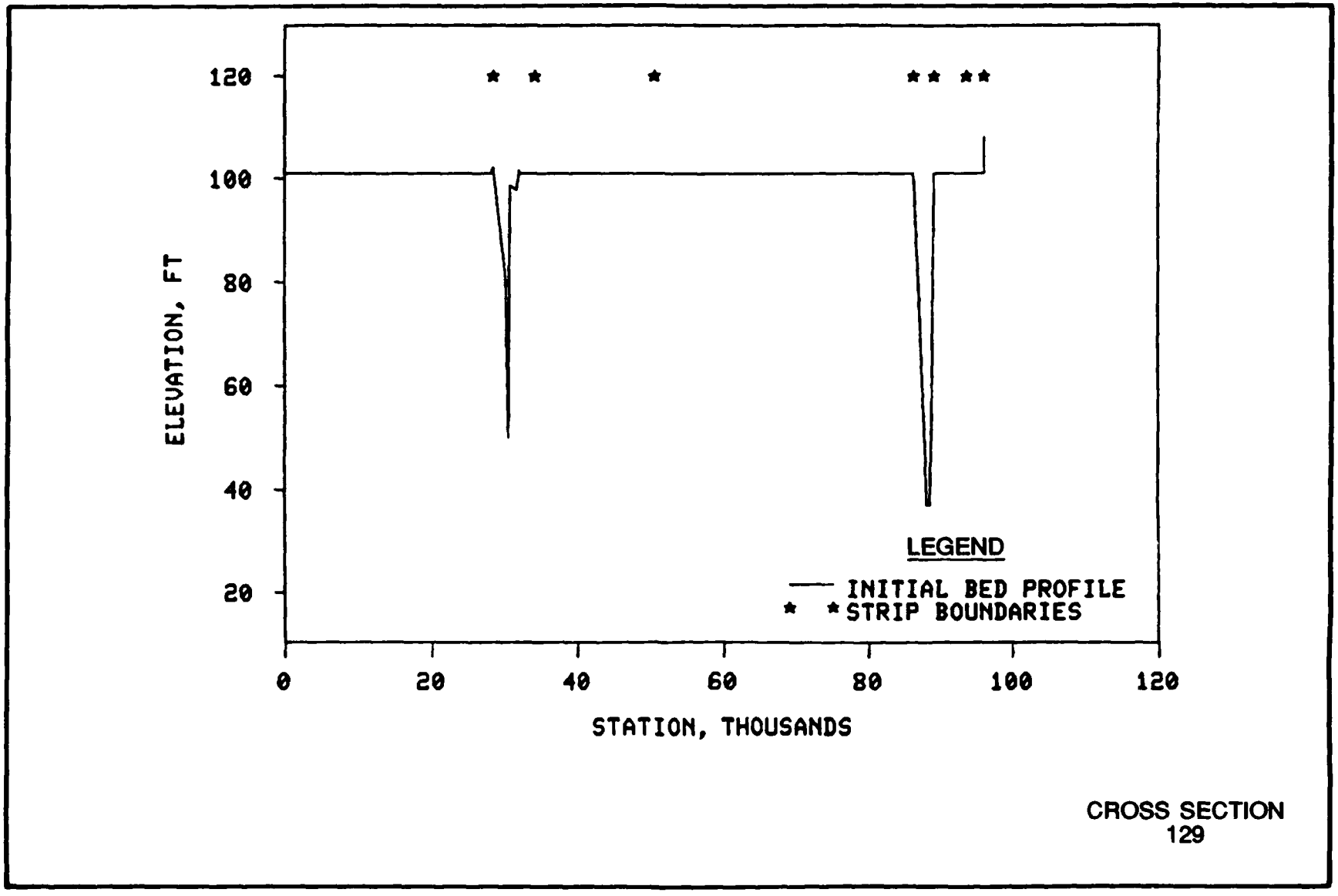
120
100
80
60
40
20
ELEVATION, FT
0
20
40
60
80
100
120
STATION, THOUSANDS
LEGEND
INITIAL BED PROFILE
STRIP BOUNDARIES
CROSS SECTION
129

PLATE 13

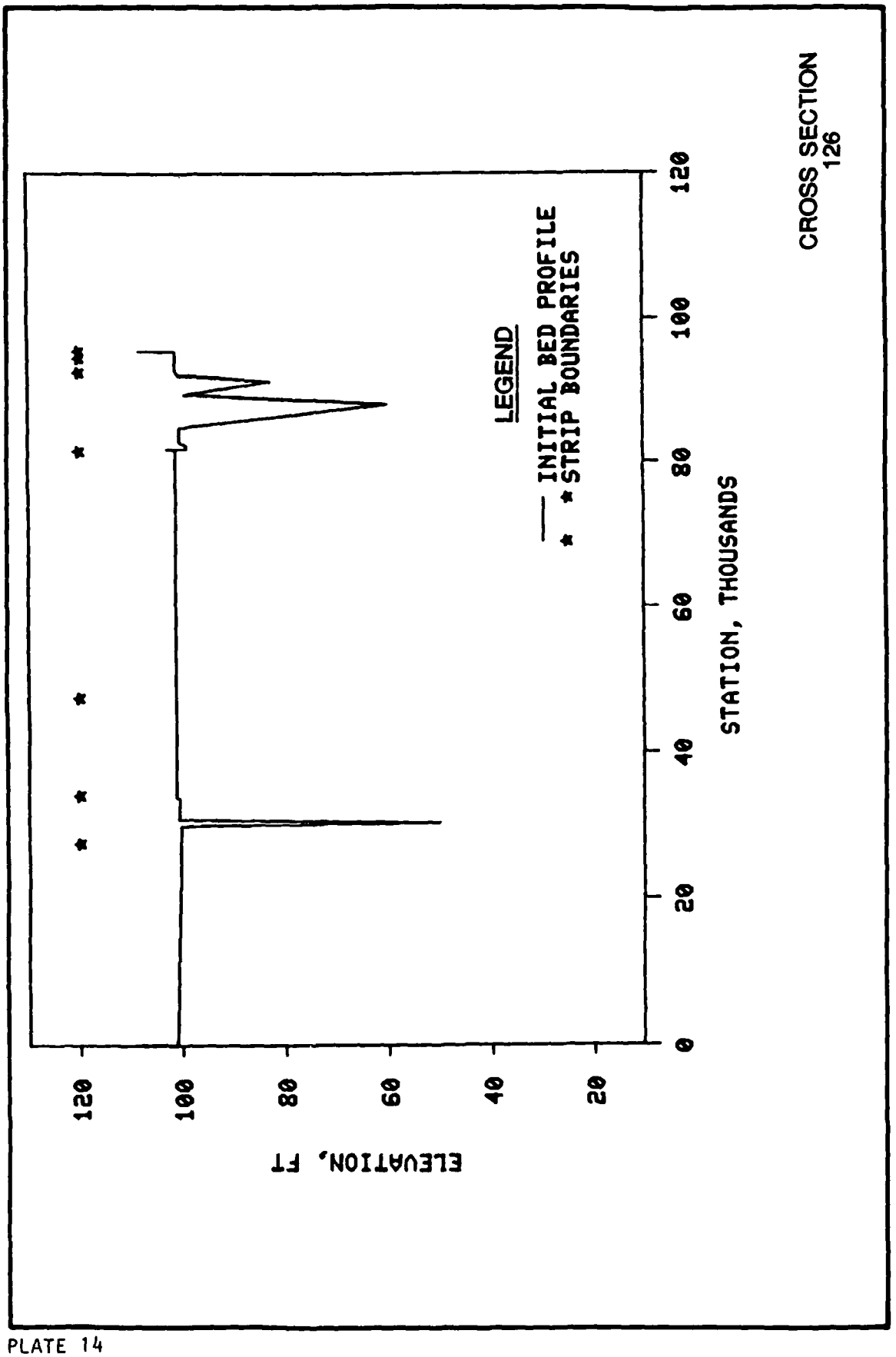
CROSS SECTION
126
LEGEND
INITIAL BED PROFILE
STRIP BOUNDARIES
STATION, THOUSANDS
0
20
40
60
80
100
120
ELEVATION, FT
20
40
60
80
100
120

PLATE 14

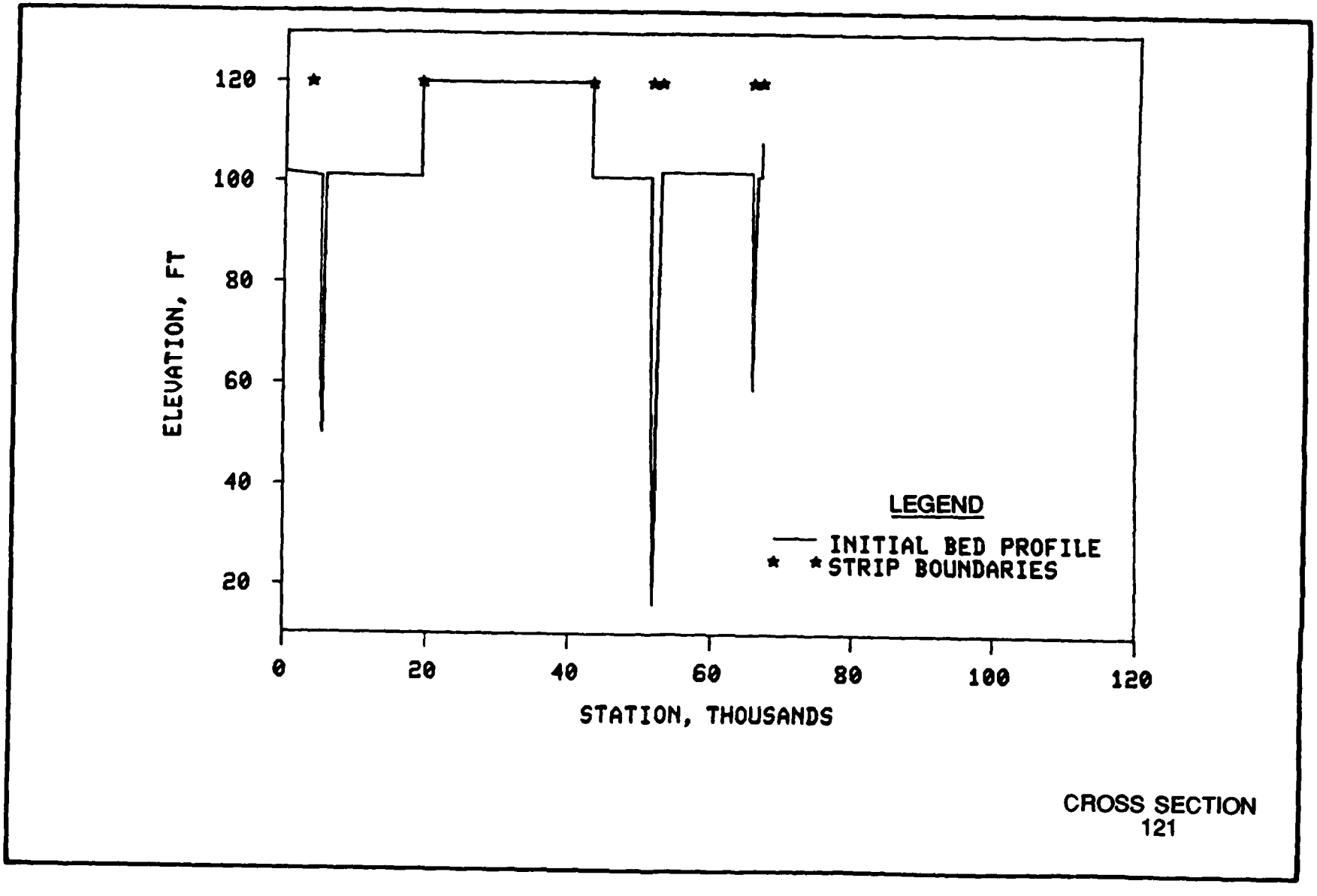
120
100
80
60
40
20
ELEVATION, FT
0
20
40
60
80
100
120
STATION, THOUSANDS
LEGEND
INITIAL BED PROFILE
STRIP BOUNDARIES
CROSS SECTION
121

PLATE 15

PLATE 16

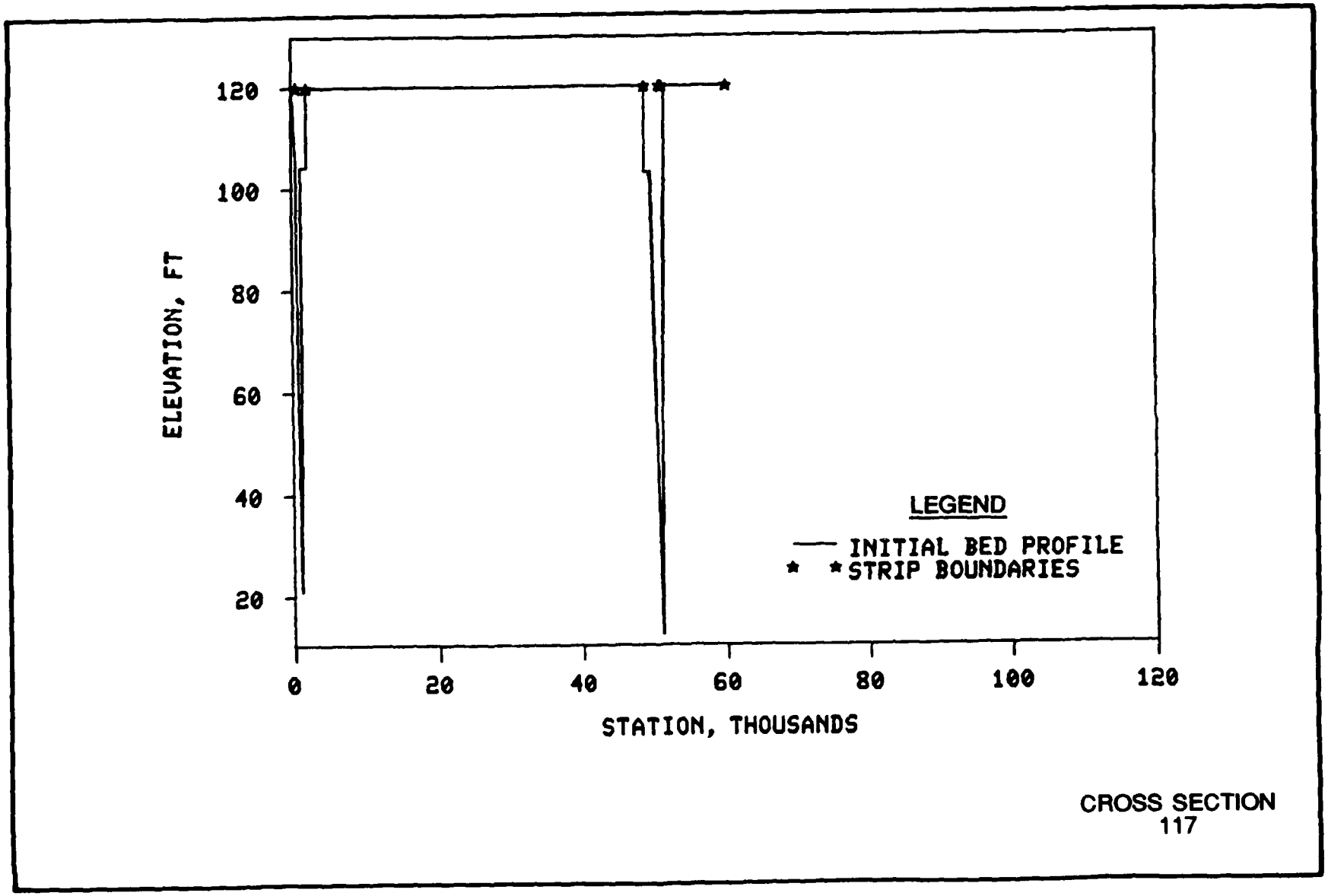
120
100
80
60
40
20
ELEVATION, FT
0
20
40
60
80
100
120
STATION, THOUSANDS
LEGEND
INITIAL BED PROFILE
STRIP BOUNDARIES
CROSS SECTION
117

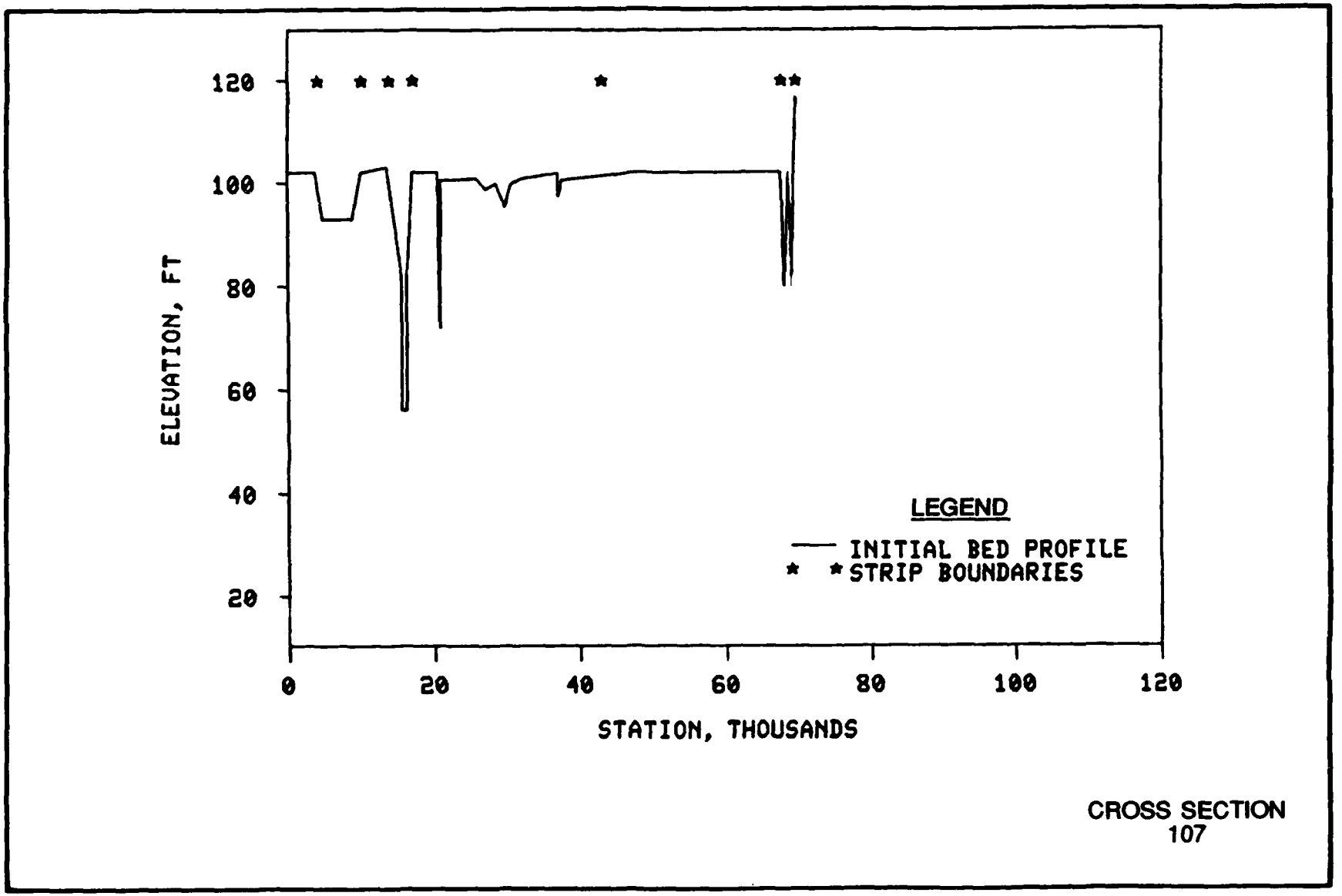

CROSS SECTION
107

PLATE 17

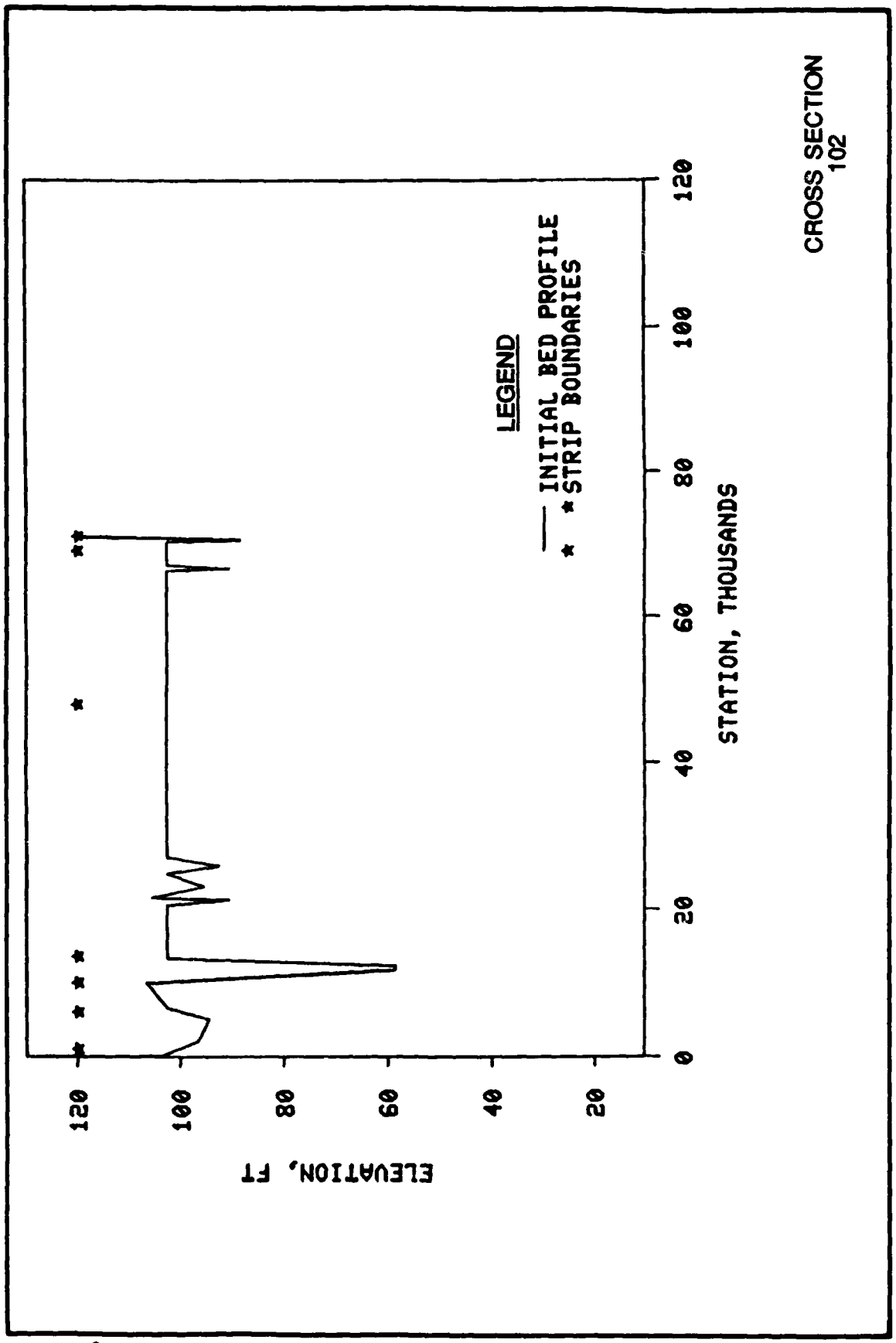
CROSS SECTION
102
LEGEND
INITIAL BED PROFILE
STRIP BOUNDARIES
STATION, THOUSANDS
0
20
40
60
80
100
120
ELEVATION, FT
120
100
80
60
40
20

PLATE 18

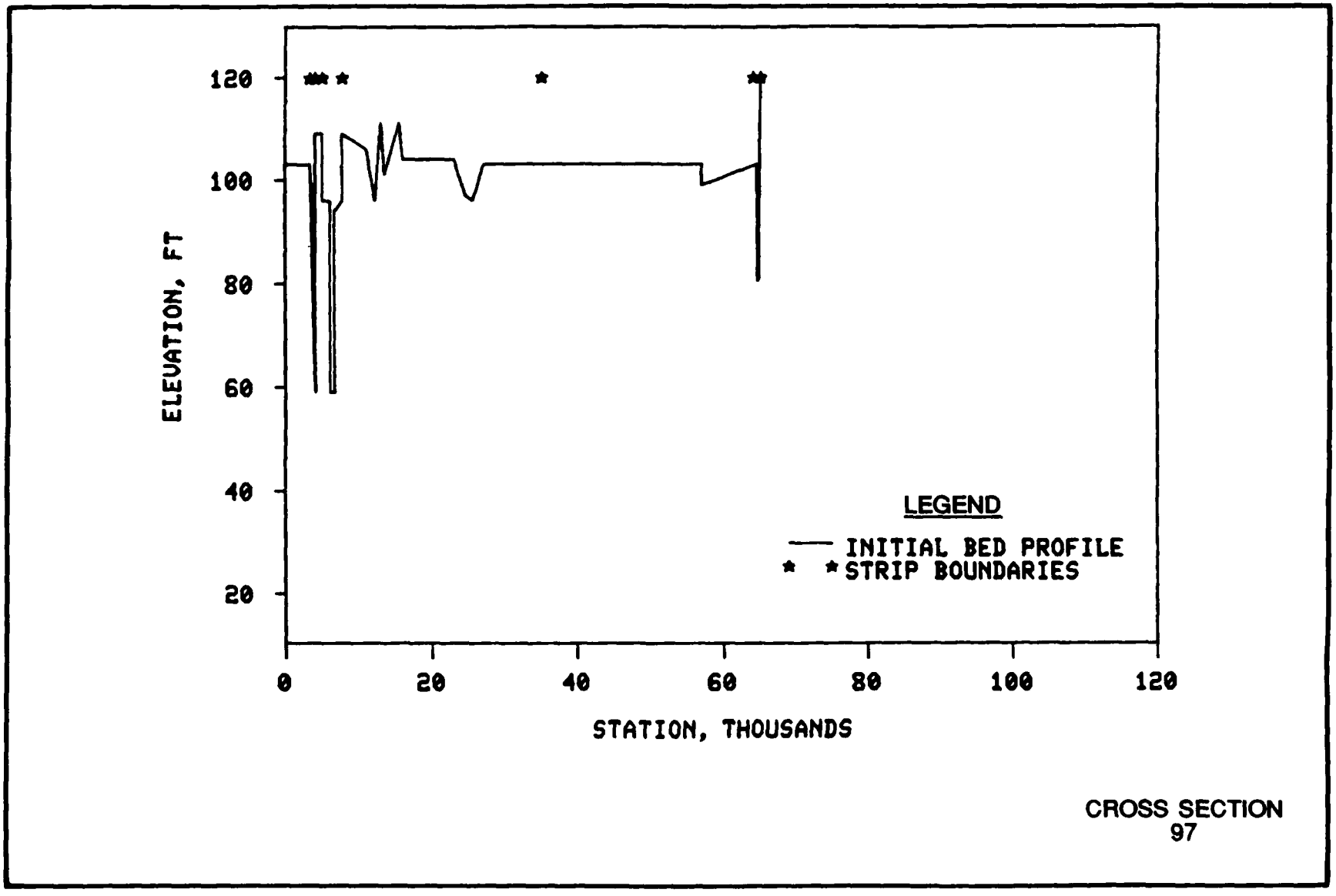
120
100
80
60
40
20
ELEVATION, FT
0
20
40
60
80
100
120
STATION, THOUSANDS
LEGEND
INITIAL BED PROFILE
STRIP BOUNDARIES
CROSS SECTION
97

PLATE 19

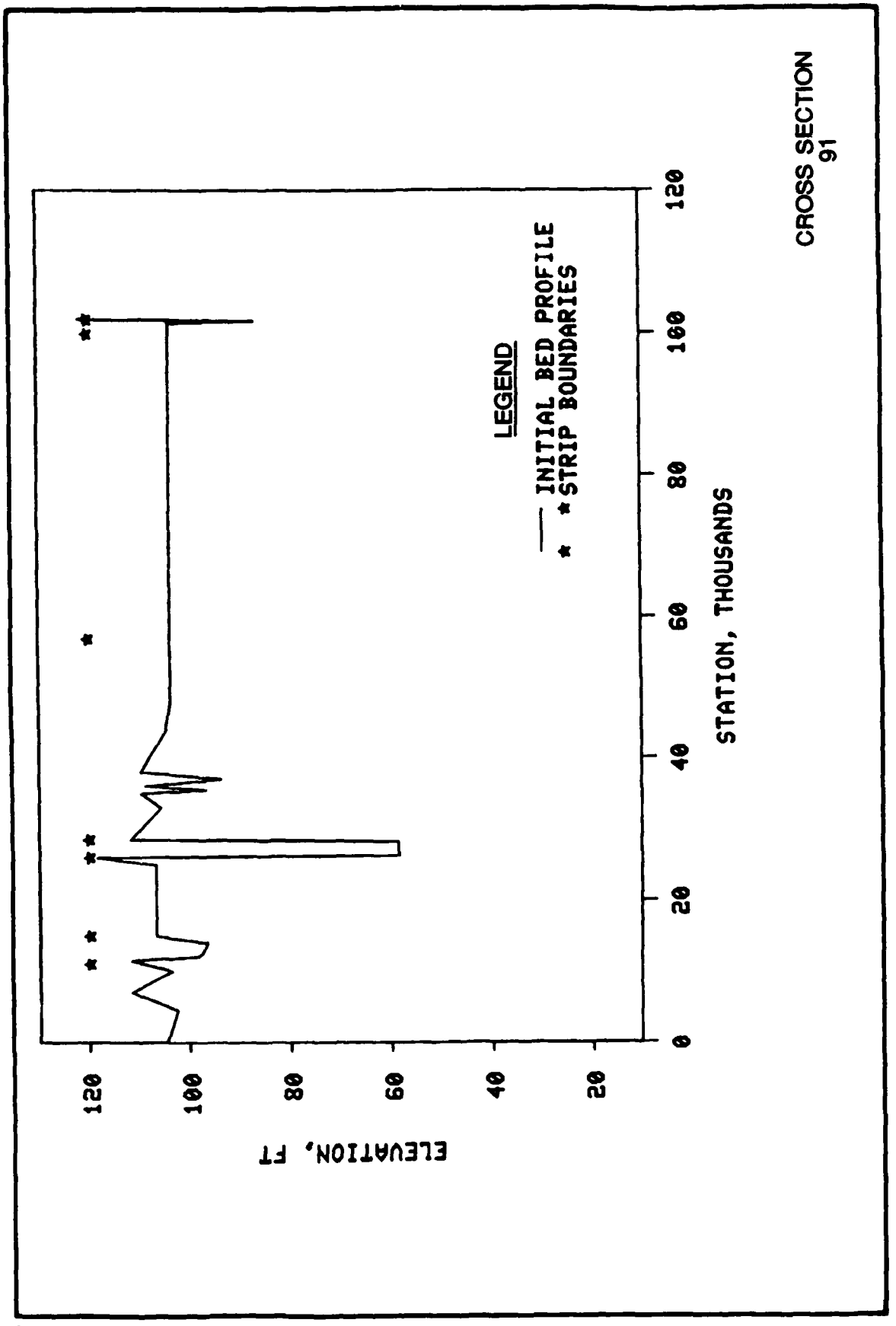
CROSS SECTION
91
LEGEND
INITIAL BED PROFILE
STRIP BOUNDARIES
STATION, THOUSANDS
0
20
40
60
80
100
120
ELEVATION, FT
120
100
80
60
40
20

PLATE 20

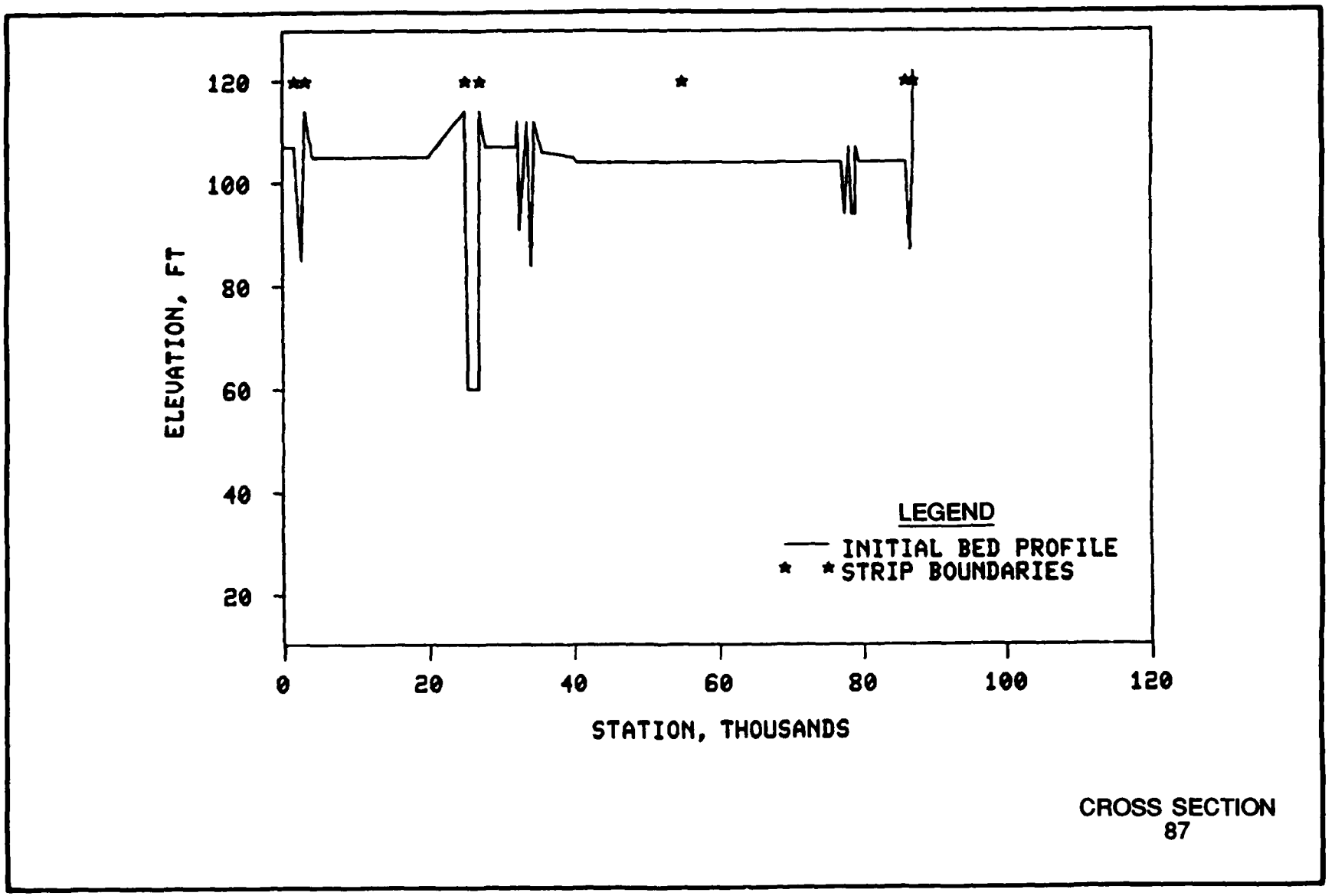

CROSS SECTION
87

PLATE 21

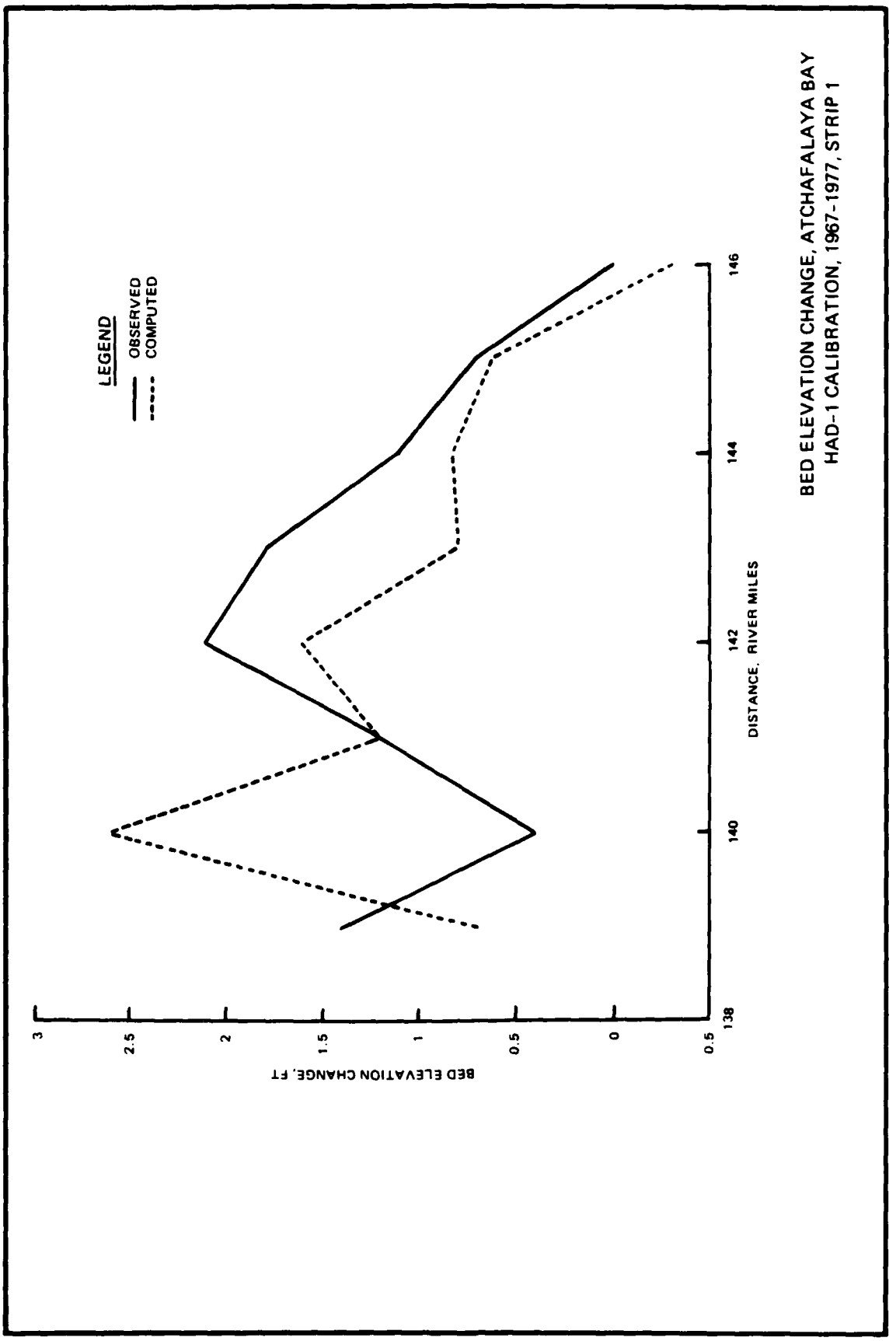

BED ELEVATION CHANGE, ATCHAFALAYA BAY
HAD-1 CALIBRATION, 1967-1977, STRIP 1

PLATE 22

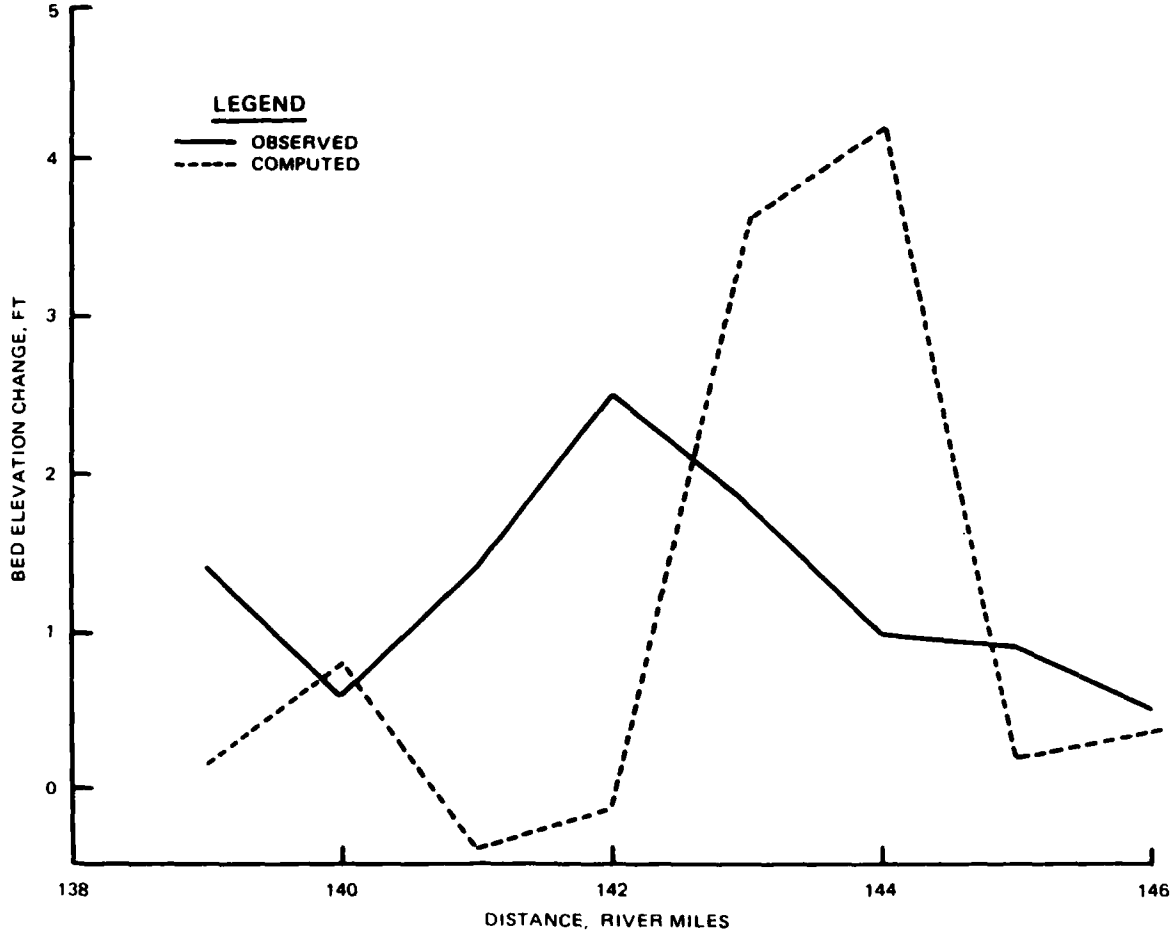

BED ELEVATION CHANGE, ATCHAFALAYA BAY
HAD-1 CALIBRATION, 1967-1977, STRIP 2

PLATE 23

PLATE 24

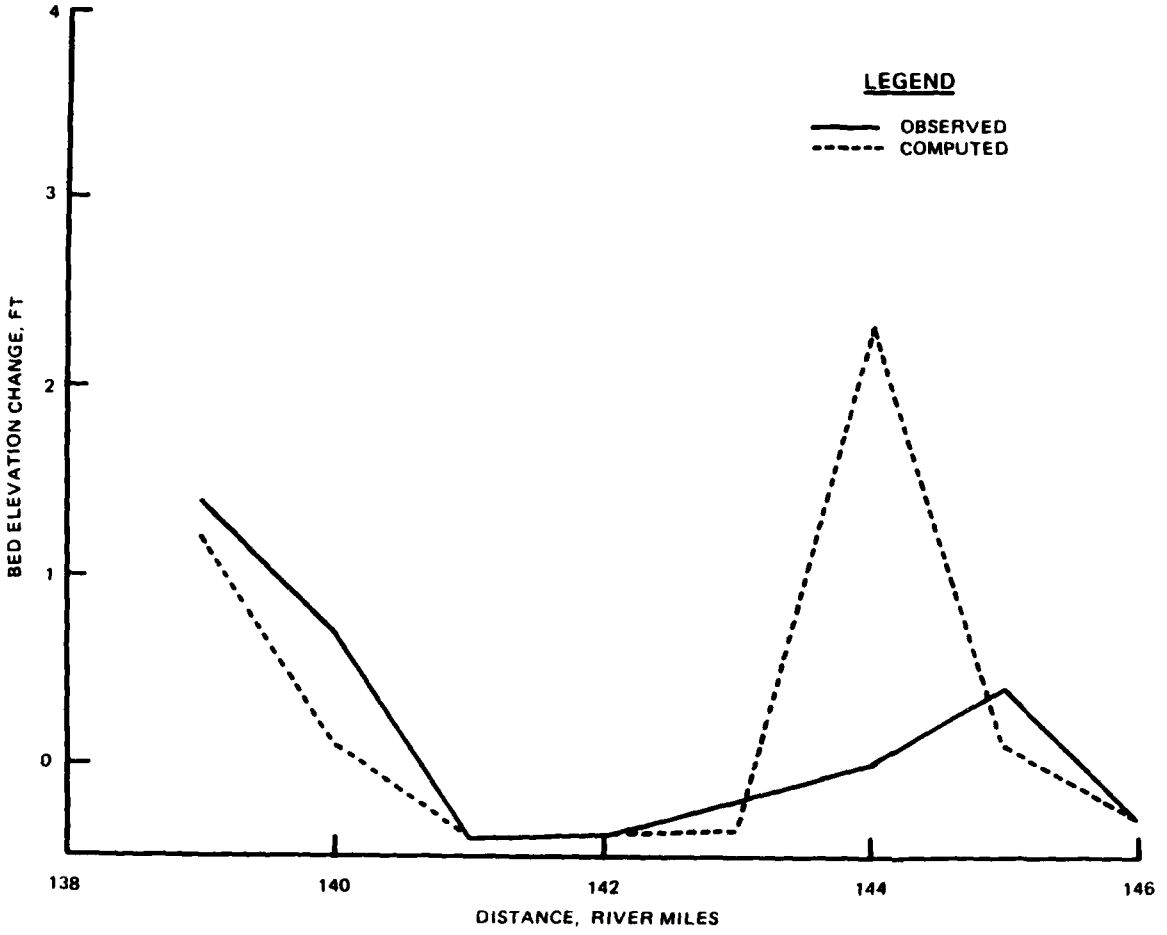

BED ELEVATION CHANGE, ATCHAFALAYA BAY
HAD-1 CALIBRATION, 1967-1977, STRIP 3

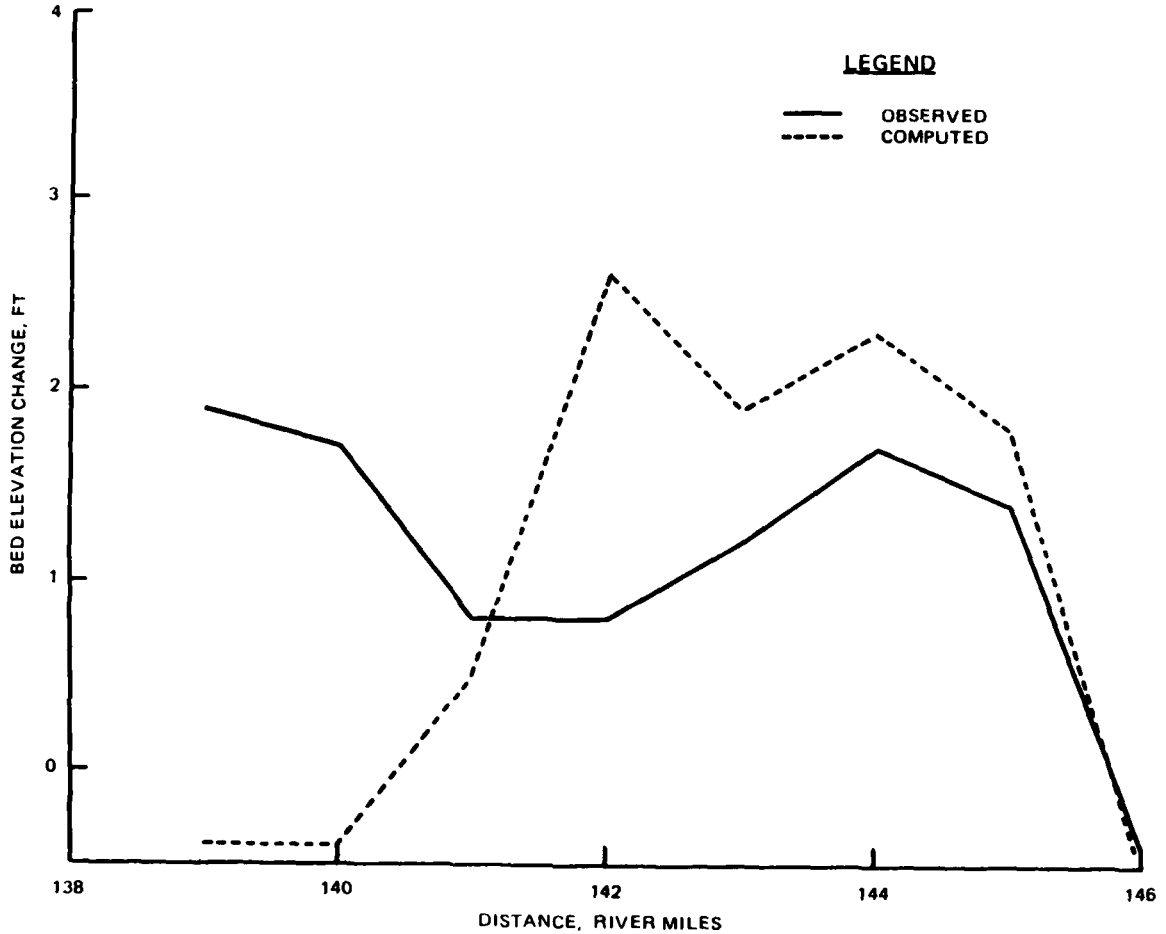

BED ELEVATION CHANGE, ATCHAFALAYA BAY
HAD-1 CALIBRATION, 1967-1977, STRIP 4

PLATE 25

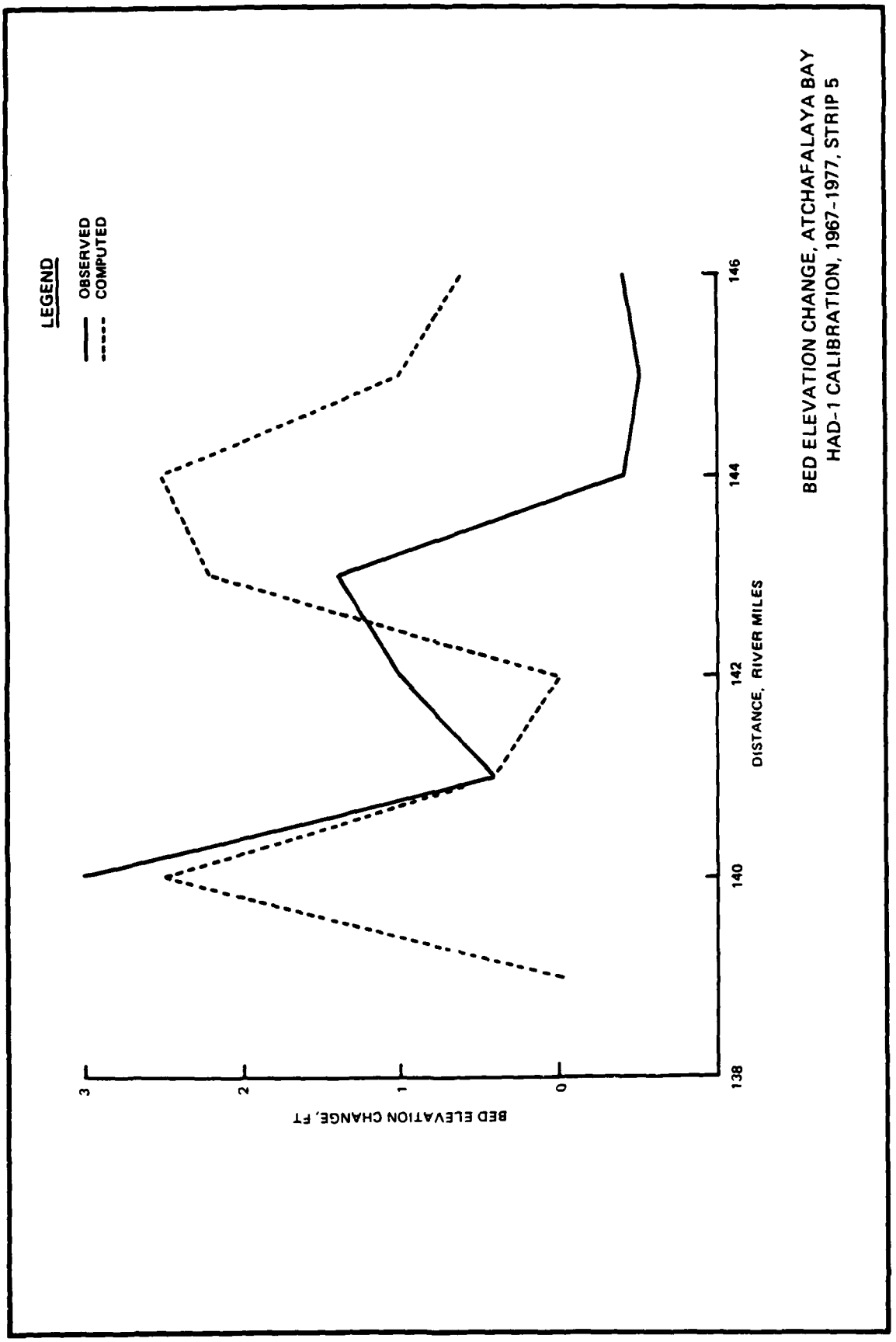

BED ELEVATION CHANGE, ATCHAFALAYA BAY
HAD-1 CALIBRATION, 1967-1977, STRIP 5

PLATE 26

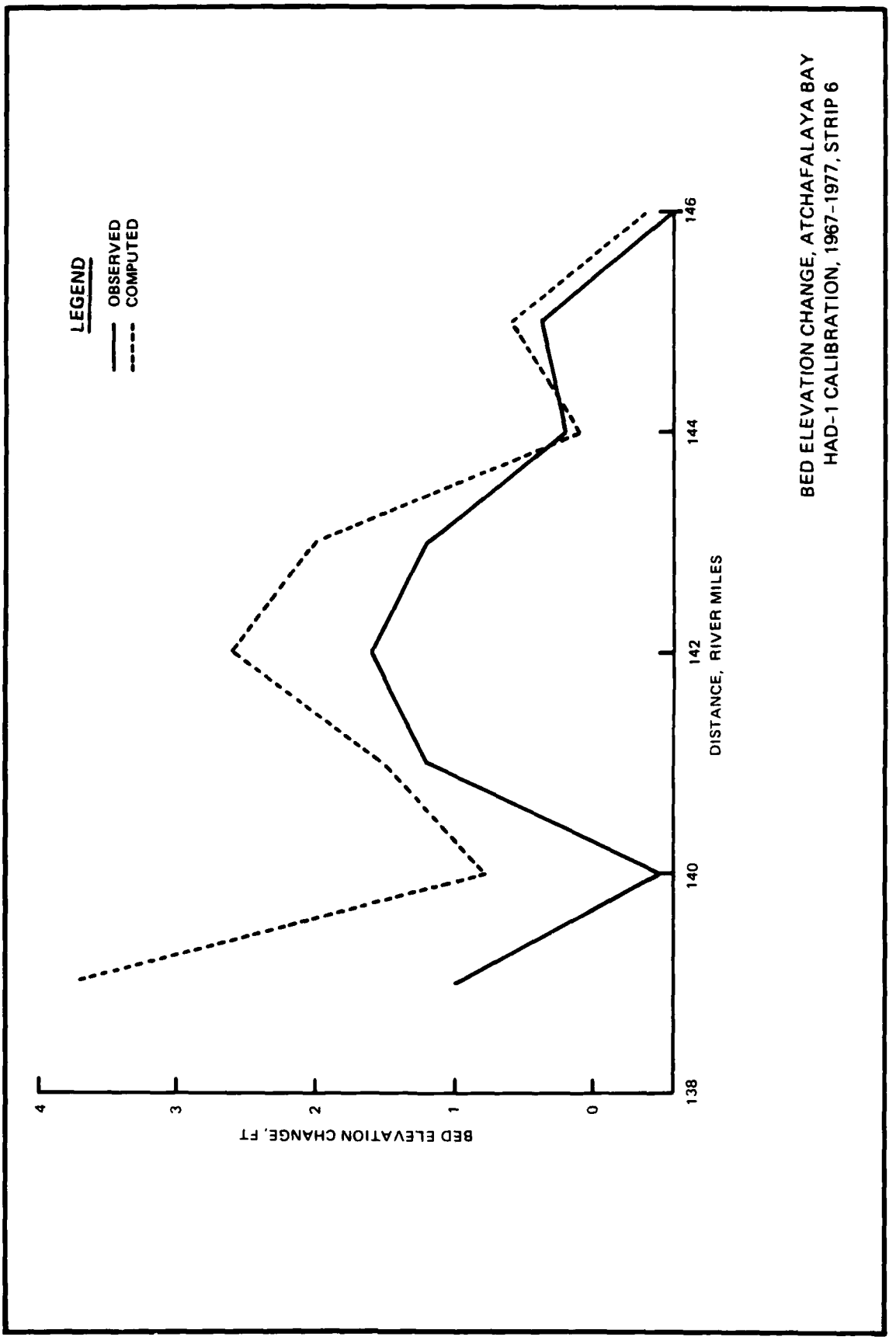

BED ELEVATION CHANGE, ATCHAFALAYA BAY
HAD-1 CALIBRATION, 1967-1977, STRIP 6

PLATE 27

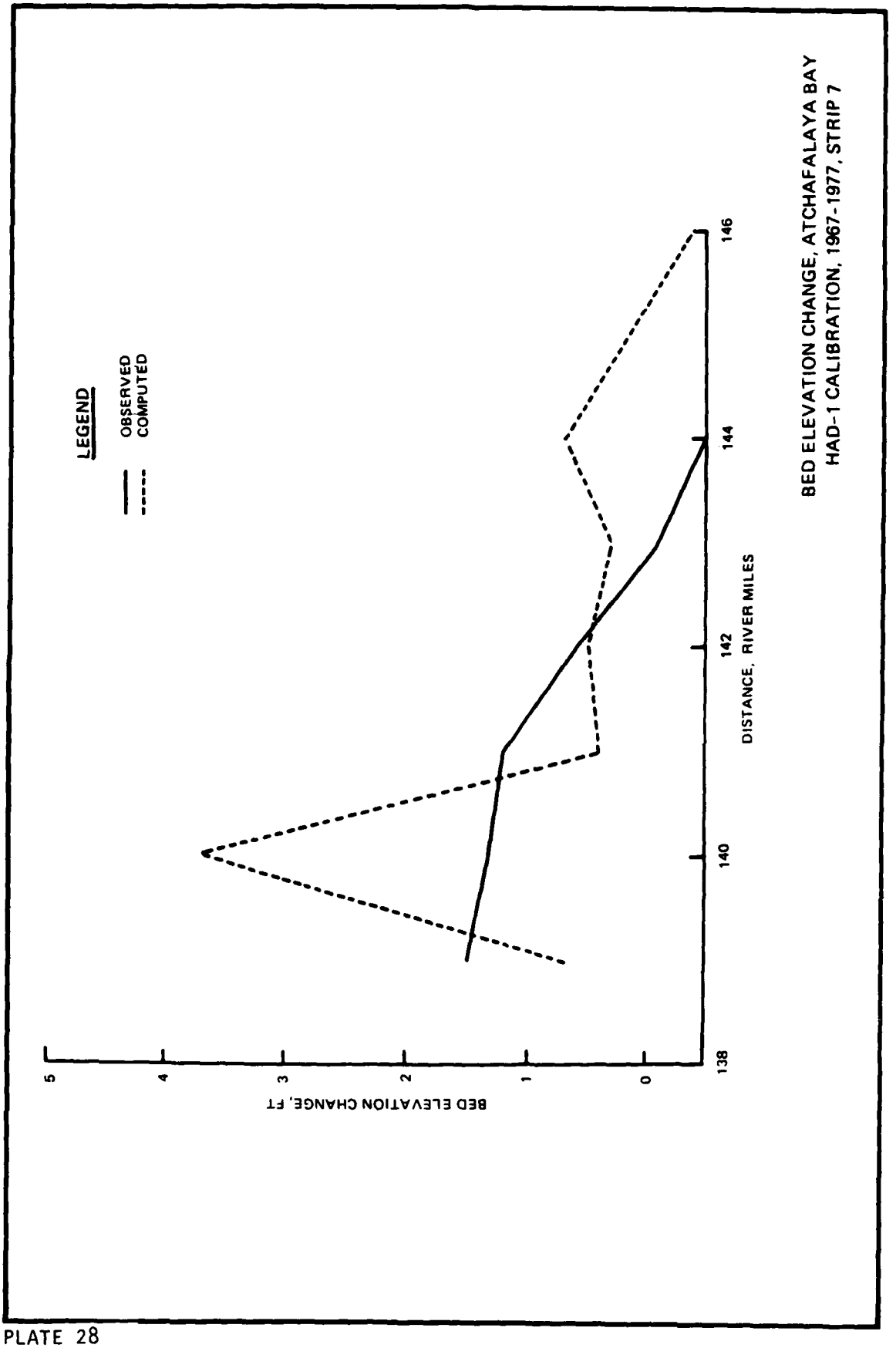
BED ELEVATION CHANGE, ATCHAFALAYA BAY
HAD-1 CALIBRATION, 1967-1977, STRIP 7
LEGEND
OBSERVED
COMPUTED
BED ELEVATION CHANGE, FT
0
1
2
3
4
5
138
140
142
144
146
DISTANCE, RIVER MILES

PLATE 28

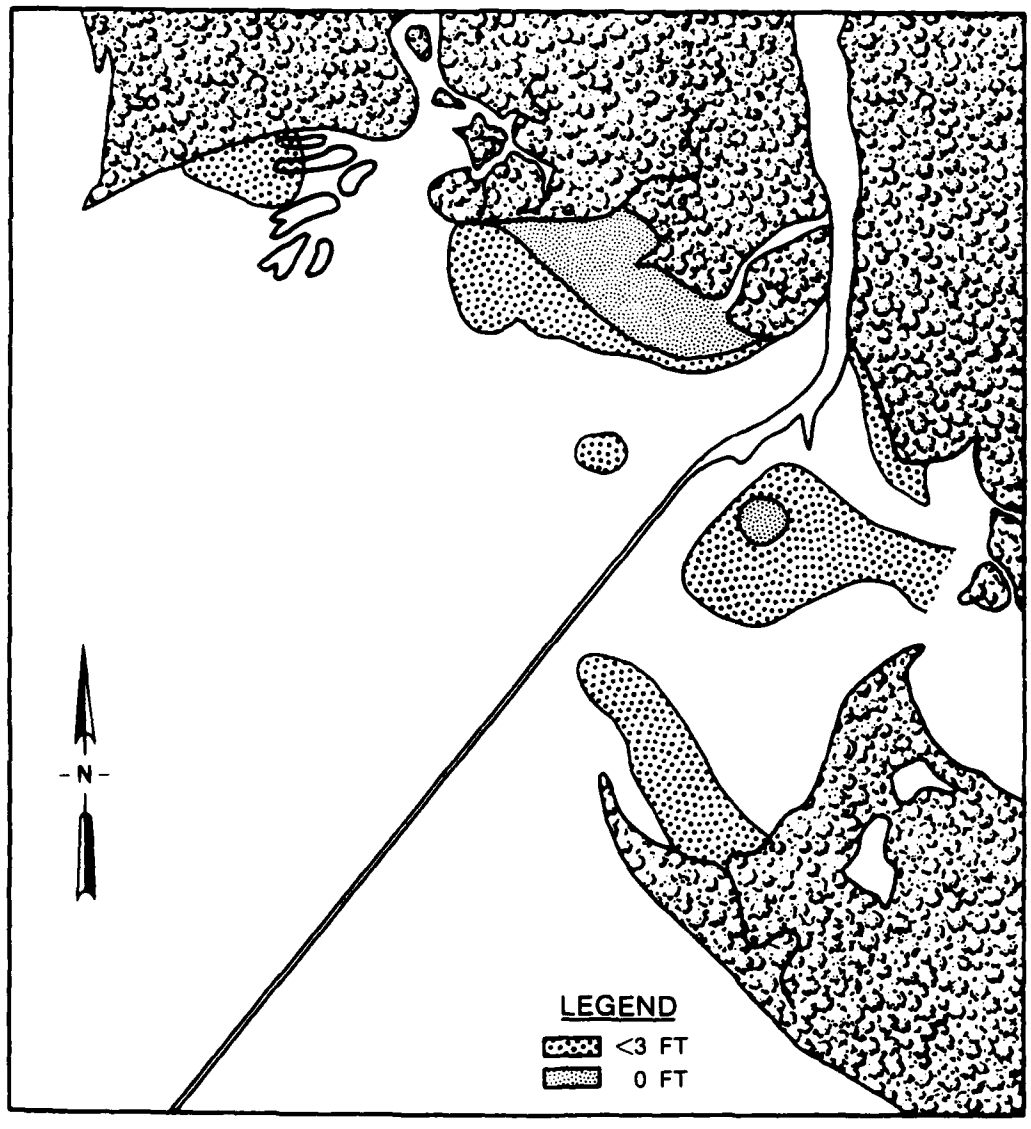

CALCULATED DELTA CONFIGURATION
BASE CONDITION

PLATE 29

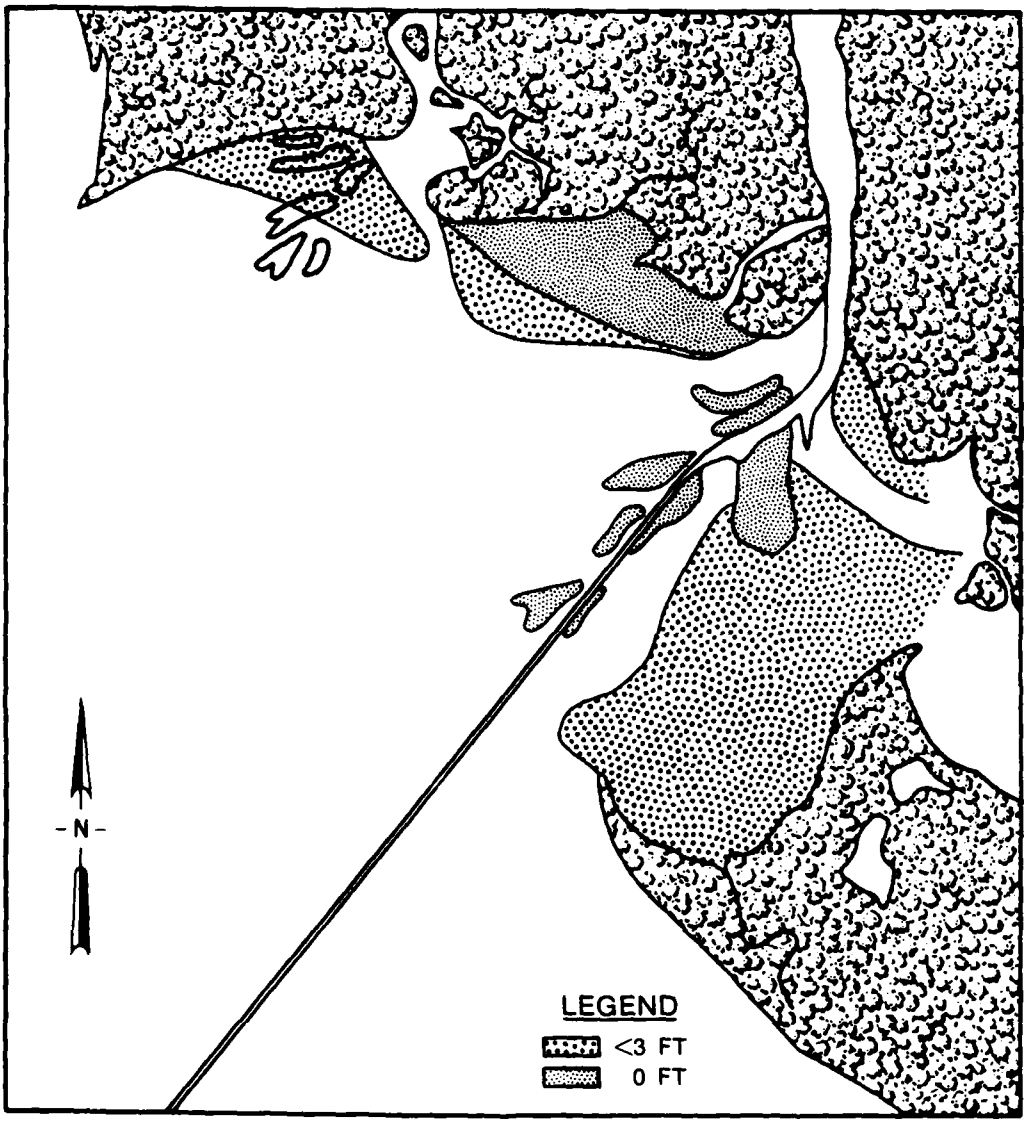

CALCULATED DELTA CONFIGURATION
YEAR 10

PLATE 30

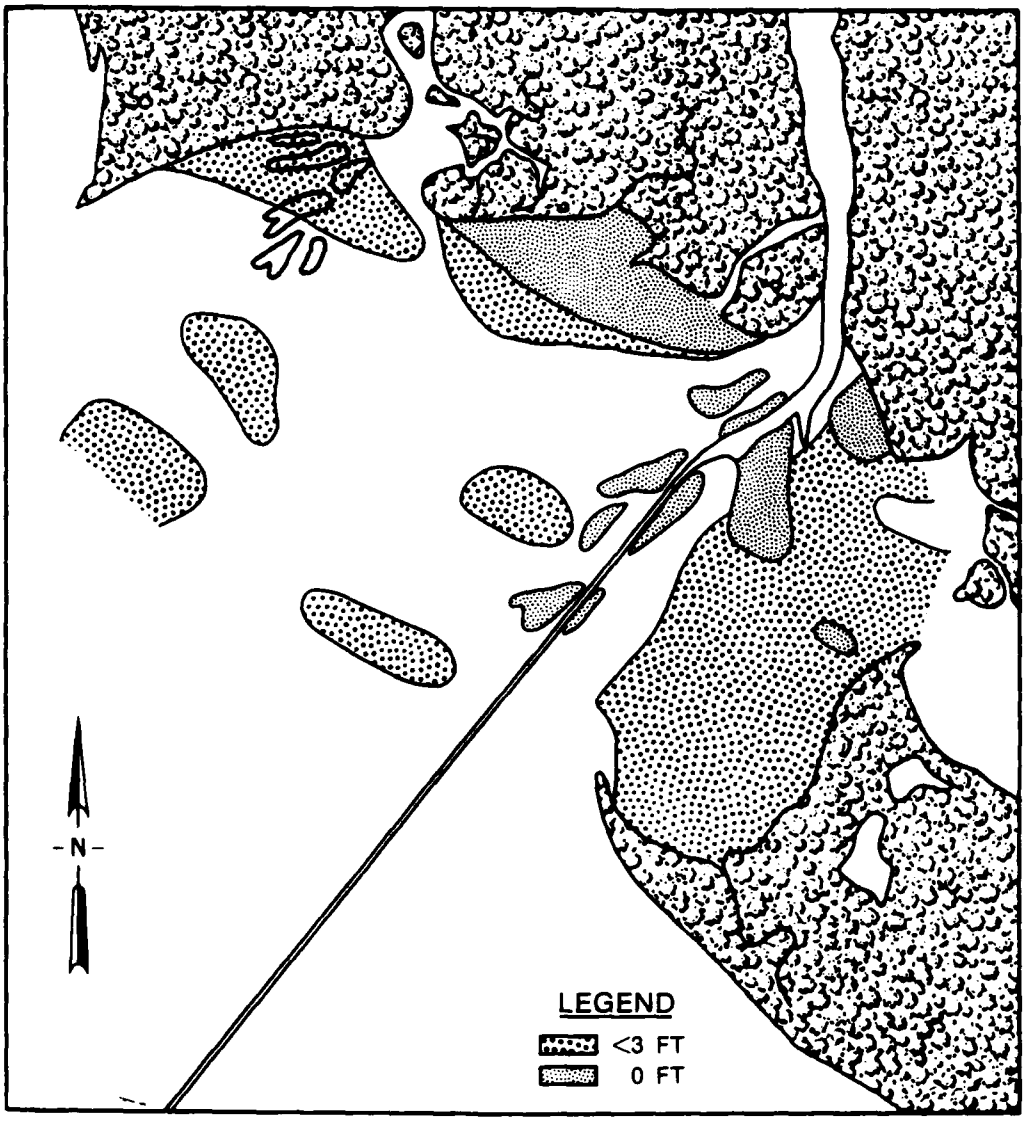

CALCULATED DELTA CONFIGURATION
YEAR 20

PLATE 31

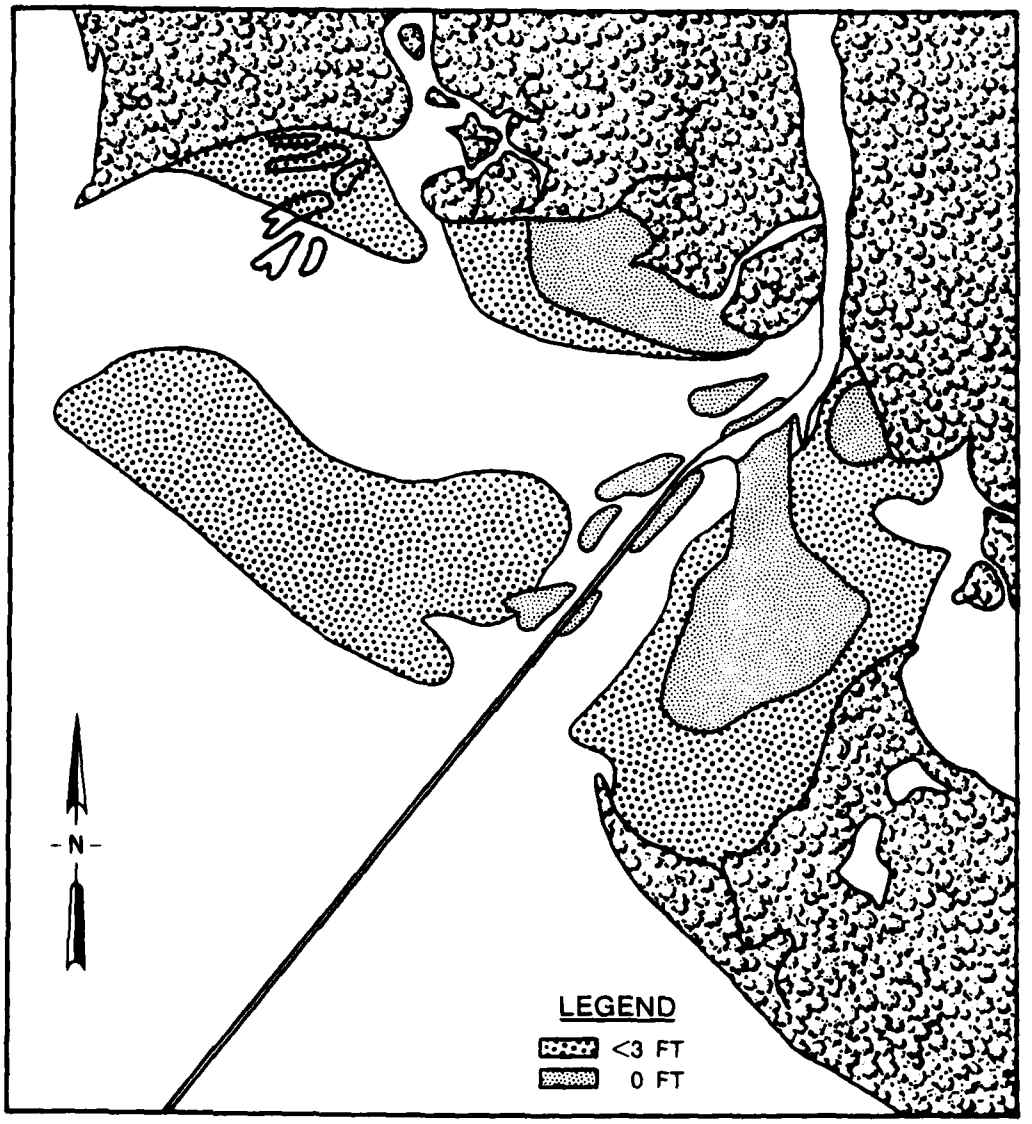

CALCULATED DELTA CONFIGURATION
YEAR 30

PLATE 32

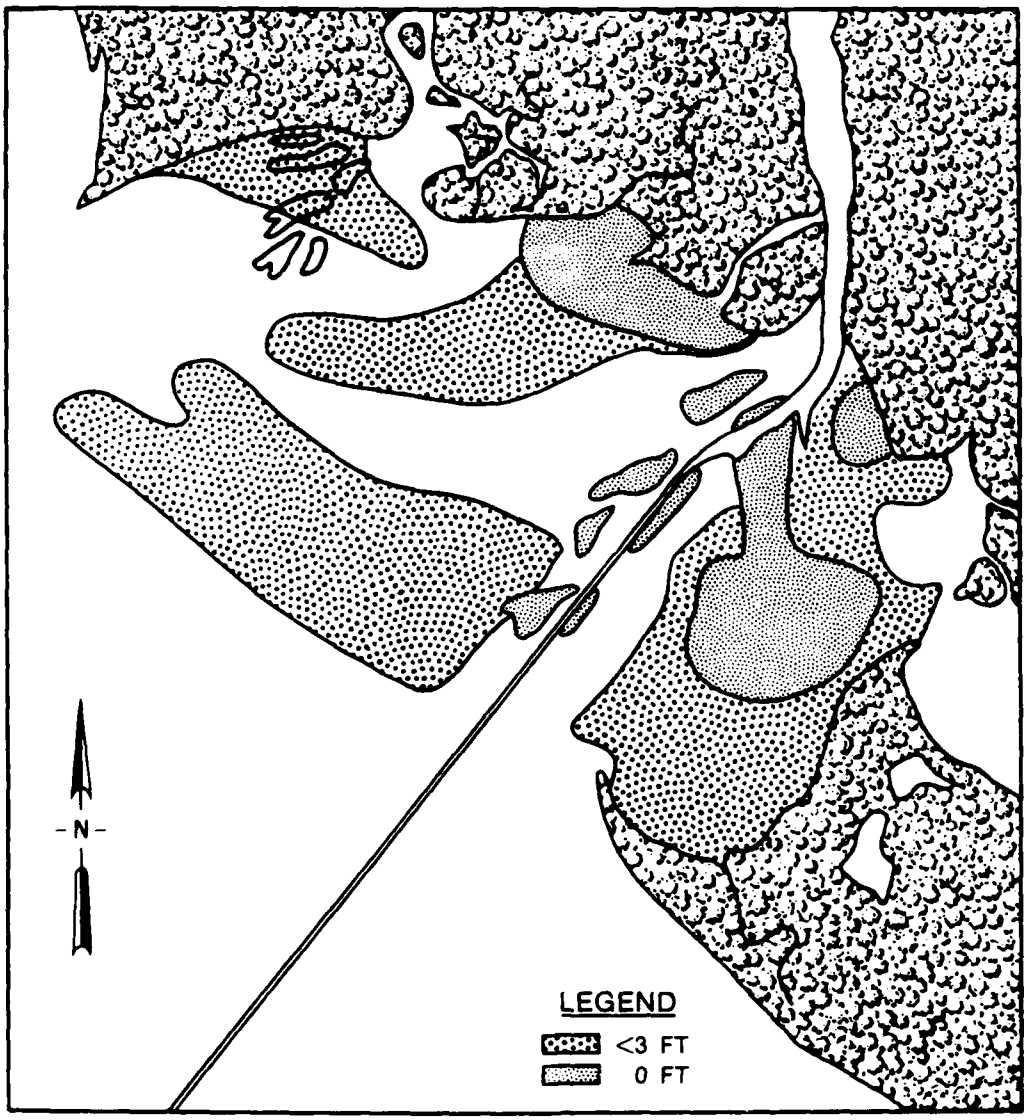

CALCULATED DELTA CONFIGURATION
YEAR 40

PLATE 33

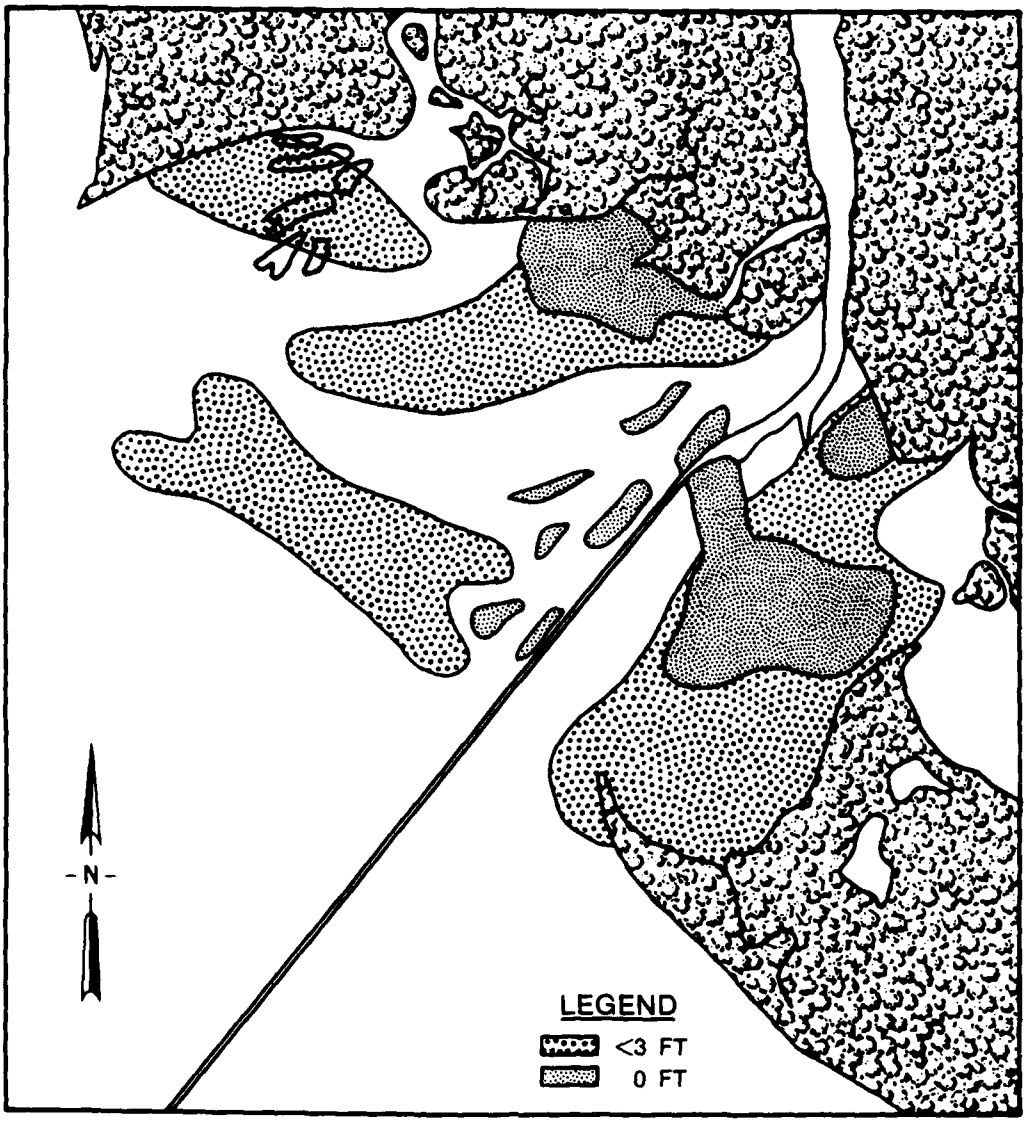

CALCULATED DELTA CONFIGURATION
YEAR 50

PLATE 34

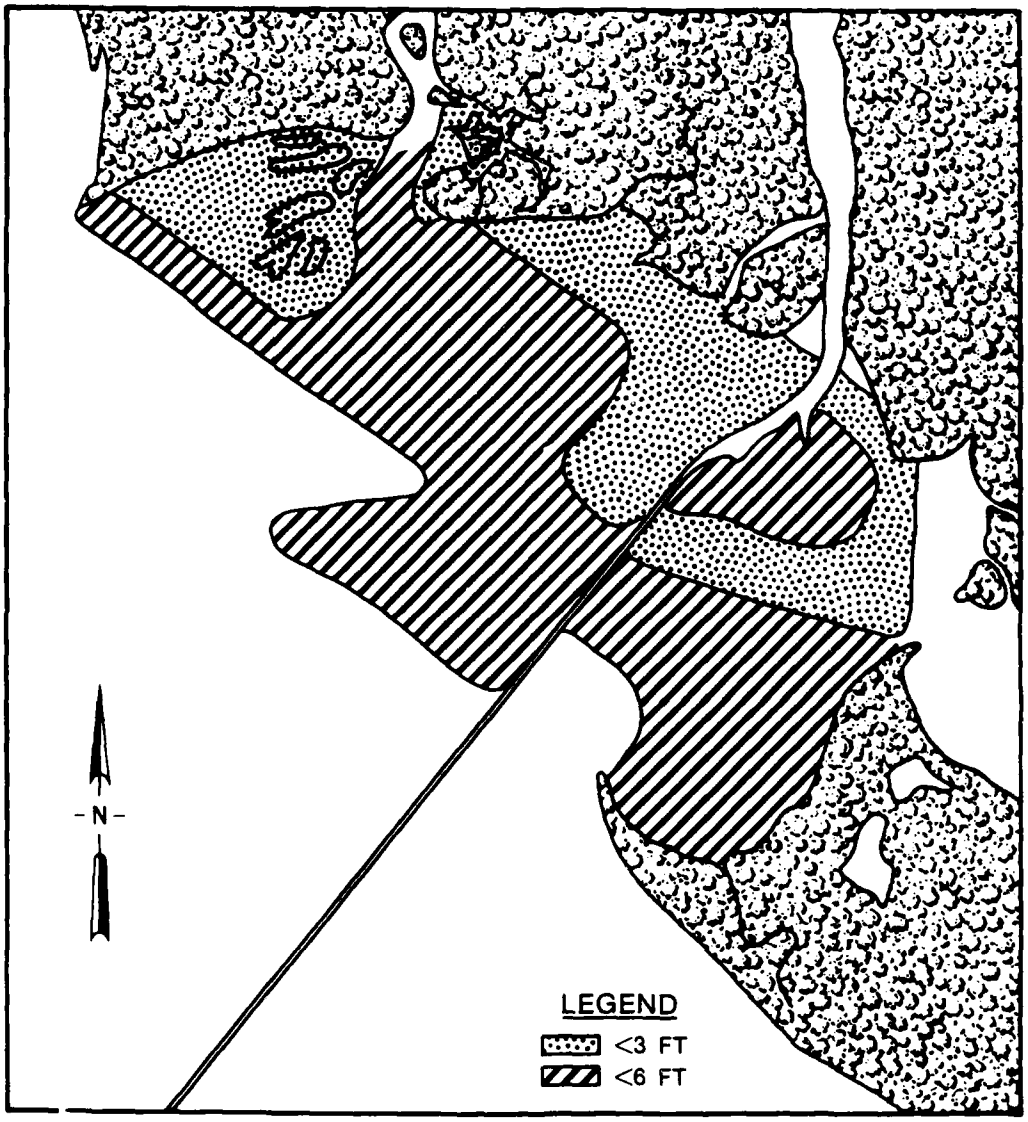

CALCULATED DELTA CONFIGURATION
YEAR 50
ALTERNATE DELTA SHAPE

PLATE 35

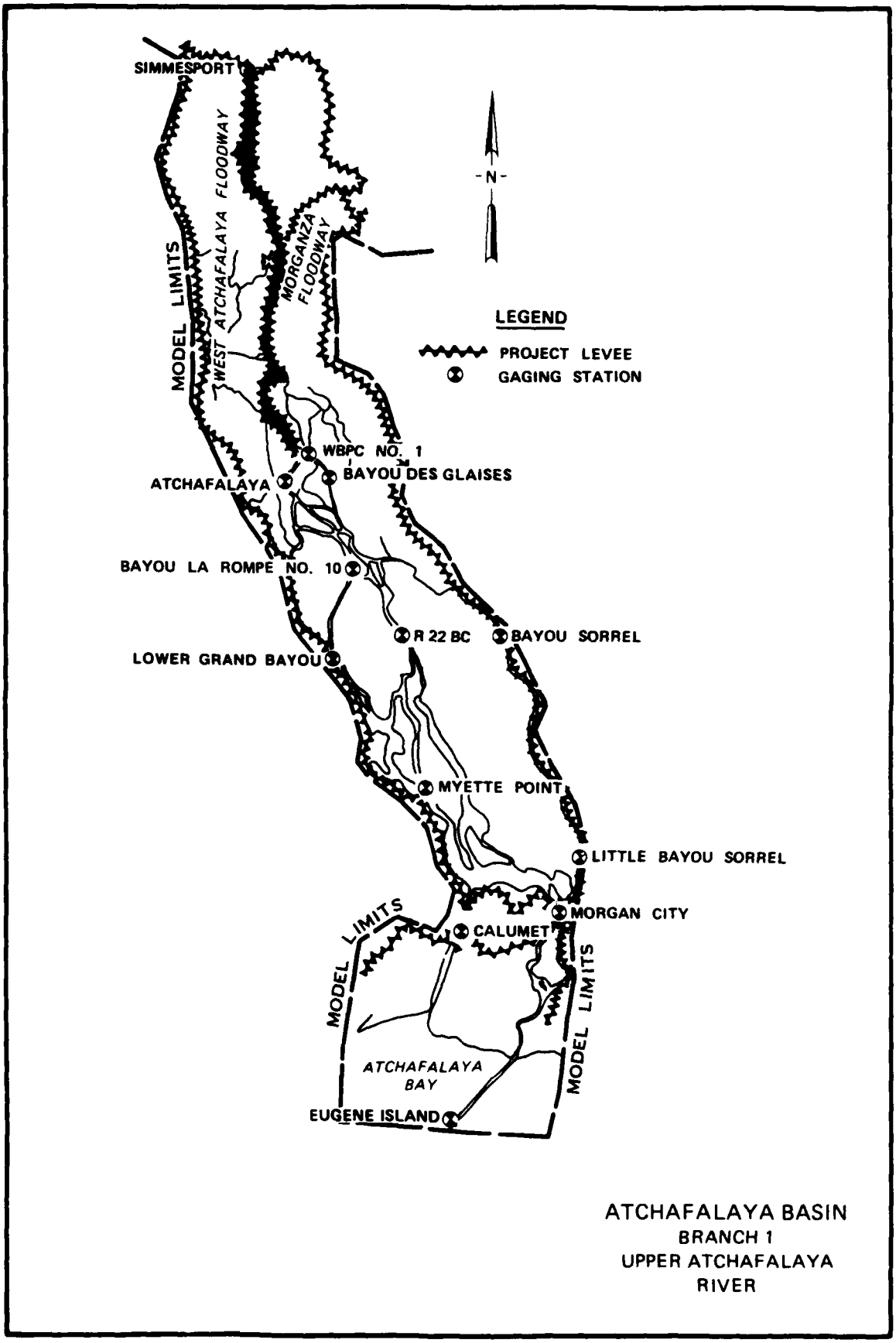
SIMMESPORT
WEST ATCHAFALAYA FLOODWAY
MORGANZA FLOODWAY
MODEL LIMITS
N
LEGEND
PROJECT LEVEE
GAGING STATION
WBPC NO. 1
BAYOU DES GLAISES
ATCHAFALAYA
BAYOU LA ROMPE NO. 10
R 22 BC
BAYOU SORREL
LOWER GRAND BAYOU
MYETTE POINT
LITTLE BAYOU SORREL
MORGAN CITY
CALUMET
MODEL LIMITS
MODEL LIMITS
ATCHAFALAYA BAY
EUGENE ISLAND
ATCHAFALAYA BASIN
BRANCH 1
UPPER ATCHAFALAYA RIVER

PLATE 36

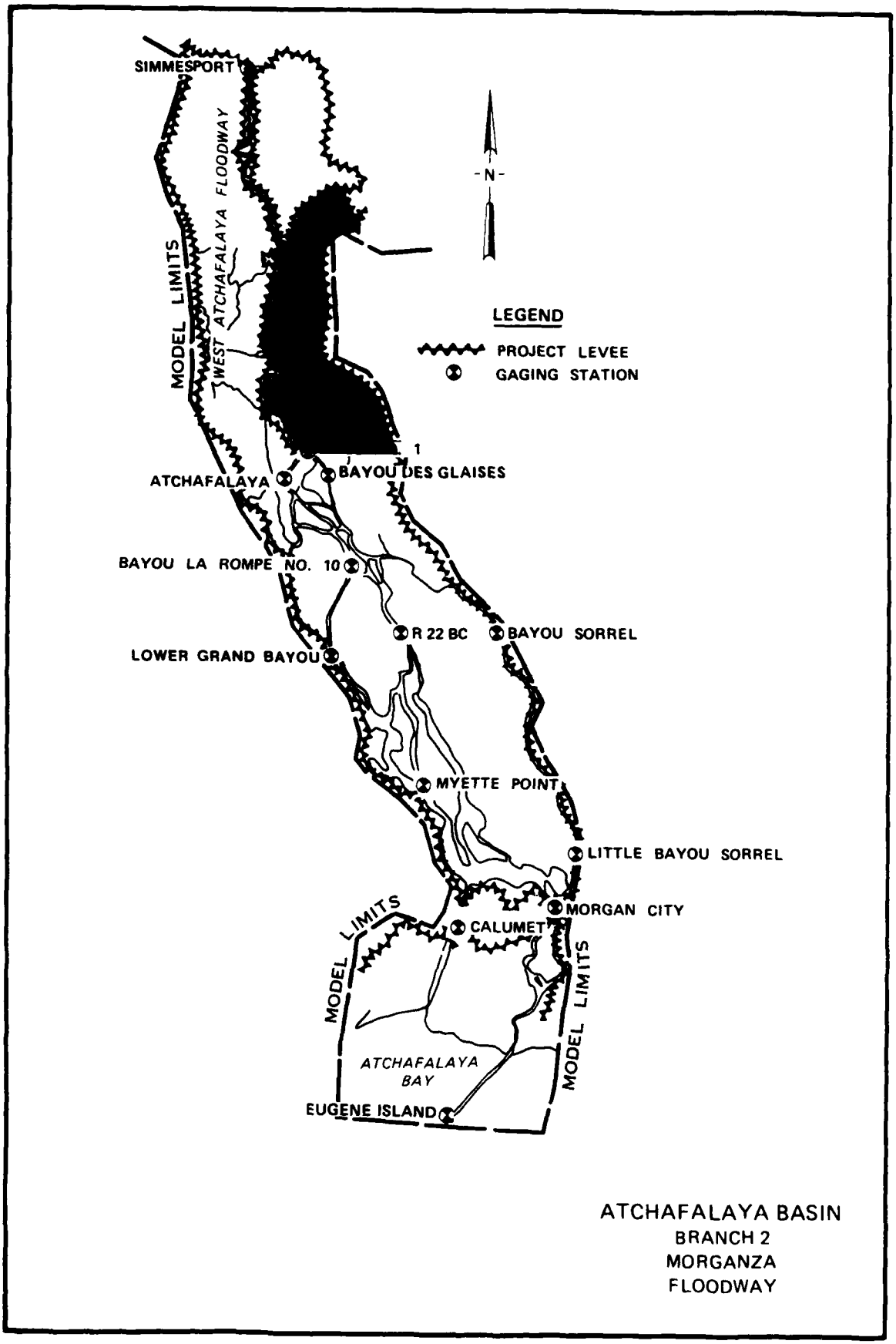

ATCHAFALAYA BASIN
BRANCH 2
MORGANZA
FLOODWAY

PLATE 37

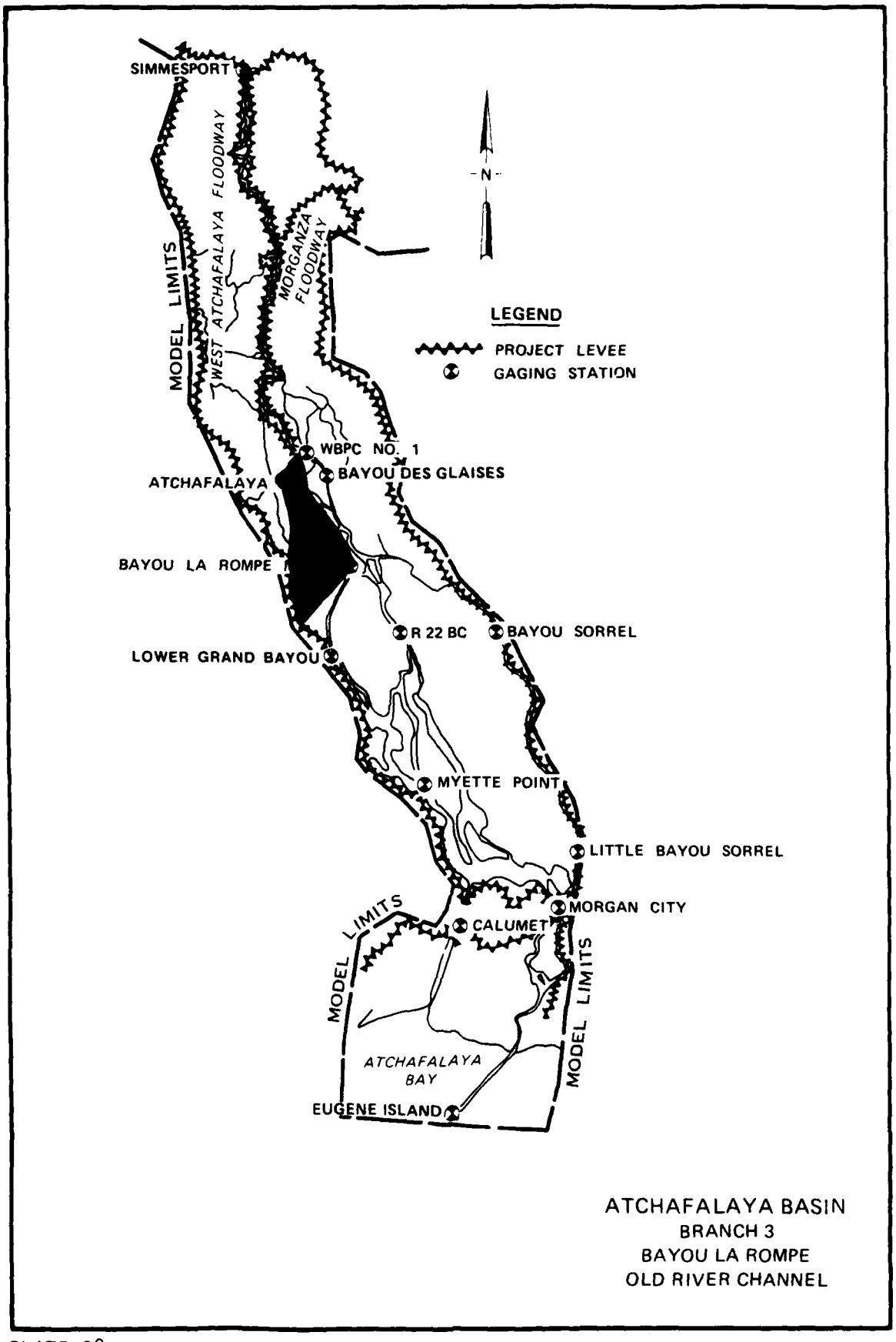
SIMMESPORT
WEST ATCHAFALAYA FLOODWAY
MORGANZA FLOODWAY
MODEL LIMITS
N
LEGEND
PROJECT LEVEE
GAGING STATION
WBPC NO. 1
BAYOU DES GLAISES
ATCHAFALAYA
BAYOU LA ROMPE
R 22 BC
BAYOU SORREL
LOWER GRAND BAYOU
MYETTE POINT
LITTLE BAYOU SORREL
MORGAN CITY
CALUMET
MODEL LIMITS
MODEL LIMITS
ATCHAFALAYA BAY
EUGENE ISLAND
ATCHAFALAYA BASIN
BRANCH 3
BAYOU LA ROMPE
OLD RIVER CHANNEL

PLATE 38

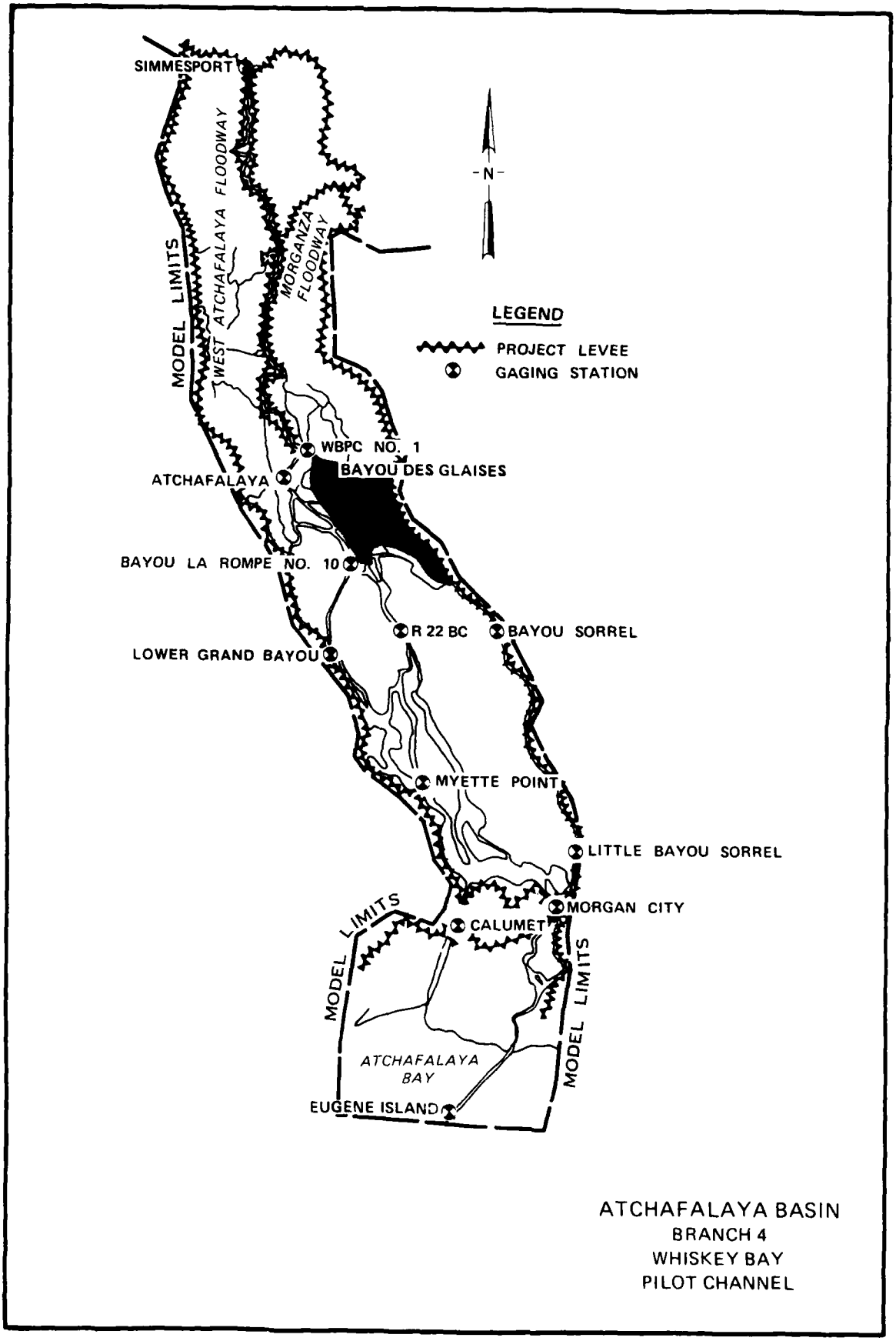
SIMMESPORT
WEST ATCHAFALAYA FLOODWAY
MORGANZA FLOODWAY
MODEL LIMITS
N
LEGEND
PROJECT LEVEE
GAGING STATION
WBPC NO. 1
BAYOU DES GLAISES
ATCHAFALAYA
BAYOU LA ROMPE NO. 10
R 22 BC
BAYOU SORREL
LOWER GRAND BAYOU
MYETTE POINT
LITTLE BAYOU SORREL
MORGAN CITY
CALUMET
MODEL LIMITS
MODEL LIMITS
ATCHAFALAYA BAY
EUGENE ISLAND
ATCHAFALAYA BASIN
BRANCH 4
WHISKEY BAY
PILOT CHANNEL

PLATE 39

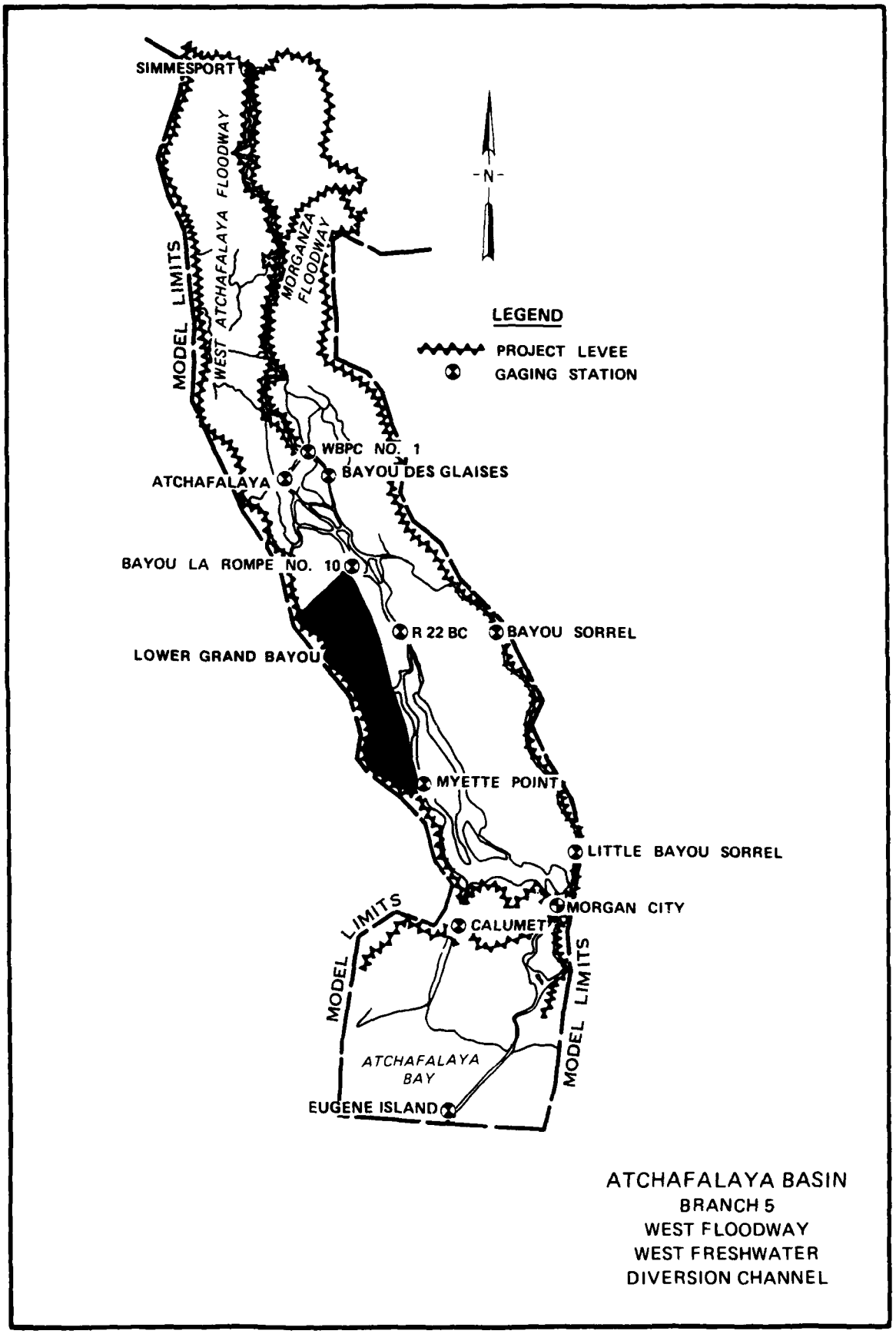
SIMMESPORT
MODEL LIMITS
WEST ATCHAFALAYA FLOODWAY
MORGANZA FLOODWAY
N
LEGEND
PROJECT LEVEE
GAGING STATION
WBPC NO. 1
ATCHAFALAYA
BAYOU DES GLAISES
BAYOU LA ROMPE NO. 10
R 22 BC
BAYOU SORREL
LOWER GRAND BAYOU
MYETTE POINT
LITTLE BAYOU SORREL
MORGAN CITY
CALUMET
MODEL LIMITS
MODEL LIMITS
ATCHAFALAYA BAY
EUGENE ISLAND
ATCHAFALAYA BASIN
BRANCH 5
WEST FLOODWAY
WEST FRESHWATER
DIVERSION CHANNEL

PLATE 40

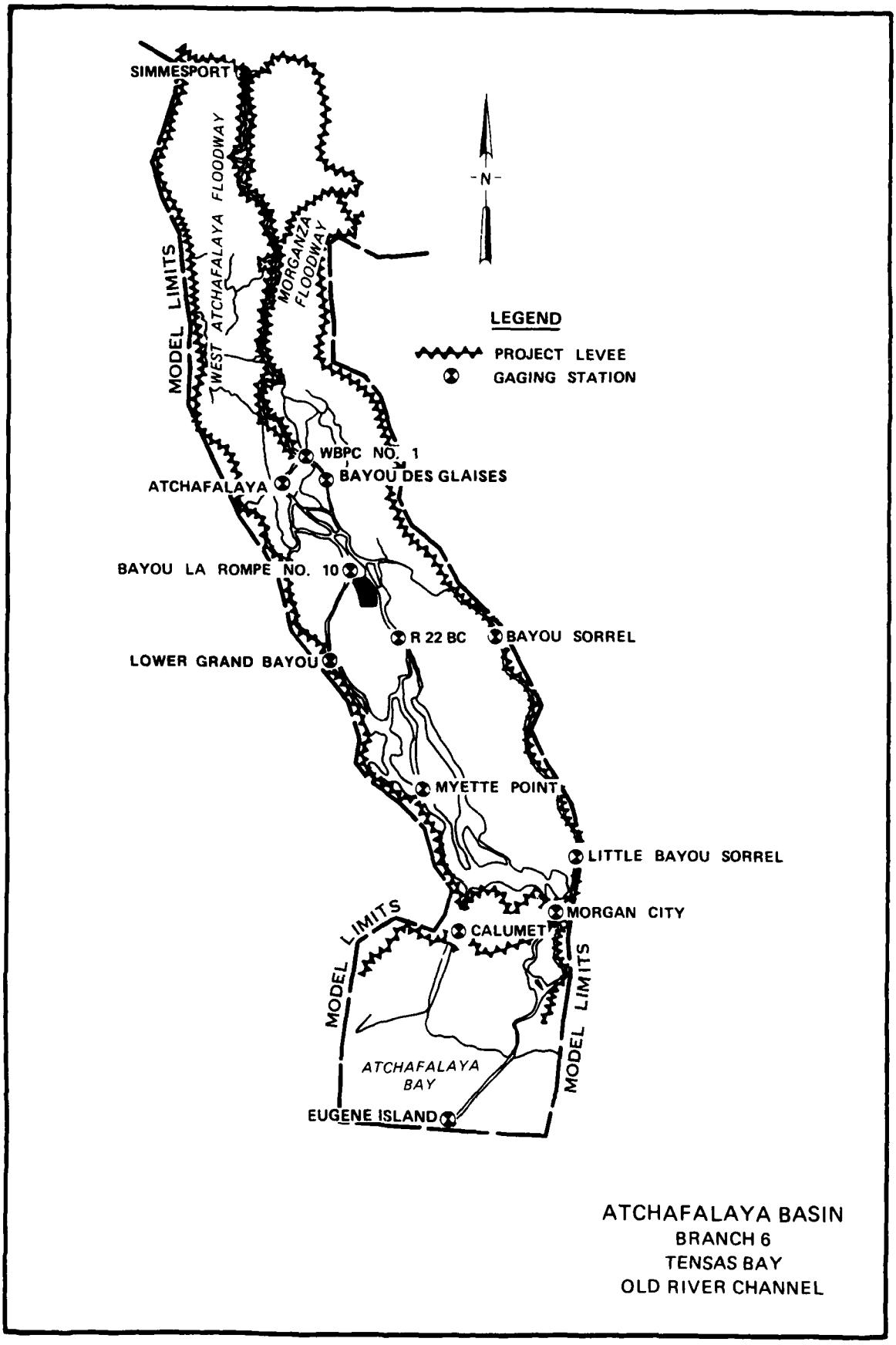
SIMMESPORT
MODEL LIMITS
WEST ATCHAFALAYA FLOODWAY
MORGANZA FLOODWAY
N
LEGEND
PROJECT LEVEE
GAGING STATION
WBPC NO. 1
BAYOU DES GLAISES
ATCHAFALAYA
BAYOU LA ROMPE NO. 10
R 22 BC
BAYOU SORREL
LOWER GRAND BAYOU
MYETTE POINT
LITTLE BAYOU SORREL
MORGAN CITY
CALUMET
MODEL LIMITS
MODEL LIMITS
ATCHAFALAYA BAY
EUGENE ISLAND
ATCHAFALAYA BASIN
BRANCH 6
TENSAS BAY
OLD RIVER CHANNEL

PLATE 41

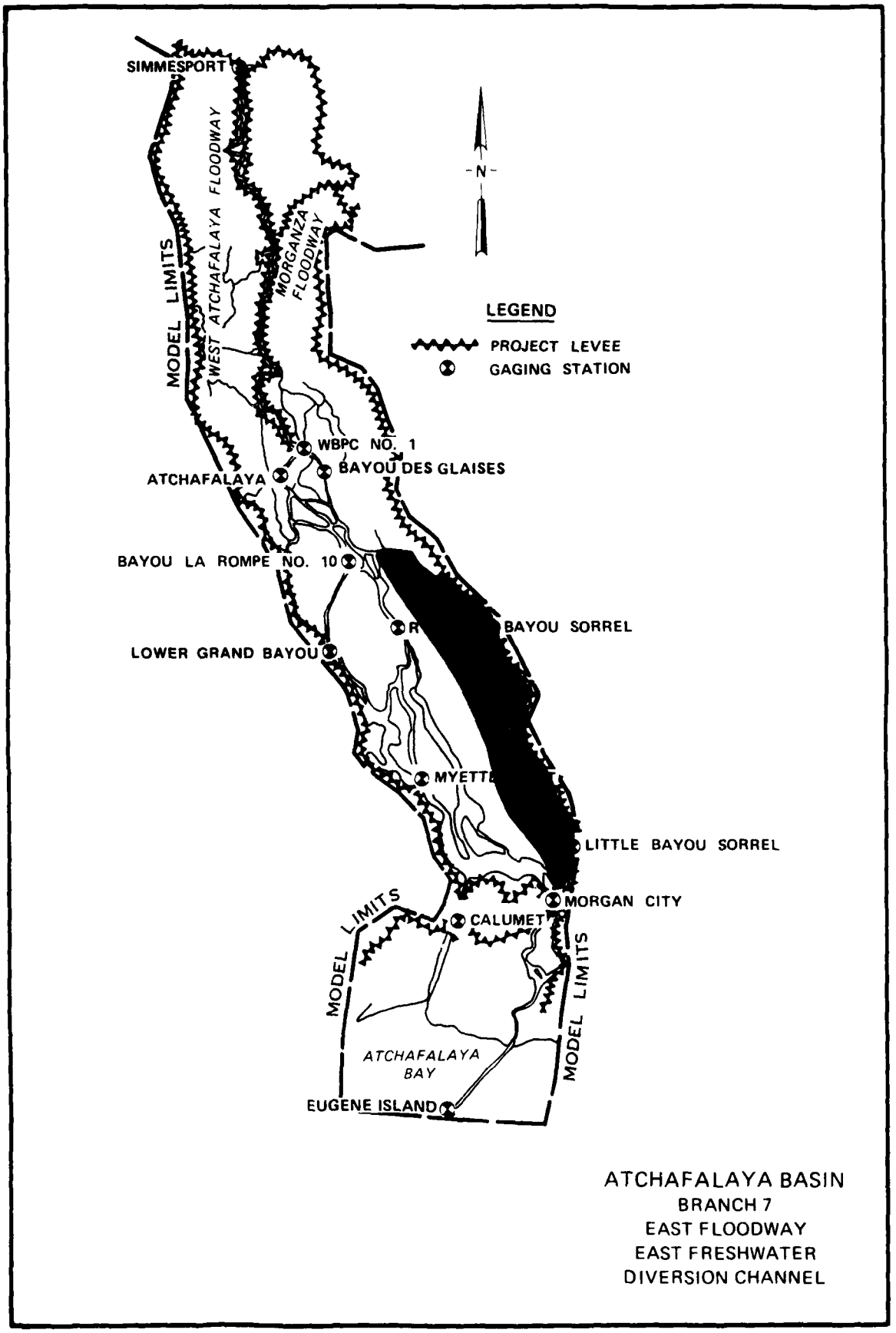
SIMMESPORT
WEST ATCHAFALAYA FLOODWAY
MORGANZA FLOODWAY
MODEL LIMITS
N
LEGEND
PROJECT LEVEE
GAGING STATION
WBPC NO. 1
BAYOU DES GLAISES
ATCHAFALAYA
BAYOU LA ROMPE NO. 10
BAYOU SORREL
LOWER GRAND BAYOU
LITTLE BAYOU SORREL
MORGAN CITY
CALUMET
MODEL LIMITS
MODEL LIMITS
ATCHAFALAYA BAY
EUGENE ISLAND
ATCHAFALAYA BASIN
BRANCH 7
EAST FLOODWAY
EAST FRESHWATER
DIVERSION CHANNEL

PLATE 42

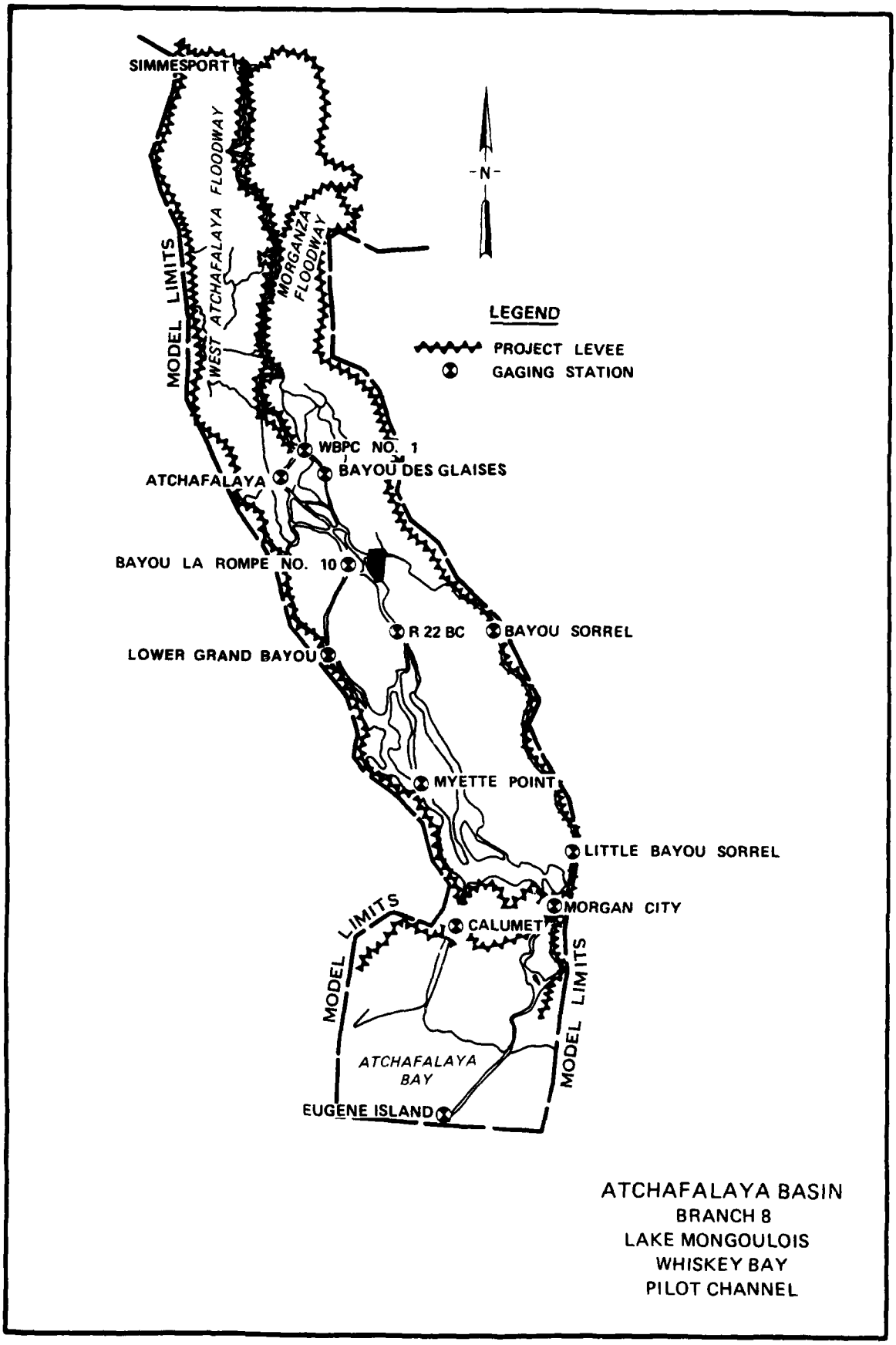
SIMMESPORT
WEST ATCHAFALAYA FLOODWAY
MORGANZA FLOODWAY
MODEL LIMITS
-N-
LEGEND
PROJECT LEVEE
GAGING STATION
WBPC NO. 1
BAYOU DES GLAISES
ATCHAFALAYA
BAYOU LA ROMPE NO. 10
R 22 BC
BAYOU SORREL
LOWER GRAND BAYOU
MYETTE POINT
LITTLE BAYOU SORREL
MORGAN CITY
CALUMET
MODEL LIMITS
MODEL LIMITS
ATCHAFALAYA BAY
EUGENE ISLAND
ATCHAFALAYA BASIN
BRANCH 8
LAKE MONGOULOIS
WHISKEY BAY
PILOT CHANNEL

PLATE 43

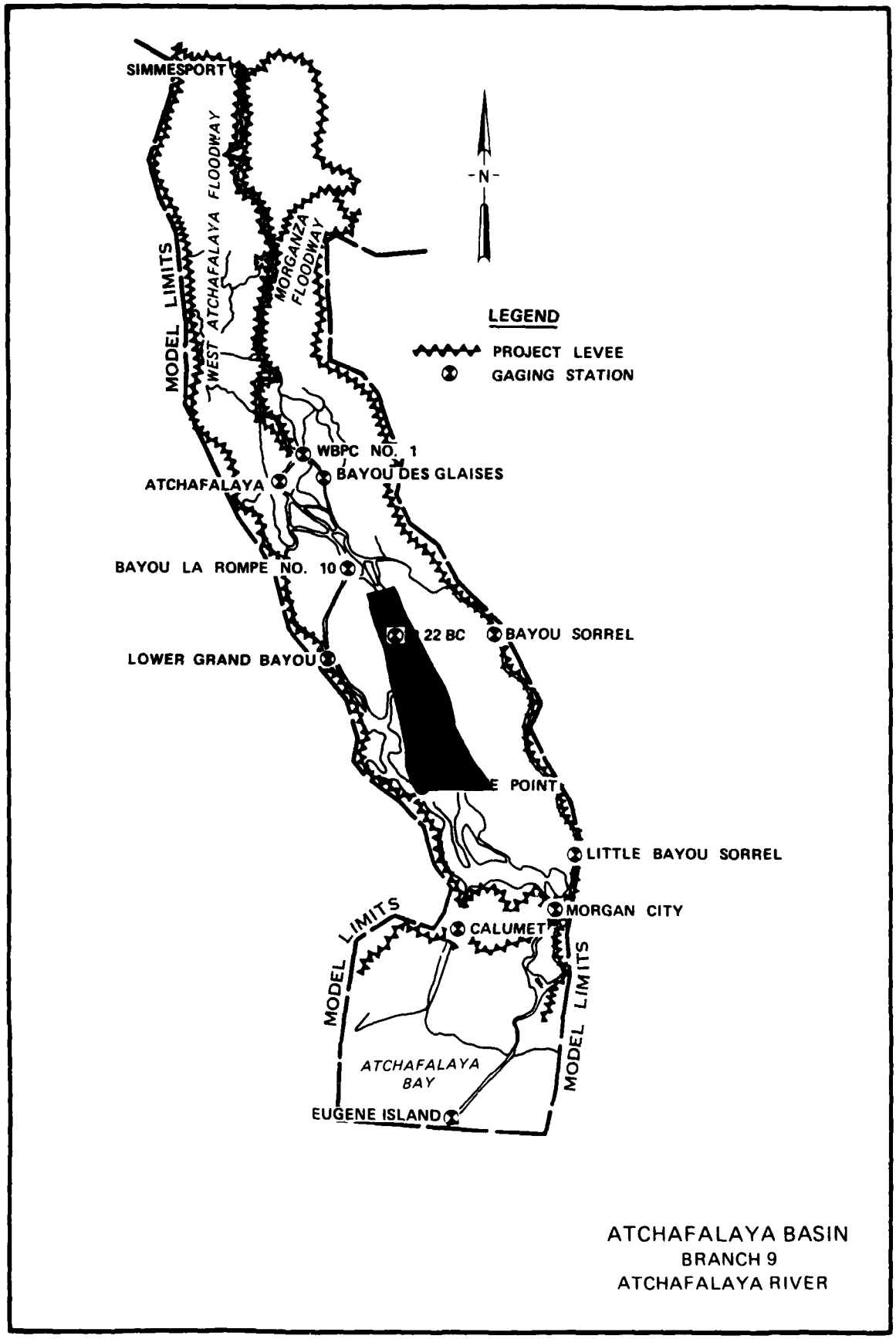
SIMMESPORT
MODEL LIMITS
WEST ATCHAFALAYA FLOODWAY
MORGANZA FLOODWAY
N
LEGEND
PROJECT LEVEE
GAGING STATION
WBPC NO. 1
BAYOU DES GLAISES
ATCHAFALAYA
BAYOU LA ROMPE NO. 10
22 BC
BAYOU SORREL
LOWER GRAND BAYOU
POINT
LITTLE BAYOU SORREL
MORGAN CITY
CALUMET
MODEL LIMITS
MODEL LIMITS
ATCHAFALAYA BAY
EUGENE ISLAND
ATCHAFALAYA BASIN
BRANCH 9
ATCHAFALAYA RIVER

PLATE 44

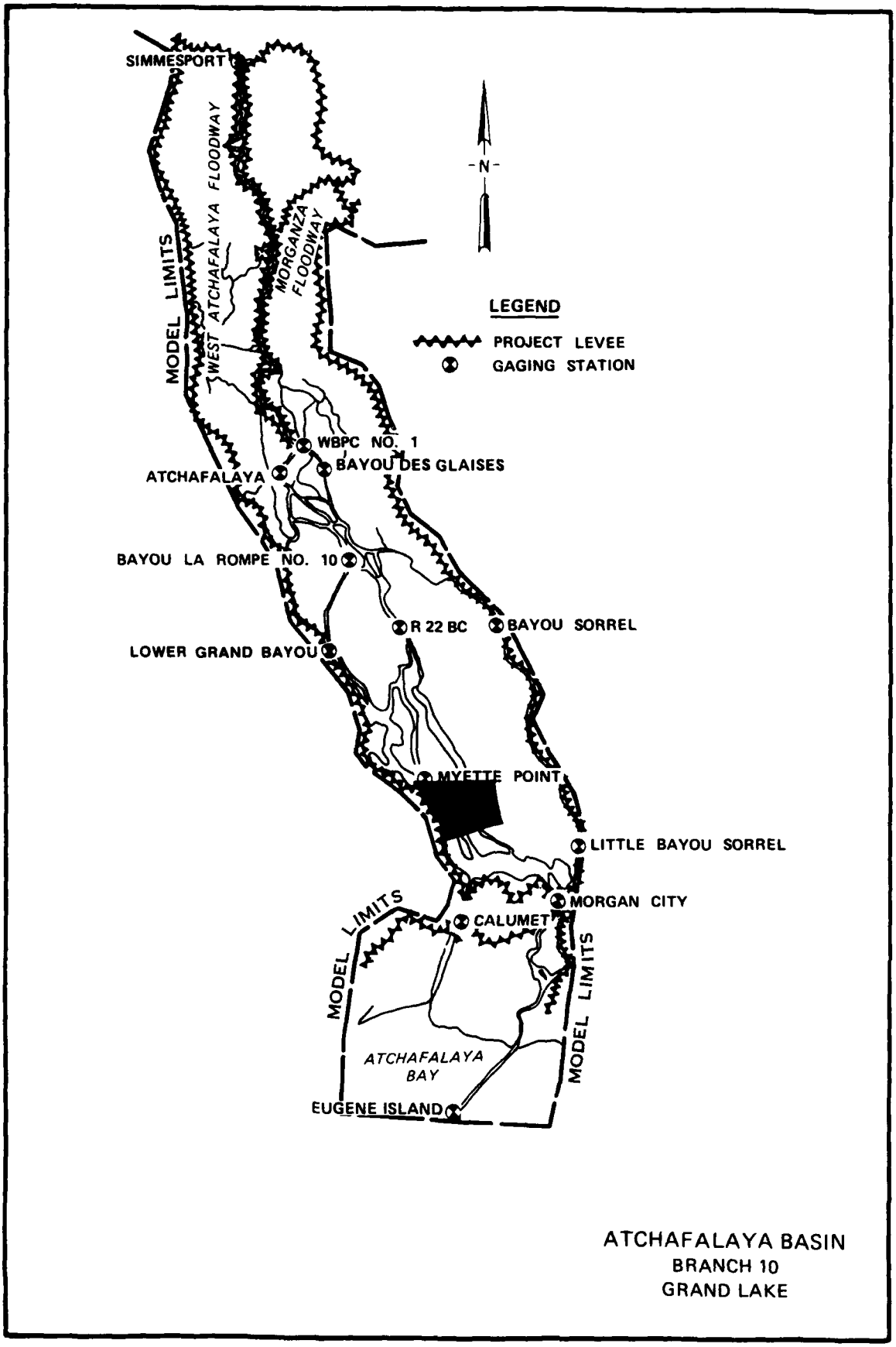
SIMMESPORT
MODEL LIMITS
WEST ATCHAFALAYA FLOODWAY
MORGANZA FLOODWAY
N
LEGEND
PROJECT LEVEE
GAGING STATION
WBPC NO. 1
BAYOU DES GLAISES
ATCHAFALAYA
BAYOU LA ROMPE NO. 10
R 22 BC
BAYOU SORREL
LOWER GRAND BAYOU
MYETTE POINT
LITTLE BAYOU SORREL
MORGAN CITY
CALUMET
MODEL LIMITS
MODEL LIMITS
ATCHAFALAYA BAY
EUGENE ISLAND
ATCHAFALAYA BASIN
BRANCH 10
GRAND LAKE

PLATE 45

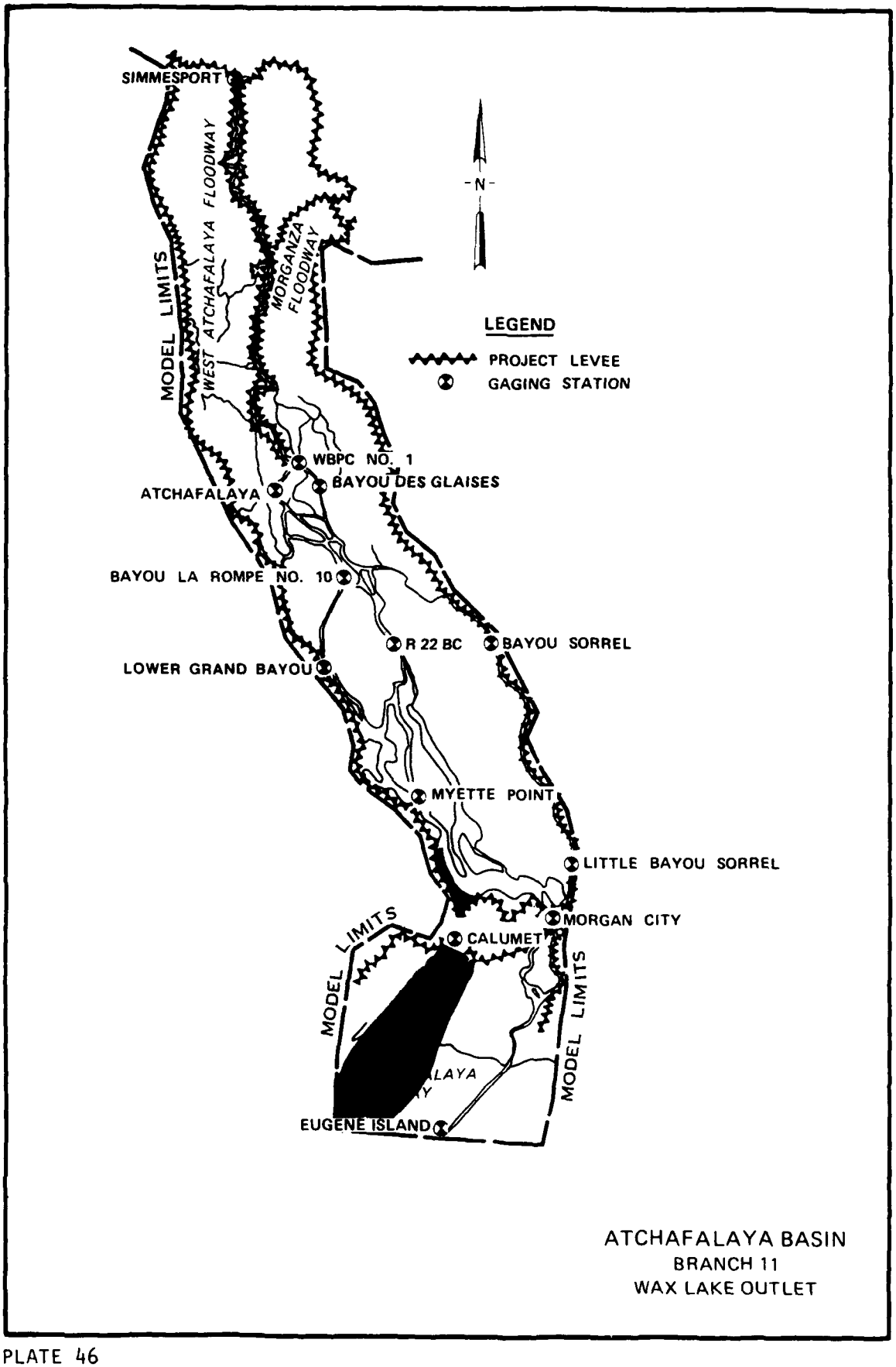
SIMMESPORT
WEST ATCHAFALAYA FLOODWAY
MORGANZA FLOODWAY
MODEL LIMITS
N
LEGEND
PROJECT LEVEE
GAGING STATION
WBPC NO. 1
BAYOU DES GLAISES
ATCHAFALAYA
BAYOU LA ROMPE NO. 10
R 22 BC
BAYOU SORREL
LOWER GRAND BAYOU
MYETTE POINT
LITTLE BAYOU SORREL
MORGAN CITY
CALUMET
MODEL LIMITS
MODEL LIMITS
EUGENE ISLAND
ATCHAFALAYA BASIN
BRANCH 11
WAX LAKE OUTLET

PLATE 46

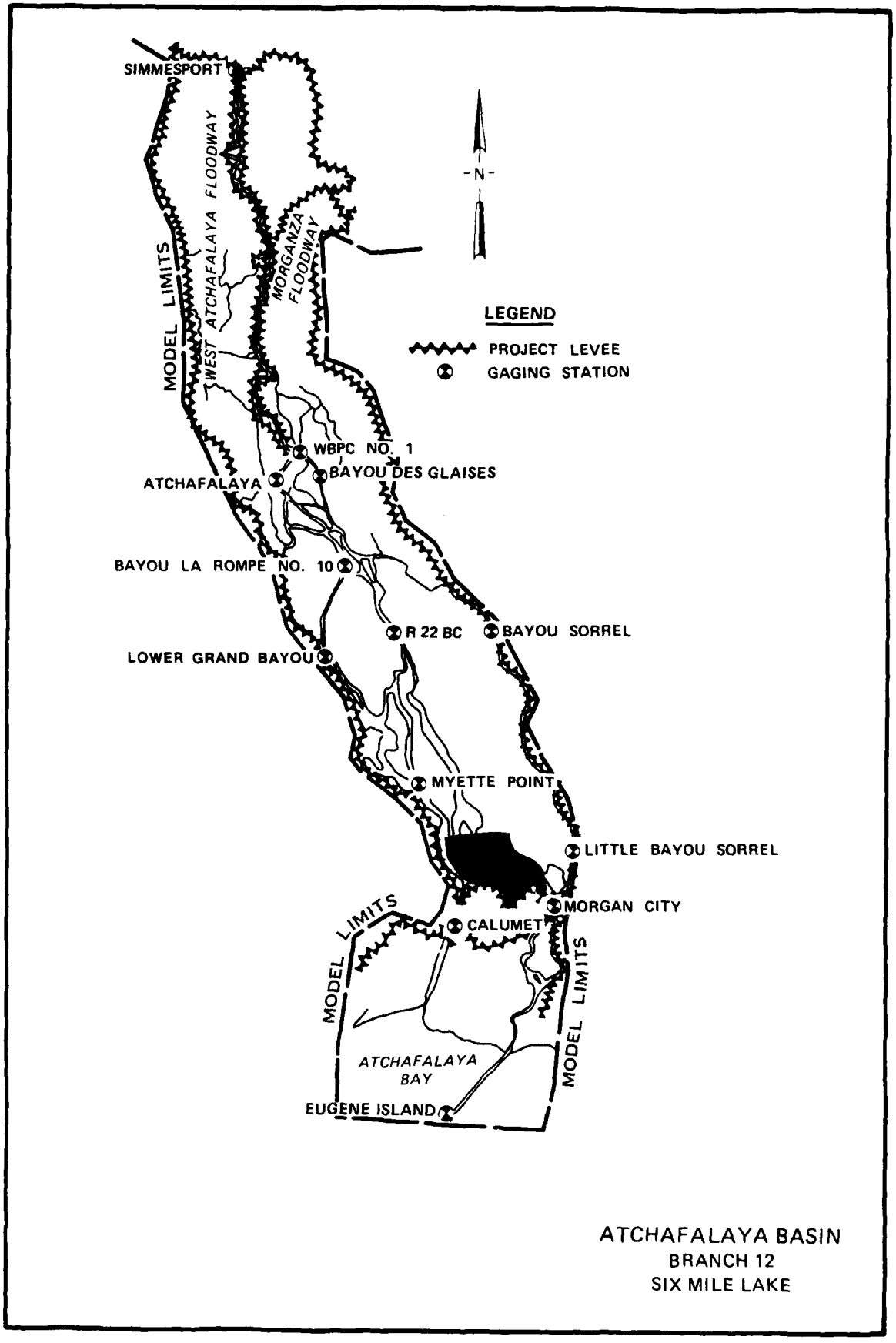

ATCHAFALAYA BASIN
BRANCH 12
SIX MILE LAKE

PLATE 47

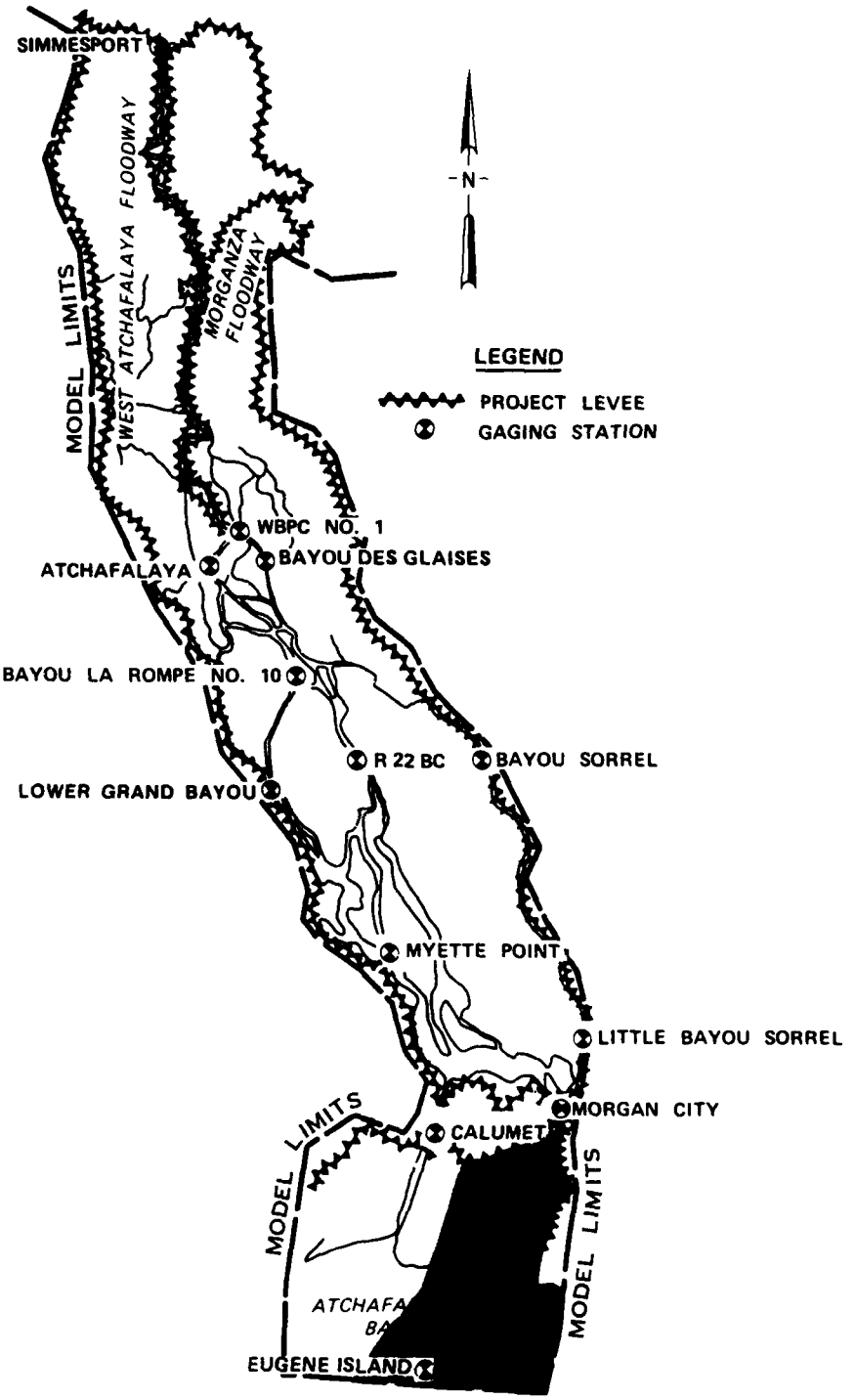

ATCHAFALAYA BASIN
BRANCH 13
LOWER ATCHAFALAYA RIVER

PLATE 48

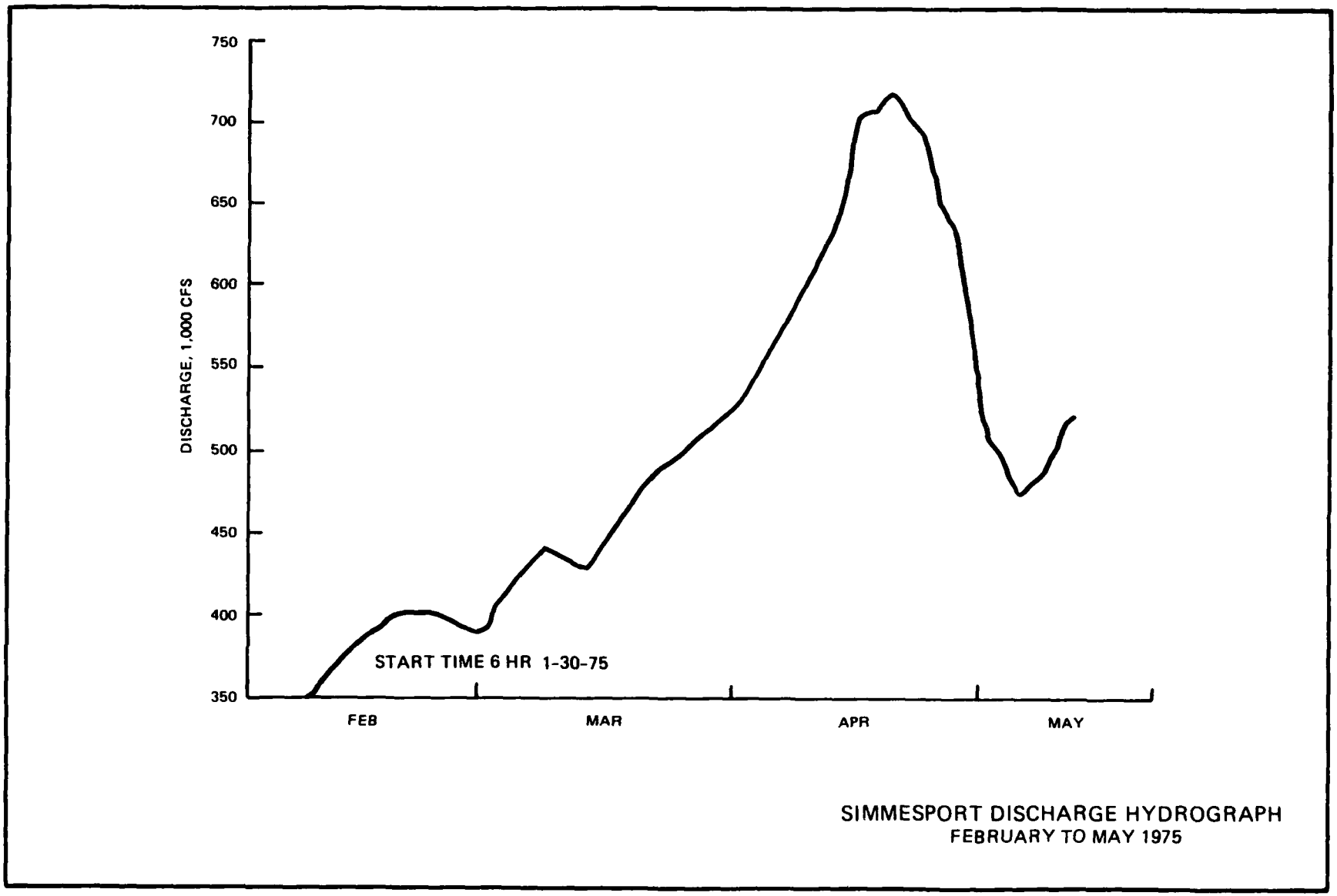

SIMMESPORT DISCHARGE HYDROGRAPH
FEBRUARY TO MAY 1975

PLATE 49

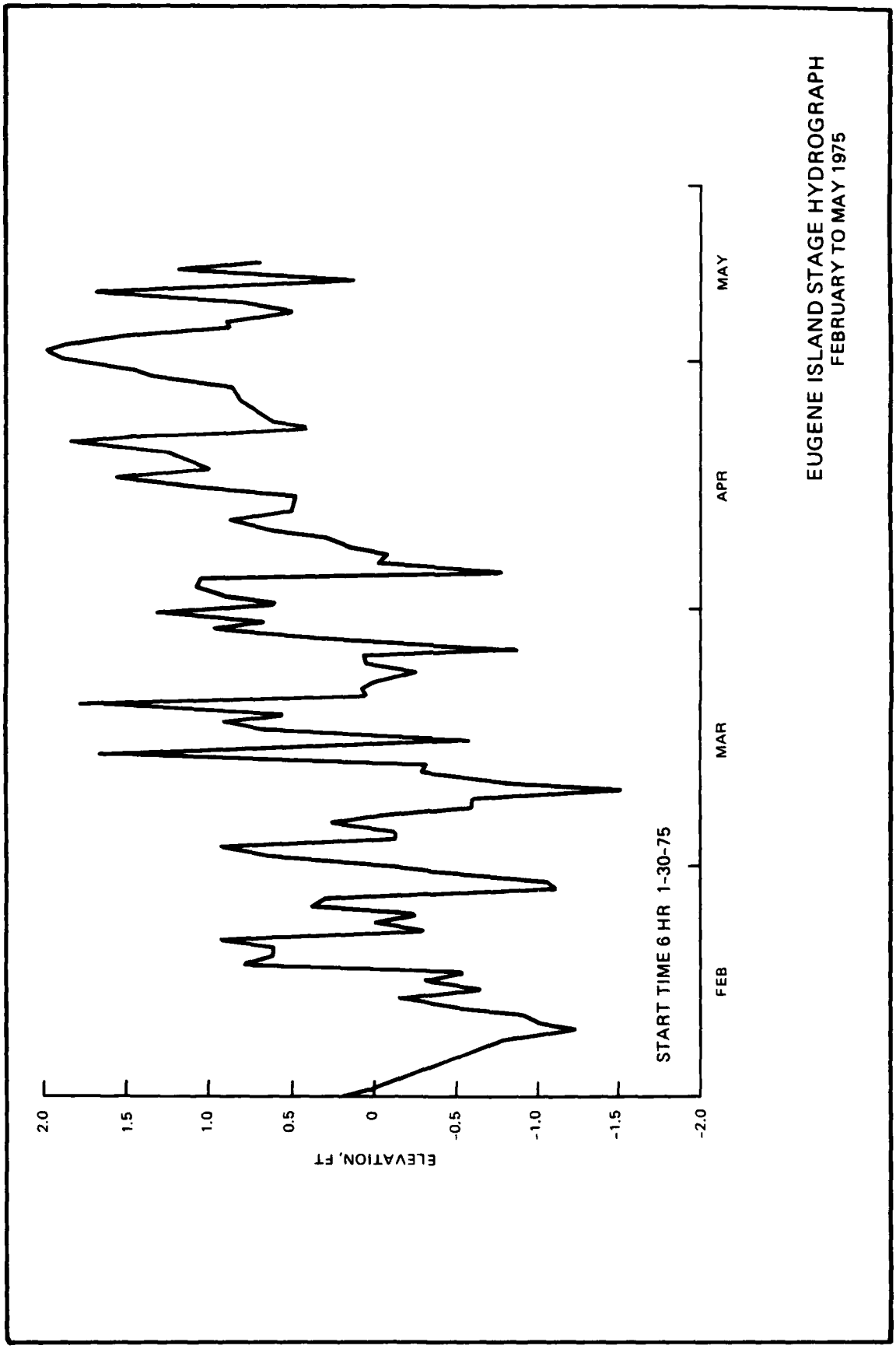
EUGENE ISLAND STAGE HYDROGRAPH
FEBRUARY TO MAY 1975
START TIME 6 HR 1-30-75
FEB
MAR
APR
MAY
ELEVATION, FT
2.0
1.5
1.0
0.5
0
-0.5
-1.0
-1.5
-2.0

PLATE 50

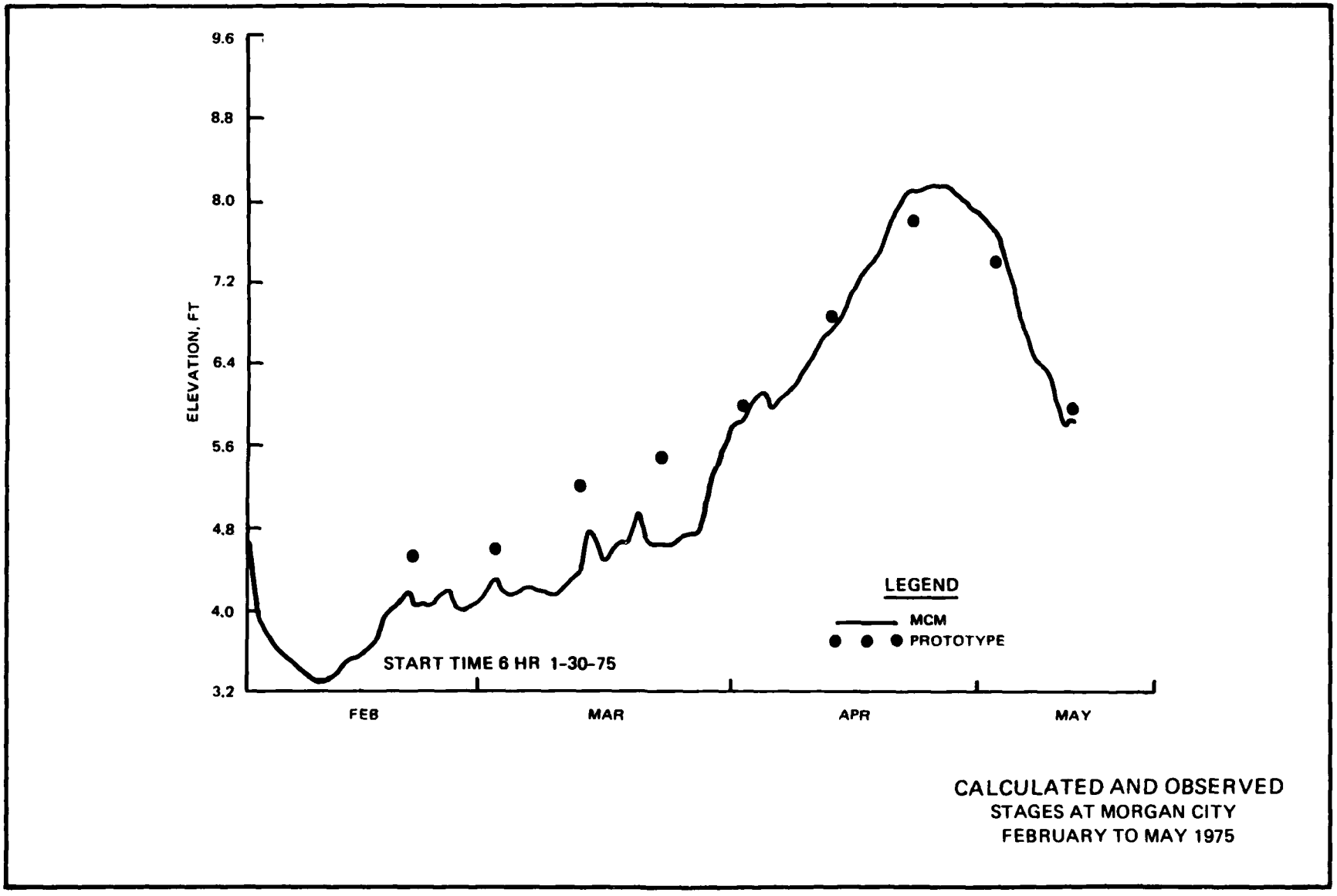

CALCULATED AND OBSERVED
STAGES AT MORGAN CITY
FEBRUARY TO MAY 1975

PLATE 51

PLATE 52

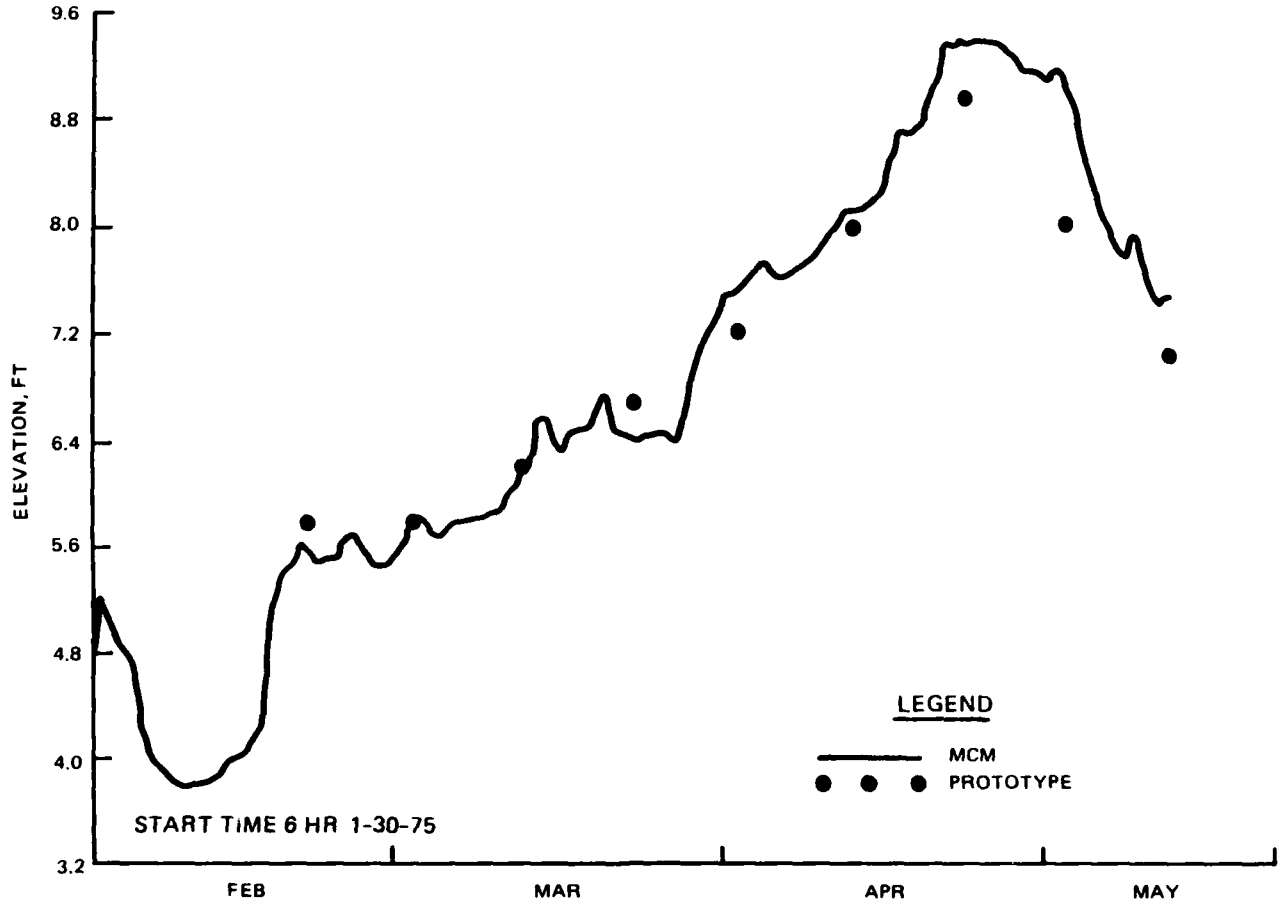

CALCULATED AND OBSERVED
STAGES AT CALUMET
FEBRUARY TO MAY 1975

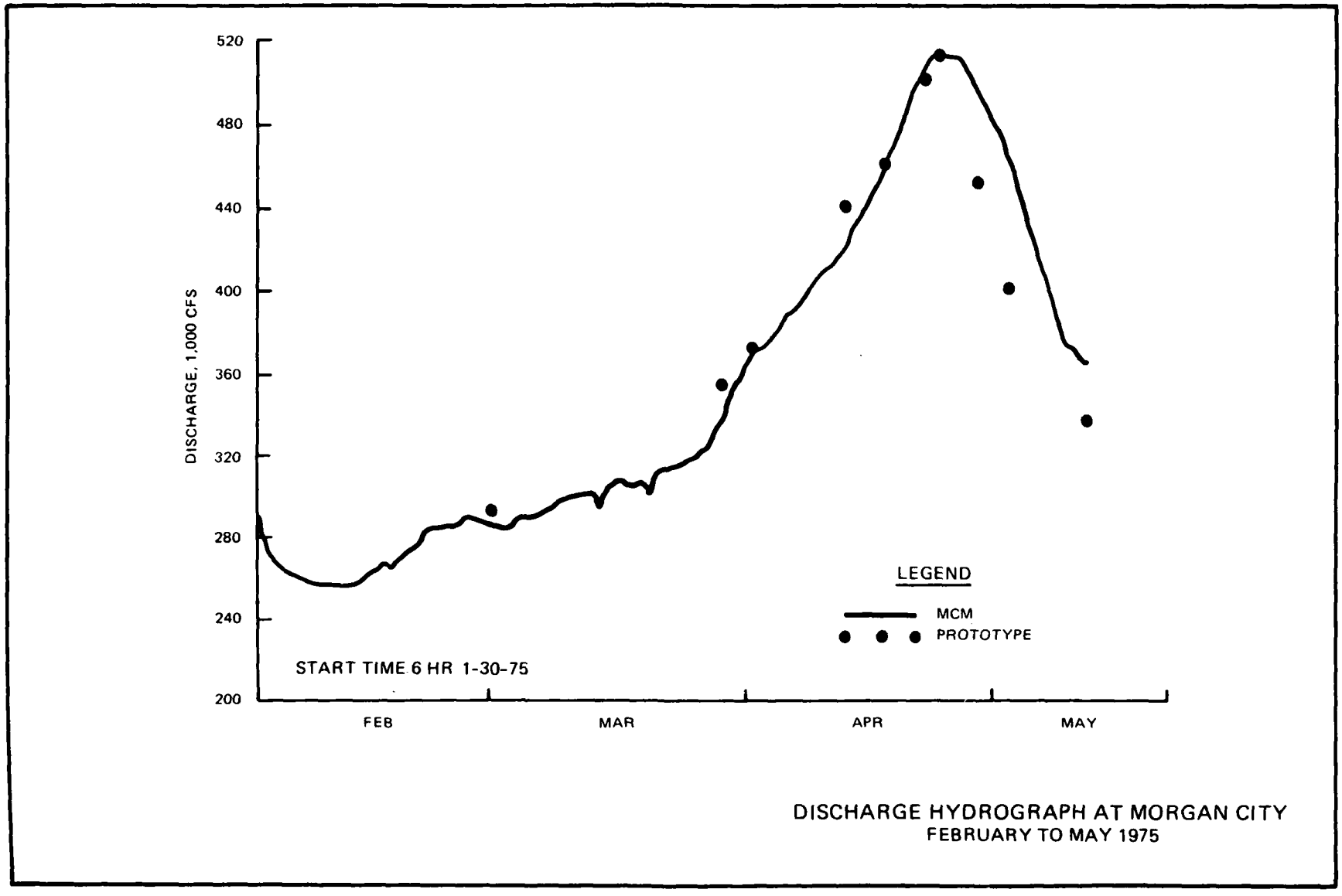

DISCHARGE HYDROGRAPH AT MORGAN CITY
FEBRUARY TO MAY 1975

PLATE 53

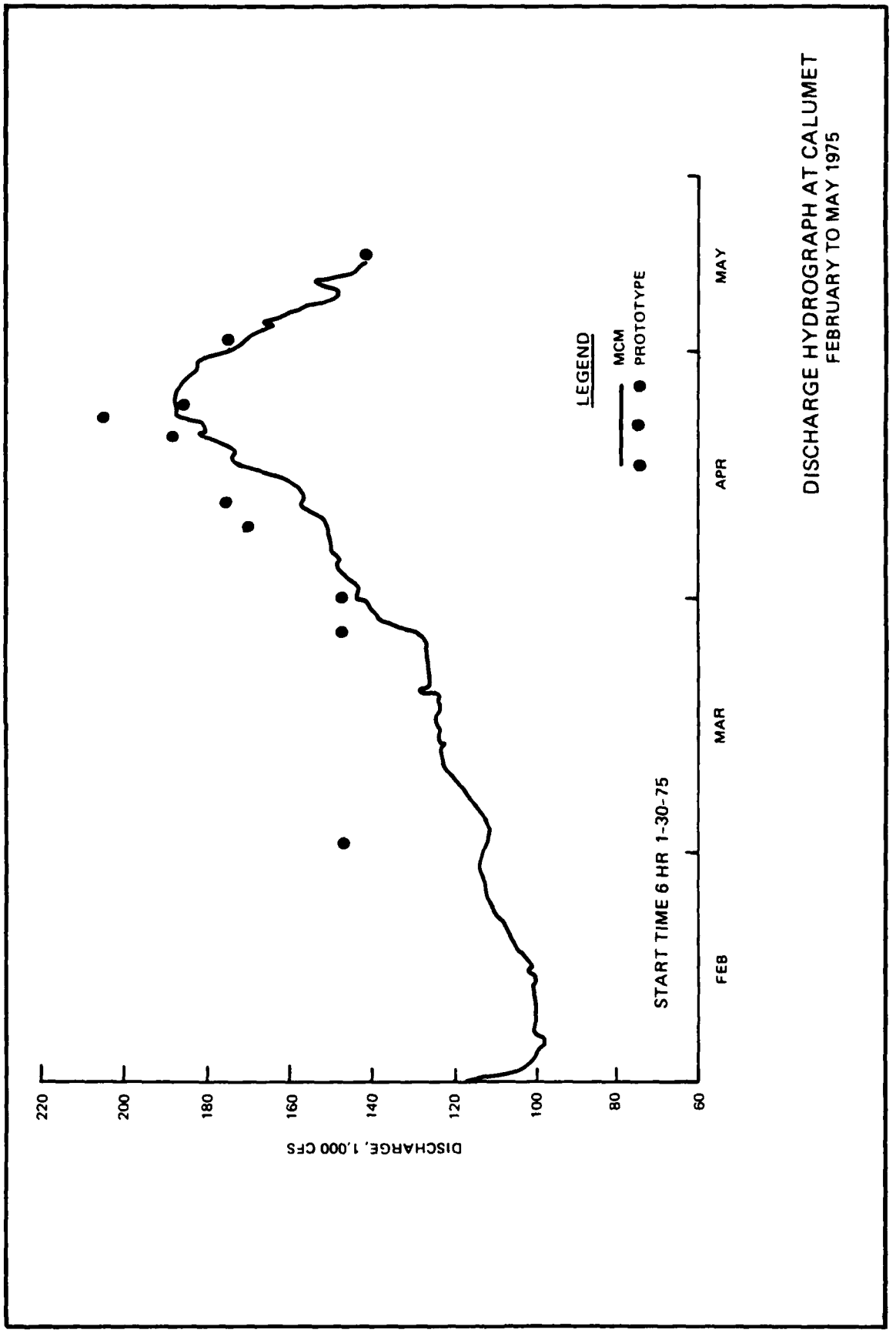
DISCHARGE HYDROGRAPH AT CALUMET
FEBRUARY TO MAY 1975
LEGEND
MCM
PROTOTYPE
START TIME 6 HR 1-30-75
FEB
MAR
APR
MAY
DISCHARGE, 1,000 CFS
220
200
180
160
140
120
100
80
60

PLATE 54

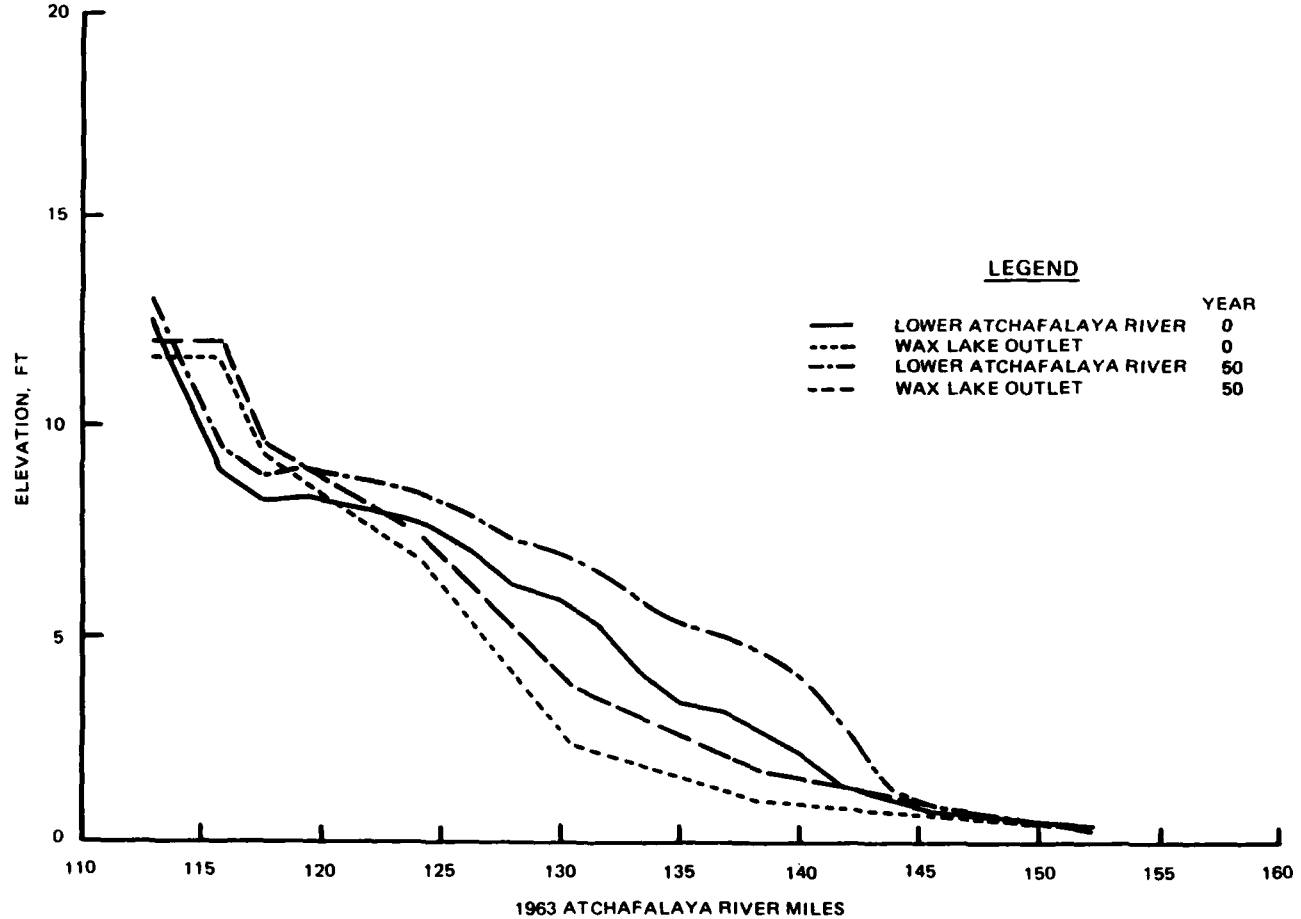

WATER-SURFACE PROFILES, SOCHMJ RESULTS
1975 FLOOD PEAK
LOWER ATCHAFALAYA RIVER
AND WAX LAKE OUTLET

PLATE 55

PLATE 56

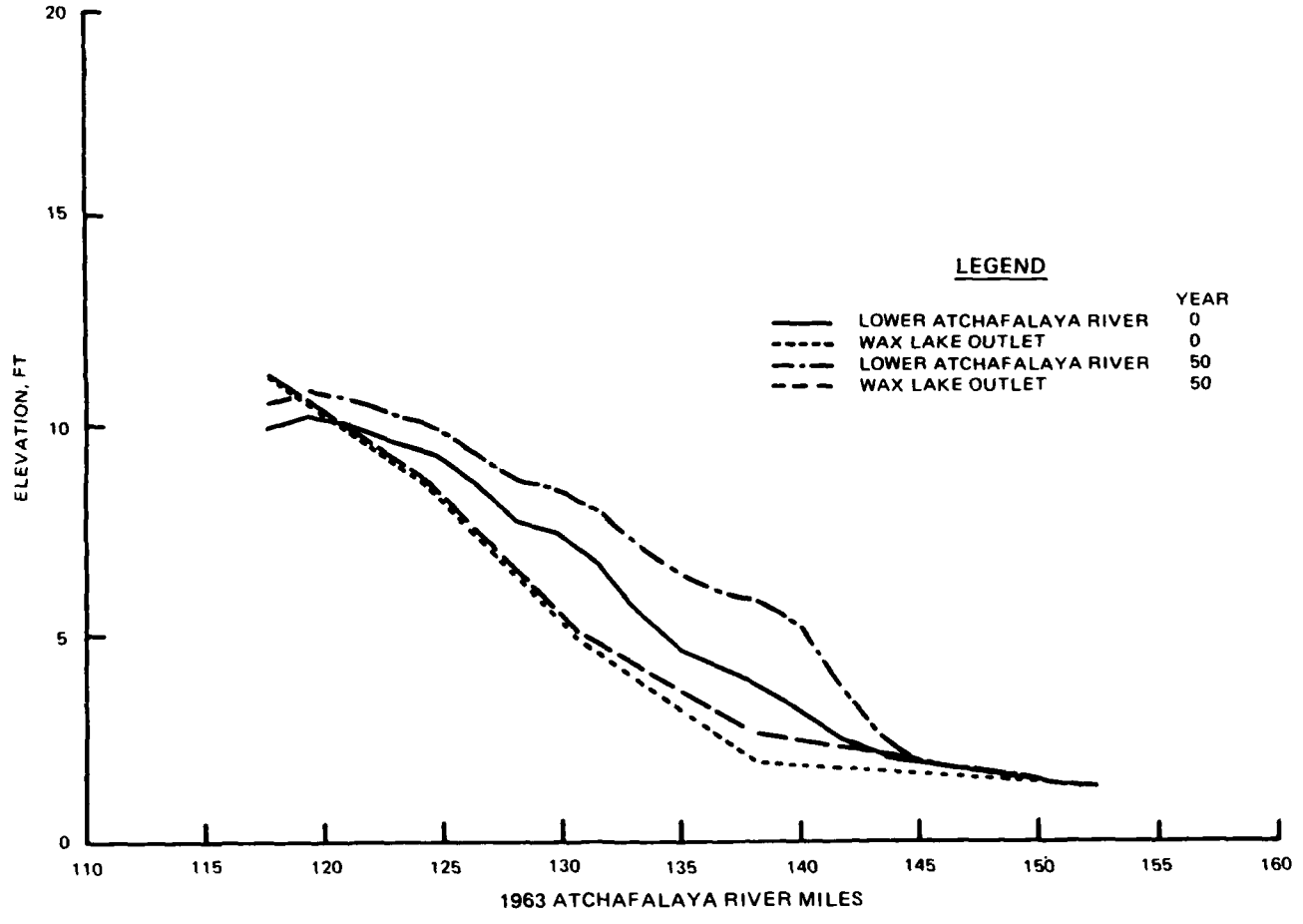

WATER-SURFACE PROFILES, SOCHMJ RESULTS
1973 FLOOD PEAK
LOWER ATCHAFALAYA RIVER
AND WAX LAKE OUTLET

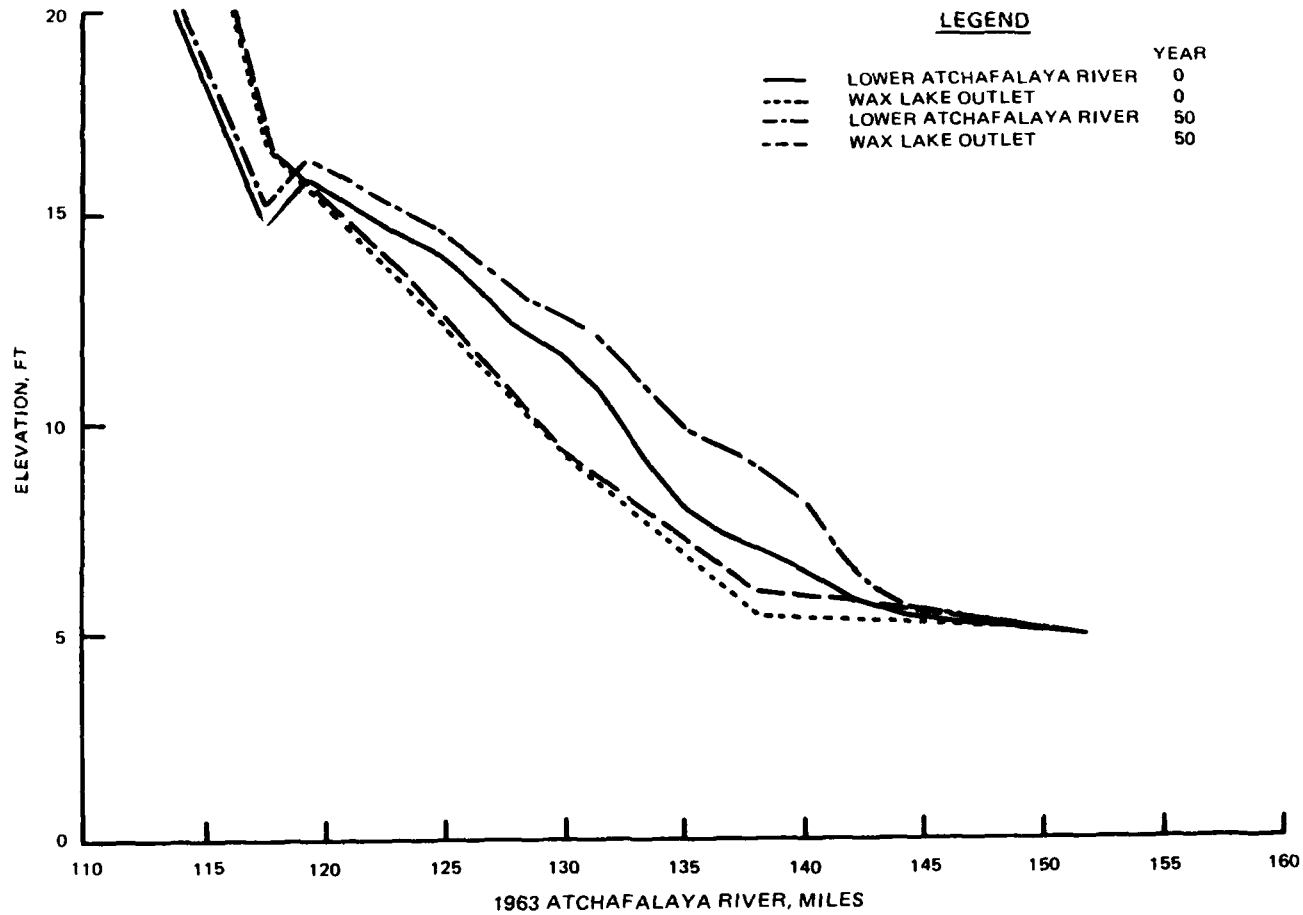

WATER-SURFACE PROFILES, SOCHMJ RESULTS
58AEN FLOOD PEAK
LOWER ATCHAFALAYA RIVER
AND WAX LAKE OUTLET

PLATE 57

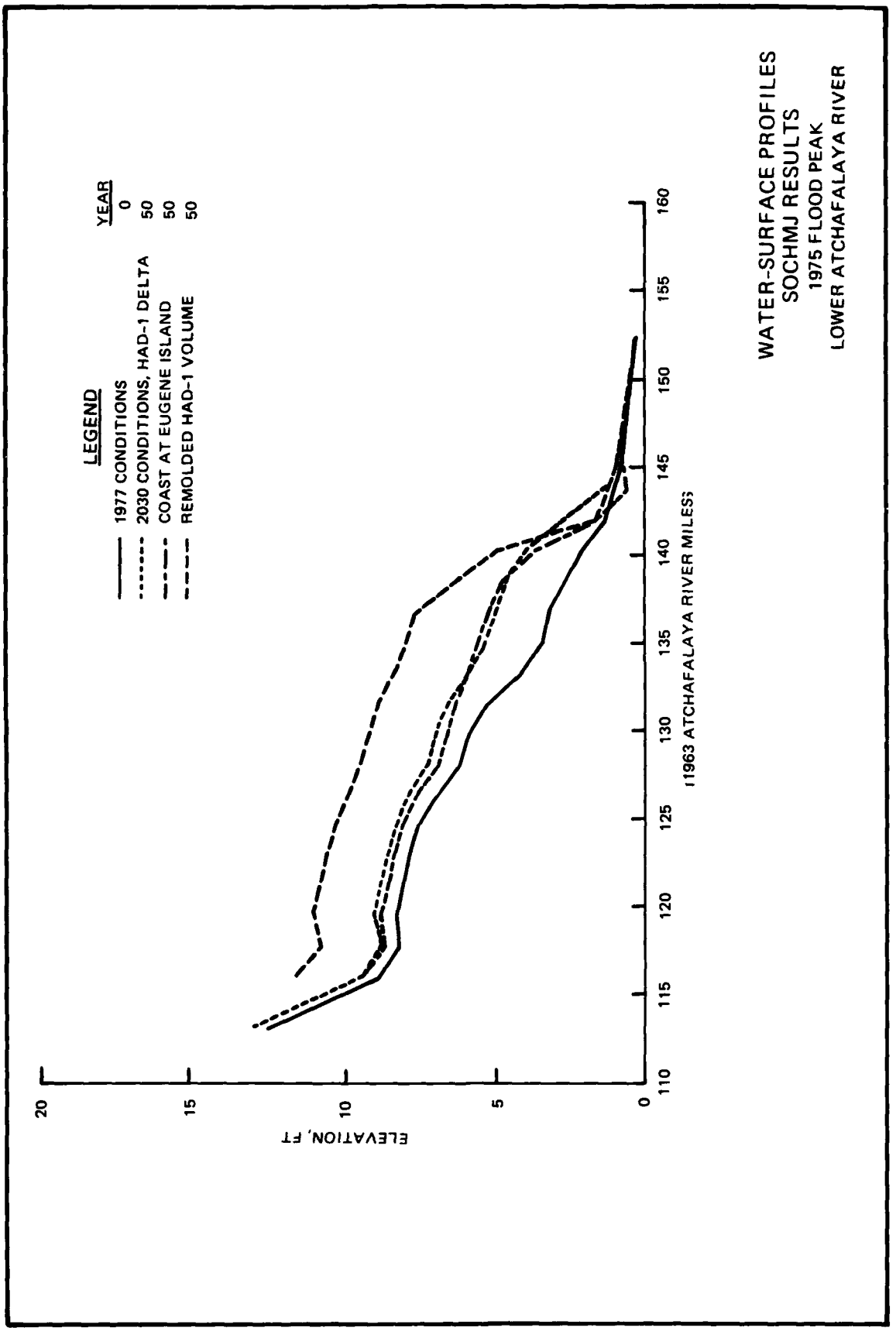
WATER-SURFACE PROFILES
SOCHMJ RESULTS
1975 FLOOD PEAK
LOWER ATCHAFALAYA RIVER
LEGEND
YEAR
1977 CONDITIONS 0
2030 CONDITIONS, HAD-1 DELTA 50
COAST AT EUGENE ISLAND 50
REMOLDED HAD-1 VOLUME 50
ELEVATION, FT
20
15
10
5
0
110
115
120
125
130
135
140
145
150
155
160
ATCHAFALAYA RIVER MILES

PLATE 58

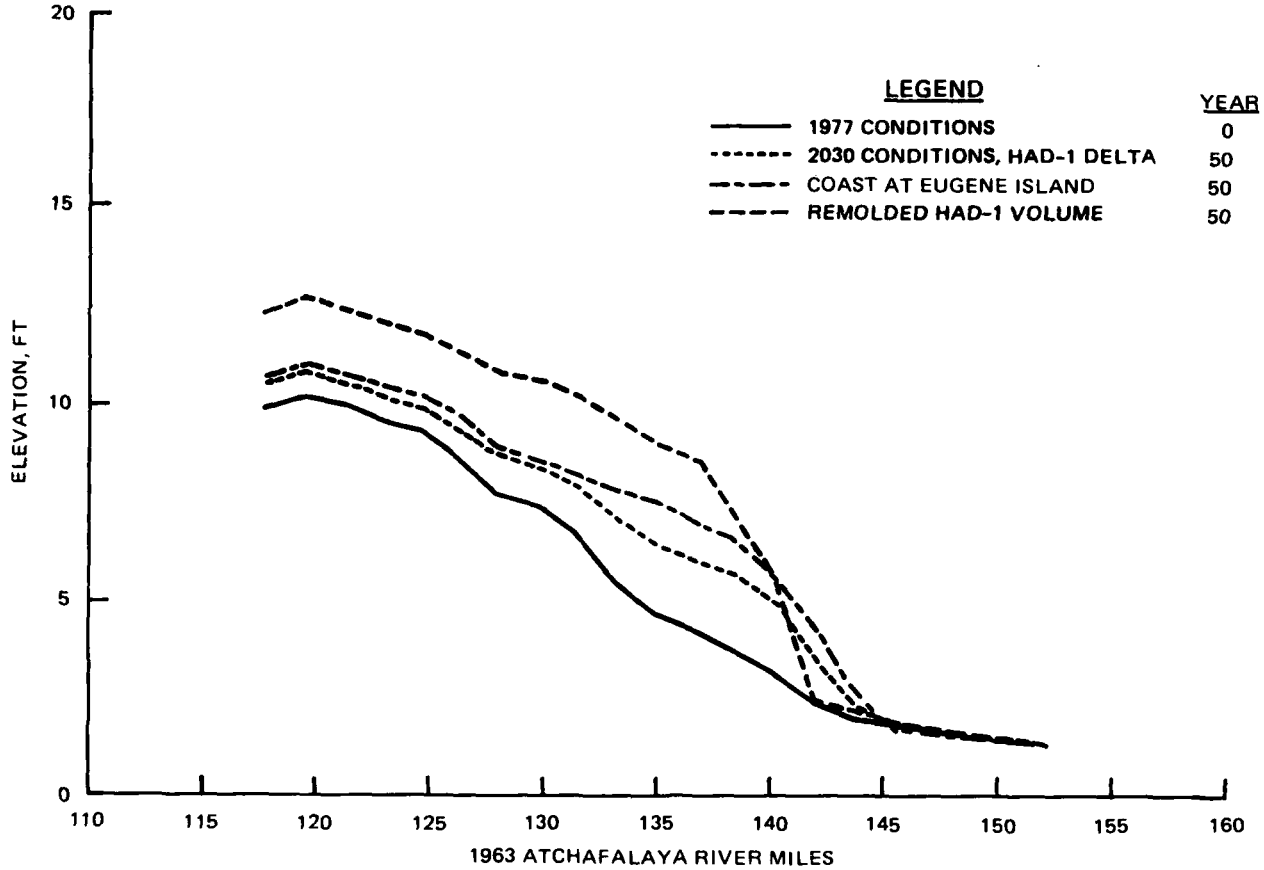

WATER-SURFACE PROFILES
SOCHMJ RESULTS
1973 FLOOD PEAK
LOWER ATCHAFALAYA RIVER

PLATE 59

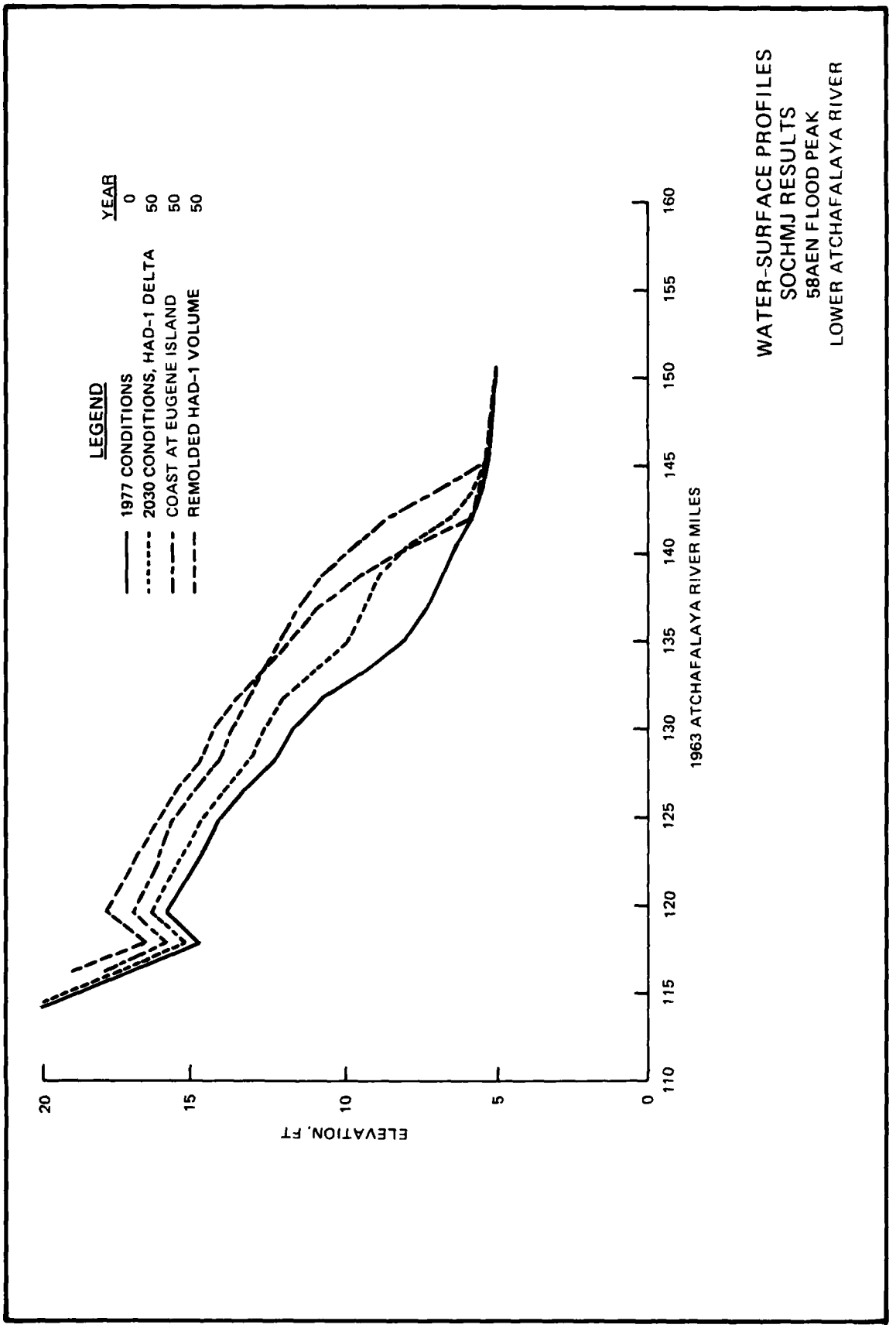
WATER-SURFACE PROFILES
SOCHMJ RESULTS
58AEN FLOOD PEAK
LOWER ATCHAFALAYA RIVER
LEGEND
YEAR
1977 CONDITIONS 0
2030 CONDITIONS, HAD-1 DELTA 50
COAST AT EUGENE ISLAND 50
REMOLDED HAD-1 VOLUME 50
ELEVATION, FT
20
15
10
5
0
110
115
120
125
130
135
140
145
150
155
160
1963 ATCHAFALAYA RIVER MILES

PLATE 60